GOING BACKWARDS TO GO FORWARDS: THE POTENTIAL USE OF MEDIAEVAL TUBERS AS FUTURE MEDICINE

A thesis presented by

Nicola Elizabeth Woods, BSc Hons

in fulfilment of the requirement for the degree of

Doctor of Philosophy

2017

Strathclyde Institute of Pharmacy and Biomedical Sciences

University of Strathclyde

This thesis is the result of the author's original research. It has been composed by the author and has not been previously submitted for examination which has led to the award of a degree.

Signed:

Date:

ACKNOWLEDGMENTS

First and foremost I would like to thank my supervisors Dr Valerie Ferro and Professor Alexander Gray for all their contributions, guidance and wisdom throughout my PhD. The support you provided was immense, and I will always be grateful for this opportunity. I would especially like to thank Val for believing in me, keeping me calm and for providing encouragement. You were always there for me with great advice and I could not have done this without you. I would like to thank Sandy for his unbelievable knowledge of natural products and NMR, and for his patience and time for helping me constantly learn - your stories will forever make me laugh, and if I have half as many to tell throughout my life as you do, I will be very happy. I would also like to give a huge thank you to Dr Rothwelle Tate (an adopted supervisor) for his support, advice and contributions to my project as well as his extensive knowledge in Molecular Biology. Thank you for taking time to help me – again it would not have been possible without your guidance and expertise.

Additionally, I would like to thank our other collaborators: Dr Ann Mitchell (University of Strathclyde), Dr Pietrro Ianetta (James Hutton Institute), Dr Greg Kenicer (The Royal Botanic Gardens of Edinburgh), Dr Brian Moffat and Mr Mark Goff (Bitter Vetch Ltd.) – the Heath Pea group. Without the help and advice from every one of you, this project could not have been successful. I greatly appreciate the help and advice from each of you.

My thanks and appreciation extend to everyone in my lab group for their friendship and support over the years, especially Dr John Igoli – if it wasn't for your guidance and support in the initial months then I would have been lost! I would also like to thank Dr Jonans Tuslimire for his friendship and expertise in various aspects of my PhD. An extended thank you also goes to Mrs Louise Young, Miss Grainne Abbott, Mr Dennis McLoughlin, Mr David Mark Thomson, Mrs Linda Horan, Mrs Carol Whitehouse, Mr Lee Wheeler, Mr Kevin O'Halloran, Mr George Walker and Mr Steven McDonald for all of their help and advice in various different aspects of my PhD.

Throughout my PhD I have made some great friends who have kept me sane – especially Claire and Samantha. An extra special thank you goes to Claire – the chocolates and pep talks you provided definitely helped me stay focused, as well as all those yoga classes which kept us calm (even if it was only for a few weeks)! Thank you for encouraging me and for your help and support during the 'really overwhelming' moments.

I would definitely not be at this stage in my life if it wasn't for the support and love from my parents Elizabeth and Raymond, and my brothers Stephen and Paul. Thank you for always believing in me. I also wouldn't have managed this without the support from my best friends - Laura, Roisin, Fe, Clare and Steph. You all deserve a medal for putting up with me through stressful times and for giving me plenty of excuses to take a break from Uni work and writing. I can now make up for all the times I had to say "No, I need to write!" - I cannot thank you all enough for being so supportive, patient and understanding.

Last, but definitely not least, my best friend, soul mate and future husband, Jordan – I don't think I can ever thank you enough for being by my side. You experienced every emotion, every mood, every up and every down, and you stayed by me. You always know the right thing to say. You inspire and motivate me every day to follow my dreams. I am very lucky to have met you (as are you to have met me!) & I can't wait to grow old with you. Thank you!

One more special mention goes to my little fur-babies, Nala and Cookie! The cutest cats on the planet. All you need in life is love… and a cat (or two). I'm so grateful I have both!

I dedicate this thesis to all of you.

PUBLICATIONS

Brain changing tubers: Gene expression changes following mediaeval tuber consumption. Woods N, Gebril A, Mitchell A, Iannetta P, Kenicer G, Tate RJ, Pickard B, Gray AI, Ferro VA. Planta Med. **2016** Dec;81(S 01):S1-S381.

Effect of Bee Venom and its Fractions on the Release of Pro-Inflammatory Cytokines in PMA-Differentiated U937 Cells Co-Stimulated with LPS. Jonans Tusiimire, Jennifer Wallace, Nicola Woods, Mark J. Dufton, John A. Parkinson, Grainne Abbott1, Carol J. Clements, Louise Young, Jin Kyu Park, Jong Woon Jeon, Valerie A. Ferro, and David G. Watson. *Vaccines* **2016**, 4(2), 11; doi:10.3390/vaccines4020011

Chemical and Antimicrobial Profiling of Propolis from Different Regions within Libya. Weam Siheri; Tong Zhang; Godwin Unekwuojo Ebiloma; Marco Biddau; Nicola Woods; Muattaz Yassein Hussain; Carol Clements; James Fearnley; Ruangelie Edrada Ebel; Timothy Paget; Sylke Muller; Katherine C Carter; Harry P De Koning; Valerie A Ferro; David G Watson. *PloS One.* **2016,** 11(5): e0155355. doi:10.1371/journal.pone.0155355

Natural vaccine adjuvants and immunopotentiators derived from plants, fungi, marine organisms and insects – Immunopotentiators in Modern Vaccines. Nicola Woods, John Igoli, Najla A Altwaijry, Jonans Tuslimire, Kanidta Niwasabutra, Reinaldo Acevedo, Alexander I Gray, David G Watson, Valerie A Ferro. *Elsevier*. **2016**

ORAL AND POSTER COMMUNICATIONS

Brain changing tubers: Gene expression changes following tuber consumption. 9th Joint Natural Products Conference. July 2016, Copenhagen, Denmark (Poster Communication)

Going backwards to go forwards: The potential of Mediaeval tubers for Future medicines. PSE-CSIC Young Scientist Meeting - Future trends in Phytochemistry in the global era of agri-food and health II. March 2015, Murcia, Spain (Oral Communication)

TABLE OF CONTENTS

LIST OF FIGURES

CHAPTER 1, General Introduction

CHAPTER 2, Collection and Identification of LL tubers

CHAPTER 3*, in vivo* preliminary screening

CHAPTER 4, Soxhlet Extraction and *in vitro* analysis

CHAPTER 5, RNA Sequencing of Hypothalamic Tissue

APPENDIX 4

APPENDIX 5

LIST OF TABLES

CHAPTER 5, RNA Sequencing of Hypothalamic Tissue

APPENDIX 2

LIST OF APPENDICES

LIST OF ABBREVIATIONS

αMSH	α-Melanotropin Stimulating Hormone	HSQC	Heteronucleur Single Bond Coherence
β-ODAP	β-N-oxalyl-L-α-β-diaminopropionic acid	HTS	High-throughput screening
5-HT	5-Hydroxytrytamine (Serotonin)	ICV	Intracerebroventricular
AChE	Acetylcholinesterase	ISSR	Inter Simple Sequence Repeat
AFLP	Amplified Fragment Length Polymorphism	JQS	Johannsen's Quadruple Stain
AgRP	Agouti Related Protein	LC-MS	Liquid Chromatography-Mass Spectroscopy
ALT	Alanine transaminase	LepR	Leptin Receptor
AMPK	AMP-Activated Protein Kinase	LH	Luteinising Hormone
ARC	Arcuate Nucleus	LHA	Lateral Hypothalamus
AST	Aspartate transaminase	LL	*Lathyrus linifolius*
BBB	Blood Brain Barrier	LPS	Lipopolysaccharide
BDNF	Brain Derived Neurotropic Factor	MC3R	Melanocortin 3 Receptor
BW	Body weight	MC4R	Melanocortin 4 Receptor
CAMS	Cell Adhesion Molecules	MCH	Melanin Concentrating Hormone
CART	Cocaine-and-amphetamine-regulated Transcript	MR	Mineralocorticoid Receptors
CCK	Cholecystokinin	MS	Mass Spectroscopy
CDRI	Central Drug Research Institute	MTT	3-(4,5-dimethylthiazol-2-yl)-2,5-diphenyltetrazolium bromide
CNS	Central Nervous System	NCI	National Cancer Institute
COSY	Correlation Spectroscopy	NMR	Nuclear Magnetic Resonance
CRH	Corticotrophin Releasing Hormone	NOESY	Nuclear Overhauser Enhancement Spectroscopy
CVD	Cardiovascular Disease	NPY	Neuropeptide Y
DMH	Dorsomedial Hypothalamus Nucleus	n.s.	Not Significant
DNA	Deoxyribonucleic Acid	NTC	No Template Control
DNP	Dictionary of Natural Products	NTRK3	Neurotropic Receptor Tyrosine Kinase 3
DOPA	3,4-dihydroxyphenylalanine)	NTS	Nucleus Tractus Solitaries
DPP IV	Dipeptidyl Peptidase IV	OXM	Oxyntomodulin
ECGC	Epigallocatechin gallate	PCR	Polymerase Chain Reaction
FFA	Formalin-aceto-alcohol	POMC	Pro-opiomelanocortin
FSH	Follicle-stimulating Hormone	PRL	Prolactin
GC	*Garcinia cambogia*	PTP-1B	Protein Tyrosine Phosphatase 1B
GC-MS	Gas Chromatography-Mass Spectroscopy	PVN	Paraventricular Nucleus

GH	Growth Hormone	PYY	Peptide YY
GHSR	Growth Hormone Secretogogue Receptor	qRT-PCR	Qualitative-Real Time PCR
GIP	Gastric Inhibitory Polypeptide	RAPD	Random Amplified Polymorphic DNA
GIP	Glucose insulinotropic polypeptide	RBGE	Royal Botanic Gardens Edinburgh
GIT	Gastrointestinal Tract	RFLP	Restriction Fragment Length Polymorphism
GL	*Ganoderma lucidum*	RNA	Ribonucleic Acid
GLP-1	Glucagon-like Peptide 1	RNASeq	RNA Sequencing
GnRH	Gonadotropin-releasing Hormone	T2D	Type 2 Diabetes
GO	Gene Ontology	TA	*Trans*-anethole
GPCR	G-protein Coupled Receptors	TB	Toludine Blue
HCA	Hydroxy Citric Acid	TBE	Tris-boric acid Ethylenediaminetetraacetic Acid
HED	Human Equivalent Dose	TM	Traditional Medicine
HFD	High Fat Diet	TNF	Tumour Necrosis Factor
HG	*Hoodia gordonii*	TOCSY	Total Correlation Spectroscopy
HMBC	Heteronuclear Multiple Bond Coherence	TRH	Thyroid Secreting Hormone
HPA	Hypothalamic-Pituitary-Adrenal Axis	UCP-1	Uncoupling Protein-1
HPG	Hypothalamic-Pituitary-Gonadal Axis	VLC	Vacuum Liquid Chromatography
HPLC	High Performance Liquid Chromatography		

MATERIALS AND REAGENTS

Material	Company
α-amylase (Porcine pancreas)	Sigma Aldrich, UK
0.2µm filter	Sigma Aldrich, UK
24 well cell culture plate	Sigma Aldrich, UK
4-methyl umbelliferyl oleate	Sigma Aldrich, UK
4-nitrophenyl α-D-maltohexaside	Sigma Aldrich, UK
5x DNA Loading Buffer	Bioline, UK
6,8-difluoro-4-methylumbelliferyl phosphate (DiFMUP)	Sigma Aldrich, UK
$75cm^2$ cell culture flasks	Sigma Aldrich, UK
96-well cell culture plates	Sigma Aldrich, UK
96-well half area plate (Black)	Grenier Bio-One, UK
ABI StepOne Plus System	Applied Biosystems, UK
Acarbose	Sigma Aldrich, UK
Acetonitrile	Sigma Aldrich, UK
Agarose (Molecular Grade)	Bioline, UK
Anti-bumping granules	BDH, UK
Bead mill (MM301)	Retsch, UK
Bis(4-trifluoromethylsulfonamidophenyl)-1,4-diisopropylbenzine (PTP Inhibitor IV, TFMS)	Sigma Aldrich, UK
Bovine serum albumin	Sigma Aldrich, UK
$CDCl^3$	Sigma Aldrich, UK
Cellosolve	Sigma Aldrich, UK
Cellulose extraction thimbles (single thickness, 123mm)	VWR, UK
Citadel 1000	Thermo Shandon, UK
Clove oil	Sigma Aldrich, UK
Cone ball (stainless steel, 6mm)	Retsch, UK
Crystal violet	Sigma Aldrich, UK
D_2O	Sigma Aldrich, UK
Diethylpyrocarbonate (DECP)	Sigma Aldrich, UK
Dipeptidyl peptidase IV	Sigma Aldrich, UK
Direct-Q 3 Ultrapure water purification system	Millipore, UK

Dithioreitol	Sigma Aldrich, UK
DMEM	Invitrogen, UK
DMEM:F12 Hams	Gibco, UK
DMSO	Sigma Aldrich, UK
DMSO-D_6	Sigma Aldrich, UK
EagleTaq Universal Mastermix	Roche, UK
Ethanol	Sigma Aldrich, UK
Ethidium bromide	Sigma Aldrich, UK
Ethyl acetate (HPLC Grade)	Sigma Aldrich, UK
Ethylene-diamine-tetra-acetic acid (EDTA)	Sigma Aldrich, UK
Exactive Orbitrap Mass Spectrometer	Thermo Fisher Scientific, Germany
Experion DNA 12K analysis kit	Bio-Rad, UK
Experion™ RNA StdSens Analysis kit	Bio-Rad, UK
Fast green	Sigma Aldrich, UK
Foetal bovine serum	Biosera, UK
Formalin	Sigma Aldrich, UK
Formic acid	Sigma Aldrich, UK
Gel Red (stock is 10,000x)	Biotium, UK
GenElute™ Plant Genomic DNA Miniprep Kit (G2N10-1KT)	Sigma Aldrich, UK
GeneSnap imaging program	Syngene, UK
Glacial acetic acid	Sigma Aldrich, UK
Gly-Pro-7-amido-4-methylcoumarin hydrobromide	Sigma Aldrich, UK
GoTaq G2 Colourless Hot Start Master Mix	Promega, UK
GoTaq Green Hot Start Master Mix	Promega, UK
HEPES	Sigma Aldrich, UK
Hexane (HPLC Grade)	Fisher Chemicals
Histoclear	Fisher Scientific, UK
Hyperladder ™ 1kb, 200bp to 10,037bp	Bioline, UK
Hyperladder™50bp, 50bp to 2000bp	Bioline, UK
INGENSUS UV imaging system	Syngene, UK
Iodine	Sigma Aldrich, UK
KOD Hot Start Polymerase	EMD Millipore, UK
Lecia EG1140 H	Lecia Microsystems, UK

Lecia RM2125RTF microtome	Lecia Microsystems, UK
L-Glutamine	Life Technologies, UK
Lipopolysaccharide (LPS) (L2630)	Sigma Aldrich, UK
Methanol (HPLC Grade)	VWR, UK
MicroAmp® Fast Optical 96-well reaction plates	Thermo Fisher Scientific, UK
Microscope	Olympus, Japan
MyTaq Polymerase	Bioline, UK
Nanodrop™ Spectrophotometer (2000C)	Thermo Scientific, UK
New born calk serum	Invitrogen, UK
Non-essential amino acids	Life Technologies, UK
Orange G	Sigma Aldrich, UK
Orlistat	Sigma Aldrich, UK
P32/98	Enzo, UK
Pancreatic lipase (type II from porcine pancreas)	Sigma Aldrich, UK
Paq5000	Agilent, UK
Paraffin wax	Sigma Aldrich, UK
Penicillan/Streptomycin	Life Technologies, UK
Phorbol 12-myristate 13-acetate (PMA) (P8139)	Sigma Aldrich, UK
Phusion High Fidelity DNA Polymerase	New England Biolabs, UK
P-nitrophenyl-α-D-glucopyranoside	Sigma Aldrich, UK
Polysine microscope slides	Thermo Scientific, UK
PowerUp™ SYBR™ Green Master Mix	Applied Biosystems, UK
Primus96 PCR machine	MWG Biotech, UK
Protein tyrosine phostphatase	Sigma Aldrich, UK
Q5 High Fidelity DNA Polymerase	New England Biolabs, UK
Resazurin sodium salt	Sigma Aldrich, UK
Reverse Phase C18 Column	Hichrom, UK
RNeasy Midi Kit	Quiagen, UK
RNeasy Mini Kit	Quiagen, UK
RPMI 1640	Lonza, UK
Safranin O	Sigma Aldrich, UK
Sodium acetate	Sigma Aldrich, UK
Sodium chloride	Sigma Aldrich, UK
Sodium phosphate dibasic heptahydrate	Sigma Aldrich, UK
Sodium phosphate monobasic	Sigma Aldrich, UK

Sodium pyruvate	Thermo Fisher, UK
Tertiary butyl alcohol	Sigma Aldrich, UK
Testosterone ELISA Kit	Alpha Diagnostic, UK
Tetro cDNA Synthesis Kit	Bioline, UK
TLC grade silica [Silica gel 60H]	Merck, UK
TNF-α ELISA DuoSet (DY201)	R&D Systems, UK
Toluidine Blue O	Sigma Aldrich, UK
TOX8 *in vitro* Toxicology Kit	Sigma Aldrich, UK
Trans-anethole (TA)	Sigma Aldrich, UK
TripLE Express	Life Technologies, UK
Tris-boric acid-ethylenediaminetetraacetic acid (TBE)	Gibco, UK
Tris-HCl	Sigma Aldrich, UK
Xylol	Sigma Aldrich, UK
Yeast α-glucosidase	Sigma Aldrich, UK

ABSTRACT

Obesity and undernourishment are two extremes with a common underlying aetiology – food intake and hunger. Both of these issues are becoming increasingly problematic worldwide, therefore there is a need to develop new therapies to address such issues. Investigation of a forgotten, mediaeval Scottish plant may hold the key to combatting both. *Lathyrus linifolius* (LL) tubers were once used as an appetite suppressant in times when food was scarce. Additionally, they are thought to be able to quench thirst, and increase alertness. The aims of this study were: 1) to collect and identify these tubers and develop a method using ISSR-PCR to confirm their identity for future commercialisation; 2) investigate the *in vivo* effects of the tuber in terms of food intake, water intake, body weight and physical activity; 3) identify possible active components in the tuber and assess the biological activity of crude extracts obtained via Soxhlet extraction; and, 4) re-assess the *in vivo* effects by conducting RNA sequencing on hypothalamic tissue. LL tubers had no effect on food intake, water intake, body weight or physical activity *in vivo*. However, evidence was generated in this study which suggests the tuber had an effect at gene expression level within the hypothalamus, which is the primary centre for appetite control. Specifically, genes involved in the hypothalamic-pituitary-adrenal axis (HPA) were effected including growth hormone (GH), lutinising hormone (LH), serotonin (5-HT), brain-derived neurotropic factor (BDNF), kisspeptin, kisspeptin receptor, prolactin (PRL), adiponectin, peptide YY (PYY) and neurotrophic receptor tyrosine kinase 3 (NTRK3). The cause of the effects are unknown, however it may be due to multiple compounds present within the tuber. Investigation of such compounds led to the identification of a novel compound, lathyrosaponin A. The biological activity of this compound remains unknown, however, the crude extract from which it was identified showed significant ($P<0.01$) inhibition of α-glucosidase. The results of this study confirm possible appetite suppressing effects of LL tubers, which correlate with their mediaeval use. Going backwards to investigate plants once used as human therapies may be the key to combating worldwide issues today.

1. CHAPTER 1, GENERAL INTRODUCTION

1.1. Introduction

Evolution has influenced many organisms in the world to accumulate body fat quickly in times of nutritional excess to allow them to withstand periods of famine. Going back in time, food was not always available as it is today, thus the evolution of organisms to cope with periods without food allowed their survival (Albrecht, 2017). In the present day, this is no longer the case. In many countries, there is a large excess of food available and excessive eating often occurs which can lead to obesity. In 2014, more than 1.9 billion adults over the age of 18 were classed as overweight, and 600 million of these were classed as obese. These figures have doubled since 1980, which highlights that this is a growing problem. Obesity is the fifth biggest killer worldwide and it is a global epidemic (Bornstein *et al.*, 2006). Being obese increases an individual's risk of developing various other pathological conditions including type 2 diabetes (T2D), cardiovascular disease (CVD), stroke and hypertension to name a few. Obesity conclusively results from an imbalance between energy intake and energy expenditure, which leads to an accumulation of body fat. The cause of this imbalance could be manifold with various environmental, genetic and lifestyle factors involved.

At the opposite end of the scale, undernourishment is also a worldwide problem. The United Nations Food and Agricultural Organisation estimated that approximately 795 million people worldwide were suffering chronic undernourishment between 2014 and 2016. The majority of these people live in developing countries, where the figures equate to 1 person in every 8. Undernourishment is caused by a lack of food, typically due to periods of famine or due to conflict. Obesity and undernourishment are two extremes with a common underlying aetiology, food intake and hunger. With the world population constantly rising (estimated to reach 9.7 billion by 2050 (Melorose *et al.*, 2015) these problems will continue to grow therefore there is a need to develop therapies in an attempt to address such issues.

With the advancement of many of today's drugs being inspired by natural products and traditional medicine, the aim of this project was to investigate the potential of

Lathyrus linifolius (LL, a forgotten, mediaeval Scottish plant) to address the issues above. Based on the effects of this plant following human consumption (information obtained by Dr Brian Moffat, Appendix 1) it is speculated that the tubers of this plant have the ability to regulate appetite, food intake and hunger.

1.1.1. Natural Product Research

The first written reports of medicinal applications for plants dates back as far as 2900 BC where it is estimated that around 1000 plant derived medicines existed (Atanasov *et al.*, 2015). Many of the formulations and herbal remedies used in these medicinal practices have been passed down generations in various cultures and now form traditional medicine (TM) as we know it today. The use of plants in TM is due to the presence of biologically active compounds (natural products), which subsequently give rise to the plants 'healing' properties.

Until the 18th century, plants were used in medicine based on indigenous knowledge rather than the pharmacological activities or active compounds present. Following the investigation of foxglove by William Withering (Cox and Balick, 1994; Withering, 1785), and poisonous herbs such as aconite and colchicum by Anton von Storck (Sneader, 2005), the need for clinical investigation of medicinal plants became apparent. This rationale led to the investigation of a number of plants, both used and not used in TM. From the 19th century onwards, many natural products were isolated from plants including nicotine, caffeine, quinine, codeine, cocaine and capsaicin. This trend continued and the development of high-throughput screening studies emerged to identify possible candidates for drug development. This approach is used by the National Cancer Institute (NCI) and the Central Drug Research Institute (CDRI) in India. NCI has developed various drugs using this approach including paclitaxel, camptothecin and calanolide A (Fabricant and Farnsworth, 2001). Today, it is thought that over 1000 new leads, based on natural products, are currently in clinical development. From 1981 to 2014, about 40% of new drugs were developed from natural products (Newman and Cragg, 2016). This statistic increases with regard to anti-infective and anti-cancer drugs, where the proportion of drugs developed from

natural products rises to about two-thirds (Kingston, 2011). Many scientists have suggested that the key to moving forward and making a significant difference in the world of drug discovery is in learning from past medicinal practises (Patwardhan and Mashelkar, 2009). Reverse pharmacological approaches are now being employed to look at TM to identify biologically active natural products with the potential of being developed into new medicines. Looking back at the traditional usage of LL to guide the development of future therapies may be the key to addressing the worldwide problems of obesity and undernourishment due to famine.

1.1.2. *Lathyrus*. L genus

Lathyrus L. is a genus of flowering plants containing approximately 160 species (Allkin *et al.*, 1986; Kenicer *et al.*, 2005) distributed throughout the northern hemisphere in temperate regions. Also known as the 'Sweet Peas' and 'Vetchlings', *Lathyrus* forms the largest genus within the Fabeae tribe of the Leguminosae family (Kenicer *et al.*, 2005). The Leguminosae, or Fabaceae family, is found on 12-15% of the worlds' arable land and accounts for approximately 27% primary crop production worldwide (Schaefer *et al.*, 2012), thus this family is very important economically. Members of the *Lathyrus* genus include various major and minor crops for food and fodder, agricultural weeds, dune stabilisers, soil nitrifiers and ideal organisms of ecological and genetic research (Kenicer *et al.*, 2005). Most *Lathyrus* members are mesophytes, however, a small number of species are typical of alpine, shoreline and drought prone areas (Kenicer *et al.*, 2005).

One of the most important members of the *Lathyrus spp.*, economically, is *L. sativus* (Grass Pea), which is an annual legume crop that has a unique ability to grow in poor soil without fertiliser and has the capability to resist infections and pests (Ghosh *et al.*, 2015). The Grass Pea is a high yielding plant which is commonly used as a cheap source of protein for human and animal consumption (Khandare *et al.*, 2013). It is widely consumed in areas of Africa and Asia as well as Pakistan, China and Russia.

One of the main concerns with the consumption of *Lathyrus* species is the development of a characteristic motor system condition called neurolathyrism (Yan *et al.*, 2006), generally associated with the consumption of the seeds and foliage of *L. sativus* as a staple diet for more than 3 months, particularly in times of famine. It causes crippling paralysis of the lower limbs and is thought to be a result of the high content of β-N-oxalyl-L-α-β-diaminopropionic acid (β-ODAP, Figure 1.1) (Khandare *et al.*, 2013), a non-protein amino acid. The prevalence of neurolathyrism is thought to be at its highest during extreme situations such as famine and drought (Singh and Rao, 2013). Food supplies would be minimal thus people would over-consume the seeds and foliage of *L. sativus* for months at a time leading to the development of this debilitating disease. When consumed as a minor component of the diet, β-ODAP appears to be tolerated with no known adverse effects (Yan *et al.*, 2006).

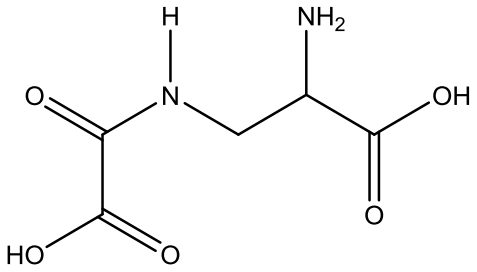

Figure 1.1: Structure of neurotoxic β-ODAP.

Symptoms of neurolathyrism include pain or cramps in the legs or lumbar spine, weakness of the lower extremities with the development of spastic movements of the legs (Khandare *et al.*, 2013). These symptoms are the result of degenerative changes in cells present in the motor cortex and their axons in the corticospinal tracts. Ultimately, these constitute the central nervous system (CNS) pathway for muscle function regulation.

Although β-ODAP is most commonly associated with *L. sativus*, it has been shown to be present in the seeds of 21 other *Lathyrus* species (mainly *L. cicera* and *L. clymenum*) as well as 17 species of *Acacia* and 13 species of *Crotalaria*. Furthermore, it is said to

be present in older ginseng roots of varying species including *P. quinquefolius, P. notoginseng* and *P. ginseng* (Yan *et al.*, 2006). Moreover, several other toxic substances have been isolated from seeds of *Lathyrus* species. These include: β-(N-γ-glutamyl)-aminopropionitrile – the γ-glutamyl derivative of β-aminopropionitrile (BAPN) which is found in *L. odoratus* (sweet pea), *L. hirsitus, L. roseus* and *L. pusillus;* and, l-2,4-diaminobutyric acid (DABA*)* which is present in the seeds of *L. sylvestris* and *L. latifolius* (Yan *et al.*, 2006).

1.1.3. *Lathyrus linifolius* (LL)

LL is a perennial plant which grows in acidic soil in Scotland. The stem of this plant can grow to 15-30cm, and it has alternate leaves with short winged stalks and large stipules. It produces long red/brown seed pods containing up to 10 seeds. This plant flowers for around two weeks in May-June where the flowers are a bright pink colour. Following this, the flower colour changes from pink to blue/purple to yellow/brown (Figure 1.2 A and 1.2 B, respectively). The leaves have no tendrils, unlike its close relative *L. alpestris,* which appears almost identical to LL, and they can either be long and thin or short and wide – the differences in leaf morphology may be a result of the differences in environmental factors such as light availability. Figures 1.3 A and 1.3 B show herbarium specimens from two different locations in Scotland from which the differences in leaf morphology can be seen. Additionally, this plant produces brown, nodular tubers which vary in size depending on the age of the plant. They can form a large intricate network underground if they remain undisturbed, sometimes reaching 50+ tubers in one network.

Figure 1.2: Photographs of *L. linifolius* (LL). Both pictures were taken by Nicola Woods on 20th May 2014 at Linn Dean Nature Reserve. The flowers of LL appear as a crimson pink colour (A) for around three weeks in May, following this the flowers turn a yellow/brown colour (B).

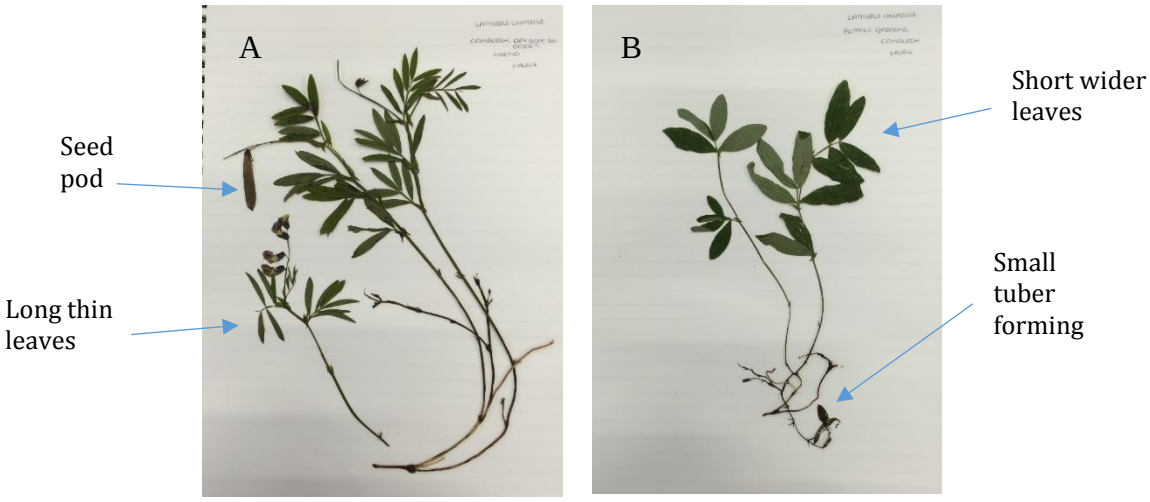

Figure 1.3: Herbarium specimens of LL. (A) Herbarium specimen taken from an area of land in Hillend, Edinburgh. (B) Herbarium specimen taken from the Edinburgh Botanic Gardens (with permission from Greg Kenicer), where the plant grew in a shaded area.

1.1.4. Taxonomic Classification of *L. linifolius*

The taxonomic classification of LL is shown in Table 1.1 below.

Table 1.1: Taxonomic classification of *L. linifolius* ("National Biodiverstiy Network 2013b. Lathyrus linifolius (Reichard) Vassler [Bitter-vetch]," n.d.)

Kingdom	Plantae
Phylum	Tracheophyta
Class	Magnoliopsida
Order	Fabales
Family	Fabaceae
Subfamily	Faboideae
Tribe	Fabeae
Species	*Lathyrus linifolius* (Reichard) Bässler

1.1.5. Nomenclature

The original name for LL was *Orobus tuberosus* ("Tropicos.org. Missouri Botanical Garden.," n.d.), although there are many synonoms of this plant species including: *L. montanus* Bernh.; *L. linifolius* var. *montanus* (Bernh.) Bässler; *O. tuberosus* L.; *O. linifolius* Reichard; *L. tuberosus* auct., non L. ("NBN Gateway - Taxon - Lathyrus linifolius (Reichard) Bässler [Bitter-vetch]," n.d.). There are also various common names for LL such as bitter vetch, caperoilie, carameile, carmele, carmeil, carmile, carmylie, charmelic, corr, Cormeille, griapperts, heath pea, karemyle, kipper nut, knapperts, liquor-knots, liquory-knots, mouse pea (seeds), napperty, napple, thetch and wood pea (Brenchley, 1920; Robertson, 1767-1771; Johnston, 1853; Pratt, 1899). LL must not be confused with wood bitter-vetch (*Vicia orobus*, or *O. sylvaticus*) (Hooker, 1821), which does not produce tubers. However, in addition to the similarities in their common name, its morphology also closely resembles that of LL. Its' flowers are white with purple veins, similar in shape to LL.

1.1.6. Going backwards: Mediaeval uses of LL

A recent excavation at Soutra Aisle, near Edinburgh, identified the remnants of LL tuber in the drains of the old mediaeval hospital. This excavation was led by Dr Brian Moffat, an expert on mediaeval remedies. Soutra Aisle was once home to the biggest mediaeval hospital in Scotland, and it is thought that the monks who inhabited the hospital used LL tubers to repel hunger and thirst. Dr Moffat regularly consumes LL tubers himself and described definite appetite suppressing abilities (see Appendix 1). Dr Moffat suggests the tubers have a sweet but sour taste, similar to liquorice or aniseed, and that after eating a small pea-sized amount daily, one would *"not eat, not want to eat and not miss eating for weeks and even into months"*. Dr Moffat also suggested that soldiers of the Scottish army regiments who were in training were educated on how to identify and collect these tubers if they were to become lost or in hiding in the wilderness. This knowledge came as the result of conversations with military veterans. When queried about the active constituents of LL tubers, Dr Moffat surmised that it is believed to be a compound known as *trans*-anethole. This knowledge was based on Dr Moffat's own research and through conversation with other scientists (see Appendix 1). Moreover, Dr Moffat gave insight into the depth of the history behind the use of these tubers, documented in Appendix 1.

According to the literature, the tubers of LL were traditionally used in late medieval times (ca. 1700s) to fend off hunger and thirst, to prevent intoxication, and as a drink flavouring. It is believed that these tubers were harvested in the winter, perhaps when crops had failed and food provisions were low. These tubers were spoken of in the late 1600s and early 1700s, when it is also recorded in historical text that there was a great famine in Scotland known as the 'Ill Years' where it is estimated that between 5-15% of the population died. In some areas, such as Aberdeenshire, this figure reached up to 25%. One of the main causes of this famine was four years of failed harvests (1695, 1696, 1698 and 1699) (Cullen, 2010). The use of these tubers may have been vital at this time in history, although there are no publications which indicate correlations between low mortality rates in specific areas with the presence and use of the tuber.

The earliest suggested use of LL tubers is thought to be by Julius Caesar who referred to the tubers as 'Charra'. It is thought that the tubers were fed to Valerius' soldiers in 48BC during the battle of Dyrrhachium (Albania). However, there are some doubts about the correct identification of the plant used. It has also been suggested that the Roman historian, Cassius Dio, referred to the plant when describing the Caledonians (indigenous people of Scotland during the Iron Age and Roman era). A quote, translated from Greek, describes the use of 'bark and roots' (LOEB Classical Library, n.d.):

> *"They can endure hunger and cold and any kind of hardship; for they plunge into the swamps and exist there for many days with only their heads above water, and in the forests they support themselves upon bark and roots, and for all emergencies they prepare a certain kind of food, the eating of a small portion of which, the size of a bean, prevents them feeling either hunger or thirst."*

It is speculated that the plant Cassius refers to is LL. Moreover, according to Scottish physician, Dr Robert Sibbald (1641-1722), joint founder of the College of Physicians of Edinburgh and of the Botanic Gardens, the plant tubers were regularly used by King Charles II to keep his mistresses slim. Dr Sibbald mentioned this plant more than any others in his book called 'Provisions for the poor in time of dearth and scarcity'. He refers to LL on numerous occasions as "*Herba Scotica Miraculosa*" – the miraculous Scottish Herb. Dr Sibbald was very keen on medicinal and health promoting plants and in his book 'Memoirs of my Lyfe', he refers to this passion at various points:

> *"I resolved to make it part of my studie to know what animalls, vegetables, mineralls, and substances cast up by the sea, were found in this country, yt might be of use in medicine, or other artes useful to human lyfe, and I began to be curious in searching after ym and collecting ym, which I continued to do so ever since."* (page 65)

> *"…It was by his incouradgement, that to the inquirie after the naturall products of the Kingdome, I added the inquyrie after what concerned ane exact geographicall description of it, and by his procurement, upon his informing King Charles the 2nd, what progresse I had made in ys matters, his Majestie gave me a patent to be his geoprapher for the kingdome of Scotland, and another to be his Physitian there, and, wt all, gave me his commands to publish the natural history of ye Country, and the geographical description of the kingdome."* (page 74)

The earliest date mentioned in Flora Celtica (which documents the evolving relationship between people in Scotland and plants) is 1767 where it was noted in James Robertson's Tour of the Highlands (1767-1771) that it was eaten by the people of Skye:

> *"[The inhabitants of Skye] eat the roots of Orobus tuberosus or as they call it Cart Mel ie a large knot of Honey, when they are thirsty and faintish."*

> *"The natives eat the root of the Orobus Tuberosus, or as they call it Charmelic, it is said to be aromatic and is eaten before drinking Strong Liquors to prevent intoxication."*

LL tubers are also mentioned in the book "History of the County Palatine and Duchy of Lancaster by Edward Baines (Baines, 1836) where its' uses are described:

> *"They are accustomed to brave hunger, cold, and all kinds of toil…They prepare a certain kind of food for all occasions, a piece of which, of the size of a bean, prevents their feeling hunger or thirst."*

The author clearly states that Sir Robert Sibbald believes this "food" to be the roots of *Orobus tuberosus* (LL), or "karemyle" as known by the Highlanders. Additionally, the taste is referred to as 'like-liquorice".

A few years later, in 1843, William Baxter published another book which mentions LL tubers. In his book "British Phaenogamous Botany, or Figures and Descriptions of the Genera of British Flowering Plants" it is mentioned that the tuberous roots of LL, referred to as Cor-meille by the Highlanders, were used to keep hunger at bay. This book also refers to the way in which these tubers were eaten

> *"… they dry and chew, as our people do tobacco, to give a better relish to their liquor… by use of them they are able to repel hunger and theist for a long time".*

Since then, this plant is mentioned several times throughout mediaeval literature (See Appendix 2) where people have spoken of its' uses, although it is thought that since the introduction of the potato to our diet in the 18th century, the use of this plant diminished rapidly and is now largely forgotten.

1.1.7. Scientific research conducted using LL

There are over 80 hits for the genus 'Lathyrus' in the Dictionary of Natural Products (a comprehensive database on natural products – search carried out in 2015), however, there were no hits for LL at the time of searching. The synonyms of LL were also searched on the DNP with one hit appearing for *L. montanas* - 7-O-β-D-glucopyranoside (oroboside), a derivative of orobol. Oroboside was first isolated from the leaves of LL in 1939 by a pharmacist named Camille Charaux (Charaux and Rabate, 1939). Since then, it has been identified in a number of plants and microorganisms including the plant species *Arctium lappa* (Chinsembu and Hedimbi, 2010), *Lagerstroemia speciose* L. (Choi *et al.*, 2010), *Sedum lineare, Baptisia spp., Lupinus spp* (Southon, 1994). *Thermopsis spp* (Zhou *et al.*, 2011), and a fungal strain (*Tritirachium sp*. F3707) (Kohyama *et al.*, 1994).

Orobol is thought to be a hypotensive agent and an inhibitor of DOPA (3,4-dihydroxyphenylalanine) decarboxylase, histidine, phosphatidylinositol kinase,

tyrosine kinase and 15-lipoxygenase. DOPA-carboxylase inhibitors prevent the synthesis of dopamine from L-DOPA. The combination of L-DOPA and a DOPA decarboxylase inhibition is the classic treatment for patients with Parkinson's disease. However, they are known to cause diverse side effects as a result of irreversible, non-specific binding (Ren *et al.*, 2014). Inhibitors of DOPA decarboxylase have also been found in other plant species including *Euonymus glabra* Roxb (Ren *et al.*, 2014). Moreover, phosphatidylinositol kinase inhibitors (including wortmannin which was isolated from *Penicillium wortmannin* (Liu *et al.*, 2009)) and tyrosine kinase inhibitors such as quercetin (a flavonoid widely found in nature) and genistein (an isoflavone isolated from *Genista tinctoria*) (Glossmann *et al.*, 1981; Levitzki and Gazit, 1995)) have been widely researched as potential candidates for the treatment of cancer. In contrast, LL has not been studied for such bioactivity despite the possible presence of orobol and/or its' derivatives.

In 1959, Pecket studied the flower colour variations within the Lathyrus genus and identified three anthocyanin compounds from the flowers of LL *(L. montanus)*. These were delphinidin, petunidin and malvidin. Anthocyanin compounds are known to have antioxidant activity, as well as being commonly used as colouring agents in the food and drink industry. Additionally, Robeson and Harborne (1980) identified phytoalexins in leaf/cotyledon samples from a number of different Lathyrus species – LL was found to contain trace amounts of four phytoalexins: maackain, variabillin, medicarpin and pisatin. Maackain, medicarpin and pisatin are known anti-fungal compounds (Martínez-Sotres *et al.*, 2012), while variabillin is said to inhibit phospholipase A_2 and have anti-inflammatory activity (Escrig *et al.*, 1997). Although there is minimal research on this particular plant species, the genus of Lathyrus is widely studied in terms of chemical composition and biological activity (Table 1.2).

Table 1.2: References of papers published on the *Lathyrus* genus

Reference	Species	Research
Fratianni *et al.*, 2014	*L. sativus*	Polyphenol composition and antioxidant activity
Pastor-Cavada *et al.*, 2010	*L. clymemum and L. annuus*	Chemical composition and functional properties of protein isolates
Mullan *et al.*, 2009	*L. cicera*	Chemical composition, nutrient content and digestible amino acid analysis
Chavan *et al.*, 2003	*L. maritimus*	Identification of phytochemical components
Porter *et al.*, 1999	*L. odoratus*	Volatile compounds of floral fragrances from Sweet Pea
Shahidi *et al.*, 1999 and Shahidi *et al.*, 2001	*L. maritimus*	Chemical composition; nutrient distribution and phenolic antioxidants
Marles and Farnsworth, 1995	*L. palestris, L. sativus, L. japonicus*	Anti-diabetic activity of various plants and their active constituents
Sousa-Cavada *et al.*, 1986	*L. cicer, L. aphaca and L. articulatus*	Amino acid sequencing
Fuchs *et al.*, 1984	*L. odoratus*	Isolation of stress metabolites

In 2006, a limited company was established called Heath Pea Ltd. which gained fame by advertising a new potential 'slimming aid'. This 'slimming aid' was in fact LL tubers – (http://www.scotsman.com/news/new-bloom-for-heath-pea-as-a-slimming-aid-1-1412434; http://www.independent.co.uk/life-style/health-and-families/health-news/medieval-appetite-suppressant-could-be-new-slimming-aid-504908.html). However, there have been no publications or recent activity by this company since; thus it is assumed the development of the 'slimming aid' was not successful. This company were also in contact with Dr Brian Moffat, who had initially supplied the tubers.

1.1.8. The Regulation and Control of Appetite

The physiological processes which regulate food intake, as well as energy expenditure, are highly complex and involve interplay from the CNS and numerous organs involved in energy homeostasis (Woods and D'Alessio, 2008). There are over 40 different orexigenic and anorexigenic hormones, enzymes, neuropeptides, signalling molecules and their receptors involved in appetite and satiety regulation (Yuliana *et al.*, 2011). In order to maintain a stable body weight (BW) over time, we must continually balance food intake and energy expenditure (Wynne *et al.*, 2005).

Central neural circuits in the brain and target peripheral tissues regulate appetite and body weight in a coordinated way which includes the involvement of positive and negative feedback mechanisms. Peripheral tissues include gastrointestinal tract (GIT), adipose tissue and liver (Yuliana *et al.*, 2011). Figure 1.5 shows an overview of pathways involved in energy balance and the regulation of food intake linking both neural circuits and peripheral tissues.

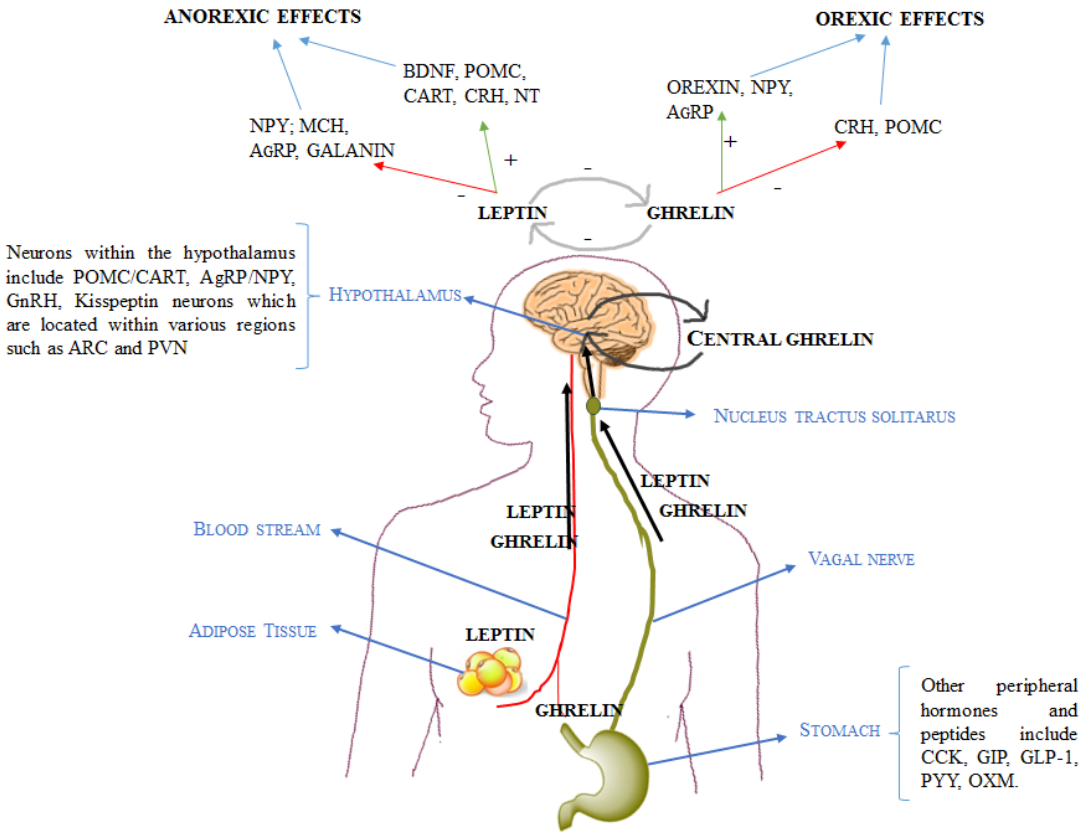

Figure 1.5: Pathways which may be involved in energy balance relating to leptin and ghrelin. AgRP, Agouti-related protein; BDNF, brain derived neutrophic factor; CART, cocaine-and amphetamine-regulated transcript; CCK, cholecystokinin; CRH, corticotropin releasing hormone; GIP, gastric inhibitory polypeptide; GLP-1, glucagon-like peptide 1; GnRH, gonadotropin-releasing hormone; MCH, melanin concentrating hormone; NPY, neuropeptide Y; OXM, oxyntomodulin; POMC, pro-opiomelanocortin; PYY, peptide YY. Adapted from Klok *et al.*, 2007.

Over the past three decades, research that has focused on rodent and human genetics, as well as molecular and physiological research, has given insight into the main orchestrators of food intake and energy homeostasis. Monogenic alterations in leptin, 5-hydroxytrytamine (5-HT; serotonin), melanocortin, and BDNF have highlighted the importance of these specific pathways in the regulation of normal food intake and

energy balance. Additionally, the importance of various gut hormones and peptides in the regulation of food intake and energy homeostasis has come to light including insulin, ghrelin, GLP-1, CCK, PYY to name a few.

1.1.8.1. Central Appetite Regulation

Central neural circuits and target peripheral tissues regulate appetite and BW in a coordinated way, which includes the involvement of a negative feedback mechanism, the main component of which involves the synthesis and release of peripheral hormones involved in metabolism. The hormones target hypothalamic nuclei which control appetite such as the lateral hypothalamus (LHA), the ventromedial hypothalamic nucleus (VMH), the dorsomedial hypothalamic nucleus (DMH), the paraventricular nucleus (PVN) and the arcuate nucleus (ARC) (Dwarkasing *et al.*, 2015). Figure 1.6 highlights the complexity of the hypothalamus with a schematic diagram showing the relationship of each of the nuclei.

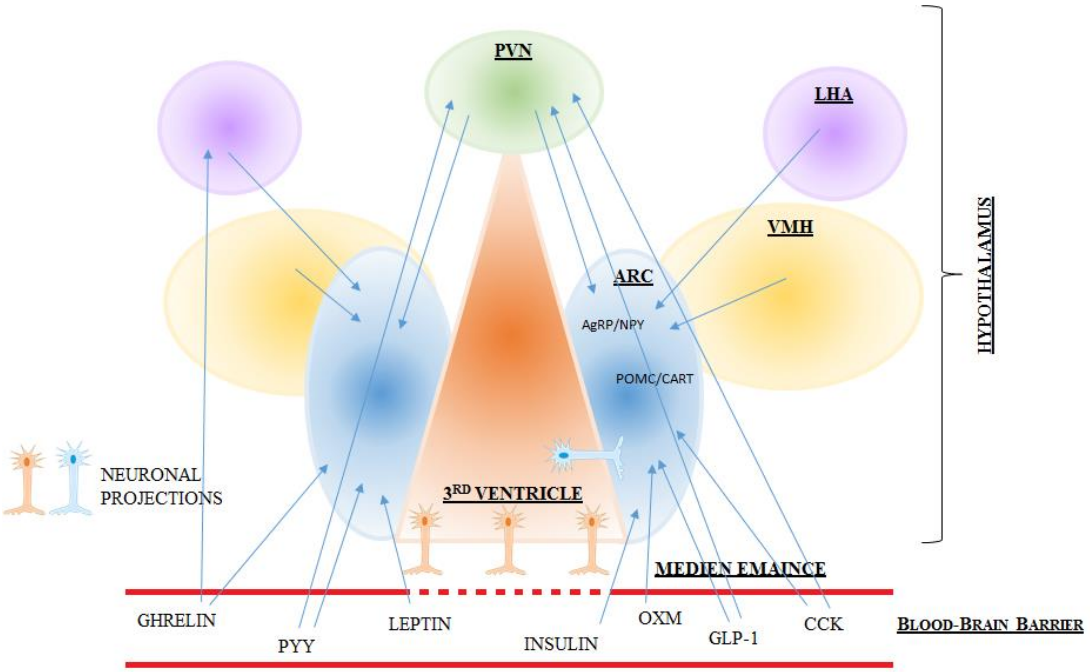

Figure 1.6: Schematic diagram of hypothalamic nuclei. AgRP, agouti related protein; ARC, arcuate nucleus; CART, cocaine- and amphetamine-regulated transcript; CCK, cholecystokinin; GLP-1, glucagon-like peptide 1; LHA, lateral hypothalamus; NPY, neuropeptide Y; OXM, oxyntomodulin; POMC, pro-opiomelanocortin; PVN, paraventricular nucleus; PYY, peptide YY.

The ARC is a privileged site situated adjacent to the median eminence (Yu and Kim, 2012). The median eminence is a circumventricular organ with a defective blood brain barrier (BBB), thus hormones and signalling molecules circulating in the blood can pass to the ARC without crossing the BBB, through semi-permeable capillaries. Additionally, the ARC surrounds the third cerebroventricle (3rd Ventricle or 3V) so hormones and signalling molecules in the cerebrospinal fluid can also pass into the fluids of the ARC. As a result of its anatomical features, the ARC is thought of as the primary nutrient sensor in the hypothalamus (Yu and Kim, 2012). Furthermore, the neurons in the ARC form complex neuronal circuits with second-order neurons in the PVN, DMH, VMH and LH as well as extra-hypothalamic neurons including the

nucleus tractus solitaries (NTS) of the brain stem (Lopaschuk *et al.*, 2010). The PVN is adjacent to the superior part of the 3V and is the primary site of CRH and thyrotropin secreting hormone (TRH). The PVN is adequately supplied with neuronal projections from the ARC, thus plays an important role in the integration of nutritional signals with the thyroid and the hypothalamus-pituitary-adrenal axis (HPA) (Neary *et al.*, 2004).

Within the ARC and PVN, there are numerous neuronal populations which influence energy homeostasis and therefore influence food intake. There are two main populations within the ARC which have opposing effects on feeding behaviour - the anorexigenic neurons which co-express POMC and CART and the orexigenic neurons which co-express NPY and AgRP (Yu and Kim, 2012). The activity of these neuronal populations is modified by multiple neuropeptides and hormones from the periphery (Sohn, 2015). Kisspeptin neurons are also found within the ARC as well as the PVN. Although primarily involved in reproduction and fertility, kisspeptin neurons are closely involved in energy homeostasis (Fu and van den Pol, 2010).

Neurons expressing POMC, of which 90% co-localise with neurons expressing CART, respond to satiety factors circulating in the blood. Upon activation, these neurons promote a negative energy balance through increased energy expenditure and decreased food intake (Lopaschuk *et al.*, 2010). POMC deficiency in humans leads to severe, early-onset obesity and adrenal insufficiency (Krude *et al.*, 1998). POMC is a precursor to the melanocortin family, and is increased following a meal and decreased when fasting. The main melanocortin involved in energy homeostasis is α-melanotropin stimulating hormone (αMSH) which is the primary endogenous agonist of MC3R (melanocortin 3 receptor) and MC4R (melanocortin 4 receptor) in the hypothalamus (Lopaschuk *et al.*, 2010). In 2000, Benoit *et al.* identified that central administration of an MC4R agonist (Ro27-3225) was able to suppress food intake in rats (Benoit *et al.*, 2000). Furthermore, an MC4R antagonist (Ro27-4680) had opposing effects as it increased food intake 4h post administration. Deletion of MC4R in mice has been shown to result in hyperphagia and obesity, thus underlying the

importance of this receptor in the regulation and control of appetite (Huszar *et al.*, 1997). As with POMC neuronal expression, CART expression is also responsive to nutritional status and is decreased during fasting and increased following consumption of a high energy meal (Rogge *et al.*, 2008). CART has been reported as a hypothalamic satiety factor (Kristensen *et al.*, 1998). In the ARC, CART mRNA levels are regulated by leptin and injections of CART peptide into the nucleus accumbens inhibits feeding in rodents (Jean *et al.*, 2007). Furthermore, injection into the ARC has demonstrated the involvement of CART in the modulation of energy expenditure as it results in an increase in mRNA for uncoupling protein-1 (UCP-1, or thermogenin) in brown adipose tissue (Lau and Herzog, 2014). Furthermore, studies of human populations have implicated CART in the regulation of food intake. One such study identified a missense mutation in CART in obese members of a family in Italy. Moreover, polymorphisms in the 5' end of the CART gene have been linked with obesity (Hill, 2010).

NPY has been shown to be an important physiological regulator of BW through its effects on energy expenditure and food intake. NPY-expressing neurons express receptors for a wide range of circulating satiety promoting factors and activation of such neurons influences a positive energy balance associated with decreased energy expenditure and increased food intake (Lopaschuk *et al.*, 2010). The NPY pathways are activated by processes associated with energy expenditure, including long-term physical exercise, loss of high energic substances such as glucose, lactation, and fasting. As a result, NPY is raised which results in increased appetite and food intake and decreased energy expenditure (Kokot and Ficek, 1999). Stanley *et al.* (1984) demonstrated that direct injections of NPY into the PVN of the hypothalamus caused a dose-dependent increase in food intake, even when food was presented up to 4h after injection. Furthermore, in genetic models of obesity such as *ob/ob* and *db/db* mice and Zucker fatty rats, hypothalamic NPY is increased (Minor *et al.*, 2009). AgRP is co-secreted with NPY and, in contrast to NPY which is expressed widely in the CNS, AgRP is only expressed in the hypothalamus (Lopaschuk *et al.*, 2010). AgRP is an antagonist and inverse agonist of receptors in the melanocortin system (MC) including MC3R and MC4R. Similar to NPY, AgRP expression is enhanced during fasting.

1.1.8.2. Peripheral and Gastrointestinal Hormones

Two peripheral hormones which play an important role in the regulation of food intake and energy balance are leptin and ghrelin.

Leptin is expressed and secreted mainly by white adipocytes, but it is also found in various other tissues such as the stomach, skeletal muscle, ovaries, testes, placenta, pituitary gland (Jin *et al.*, 1999) and lymphoid tissue (Bado *et al.*, 1998; Jin *et al.*, 1999; Park and Ahima, 2014; Senaris *et al.*, 1997). Circulating levels of leptin are directly proportional to fat mass and thus leptin levels reflect the status of long term energy stores. The idea that circulating signals generated in response to fat mass could influence food intake and energy expenditure was first proposed in the 1950s (Kennedy, 1950). Subsequently, in 1994, the *ob* gene was identified by Zhang *et al.* (1994) following studies of naturally occurring obese mice. These mice were found to have a mutation in the *ob* gene which caused loss of function of this gene, now known as the leptin gene. Additionally, a second strain of naturally occurring obese mice were found to have a mutation in the *db* gene (Yeo and Heisler, 2012) which encodes the receptor for leptin (LepR). Both groups of mice displayed similar phenotypes consisting of severe and early onset obesity, extreme resistance to insulin, decreased energy expenditure, hyperphagia and infertility (Magni *et al.*, 2000). It was identified that central and peripheral administration of leptin results in a dose-dependent reduction in BW as well as a reduction in food intake and an increase energy expenditure (Halaas *et al.*, 1995; Pelleymounter *et al.*, 1995) in wild type mice. It also causes a reduction in weight in *ob* deficient mice. However, there was no effect in *db* deficient mice (Halaas *et al.*, 1995). Administration of leptin was found to be more potent when given via the intracerebroventricular (ICV) route, thus suggesting that leptin signalling is primarily mediated through the hypothalamus (Halaas *et al.*, 1997).

Leptin acts upon neurons in the hypothalamus which express LepR such as neurons in the ARC, VMH, PVN, LH and DMH. In the ARC, leptin is able to activate neurons which synthesise POMC and CART, and inhibit neurons which synthesise AgRP/NPY (Park and Ahima, 2014) thus inhibiting food intake. NPY is thought of as a major target

for leptin. It stimulates food intake whilst inhibiting brown fat thermogenesis and increasing plasma insulin and steroid levels (Moran and Phillip, 2003). During fasting or starvation, leptin levels fall which activate behavioural, metabolic and hormonal responses. On the other hand, a gain in weight leads to increased plasma leptin which elicits the opposite response leading to a deficit in energy balance. Neurons within the hypothalamus are thought to respond in various ways to changes in plasma leptin (Friedman, 2002). Furthermore, leptin plays an important role in reproduction which is directly related to energy balance.

The GIT is also thought to play a major role in the regulation of appetite through the release of various regulatory peptides including ghrelin, GLP-1, CCK, OXM, pancreatic polypeptide YY (PYY3-36) and enterostatins.

Ghrelin is produced in the stomach and is the only known orexigenic (appetite stimulating) gut hormone identified to date (Perry and Wang, 2012). It is a ligand of growth hormone secretogogue receptor (GHSR) and activation of the receptor stimulates growth hormone (GH) secretion from the pituitary gland. The actions of ghrelin are opposed by those of leptin, and it is widely known as the 'hunger hormone'. It is predominately expressed in the gut mucosa, although it is widespread across the body (Kola *et al.*, 2005) including the brain. Levels of ghrelin in the body fluctuate depending on energy levels – levels are high when fasting and in subjects with low body mass index, and low following food intake and in patients with insulin-sensitive disorders including T2D and polycystic ovary syndrome. Previous studies have shown that administration of ghrelin caused an increase in weight as well as adiposity in rodents through increasing food intake and reducing fat utilisation or energy expenditure. The effects of centrally administered ghrelin on food intake are thought to be independent of its ability to stimulate GH release, and instead result from its direct action in the hypothalamus (Wortley *et al.*, 2004). It has been shown that ghrelin increases mRNA expression of AgRP and NPY in the ARC (Wang *et al.*, 2002). This enhances the upregulation of NPY and stimulates appetite by suppressing POMC pathways.

Whilst ghrelin stimulates appetite, the other gut hormones and peptides are believed to be involved in the suppression of appetite and food intake. CCK was the first gut hormone shown to inhibit feeding in rodents (Neary *et al.*, 2004). CCK promotes digestion though bile and enzyme release and slows down gastric emptying (Halford and Harrold, 2012). GLP-1 and PYY $_{(3\text{-}36)}$ (PYY) are co-secreted in response to nutrients in the gut. Both induce a significant decrease in food intake when administered peripherally in rodents (Neary *et al.*, 2004). GLP-1 is thought to act as a satiety factor within the hypothalamus (Beiroa *et al.*, 2014). Tang-Christensen *et al.* (1996) showed administration of GLP-1 to rats reduced food intake and water intake in a dose dependant manner. PYY, a member of the NPY protein family, is secreted by endocrine cells lining the bowel and colon in response to food and has been found to remain at high levels in the blood in between meals. Batterham *et al.* (2003) showed that infusion of PPY significantly reduced food intake of obese and lean human patients when compared to patients infused with saline solution. PYY activity also involves the ARC in the hypothalamus as it binds to Y2 receptors on NPY neurons, and subsequently inhibits NPY/AgRP neurons. The inhibition of NPY/AgRP neurons subsequently allows activation of the POMC neurons, thus food intake is reduced.

5-HT has also been classified as an important player in the regulation of food intake and energy balance. 5-HT is a neurotransmitter thought to mediate its effects through receptors in the hypothalamus, which change the activities of NYP/AgRP and POMC neurons. 5-HT can inhibit NPY signalling whilst activating POMC neurons (Dwarkasing *et al.*, 2015). Additionally, administration of 5-HT reduced food intake and stimulated energy consumption in both humans and rats (Fang *et al.*, 2013). Serotonergic drugs are widely used in the treatment of obesity as they exert their appetite suppressing effects by increasing the availability of 5-HT. Furthermore, 5-HT is thought to be able to inhibit the orexigenic activity of ghrelin (Dwarkasing *et al.*, 2015).

As well as the above peptides and hormones, there are numerous other potential peptides and hormones which can play a role in the regulation of food intake and

energy metabolism. These include AMPK (Stark *et al.*, 2013), oxyntomodulin (Cohen *et al.*, 2003), adiponectin (Kubota *et al.*, 2007; Yamauchi and Kadowaki, 2008), and spexin (Walewski *et al.*, 2014) to name a few.

Overall, appetite regulation and the control of BW and food intake is a very complex process. The tubers of LL may act upon any of these mechanisms plus many more. Thus, the aim of this project was to determine possible mechanisms of action of these tubers, and identify potential biologically active components causing the appetite-suppressing effects. This will be discussed throughout the following three chapters and is outlined in Figure 1.7.

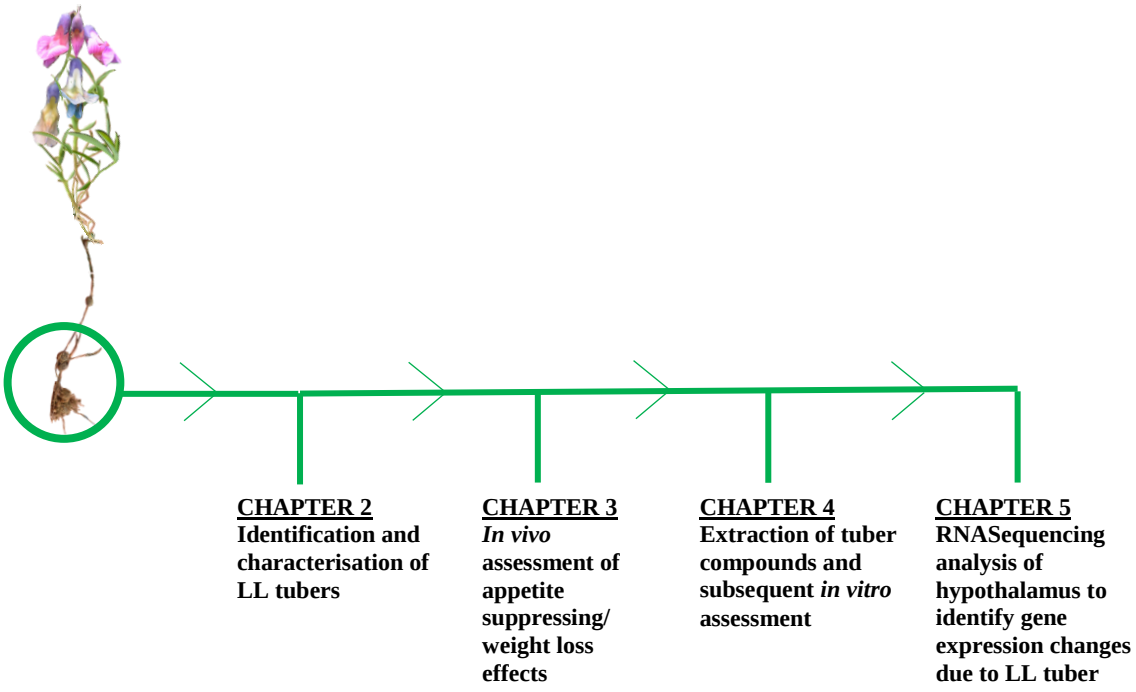

Figure 1.7: Schematic diagram outlining the focus of each subsequent chapter

Specifically, Chapter 2 will focus on the collection of plant material and plant identification. Following collection of the tubers, an *in vivo* study was conducted to investigate the effect of the tubers on food intake and BW in a normal rat model, which forms Chapter 3. Subsequently, the tubers were subjected to Soxhlet extraction to allow the identification of individual compounds which could be biologically active. The resulting extracts were screened for biological activity. These results collectively form Chapter 4. Lastly, to examine the effect of the tuber on specific appetite-associated genes, RNA sequencing (RNASeq) was carried out on hypothalamic tissue. The results for RNASeq are discussed in Chapter 5.

2. CHAPTER 2, COLLECTION AND IDENTIFICATION OF LL TUBERS

2.1. Introduction

As a safety precaution, and due to other *Lathyrus* species being associated with neurolathyrism (*L. sativus*), there is a requirement for the correct identification of LL tubers. Without expert knowledge, tubers or rhizomes from different plant species which grow close by could be collected in error. In this instance, the appetite-regulating properties would not be identified. Moreover, correct identification would be required in order to control the collection process in the case of commercialisation. Identification of the plant, and subsequent 'batch testing' would be required to ensure the correct plant was being used. Moreover, LL grows in various places around Britain as well as throughout Europe. Collection of large numbers of tubers would be required if this plant was to be used in the development of a new therapeutic. Thus a quick, reliable and inexpensive method of identification would be required. The aims of this chapter were to characterise the morphology of LL tubers and develop a quick and reliable method of identification. Moreover, to confirm the specificity and sensitivity of the method, other *Lathyrus* species were also tested which are closely related to LL. A phylogenetic tree was compiled using the results to confirm the reliability and accuracy of the identification in comparison to other methods previously reported throughout the literature.

Traditional species identification consists of analysing multiple morphological features, either within the plant's habitat or using a herbarium specimen (Dasmahapatra and Mallet, 2006); this is usually carried out by a botanical expert. There are various issues which can arise in this method of identification. Although vegetative traits are highly variable amongst different plant species within an environment, some plants from different species may have very similar features. Additionally, morphological features can change within species depending on environmental conditions. Plants can also be identified by their floral features, however, in many instances, these features are absent for much of the year. Therefore, without expert opinion, it may be very difficult to correctly identify specific plants.

In the era of 'omics technologies, DNA fingerprinting or barcoding (Ajmal Ali *et al.*, 2014; Dasmahapatra and Mallet, 2006) methods are widely used to address issues of identification, as well as phylogeny, relatedness and diversity within plant populations. The former term was initially coined in a method developed in 1985 by Sir Alec Jefferys and his colleagues (Karihaloo, 2015) and there are various molecular methods which have been used today including random amplified polymorphic DNA (RAPD), restriction fragment length polymorphism (RFLP), amplified fragment length polymorphism (AFLP) and inter-simple sequence repeats polymerase chain reaction (ISSR-PCR). However, due to large variations in the protocols used, some of these methods are seen as unreliable and prone to errors in identification (Dasmahapatra and Mallet, 2006). A combination of traditional morphological identification with DNA barcoding may solve this issue.

ISSR PCR is a DNA fingerprinting technique first developed by Zietkiewicz *et al.* (1994). ISSR PCR is based on genomic variations found in regions between microsatellites and has been described as a powerful technique to assess genetic diversity among closely related species and to identify similarities both between and within species (Ghorbel *et al.*, 2014). This technique is fast and inexpensive with multiple primer sets available, each containing over 100 primers.

2.2. Aims and Objectives

This chapter focuses on the characterisation and identification of LL tubers. The specific aims of this chapter are to:

- Characterise LL tuber morphology using histological staining techniques
- Develop an identification method using ISSR PCR and compile a phylogenetic tree of various *Lathyrus* species

2.3. Materials and methods

2.3.1. Herbarium Specimens

Herbarium specimens were collected from the Royal Botanic Gardens Edinburgh (RBGE) with permission from Dr Greg Kenicer (Head of Education), and from Hillend, Edinburgh with permission from Midlothian Council, Edinburgh, Scotland. Two herbarium specimens were taken to highlight leaf morphology changes due to changes in the growing habitat. Plant identity was confirmed by Dr Kenicer, who studied the *Lathyrus* genus during his doctorate, and by Dr Brian Moffat, who is leading the excavation at Soutra Aisle.

2.3.2. Plant Material

LL tubers obtained for this study were kindly supplied by Mr Mark Goff, the founder of a company called Bitter Vetch (http://www.bitter-vetch.com). The tubers supplied were grown from seeds originating from Soutra Aisle. See Appendix 3.

2.3.3. Histology and Staining

To characterise the morphology of the LL tubers, histological staining was carried out. Small sections of fresh LL tuber were fixed in formalin-aceto-alcohol (FFA) (90ml 70% v/v ethyl alcohol; 5ml glacial acetic acid; 5ml commercial formalin) over night for a minimum of 24h prior to processing. The tissues were then processed in a Citadel 1000 (Thermo Shandon, UK) processor overnight using the protocol shown in Table 2.1.

Table 2.1 Tissue processor protocol for fixed tissues.

Solution	Time (h)
70% v/v ethanol	3
90% v/v ethanol	3.5
100% ethanol	2
100% ethanol	1
1:1 (v/v) ethanol: Histoclear	1
100% Histoclear	1
100% Histoclear	1
Paraffin wax	2
Paraffin wax	2

The tissues were embedded in paraffin wax using a Lecia EG1140 H (Lecia Microsystems, UK) embedder and 8µm sections were cut using a Lecia RM2125RTF (Lecia Microsystems, UK) microtome. The tissue sections were floated onto polylysine microscope slides (Thermo Scientific) using a water bath at 60°C. The slides were placed on a hotplate over night before being processed for staining.

Before carrying out histological staining, the tissue sections were rehydrated using the method shown in Table 2.2.

Table 2.2: Rehydration method for histological staining

Solution	Time (min)
Histoclear	5
Histoclear	5
100% ethanol	5
100% ethanol	5
95% v/v ethanol	2
70% v/v ethanol	2
Tap water	2

Tissues were stained in either Toluidine Blue (Toluidine Blue O) in distilled water (dH_20) for 20 min, Iodine (20 min), or Johannsson Quadruple Stain (Solution A, 1% Safranin O (v/v) in cellosolve (50mL), 95% v/v alcohol (25mL), dH_20 (25mL), sodium acetate (1g), formalin (2mL)) for 24-48h followed by a wash in dH_20; Solution B (crystal violet 1% w/v aqueous) for 15 min followed by a wash in dH_20; Solution C (95% v/v alcohol (25mL), cellosolve (25mL), tertiary butyl alcohol (25mL)) for 15 s; Solution D (Fast green, FCF, saturated in equal parts clove oil and cellosolve (20mL), 95% v/v alcohol (60mL), tertiary butyl alcohol (60mL)) for 20 min; Solution E (95% v/v alcohol (30mL), tertiary butyl alcohol (30mL), glacial acetic acid (0.15mL)) for 2 s; Solution F (Orange G saturated in cellosolve (20 mL), 95% v/v alcohol (20mL)) for 3 min; and, solution G (clove oil (10mL), absolute alcohol (10mL), xylol (10mL)) for 2 s.

At the end of the staining process, the slides were dehydrated using the protocol shown in Table 2.3.

Table 2.3: Dehydration process following staining process

Solution	Time (min)
dH20	Dip
70% ethanol	Dip
95% ethanol	2
100% ethanol	5
Histoclear	5
Histoclear	5

Each slide was then mounted in DPX and left at room temperature to dry before imaging using a Nikon camera connected to a microscope (Olympus, Japan).

2.3.4. Genetic Characterisation of LL

2.3.4.1. DNA Extraction

Leaf samples from various species growing at RBGE were taken with permission from Dr Greg Kenicer. Plant identification is listed in Table 2.4 including the Botanical Garden Reference. Additionally, LL leaf samples were provided by Mark Goff which originated from two distinct locations – Black Aisle and Soutra Aisle. Identification codes and details of these samples are also listed in Table 2.4. All leaf samples were collected in paper bags, labelled, and stored at -20ºC until required. Total cellular DNA was isolated from the leaf samples using a GenElute™ Plant Genomic DNA Miniprep Kit (G2N10-1KT). The kit protocol was followed with the exception of the initial disruption step.

Briefly, the plant leaf samples were added to 2ml tubes with 350µl lysis solution A. The tubes were then placed in a bead mill along with a cone ball (stainless steel, 6mm

cone ball), and mixed at maximum speed (30 Hz) until the plant samples were fully homogenised. Before use, cone balls were decontaminated with diethylpyrocarbonate (DEPC) (0.1% v/v in dH_2O) and autoclaved. All plasticware used including pipette tips were RNAse/DNAse free. Following this, 50µl of lysis solution B was added and the cone bead removed before proceeding with the manufacturer's protocol. Quality and quantity of the DNA obtained was measured using a Nanodrop™ Spectrophotometer (2000C; Thermo Scientific). Each sample was diluted in elution buffer to a concentration of 5ng/ml.

Table 2.4: Plant identification of samples taken at RBGE

ID#	Name	RBGE code
1	*L. aureus*	1936.2795.B
2	*L. sativus*	20080538.C
3	*L. pannonicus*	2006.0076.A
4	*L. venetus*	20020546.B
5	*L. vernus*	1987.0593.E
6	*L. japsonii var. californicus*	2003.0155.A
7	*L. laxiflorus*	N/A
8	*L. niger*	2006.0073.A
9	*L. pratensis*	2009.1754.A
10	*L. linifolius*	Black Aisle
11	*L. linifolius*	Soutra Aisle

2.3.4.2. ISSR PCR

2.3.4.2.1. Primers

Ten oligonucleotides, from the University British Columbia ISSR Set #9, were selected to allow for the identification of the optimum primers to use for this analysis. The sequences are shown in Table 2.5.

Table 2.5: Primer sequences used in ISSR-PCR

UBC Set 9 Primer #	ID #	Sequence (5' – 3')
UBC9 807	1	AGAGAGAGAGAGAGAGT
UBC9 816	2	CACACACACACACACAT
UBC9 845	3	CTCTCTCTCTCTCTCTRG
UBC9 849	4	GTGTGTGTGTGTGTGTYA
UBC9 861	5	ACCACCACCACCACCACC
UBC9 862	6	AGCAGCAGCAGCAGCAGC
UBC9 875	7	CTAGCTAGCTAGCTAG
UBC9 889	8	DBDACACACACACACAC
UBC9 895	9	AGAGTTGGTAGCTCTTGATC
UBC9 899	10	CATGGTGTTGGTCATTGTTCCA

2.3.4.2.2. GoTaq Green Polymerase

Amplification was performed in a total volume of 25µl including 10ng of total cellular DNA, 10pmol of primer, 12.5ul of 2x GoTaq Green Master Mix with the remaining volume made up using nuclease-free H_2O. PCR amplifications were performed in a Primus96 PCR machine (MWG Biotech, Milton Keynes, UK) as follows: an initial step of 2min at 95°C, followed by 25 cycles, each one including 30s at 95°C for denaturation, 30s at 50°C for annealing, and 2min at 72°C for elongation. A final 5min step at 72°C was used for final extension.

The final products of PCR were separated by electrophoresis on 1% agarose gel [0.5g agarose (Molecular Grade) in tris-boric acid-ethylenediaminetetraacetic acid (TBE)] for 1 h at 50 V. The agarose gel and running buffer contained 0.5µg/mL ethidium bromide or 1x Gel Red (stock was 10,000x) to allow visualisation under ultra-violet (UV) light at 605nm. All samples were loaded with 5x DNA Loading Buffer. Molecular weight markers were loaded onto each gel (Hyperladder ™ 1kb, 200bp to 10,037bp, H1, and Hyperladder™50bp, 50bp to 2000bp, H2) alongside the PCR products for each DNA sample. The gels were visualised using an INGENSUS UV imaging system (Syngene) and images were captured using the GeneSnap imaging program (Syngene).

2.3.4.2.3. MyTaq DNA Polymerase

Amplification was performed in a total volume of 25µl which included 10ng of total cellular DNA, 1.25µl 10pmol/µl primer, 5µl MyTaq 5X reaction buffer, 0.75µl MyTaq DNA Polymerase and 16µl nuclease-free H_2O. PCR amplifications were performed in a Primus96 PCR machine (MWG Biotech, Milton Keynes, UK) as follows: an initial step of 2min at 95°C, followed by 30 cycles, each one including 30s at 95°C for denaturation, 30s at 58°C for annealing, and 35s at 72°C for elongation. A final 2min step at 72°C was used for the final extension. A negative control was used in each run to reduce the possibility of interference due to contamination. The final products of PCR were separated by electrophoresis on a 1% agarose gel as in section 2.3.4.2.2.

2.3.4.3. Experion ™ DNA 12K Analysis

To increase the resolution of the resulting banding patterns, and overall sensitivity of the experiment, an Experion automated electrophoresis system was used. Experion™ DNA analysis enables reproducible and accurate results using minimal sample volume. An Experion DNA 12K analysis kit was used as per the manufacturer's instructions. This allows sensitive, high resolution analysis of DNA fragments in the range of 50-17,000bp via a microfluidic lab-on-a-chip system. Briefly, each chip was primed and loaded with Gel-Stain solution before adding 5µl of DNA loading buffer and 1µl of the ISSR PCR reactions (resulting from MyTaq ISSR-PCR) to appropriate wells. Distilled water was used as a blank. The chip was then vortexed and loaded onto the Experion electrophoresis station within 5min of preparing the chip. Analysis of the ISSR PCR amplicons was performed on the Experion software Version 3.0 and virtual gel images obtained.

2.3.4.4. Phylogenetic Tree Analysis

Phylogenetic analysis was carried out on the ISSR PCR banding patterns from the Experion virtual gel images using PyElph 1.4 software and data was compared to the literature. PyElph (Pavel and Vasile, 2012) is a software tool which captures data from gel images and computes the molecular weights of each fragment in order to generate a phylogenetic tree.

2.4. Results

2.4.1. Histology and Staining

Slices of LL tuber were stained using histological methods to characterise morphological features which could aid in the identification of the tuber. A red/orange outer layer is evident in Figure 2.1 which is representative of the periderm, or skin, of the tuber. This image also indicates the presence of sac-like structures in the inner surface of the tuber. Following staining with iodine (Figure 2.2), the presence of large, round starch grains was evident within the tuber slice. It is possible that these grains are contained within the sac-like vesicles evident in the unstained image. Further

structures were stained using Toludine Blue (TB). TB is a cationic dye which binds to positively charged groups. Figure 2.3 shows two images of LL tuber stained with TB. Lignified cells can be identified in the top image (see red arrow) as they are stained blue/green. These cells may be, for example, xylem cells or phloem cells. Additionally, dark purple/pink areas indicate the presence of polysaccharides, which is evident surrounding the sac-like vesicles in the tuber slice. The bottom image in Figure 2.3 also highlights the sac-like vesicles present in the tuber slice. TB does not stain starch, thus this image correlates with the iodine stained images and again suggests the starch grains are present in the vesicles. The inner layers of the LL tuber (known as the perimedullar zone) show a mild pink/purple tone which may highlight the presence of carboxylated polysaccharides. Lastly, LL tuber slices were stained with Johansen's Quadruple Stain (JQS, Figure 2.4). Both green and blue stained structures were visible in the top image (highlighted by red arrows). JQS gives rise to a green colour (due to the presence of Fast Green) when cellulose is present. This structure may represent vascular cell walls in the tuber slice, possibly a xylem bundle. The blue colour arises when JQS is in contact with basic solutions, of which there may be many basic compounds present in the tuber. The bottom image in Figure 2.4 again highlights bright green structures, as well as purple grain-like structures with hints of orange. The green structures represent cellulosic cell walls. Crystal violet, contained within the JQS, stains starch a purple colour, thus the presence of purple, grain-like structures again indicates large starch grains. Many of these features helped to aid in the identification of LL tubers. However, the features are not unique to LL tuber, thus other methods of identification are still required.

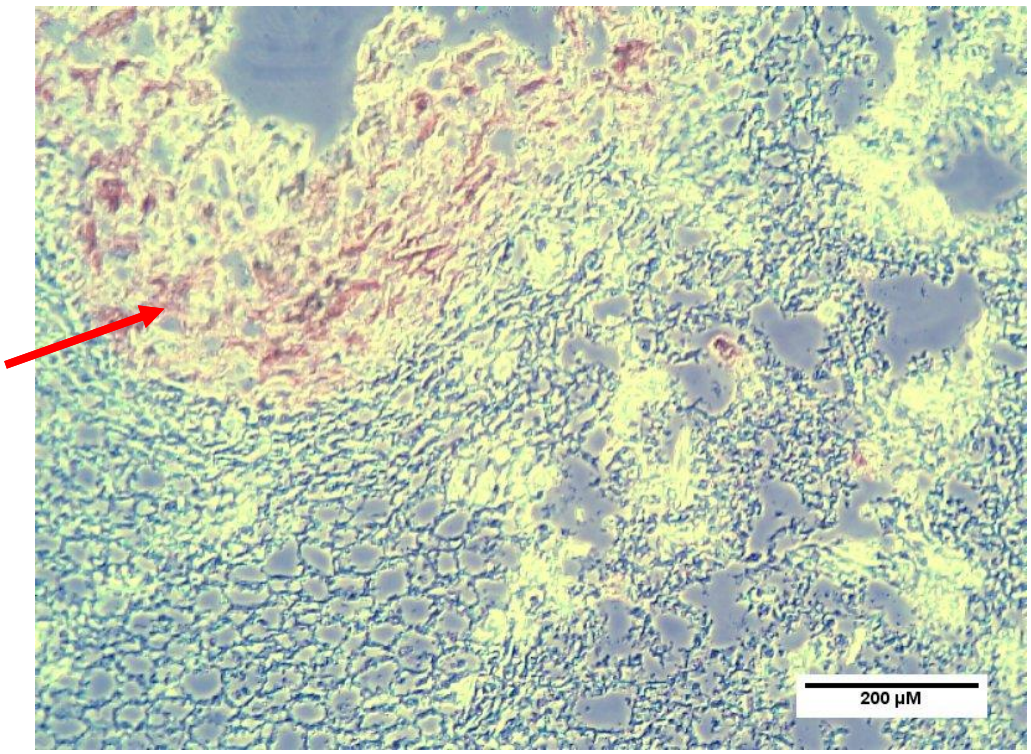

Figure 2.1: Unstained images of LL tuber. Scale bar represents 200µm, 10x objective magnification. Red arrow highlights outer layer of tuber. Red arrow points to the periderm or skin of the tuber.

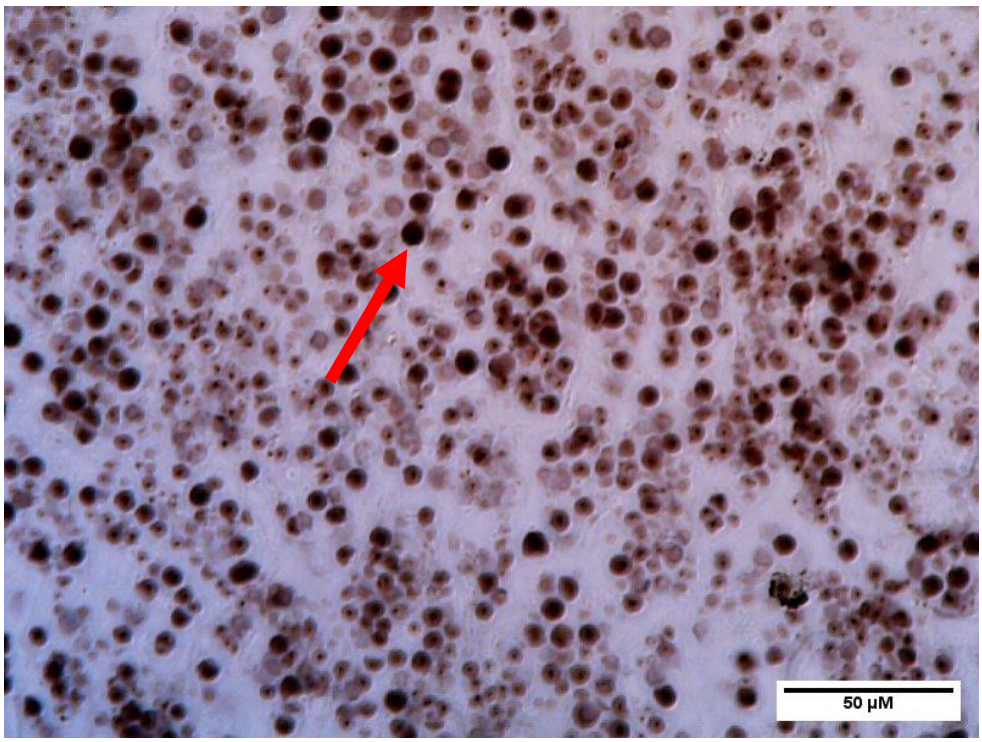

Figure 2.2: Slices of LL tuber stained using Iodine. Scale bar represents 50µm, 40x objective magnification. Red arrow points to an individual starch grain which is stained dark brown in the presence of iodine.

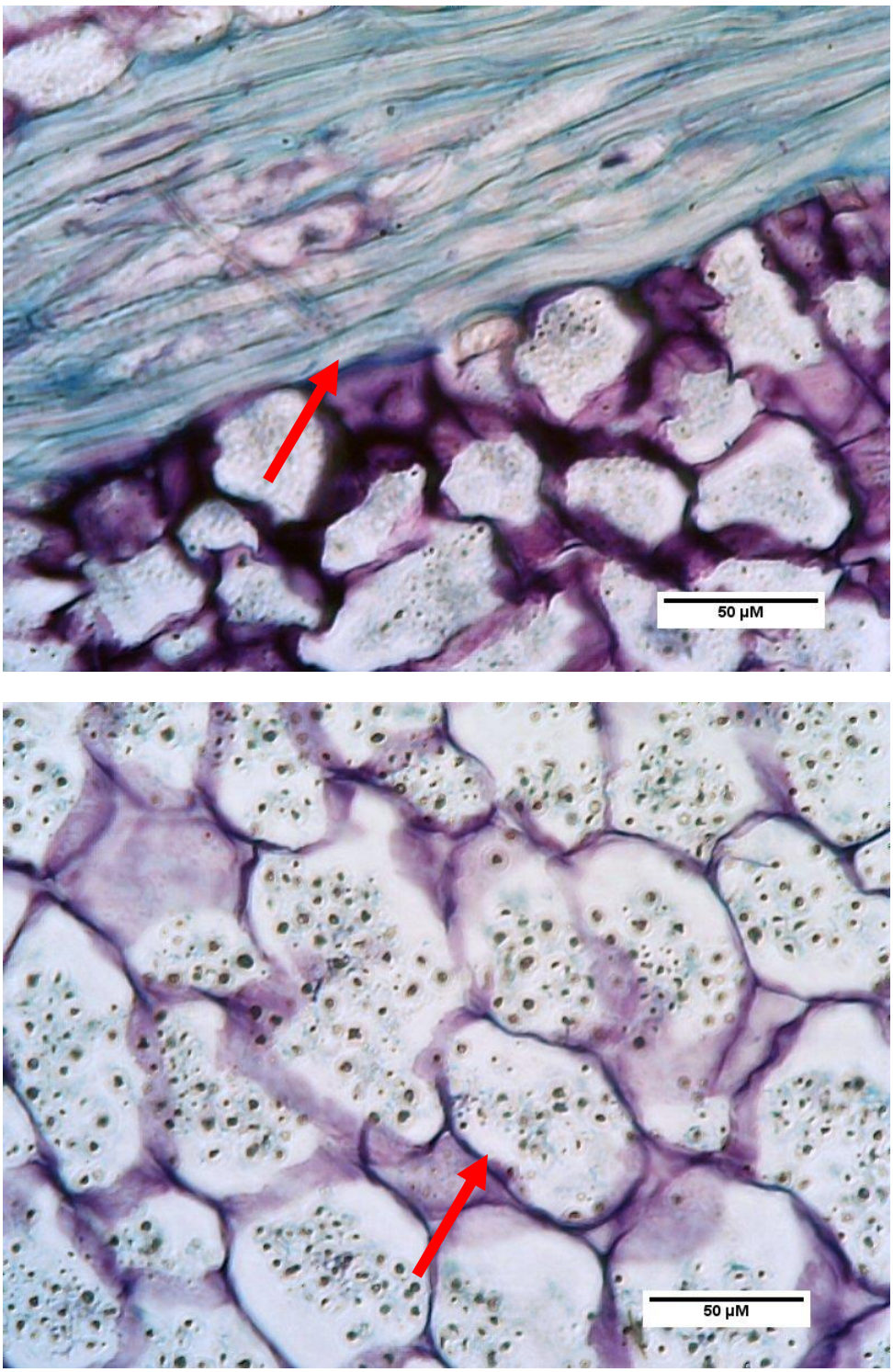

Figure 2.3: Slices of LL tuber stained using Toludine Blue. Scale bar represents 50µm, 40x objective magnification. Red arrows highlight lignified cells (top image) and the presence of polysaccharides stained pink/purple (bottom image). Additional vesicle-like cells can be seen in the bottom image representing potential starch grains.

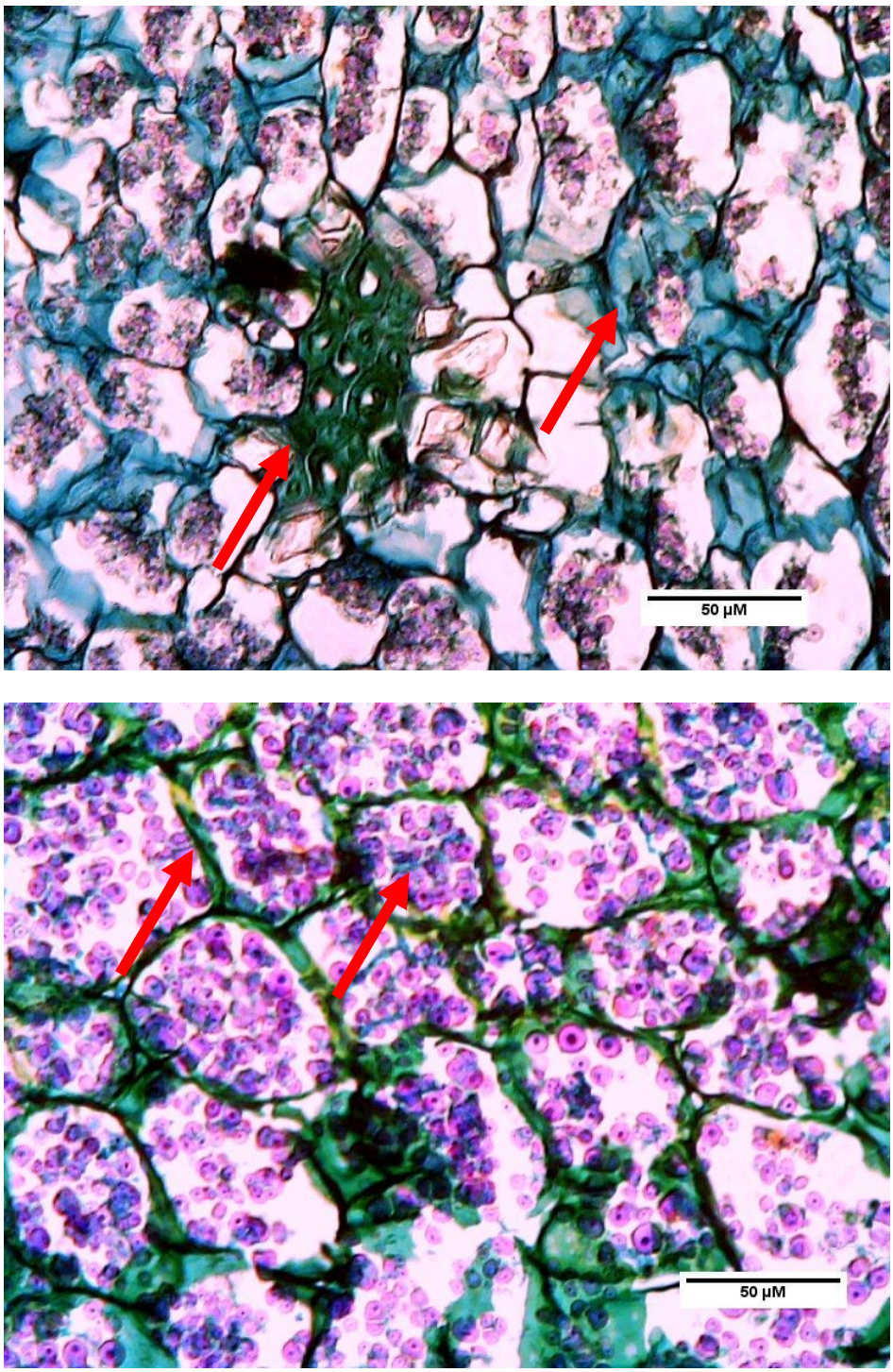

Figure 2.4: Slices of LL tuber stained using Johansen's Quadruple Stain. Scale bar represents 50µm, 40x objective magnification. The red arrow to the left of the image points to green stained structures where cellulose is present. The arrow to the right points to purple grain-like structures which could be starch grains.

2.4.2. ISSR PCR and Phylogenetic Tree Analysis

2.4.2.1. DNA Extraction

The concentration and quality of DNA from each leaf sample was determined using a spectrophotometer. The ratio of absorbance at 260nm *vs* 280nm is used to assess the purity of DNA. A ratio of approximately 1.8 is accepted as 'pure' for DNA, and a ratio of about 2.0 is accepted as 'pure' for RNA. Table 2.6 shows the 260:280 ratio for each sample, as well as the concentration of DNA in each sample. Some ratios were lower than expected, which could be due to the presence of proteins, which can absorb strongly at 280nm. Moreover, higher values (as in sample #7) may suggest the presence of RNA carry-over. The concentration of DNA ranged from 7.5ng/µL to 109.2ng/µl. This was due to differences in the percentage recovery from each leaf sample as some leaves were frozen within 1-2 h following collection, while others were stored at room temperature overnight before being frozen.

Table 2.6: Nanodrop™ data for each extracted DNA sample

ID #	260:280	Concentration (ng/µl)
1	1.49	20.3
2	1.74	72.1
3	1.74	109.2
4	1.61	24.9
5	1.80	99.7
6	1.82	96.0
7	2.17	7.5
8	1.81	90.6
9	1.87	37.7
10	1.77	68.2
11	1.85	43.1

2.4.2.2. ISSR PCR and Gel Electrophoresis

GoTaq Green was used for the initial selection of appropriate ISSR primers capable of discriminating between L*athyrus* cultivars. GoTaq Green was selected as it is an inexpensive, pre-mixed, ready-to-use solution, which contains two dyes (blue and yellow) that allows direct loading of the PCR reactions into gels and monitoring of the electrophoresis process, thus it minimises the steps taken from PCR to gel electrophoresis. The Experion™ DNA system uses a fluorescent stain which is bound to each sample and is excited by a laser to allow the each band to be simultaneously detected and quantified. The tracking dyes present in GoTaq Green were found to interfere with this detection system, thus creating high background noise. Therefore,

GoTaq Green was replaced with MyTaq polymerase in Experion DNA™ experiments.

The ISSR primers should give rise to specific banding patterns on an agarose gel depending on the number of inter-simple sequence repeats in the DNA sample the primers bind to. The unique banding pattern would then be associated with a particular species. This method thus could be used to confirm the identification of LL from different 'batches', or different habitats. The differentiation between closely related *Lathyrus* cultivars will portray the reliability and accuracy of the method.

For the initial testing of the ISSR primers, plant DNA samples (samples 1 to 6, see Table 2.4) were used in ISSR PCR primer assay with 10 different primers. Each ISSR PCR primer assay also ran a NTC reaction, in which the DNA sample was replaced with ultrapure RNase/DNase-free water. No amplification was observed in the NTC samples, confirming that the ISSR PCR assays did not create false positives via environmental contamination of the reactions. Based on the quality of the banding patterns and differentiation between the species, only two primers (Primer 5 and Primer 6) were carried forward for use in Experion DNA™ experiments. The results for all ten Primers are shown in Appendix 4.

Figure 2.5 shows the initial gel electrophoresis image of the resulting ISSR PCR products using Primer 5. There were clear, discrete bands for all *Lathyrus* samples tested excluding lane 9 which had an aliquot of the ISSR PCR reaction for *L. laxiflourus*. The lack of bands for this sample may have been due to the low concentration, or low quality of DNA produced following DNA extraction. Due to the clarity of the remaining bands, it was possible to analyse them straight from the gel. However, interpretation error from electrophoretic migration artefacts and detection of weak bands could influence phylogenetic analysis. Therefore, to help reduce variation and subjectivity in the analysis of the ISSR PCR, the reactions were subsequently subjected to Experion™ DNA Analysis. Figure 2.6 shows the gel electrophoresis image following ISSR PCR using Primer 6. Using this primer, with the same conditions as before, it was evident that the banding pattern for each primer was not

so clear. However, there were visible differences between each sample. The reaction aliquot in lane 10 (*L. laxiflourus)* was fainter in comparison to the other samples suggesting reduced quality or quantity of *Lathyrus* DNA used leading to a lower PCR yield. Although the banding pattern was not as clear as when using Primer 5, these samples were also analysed using Experion ™ DNA Analysis for comparison purposes. Based on the results obtained for Primer 5 and Primer 6, no further primers were required.

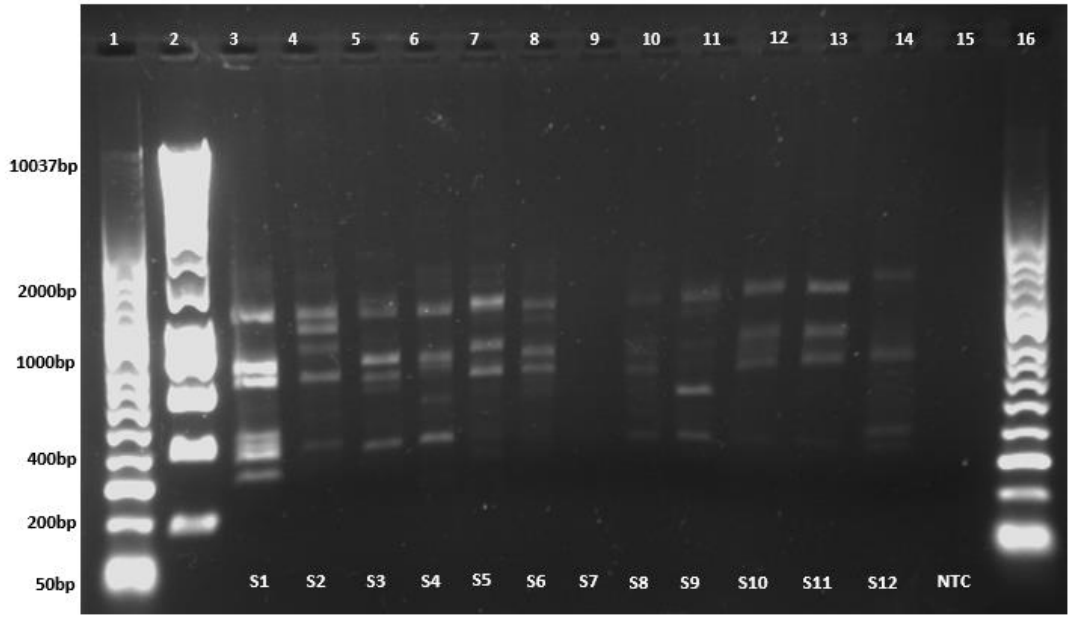

Figure 2.5: ISSR PCR of Lathyrus DNA Samples with ISSR Primer 5 using MyTaq Polymerase. Aliquots of ISSR PCR products following amplification of *Lathyrus* DNA samples, S1-12 (as detailed in Table 2.5) with ISSR Primers 5 (as detailed in Table 2.7) were resolved on a 2% agarose gel and visualised by ethidium bromide staining. NTC lanes contain aliquots of the reactions from the no template control reactions for each ISSR PCR assay. The size markers (measured in basepairs) were Hyperladder 1kb (lanes 2 and 16) and 50bp (lane 1).

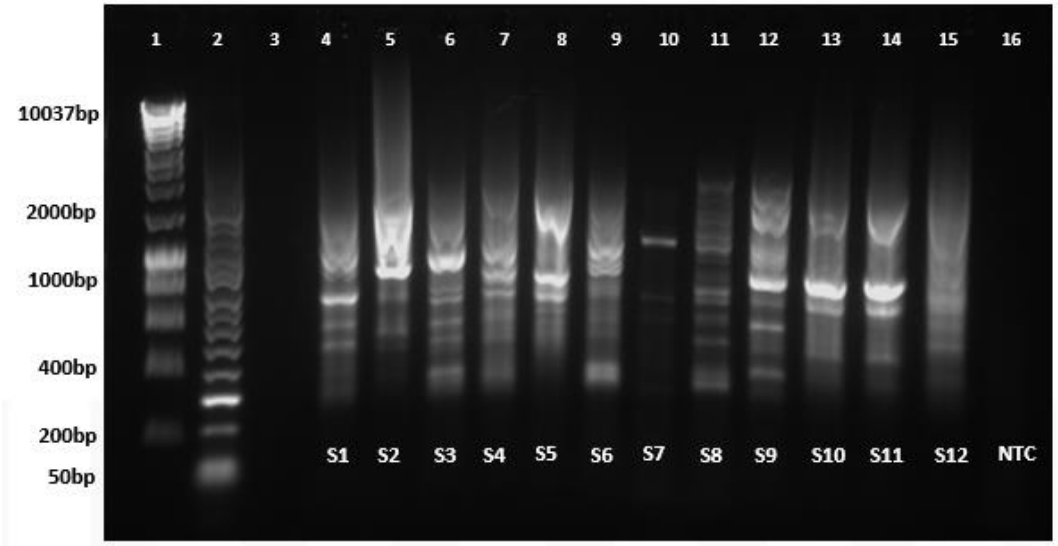

Figure 2.6: ISSR PCR of Lathyrus DNA Samples with ISSR Primer 6 using MyTaq Polymerase. Aliquots of ISSR PCR products following amplification of *Lathyrus* DNA samples, S1-12 (as detailed in Table 2.5) with ISSR Primers 6 (as detailed in Table 2.7) were resolved on a 2% agarose gel and visualised by ethidium bromide staining. NTC lanes contain aliquots of the reactions from the no template control reactions for each ISSR PCR assay. The size markers (measured in basepairs) were Hyperladder 1kb (lanes 1) and 50bp (lane 2).

2.4.2.3. Experion ™ DNA Analysis

Figures 2.7 and 2.8 show the comparisons between the agarose gel electrophoresis (A) and the virtual gel image produced following Experion ™ DNA analysis (B) for Primers 5 and 6, respectively. In both cases, the banding patterns were very similar, with greater resolution and sensitivity seen when using the Experion ™ DNA analysis. Some bands in the agarose gel (A) appear to be smeared, and some were extremely close together. However, these issues appear to be resolved in the virtual gel image due to increased resolution when using Experion DNA ™. Not all samples were tested in the Experion DNA™ system as the microfluidic chip only had a capacity of 11 samples in total. An upper and lower marker are present in the loading dye which is added alongside each sample and can be seen in each lane in Figure 2.7(B) and 2.8(B). The lack of bands, other than the loading markers, in the NTC lane confirms there was no contamination of the samples during the ISSR PCR reaction. This was also confirmed in the agarose gels. Due to the increased resolution and sensitivity, the gel image obtained via the Experion™ DNA system was used in phylogenetic tree analysis using PyElph 1.4 software (Figure 2.9(A) and (B)). PyElph uses images of the gels to generate a phylogenetic tree. The software packages require input from the user to identify the molecular weight markers, as well as the lanes to be analysed. Thus, it is important that the images used are clear, and the bands are distinct. The Experion™ DNA virtual gel was used in this software package as the sensitivity and clarity of the bands was greater in comparison to the agarose gel images. Moreover, the migration of the bands along each lane is more parallel in comparison to the agarose gels where the lanes can appear at an angle. This can cause issues when carrying out analysis using PyElph. Furthermore, the Experion™ DNA analysis was able to detect very faint bands in the *L. laxiflourus* lanes (lane 7 in Figure 2.7(B) and 2.8(B)), which appeared blank when visualised on the agarose gel (lane 9 in Figure 2.7(A), lane 10 in Figure 2.8(A)), thus highlighting the increased sensitivity even when using lower volumes of each PCR product.

The phylogenetic tree analysis (Figures 2.9) shows the relationship between each species based on the banding pattern obtained using primer 5 (A) and 6 (B)

respectively. Using Primer 5, LL (BA) and LL (SA) were shown to be closely related to *L. vernus* followed by *L. venetus*, while *L. aureus* was seen to be the most distant as it appeared on a separate branch from the initial starting point. Primer 5 also grouped together *L. laxiflourus, L. pannonicus, L. pratensis* and *L. niger*. Using Primer 6, LL (SA) and LL (BA) appear to be closely related to *L. vernus* and *L laxiflourus* followed by *L. pratensis*. The most distant species were shown to be *L. niger, L. aureus, L. pannonicus, L sativus* and *L. venetus.* The differences in the phylogenetic tree analysis is based on the relationship of similar banding patterns following ISSR PCR. This method is quick and inexpensive, however, to obtain the exact relationship status, more in depth methods are required. In terms of identifying LL species, both Primers 5 and 6 differentiate LL (BA) and LL (SA) samples not only from the other *Lathyrus* species but also from one another. These two samples are from the same species, however, they were grown in separate environments in different parts of the United Kingdom. Thus, these results suggest that there are genetic differences between the same species grown in the two different locations. Ultimately, the technique of ISSR PCR combined with Experion™ DNA Analysis can be used to distinguish between LL samples as well as different *Lathyrus* species from various locations with quick and accurate results.

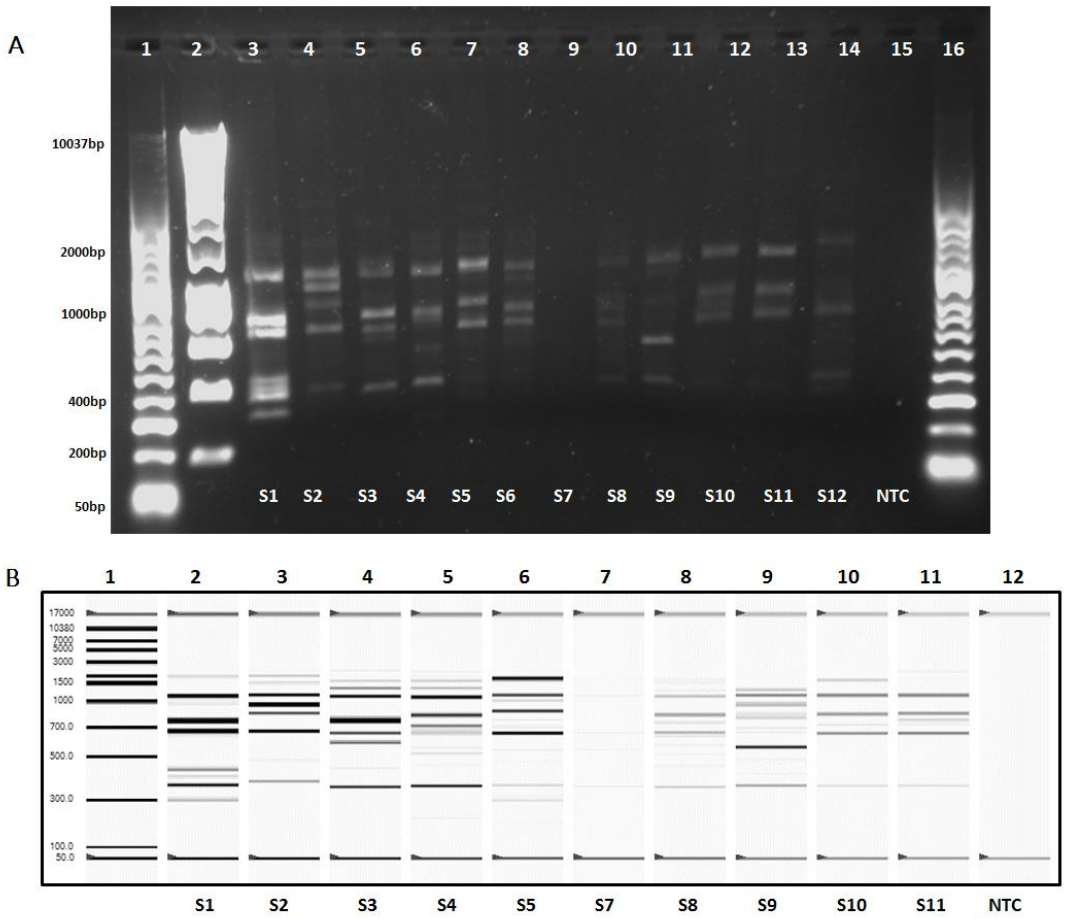

Figure 2.7: Gel electrophoresis of ISSR PCR samples using Primer 5. Image (A) shows the conventional agarose gel, while (B) shows the virtual gel obtained using the Experion™ DNA Analysis system. The same *Lathyrus* DNA samples, and ISSR PCR products, were used for both agarose gel electrophoresis and Experion™ DNA analysis. Due to the maximum capacity of the microfluidic chip being 11 samples, two samples were excluded in the Experion™ DNA analysis – these samples are shown in lanes 8 and 14 of the agarose gel (Sample 6 and 12). The numbering above both gel images represents the lane number. The numbering below each gel image refers to the sample number (Table 2.5). NTC refers to the no template control. Lanes 1, 2 and 16 of (A) show the molecular weight markers (Hyperladder 1kb and 50bp). Lane 1 in (B) shows the molecular weight marker in the Experion™ DNA analysis. Each lane in (B) also shows quality control markers at 50bp and 17,000bp.

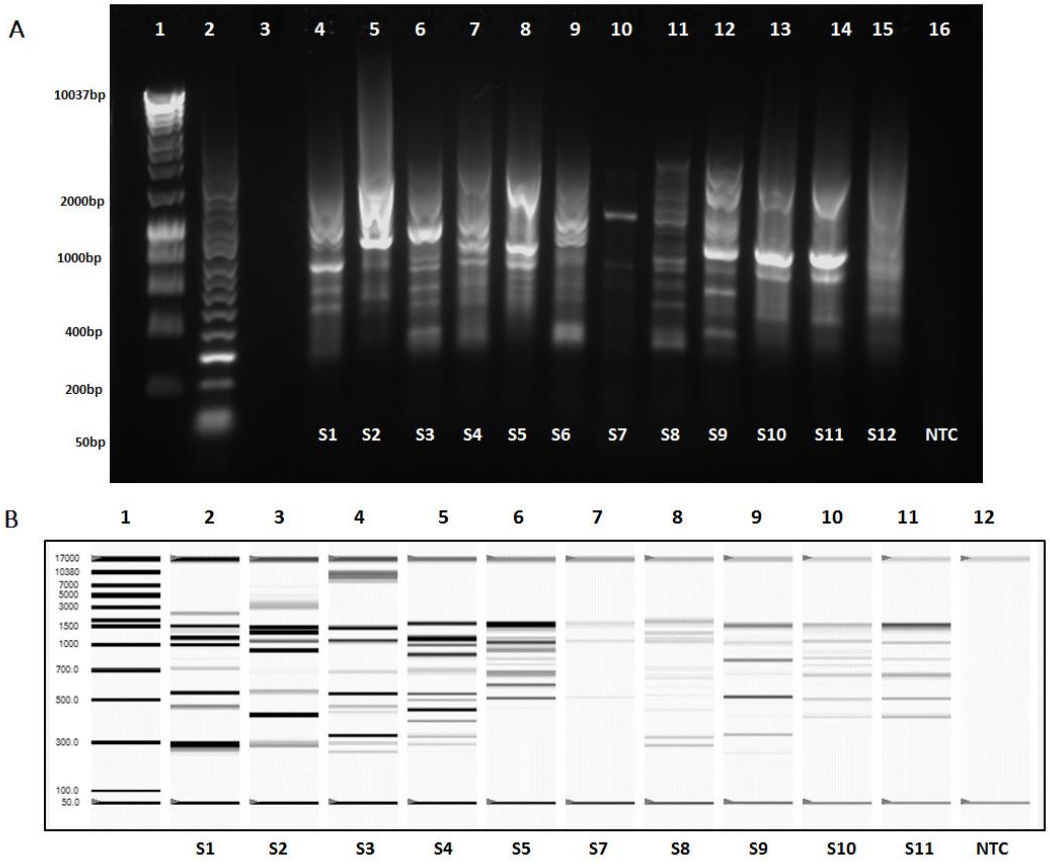

Figure 2.8: Gel electrophoresis of ISSR PCR samples using Primer 6. Image (A) shows the conventional agarose gel, while (B) shows the virtual gel obtained using the Experion™ DNA Analysis system. The same *Lathyrus* DNA samples, and ISSR PCR products, were used for both agarose gel electrophoresis and Experion™ DNA analysis. Due to the maximum capacity of the microfluidic chip being 11 samples, two samples were excluded in the Experion™ DNA analysis – these samples are shown in lanes 8 and 14 of the agarose gel (Sample 6 and 12). The numbering above both gel images represents the lane number. The numbering below each gel image refers to the sample number as mentioned in Table 2.5. NTC refers to the no template control. Lanes 1 and 2 of (A) show the molecular weight markers (Hyperladder 1kb and 50bp). Lane 1 in (B) shows the molecular weight marker in the Experion™ DNA analysis. Each lane in (B) also shows quality control markers at 50bp and 17,000bp.

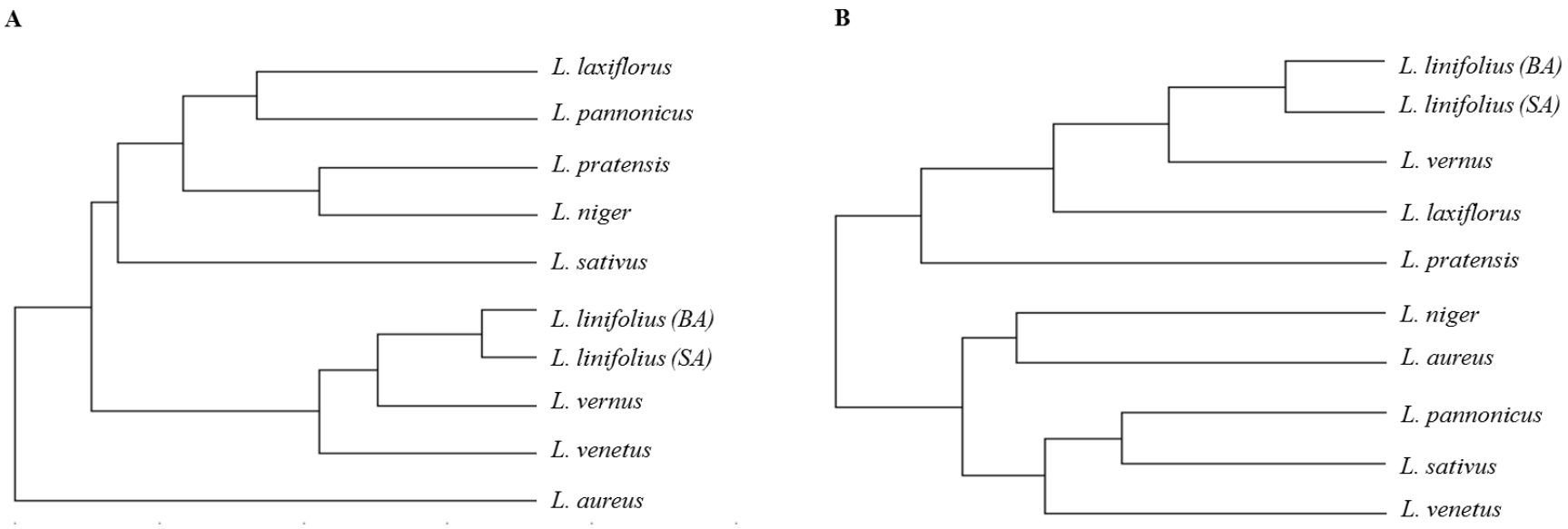

Figure 2.9: Phylogenetic tree analysis based on ISSR PCR using Primer 5 (A) and Primer 6 (B). Samples, generated using the same ISSR PCR method, were tested using Experion ™ DNA analysis. The virtual gel image shown in Figure 2.21 (B) was analysed using PyElph to generate a phylogenetic tree based on similarities and differences in the banding pattern generated by each sample.

2.5. Discussion and Conclusions

Characterisation of LL tuber using general plant staining techniques were utilised which showed various differences in the structural make-up of LL tubers and it is clear that the tuber has some distinct features. The presence of large grains of starch throughout the tuber slice, which appear to be held in sac-like vesicles (Figure 2.4), are similar to that of the common potato (data not shown). The LL tubers also have a characteristic red/orange outer layer, which can be identified even when slices remain unstained. Thus, this feature could be an identifying factor when collecting such tubers in a wild habitat. The pattern of staining seen when using Toludine blue also highlights distinctive features. The pink/purple colouring, indicating the presence of carboxylic acids, could represent areas in which the active components are stored. The method of identification through characterisation of the anatomy is simple, inexpensive and robust. However, various other tubers may give similar staining and tuber morphology may change throughout the seasons, therefore, based on these results alone, the identification cannot be definite. Future studies could examine other Lathyrus tubers to confirm similarity. Thus, these results were coupled with genetic characterisation using ISSR PCR, to improve the process of identification.

ISSR PCR has been proven to be applicable to studies looking at intra- and inter-specific variation in plant populations as well as marine populations, and fungi. Belaïd *et al.*, (2005) and Ghorbel *et al.* (2014) both utilised ISSR PCR to map the phylogeny between different populations of *Lathyrus* species. Using this technique, they were able to characterise and differentiate between different genotypes. Furthermore, Djamila *et al.* (2012) studied genetic polymorphisms of pistachio (*Pistacia vera* L.) using ISSR PCR and were able to characterise plants from this species from different cultivars in Algeria. ISSR PCR has also proven useful in identifying between species other than plants. Chiu *et al.*, 2015 used ISSR PCR to identify types of seafood. The purpose of their study was to develop molecular marker methods to determine genetic variation inter- and intra-species and they were able to conclude that ISSR PCR was able to distinguish between different species within one genus. Additionally, Roux *et al.* (2007) utilised ISSR PCR in a study to distinguish between several moth

populations worldwide. Thus, these studies highlight the effectiveness of this technique in identification protocols in various organisms. One advantage of ISSR PCR in comparison to other molecular marker methods is that it does not require prior knowledge of the DNA sequence and therefore can be used to identify and distinguish between unknown samples (Chiu *et al.*, 2015). Moreover, ISSR PCR has been shown to have high reproducibility and requires less than 50ng of DNA compared to over 100ng when using AFLP (Ng and Tan, 1994). Poyraz (2016) conducted a study to compare various molecular marker techniques including RAPD-PCR, ISSR-PCR, and ITS Sequencing (Internal Transcribed Spacer regions). They determined that RAPD-PCR and ISSR PCR are more sensitive in detecting genetic diversity in populations of similar habitats than ITS Sequencing. However, the effectiveness of these techniques decreases when discriminating between populations further on the phylogenetic tree (Poyraz, 2016).

In this study, a method to help in the identification of *Lathyrus* species was developed using two primers from Set 9 in the UBC database. Using these primers, unique profiles for each plant species were obtained. Each species showed a unique banding pattern, with some bands appearing in more than one species. Moreover, the two LL samples tested from different locations showed almost identical banding patterns, confirming the reliability of this method. The banding patterns had minor differences, which may be a result of different environmental conditions in which the plants were growing. The results confirm that this technique can be used in future studies to identify LL tubers in the wild in comparison to other *Lathyrus* species. To reduce time and increase the sensitivity of the ISSR PCR analysis, Experion™ DNA analysis was carried out using the ISSR PCR products. This method allows gel electrophoresis to be automated, whilst minimising electrophoresis artefacts and reducing subjectivity in the analysis. Experion ™ DNA analysis kits provided accurate, reliable and quantitative DNA analysis within 40 min. Furthermore, the microfluidic chips used have high sensitivity and excellent resolution over a broad dynamic range (down to 5bp), using only 1µl of sample. Thus, this technique could be used to develop a fast, reliable, and high quality method which can help distinguish LL samples from other *Lathyrus* species. Additionally, the increased sensitivity allows for more accurate

analysis which is beneficial when creating a phylogenetic tree to compare each sample with the others, and with the literature values.

The unique profiles were subsequently used to create a phylogenetic tree of the *Lathyrus* species tested to determine the accuracy of the method in comparison to other methods used previously in the literature. However, both phylogenetic trees appear to show differing relationships between the *Lathyrus* species. This may be due to different genetic polymorphisms being apparent when utilising different primers (Poyraz, 2016). Debnath *et al.* (2008) identified variations between primers in their ability to distinguish between genotypes of strawberry species. They noted that this may be due to differences in the resolving power of the primers used. Nevertheless, the LL samples were distinguishable and consistently grouped together, despite minor differences in the banding patterns, thus confirming the ability of this technique to identify intra- and inter-species relationships. This technique relies on the amplification of segments found in between microsatellite markers, and not on the exact DNA sequence of the plants being studied. Kenicer *et al.* (2005) carried out a systematic and biogeographical study of *Lathyrus* using combined ITS *trnL-F* and *trnS-G* sequencing. When comparing the phylogenetic data presented by Kenicer *et al.* (2005) to the data shown in this study (Figure 2.10), *L. linifolius* is consistently close to *L. vernus,* suggesting that this is the most closely related species. When looking at the results from Primer 6 in comparison to ITS sequencing by Kenicer *et al.,* LL is also closely related to *L. laxiflourus.* However, primer 5 shows that this species is grouped in a separate clade of the phylogenetic tree. There are also differences in the relationships between the other *Lathyrus* species tested. These differences are possibly a result of the different techniques used as well as the analysis process. Additionally, the techniques used by Kenicer *et al.* are based on the specific DNA sequence of the plant species and thus may present a more in-depth analysis of mutations and polymorphisms. Only two primers were used in this study, therefore, many other primers could be tested. One sample (*L. laxiflourus*) did not give a clear banding pattern, thus it is possible that it is due to the primers used. Arnau *et al.* (2002) were able to identify 30 different strawberry varieties using only one ISSR primer. Thus, testing a larger pool of primers may result in identification of a primer which gives a

unique and clear banding patterns for all samples tested. Overall, ISSR PCR is inexpensive in comparison to DNA sequencing techniques and the method is robust and simple. The method used in this study would help in the identification of LL tubers from various locations as a 'batch' test to confirm the correct tuber is being used. This is an important aspect due to the potential of other *Lathyrus* species to cause neurolathyrism.

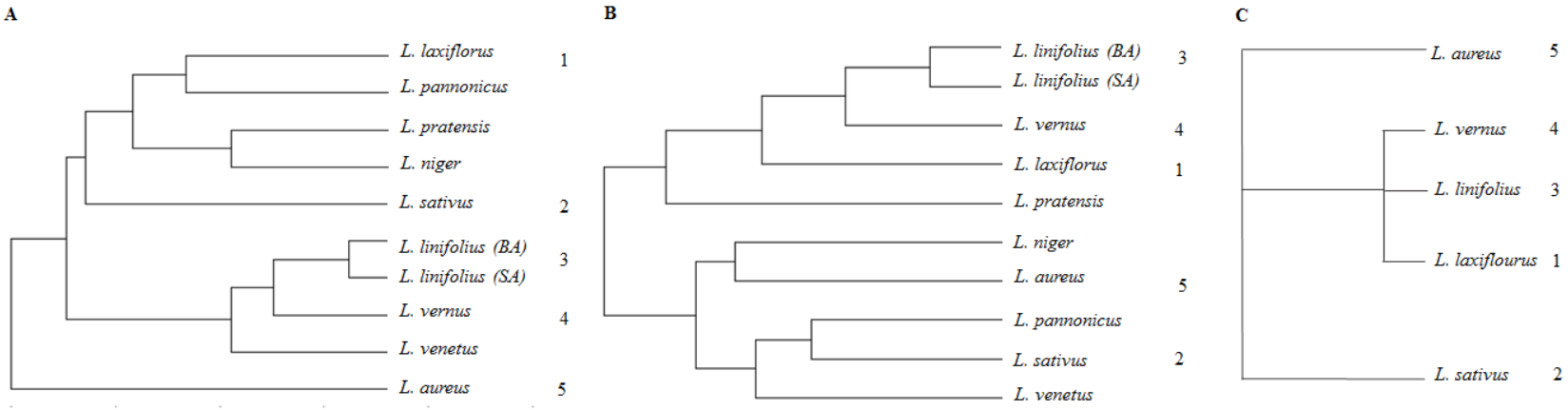

Figure 2.10: Comparison of results between ISSR PCR phylogenetic tree analysis and ITS sequencing analysis carried out by Kenicer *et al.* (2005). (A) ISSR PCR Primer 5 results using PyElph Phylogentic analysis (Figure 2.14), (B) ISSR PCR Primer 6 results using PyElph Phylogentic analysis (Figure 2.15), (C) representative of the relationship reported by Kenicer *et al.* (2005) using a different technique which consisted of combined ITS, *trnL-F* and *trnS-G* sequencing and gap characters. Numbering highlights position of individual species common to all figures, and their representative position for comparison purposes.

3. CHAPTER 3, *IN VIVO* PRELIMINARY SCREENING

3.1. Introduction

As noted in mediaeval literature (Chapter 1 Introduction, section 1.4.5), LL tubers were eaten and chewed whole, thus any effects experienced in humans may be due to one or more of the biologically active compounds acting upon one or more sites. To replicate these effects, an *in vivo* study on a normal rat model was conducted to determine the effects of the tuber on food and water intake. In addition to this, BW and the effect on physical activity were also monitored as it is possible that the effects of the tuber may also influence other aspects of energy metabolism. Sex hormones such as testosterone and estrogen are also known to be involved in the regulation of food intake. Specifically, testosterone is an anabolic steroid and can reduce food intake. Research has shown that castrated rats experience weight gain and hyperphagia which is reversed when administered with testosterone (Begg and Woods, 2013). Due to this, blood serum testosterone levels were also measured post-treatment.

Many plant species have been studied *in vivo* for their ability to control or regulate appetite and for their anti-obesity potential. Due to adverse effects associated with some anti-obesity drugs, many drug trials have opted for natural sources. The anti-obesity action of gingerol, obtained from rhizomes of ginger (*Zingiber officinale*) was investigated in obese, Wistar rats (Saravanan *et al.*, 2014). Saravanan *et al.* found that in addition to a significant ($P<0.01$) reduction in BW, gingerol (at concentrations of 25mg, 50mg and 75mg) was able to significantly ($P<0.01$) reduce serum glucose, insulin and leptin levels in comparison to the HFD control. Furthermore, treatment with gingerol significantly ($P<0.001$) lowered lipid levels in the plasma and liver to near normal levels, and reduced α-amylase and pancreatic lipase activity which was elevated in the HFD group. This group concluded that the anti-obesity mechanism could be due to the inhibition of the metabolism of dietary fats in the intestine, as well as hypolipidemic activities.

Green tea, brewed from unfermented leaves of *Camellia sinensis*, is commonly

associated with appetite suppressing properties and effective weight loss. It is known to have high amounts of polyphenols including epigallocatechin-3-gallate which is thought to be the most bioactive compound present. It is hypothesised that this plant acts on CNS activity increasing energy expenditure and thus promoting fat oxidation (Astell *et al.*, 2013). There have been many studies on this plant, however, the results have been inconsistent. It is also thought that extracts of green tea, as well as black tea and mulberry tea, cause malabsorption of carbohydrates, which could influence blood glucose levels following a meal (Zhong *et al.*, 2006). Kao *et al.,* (2000) investigated the effect of (-)-epigallocatechin gallate (EGCG) from green tea on the food intake and endocrine systems using Sprague Dawley and Zucker rats. A decrease in BW was identified following i.p. injection of ECGC in Sprague dawley rats (administered 82mg/kg BW) as well as lean (administered 81mg/kg BW) and obese Zucker (administered 92mg/kg BW) rats. Furthermore, leptin and testosterone levels were significantly ($P<0.05$) lowered following treatment. Of note, the effects observed were lower or not seen when ECGC was administered orally.

Hoodia gordonii is another very popular plant in terms of its appetite suppressing abilities. *H. gordonii* is a succulent plant, which grows in South Africa and Namibia. It is thought that this plant was used by the Khoisan people to suppress hunger and thirst while on long hunting trips or in times of famine. Fresh stems were peeled and chewed or kept in the buccal cavity before swallowing (Vermaak *et al.*, 2011). In 2002, Van Heerden *et al.* (2002) isolated the steroidal glycoside P57 from *H. gordonii*. Following this, the anti-obesity activity of this compound was published (van Heerden *et al.*, 2007) and approximately 40 more glycosides have been isolated. Van Heerden *et al.* established appetite suppressant activity following an *in vivo* feeding trial. They isolated P57 before testing it on female Wistar rats. The rats were treated on day 1 and monitored for 8 days. They concluded that P57 caused a reduction in food intake and body mass gain, however, there was no effect on water consumption. Following this, MacLean and Luo (2004) hypothesised that this action may be due to altered ATP production/content in the hypothalamus. They also showed that third ventricle administration of P57AS3 to rats caused a reduction in food intake by 40-60% 24h post treatment. Moreover, they found that hypothalamic ATP in rats following 4 days

of moderate food deprivation was reduced. However, administration of their compound, P57AS, (via intracerebroventricular (i.c.v) injection) reversed this reduction in ATP. As a result of this finding, they not only hypothesised a mechanism of action for HG, but also a key process involved in appetite regulation within the hypothalamus. In 2010, there were over twenty patents/registrations on HG relating to appetite suppressant and anti-diabetic activity as well as for the treatment of gastric acid secretion (Tucci, 2010).

Garcinia cambogia (GC) a native plant of Southeast Asia, is widely known as an ingredient in weight loss supplements. The active component, hydroxy citric acid (HCA), has been shown to be a competitive inhibitor of ATP-citrate lyase which catalyses cleavage of citrate to acetyl-coA and oxaloacetate. The inhibition of ATP citrate lyase causes a reduction in acetyl-coA which therefore limits the biosynthesis of fatty acids and cholesterol (Saito *et al.*, 2005). Subsequently this results in the suppression of body fat accumulation. HCA has also been shown to suppress appetite in experimental animals (Greenwood *et al.*, 1981) by inhibition of serotonin (5-HT) uptake and subsequently increasing the availability of 5-HT (Ohia *et al.*, 2002) *in vitro* in brain cortex slices. The majority of animal studies on this compound used a dose of around 50mmol/kg BW, however, this dose was found to be ineffective in suppressing body fat accumulation in obese Zucker rats (Greenwood *et al.*, 1981; Saito *et al.*, 2005). It was concluded that this may be due to the genetics and metabolic characteristics of this strain of animal. These results may also apply to humans who are genetically predisposed to modifications in lipid metabolism. However, results from clinical trials have been controversial with some studies indicating there are no significant differences in treatment groups vs. control groups, while other studies show significant weight loss. Kim *et al.* (2013) showed that there was significant ($p < 0.05$) reduction in visceral fat accumulation and adipocyte size following supplementation of GC, however there were no significant changes in body weight and food intake between the groups. Moreover, there are other issues associated with this natural product including hepatotoxicity. Kim *et al.* (2013) identified that supplementation with GC caused accumulation of collagen in the liver in addition to an increase in mRNA levels of genes associated with oxidative stress and inflammation.

3.2. Aims and Objectives

This chapter will focus on the actions of LL tubers *in vivo* in a normal rat model to provide evidence of the biological activity of the tubers in relation to their traditional use. The specific aims of this chapter are:

1. To determine the effect of the tuber on food intake and water intake. LL tubers have been mentioned numerous times in the literature to be appetite suppressing and to be able to quench thirst, therefore a reduction in food intake and water intake are speculated to highlight these properties.
2. To determine the effect of LL tuber on BW. It is speculated that a reduction in food and water intake will ultimately lead to a reduction in BW.
3. To determine the effect on the physical activity of the rats. Dr Moffat suggested an active component of the tuber was *trans*-anethole (TA), which may be metabolised to amphetamine-like compounds within the body (Sangster *et al.*, 1984). Therefore, an increase in these compounds would be believed to cause an increase in physical activity.
4. To determine the effect of LL tuber on testosterone levels. The HPG-axis closely correlates to food intake and energy regulation; thus the aim was to identify if the treatments had any effect on testosterone levels.

3.3. Materials and methods

3.3.1. Animals

Male Sprague-Dawley rats aged 12 weeks (weighing between 270-349g) were monitored and acclimatised, three weeks prior to treatment. Treatment began when rats were aged 15 weeks. Rats were bred in-house and originally obtained from Charles River Laboratories. Rats were fed *ad libitum* at all times unless otherwise stated and had access to water at all times. Food was supplied in a metal hopper and water in a plastic bottle with an attached stainless steel feeding tube. The rats were housed individually and the housing area was maintained at 21°C ± 2°C with a humidity of 55% ± 10% and a 12h light-dark cycle. Cages were lined with sawdust and were cleaned every third day, or more frequently if necessary. All experimental protocols were conducted in accordance with Home Office UK License PL 60/4562, and animals

were maintained in-house.

3.3.2. Group Allocation and Treatment

The rats were randomly assigned experimental groups based on their BW – there were no significant differences between the mean BW of each group. The study consisted of 18 rats assigned to three groups (n=6 per group). All treatments were administered via oral gavage. Group 1 were treated with 0.9% (v/v) saline as a sham control. Group 2 were treated with 42mg/kg BW of LL tuber, which was prepared using dried, ground tuber mixed in 1ml of deionised (dH_2O) water. The ground tuber did not dissolve in dH2O, however it was sonicated to ensure it was mixed evenly immediately before the animals were dosed. The dosage of tuber was based on mediaeval human dosage guidelines provided by Dr Brian Moffat who suggested one would chew on a small tuber (weighting approximately 1g) and quantified for rats using the calculation below according to Reagan-Shaw *et al.* (2008):

$$\text{HED (mg/kg)} = \text{Animal dose (mg/kg)} \times \left(\frac{\text{Animal } km}{\text{Human } km}\right)$$

The Km values were roughly based on Reagan-Shaw *et al.* (2008) are shown in Table 3.1.

Table 3.1: Km values for Human and Rat based on Reagen-Shaw *et al.* (2008).

Species	Weight (kg)	BSA* (m^2)	K_m factor
Human (Adult)	60	1.6	37
Rat	0.15	0.025	6

*BSA – Body Surface Area

TA was used as a positive control and was given at the same dosage as the ground tuber

– 42mg/kg BW - mixed in 1ml of dH_2O to match the tuber preparation. The rats treated with TA were identified as Group 3.

Rats were treated orally by gavage to ensure the treatment dose reached the stomach. Rats were treated on day 1 and on the final day of the experiment. On the final day, rats were treated with an increased dose of 210mg/kg/BW for both the tuber and TA to maximise the effects, 4h prior to being anaesthetised, which was carried out using pentobarbitone sodium tartrazine (20% v/v, 0.1ml per 100g BW).

3.3.3. Measurement of Experimental Parameters

BW (g), food intake (g) and water intake (ml) were measured on a daily basis. These measurements were taken every 24h ± 30min. The rats were monitored prior to treatment and for 17 days following treatment. All measurements were made using an electronic balance with a tolerance of 1g. Intake of food and water were calculated from the weight and volume consumed from the hopper and water bottle over a period of 24h.

3.3.4. Measurement of Physical Activity

Following administration of the treatments, rats were immediately relocated to a separate room to begin the monitoring of physical activity. The monitoring of physical activity lasted 1h, and the rats had no access to food or water during this period. Rats were carefully placed into one of 4 square plastic boxes measuring 40cmx40cmx40cm. The boxes were not enclosed, but height of each box was large enough to ensure the rats could not escape. The movements of each rat was tracked using an EthoVision tracking system XT v8.5 using centre point detection. This software detects centre of the rat then records movement by drawing a line to represent distance moved. It is also able to measure velocity (cm/s). Rats were monitored for 1h each day for 5 days following treatment. The distance travelled was used as a measure of physical activity to detect an increase or decrease in movement of the rats post-treatment.

3.3.5. Blood Sampling and Preparation

Blood samples were taken from the tail vein at 4h and 24h following treatment. No more than 0.5ml of blood was taken per animal in accordance with local rules on blood sampling. Blood samples were kept at 4°C overnight before being centrifuged at 1500g for 10min to separate the red blood cells (RBC) from the serum. The serum was then removed and stored at -80°C until required. Cardiac blood was taken immediately following anaesthetisation. Blood samples were treated as above and serum was stored at -80°C in 0.5ml aliquots until required.

3.3.6. Testosterone ELISA

Serum testosterone levels were measured using a commercial Testosterone ELISA Kit following the manufacturer's instructions. Briefly, serum samples were diluted 2-fold in assay buffer before being added to a pre-coated (Anti-Rabbit IgG) 96-well plate (50µl) with 100µl of enzyme conjugate. Testosterone standards and positive controls were also added to the 96-well plate simultaneously with the samples. The plate was then incubated on a plate shaker (approximately 200 rpm) at room temperature for 1h. Following this, the plate was washed 3x with wash buffer, before 150µl of 3,3',5,5'-Tetramethylbenzidine (TMB) substrate was added to each well. The plate was incubated for a further 15min until a blue colour developed in the standards and positive control wells. The reaction was stopped by adding 50µl of stop solution. The absorbance was then read at 450nm using a M5 Spectramax plate reader.

3.3.7. Dissection of Animals

Following cardiac puncture, rats were dissected and the hypothalamus was taken for further analysis. To preserve RNA, the hypothalamus was incubated in RNALater solution for 24h before the solution was removed and tissue was stored at -80°C. See Chapter 5 for further experimental work using the hypothalamus.

3.3.8. Statistical Analysis

Statistical analysis was carried out using two-way ANOVA with a Dunnet's post-test using MiniTab 16. Graphs were plotted using GraphPad Prism 4.0. Data represents the mean ± SEM, n=6.

3.4. Results

3.4.1. Effect of treatments on food and water intake

Animals were monitored prior to treatment to give an indication of their food and water intake. Following treatment of either 0.9% (w/v) saline solution (control), 42mg/kg BW of LL tuber, or 42mg/kg BW of TA, animals were monitored for up to 7 days. Figures 3.1 (A) and 3.1 (B) show the effect of treatment with LL tuber and TA compared to the control, on food intake and water intake. On day 1 post-treatment, it is evident that food intake is reduced in all three groups (Figure 3.1 (A)). However, this reduction is not significantly different between groups. By day 2 post-treatment, it appears that food intake returns to the baseline level pre-treatment. On the other hand, water intake increases on day 2 post-treatment (Figure 3.1 (B). At all of the time points investigated, water intake appears to be more variable, with no significant differences between the groups tested. This may be a result of spilling of the water bottle. These results suggest that the treatments given to each animal group had no effect on food intake or water intake up to 7 days post-treatment.

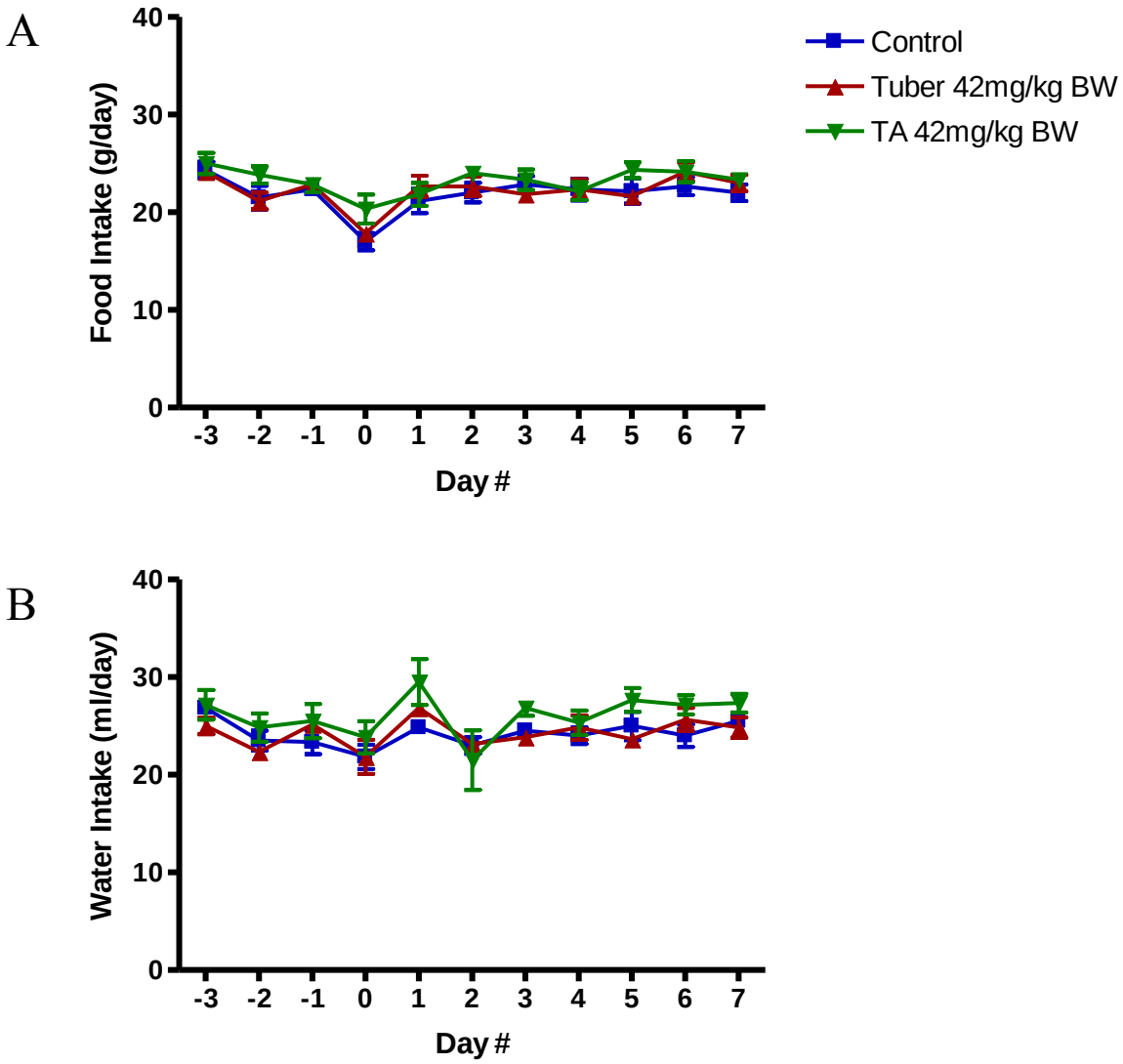

Figure 3.1: Effect of treatments on (A) food intake (g) and (B) and water intake (ml). Treatments were administered on Day 0. Animals were monitored for 3 days prior to treatment. Measurements were recorded 24h ± 30 min.

3.4.2. Effect of treatments on BW

Following administration of each treatment at day 0, there were no significant effects on BW throughout the 7 days (Figure 3.2).

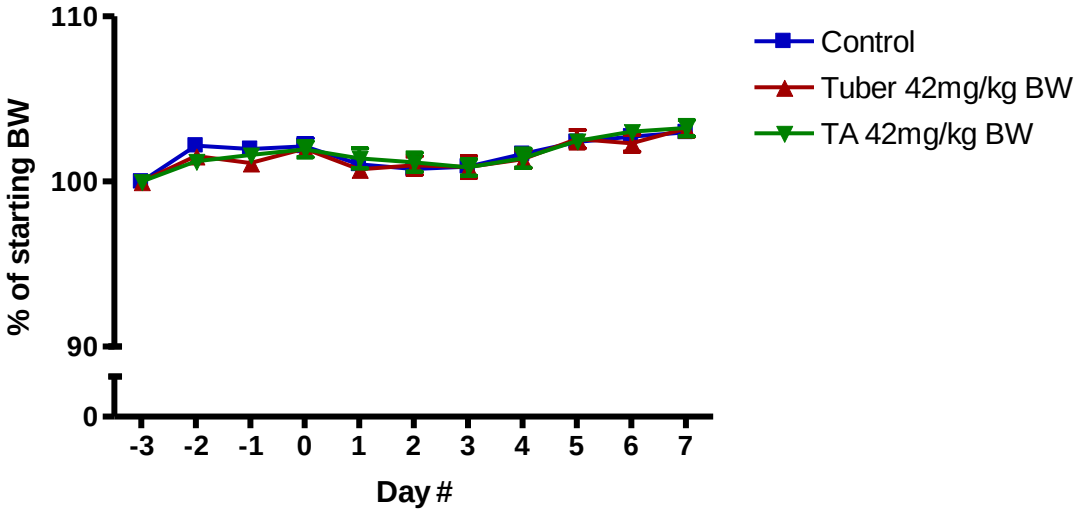

Figure 3.2: Effect of treatments on bodyweight (g). Treatments were administered on Day 0. Bodyweight prior to treatment was used at the initial starting weight. Measurements were recorded 24h ± 30 min.

3.4.3. Effect of treatments on physical activity

Immediately following treatment, and at 24h and 48h post treatment, the physical activity of each group was monitored. This was carried out by monitoring the movement of each animal over a specified period of time. The purpose of this study was to determine if the LL tuber had any effect of the physical activity of the animals. It was hypothesised that if the tuber was to boost energy levels there would be an increase in movement of the animals treated. By monitoring the movement of each group, the total distance can be calculated and compared. As seen in Figure 3.3 (A), immediately following treatment, there were no significant differences between the distances travelled in each group. The initial 10 min time-bin showed a high degree of movement in each group, which gradually decreased towards the end of the experiment. The high level of movement seen in the first 10 min could be attributed to

'fight or flight' mode experienced by the animals due to a change in their surroundings. The survival instinct for rats would be to avoid open spaces, thus as they adapt to the new environment, their movement is increased. Their movements gradually decreased as the animals became more comfortable with the new environment. Again at 24h (Fig 3.3 (B)) and 48h (Fig 3.3 (C)) post treatment, there were no significant differences in the movement of each group. However, a similar pattern was evident, with the initial 10 min showing a higher degree of movement which then decreased over time.

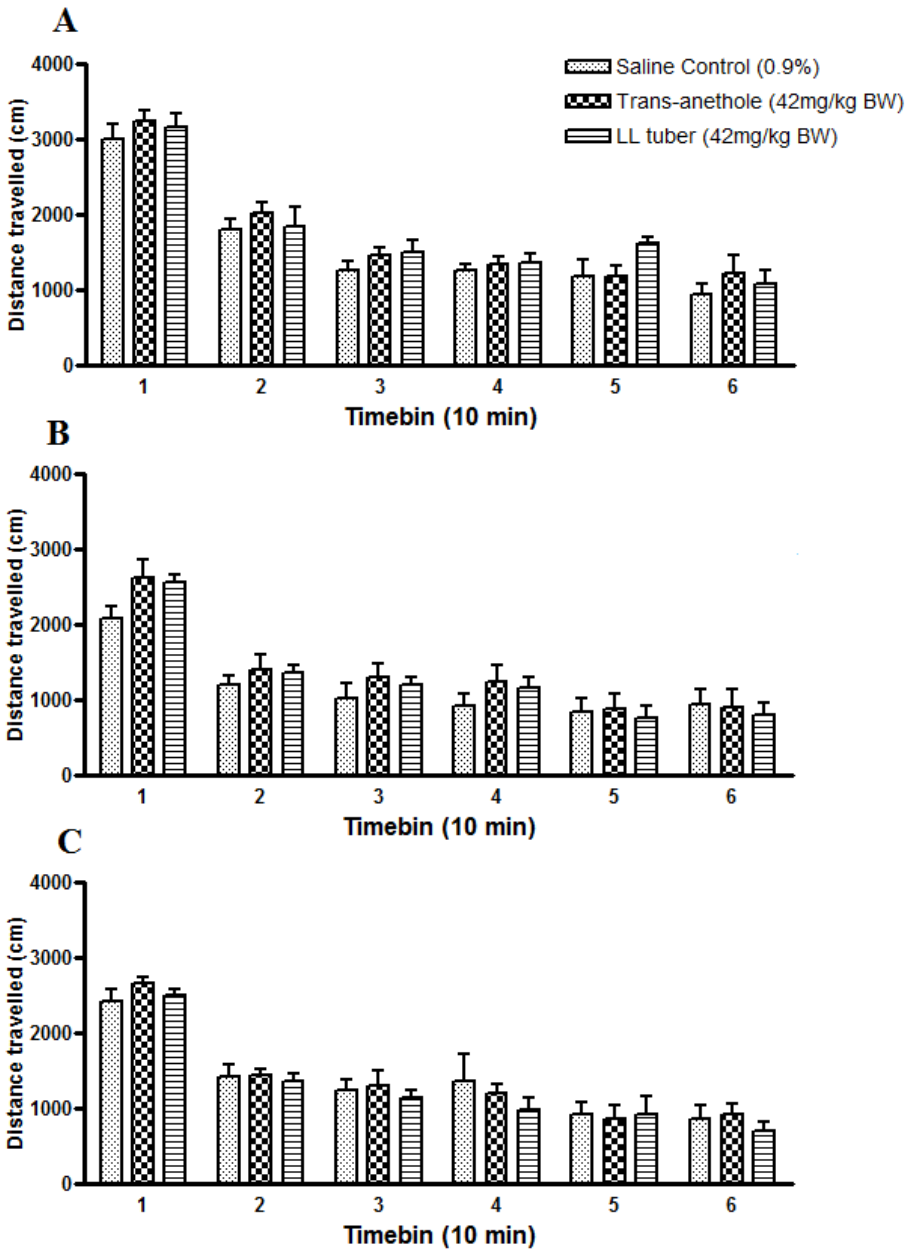

Figure 3.3: Effect of treatment on physical activity. Distance travelled was taken as a measure of physical activity immediately following treatment. (A) Immediately post-treatment of control, tuber and TA, (B) 24h post treatment, and (C) 48h post-treatment.

3.4.4. Effect of treatments on blood serum testosterone levels

Serum testosterone levels were measured in the blood serum at various time points post-treatment. Serum was separated from blood samples taken at 4h, 24h, and at the end of the experiment via cardiac puncture. Subsequently, serum testosterone levels were measured using a commercial ELISA kit. Figure 3.4(A) shows results of the 4h and 24h blood samples post-treatment for the control group and two treatment groups, tuber treated and TA treated. At 4h post-treatment, there were no significant differences between the testosterone levels of each group, however, although not significant, it appears that TA increased testosterone levels compared to the control group. Similarly, there were no significant differences at 24h post treatment between each of the three groups. In terms of changes between 4 h and 24h, there appeared to be more variability in the measurements for the control group at 24h in comparison to 4h. On the other hand, at 24h for the tuber and TA group, the results appeared less variable. For the TA group, there was a significant ($p<0.05$) decrease in testosterone levels at 24h compared to 4h post-treatment.

The final blood sample was taken via cardiac puncture, 4h following a final treatment. The treatment administered to each group was 5 times more concentrated (210mg/kg BW compared to 42mg/k BW) than the previous treatment in the hope of inducing a larger response. The results of the higher dose on testosterone levels 4h post-treatment are shown in Figure 3.4(B) There was a significant reduction in blood serum testosterone levels following treatment with LL tuber in comparison to the control. Thus, it may be possible that a dose of 42mg/kg BW was too low to see any physiological changes. TA did not have any significant effect on serum testosterone levels at a higher concentration.

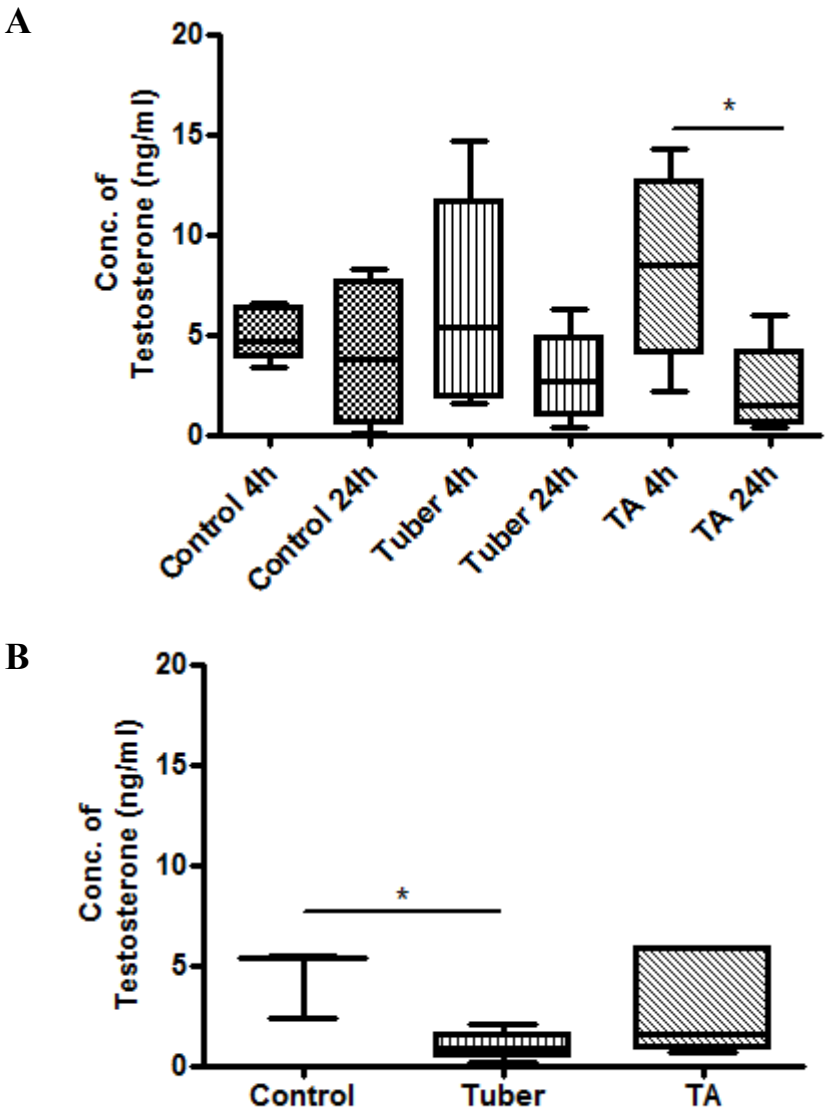

Figure 3.4: Effect of two different tuber concentrations (42 mg/kg and 210mg/kg) on serum testosterone testosterone (ng/ml). (A) Samples were taken at 4h and 24h post-treatment from animals treated with either 0.9% (v/v) saline, 42mg/kg BW tuber or 42mg/kg BW TA. (B) Samples were taken at 4h post-treatment from animals treated with either 0.9% (v/v) saline, 210mg/kg BW tuber or 210mg/kg BW TA. n=5 for control, n=6 for tuber treated group. Data represents mean ± SEM. *P<0.05, vs Control.

3.5. Discussion and Conclusions

At a dose of 42mg/kg BW, LL tubers and TA did not have an effect on food intake, water intake, BW or physical activity. However, this does not conclude that the tubers do not affect appetite or food intake within the central or peripheral pathways. There may be several reasons for the above results. Firstly, the timing of treatment and/or measurements. The measurements were taken once daily (24 h ± 30 min) thus any effects caused before the 24h point would not have been observed. Moreover, treatments were given in the light phase (between 8am-6pm). Rats are nocturnal animals that usually eat in the dark phase (6pm-8am), thus it is also possible that due to this, any effects of the treatments were not seen due to the delay in eating. The effects of the tuber or TA may be immediate and could have diminished by the time the animals began to eat. Kim *et al.* (2016) conducted a study to look at the effect of metformin on neuronal activity in mice fed a high fat diet. This study looked at C57BL/6 mice, which were fed a high fat diet before being treated with 300g/kg BW metformin. Treatments were given once a day for 1 day or 3 days, by oral gavage immediately prior to the dark cycle (6pm). The group treated once with metformin showed no significant change in BW. However, the group treated for 3 days showed a significant decrease in BW compared to both the control and the group treated only once. Batterham *et al.* (2003) showed that an intraperitoneal (ip) injection of PYY_{3-36} was able to significantly decrease food intake in rats. However, as mentioned above, the timing of the injection was an important factor - PYY was administered before the dark phase. Halatchev *et al.,* (2004) were also able to show this reduction in food intake following ip injection of PYY to rats. However, they also identified that in stressful conditions, there was no reduction in food intake. Thus, the timing and number of treatments seems to be important, as well as the stress levels of the rats, and these may limit the interpretation of data in this study.

Secondly, the dosage may be too low to show physical effects on BW, food intake and water intake. The dose was calculated based on knowledge of the traditional usage of the tuber where a ‘hazelnut size amount’ of tuber was chewed on. However, it is not possible to know whether tubers today are of similar dimensions as there are no

measurements published in the mediaeval literature. The dose given to the animals was increased by 5-fold before anaesthesia to maximise the effect of the tuber components within the tissues. However, it was not possible to determine the effects of the higher dose on BW or food and water intake due to time constraints.

Further to this, the method of delivery may not be optimal. Traditionally, the tuber was chewed on, thus, it is possible that the active components are absorbed through the buccal cavity rather than in the stomach. The bioavailability of the tuber components may be higher in the oral cavity in comparison to the stomach. Furthermore, the metabolism of such compounds could also be affected depending on the delivery method. Glycyrrhizin has poor oral bioavailability, however after oral ingestion in humans, glycyrrhizic acid is hydrolysed to glycyrrhetic acid by bacteria in the intestine. Glycyrrhetic acid is a more potent inhibitor (200-1000 times more potent) of 11-β-hydroxysteroid dehydrogenase than glycyrrhizic acid (Omar *et al.*, 2012). This emphasises the importance of the metabolism of a drug. Kao *et al.*, (2000) conducted a study looking at natural products from green tea – ECGC. It was noted that the method of delivery had an effect on the results. If administered i.p. at 85mg/kg BW, there was a reduction in BW by approximately 15-21%, relative to the starting weights. However, this reduction was not evident, or was much less, when ECGC was administered orally. Ip administration is useful for drugs which are degraded in the GIT, or are not fully absorbed. This method gives higher bioavailability, however it is not a clinically relevant route of administraion. Kao *et al.* administered purified ECGC for 7 days before measuring BW, whereas LL tuber and TA were administered once and monitored daily to reflect the traditional usage. Saravanan *et al.* (2014) looked at the anti-obesity effect of gingerol. They administered gingerol at various concentrations (25, 50 and 75mg/kg BW) over a period of 30 days using an intragastric tube. Thus, future work could include a longer trial with more frequent doses.

Moreover, LL tuber is a mixture of components rather than a purified compound, thus higher doses may increase the dose of any active components allowing specific effects to be observed more easily. Future work in this area would include dose-response

experiments as well as optimisation of the delivery method. It may be possible to produce oral films with LL tuber material which could be placed within the oral cavity of the animal. Another method which could be investigated is to add the tuber to the normal rat chow to maximise the chewing and thus mimic the traditional method of delivery. Additionally, tuber extracts or pure compounds of the tuber could be tested alongside the whole tuber.

The traditional usage of LL tuber is based on human consumption, therefore using an animal model may not result in the same effects. One reason for this may be due to the gut microbiota. Gut microbiota plays an important role in the bioavailability of therapeutic drugs and has been attributed to the mechanism of action of various natural products, and has also been linked to several conditions including metabolic syndrome, T2D and obesity (Lecomte *et al.*, 2015). Moreover, it has been suggested that gut microbiota plays a role in the physiology of eating disorders as it is able to partially mediate the control of energy and metabolism (Queipo-Ortuño *et al.*, 2013). Chen *et al.* (2016) conducted an informative review of the role of the gut microbiota in terms of bioavailability of traditional herbs delivered orally.

Several clinical and non-clinical studies show the effect of traditional herbs and extracts on the gut microbiota, and in turn, on several disease states. For example, Chang *et al.* (2015) demonstrated that a water extract of a well-known Chinese Traditional Medicine, *Ganoderma lucidum* (GL), was able to modulate the gut microbiota, and subsequently reduce obesity in mice. Mice fed a high fat diet supplemented with an 8% GL extract showed significantly less weight gain than mice fed a high fat diet with no supplementation. Chang *et al.* (2015) attributed this anti-obesity effect to the change in microbes in the gastrointestinal tract as a result of the natural product extract. Further to this, Zhang *et al.* (2015) showed that two clinically effective drugs, berberine and metformin, used in the treatment of diabetes and obesity, also modulate the gut microbiota in favour of the host, male Wistar rats. It is speculated that the gut microbiota plays an important role in the mechanisms of action of both of these drugs. Kostic *et al.* (2013) highlighted the different composition of microbiota

present in various species, with mice and humans differing, however rats were not mentioned in the review. Lecomte *et al.* (2015) suggested that rats are the ideal model for studying gut microbiota as the microbes of rats and humans consist of the same four predominant bacteria phyla – Bacteroidetes, Firmicutes, Actinobacteria and Proteobacteria. Although this may be true, there are over 10^{14} bacteria and over 1000 different species present within the gut, thus there will still be differences between both species. Further to this, the diet of humans and rodents is entirely different with rodents being herbivores and humans omnivores. This difference would also result in different gut microenvironments, as well as differences in digestion and metabolism of food.

In terms of the effect of the treatments on testosterone levels, 42mg/kg BW of LL tuber had no significant effect at 4h or 24h post treatment. At 24h post-treatment, TA significantly ($P<0.05$) reduced serum testosterone levels in comparison to the 4h post-treatment timepoint. When increasing the dose to 210mg/kg BW, a significant ($P<0.05$) reduction in serum testosterone levels was seen in the tuber group compared to the control. The effects of LL tuber and TA do not appear to be similar in this experiment, thus this suggests the effects are not due to TA present within the tuber. However, the quantity of TA present in the tuber remains unknown and therefore it was not possible to give an equivalent dose. To speculate, it is possible that in reducing testosterone levels, LL tuber indirectly affects food intake and energy regulation. Kao *et al.* (2000) showed a reduction in testosterone levels by up to 70% in male Sprague Dawley rats administered EGCG. These results were in combination with a reduction in BW as described above. This further reiterates that the dose of LL tuber may have been too low to exert physical effects at the lower dose of 42mg/kg BW as the change in testosterone levels were not apparent at this dose. Moreover, decreases in testosterone levels can lead to increased body fat and reduced muscle mass in men (Blouin *et al.*, 2008).

Due to the lack of findings in the *in vivo* experiment, the next step was to go back to the tuber itself. It is possible that the model used was not optimal, and therefore it was anticipated that looking at the chemical constituents of the tuber would provide insight

into the potential biological activity. The following chapter details the extraction and isolation of compounds present in the tuber, as well as preliminary *in vitro* screening experiments.

4. CHAPTER 4, SOXHLET EXTRACTION AND *IN VITRO* ANALYSIS

4.1. Introduction

There are various methods available to extract natural products depending on the physiochemical properties of the compounds being targeted. In general, the main conventional methods used to extract compounds within a laboratory setting include cold pressing, Soxhlet solvent extraction, maceration and hydrodistilliation (Azmir *et al.*, 2013). Over recent years, other modern techniques have also been used such as supercritical fluid extraction and pressurised fluid extraction. In all cases, researchers are constantly attempting to increase the yield, reduce the extraction time, decrease the volume of solvent used and improve the quality of the end product (Uribe *et al.*, 2011). One of the benefits of researching compounds isolated from plants is that the compounds present are produced within a live cell rather than being designed synthetically, and thus their chemical structure is designed specifically to interact with biological molecules such as lipids, proteins and carbohydrates. Therefore, when transferred to another organism, they have the potential to effectively bind to targets and either inhibit or enhance specific processes (Sadot, 2014). This property makes natural products excellent leads for drug development. Following extraction and isolation of natural products, preliminary screening methods can be used to identify possible biological activity (Figure 4.1).

Initial screening bioassays can be of two different forms: (i) cell-based screening and, (ii) biochemical assays. One of the most common cell-based screening assay, which is non-expensive, reliable and can be adapted to HTS formats, is the Alamar blue® (resazurin) cell viability assay (Baker *et al.*, 2007). Resazurin is a blue dye which is irreversibly reduced to a pink, highly fluorescent compound called resorufin. It effectively measures metabolic activity of cells which is proportional to the number of alive cells present (Baker *et al.*, 2007). This assay can be used to test initial toxicity of natural product extracts or isolated compounds against cell lines *in vitro*. Furthermore, this assay can also indicate potential anti-cancer activity if extracts or compounds are identified as killing cancer cells, but not the normal cell equivalent. The MTT (3-(4,5-

dimethylthiazol-2-yl)-2,5-diphenyltetrazolium bromide) tetrazolium assay may also be used in this way, however, resazurin has been found to be more sensitive (Hamid *et al.*, 2004). MTT is converted to formazan following incubation with the cells. The quantity of formazan is proportional to the number of viable cells. Formazan accumulates as an insoluble precipitate which then requires solubilisation prior to reading the absorbance (Boncler *et al.*, 2014). Resazurin is also the favoured assay as it can be multiplexed with other methods such as measuring caspase activity to gain more insight into mechanisms of action of the samples.

Although these methods are commonly used, there are various issues associated with them. Firstly, the amount of resorufin/formazan product is proportional to the number of metabolically active cells which are in log phase growth. However, if cells become over confluent (adherent cells), growth may slow down due to contact inhibition, therefore reducing metabolic activity. Subsequently, the amount of resazurin/MTT reduced will be lower. This then causes a loss of linearity between the absorbance and the cells number. Moreover, improper culture of cells, or depletion of essential nutrients may also reduce cell growth and metabolism. Metabolic activity can also vary between cell types, and during the life cycle of a cell (Boncler *et al.*, 2014). Thus, proper controls must be included in each experiment as results cannot be directly compared without normalising against a control. MTT, as well as the solvents used to solubilise the formazan crystals, are also toxic to cells at high concentrations, therefore optimisation of the concentrations used in the assay is imperative. Lastly, reducing compounds can interfere with reduction assays. For example, ascorbic acid can reduce MTT salts non-enzymatically, leading to increased signal in the assay, which then leads to false positive results. Due to this, samples must be assessed with and without cells to establish if the compounds present interfere with the assay results.

Biochemical assays can exist in various forms, with one of the main methods using enzymes. A key aspect of drug discovery is the identification of compounds with enzyme inhibitory activity (Ata *et al.*, 2011). Enzymes are vital in many biological and physiological processes including metabolism, cell cycling, cellular signal

transduction and cellular development. If these systems fail, this often leads to disease of which the root cause could be an overexpression or hyper activation of the enzyme involved. Understanding such diseases, and the mechanisms behind the dysfunction, has lead scientists to the discovery of enzyme inhibitors which can then be used therapeutically. One such inhibitor which is currently used clinically is galanthamine. Galanthamine is a potent acetylcholinesterase (AChE) inhibitor used in the treatment of Alzheimer's disease (Ata *et al.*, 2011).

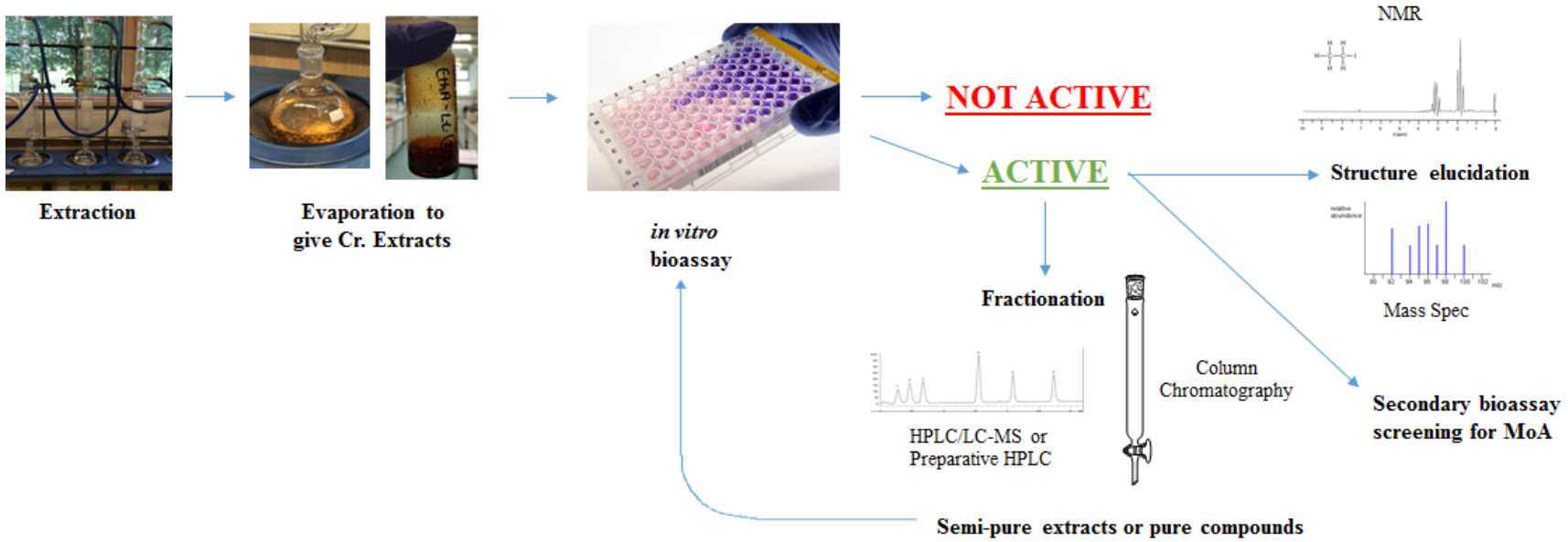

Figure 4.1: Screening process for Natural Products from extraction to structure elucidation. Cr. extracts are screened for potential activity before being subject to further fractionation and purification. Various techniques are used in combination such as column chromatography, high performance liquid chromatography (HPLC), liquid chromatography-mass spectroscopy (LC-MS), mass spectroscopy (MS) and nuclear magnetic resonance (NMR). Abbreviations: Cr. extracts – crude extracts; MoA, mechanism of action.

To identify the therapeutic potential of LL extracts in terms of obesity, as well as associated disorders such as diabetes, various *in vitro* assays were conducted. Cytotoxicity of the extracts on adipocytes and neuronal cells were conducted, as well as various enzyme based assays including dipeptidyl peptidase IV (DPP IV or DPP 4), Protein-Tyrosine-Phosphatase 1B (PTP1b), α-amylase, α-glucosidase and pancreatic lipase.

DPP IV is a pleiotropic enzyme which cleaves and inactivates various peptide hormones. It is involved in immune functions, satiety and regulation of hunger, inflammation and psychomodulation. Moreover, it has also been shown to be increased in obese patients in comparison to normal patients and has a positive correlation with BMI (Stengel *et al.*, 2014). Two intestinal hormones which are inactivated by DPP IV are glucagon-like peptide 1 (GLP-1) and glucose-dependent insulinotropic polypeptide (GIP) (Green *et al.*, 2006) (see Figure 4.2). These hormones are two of the most important incretins (metabolic hormones) and they have gained wide interest due to their potent insulin secretory activity following oral administration of glucose, and subsequent lowering of plasma glucose (Ahrén, 2007). In addition to this, GLP-1 can decrease gastric emptying intestinal motility thus reducing appetite. Through these actions, GLP-1 contributes to the ileal break – an inhibitory feedback mechanism with the main purpose of optimising nutrient absorption (Dailey and Moran, 2013). Furthermore, GLP-1 is associated with increased thermogenesis of brown adipose tissue (Beiroa *et al.*, 2014), thus, an increase in this peptide-hormone could potentially help in the treatment of obesity as well as diabetes. When GIP and GLP-1 enter the capillaries, they are rapidly degraded by DPP IV which is present on capillary walls throughout the body. Thus, the inhibition of DPP IV would lead to an increase in the levels of GLP-1 and GIP. Therefore, the search for new DPP IV inhibitors is gaining vast interest. There are many examples of clinically used DPP IV inhibitors including sitagliptin, vildagliptin, and saxagliptin (Saleem *et al.*, 2014). In addition, there are many plant extracts which can inhibit DPP IV including from *Fagonia cretica* and *Hedera nepalensis* (Saleem *et al.*, 2014).

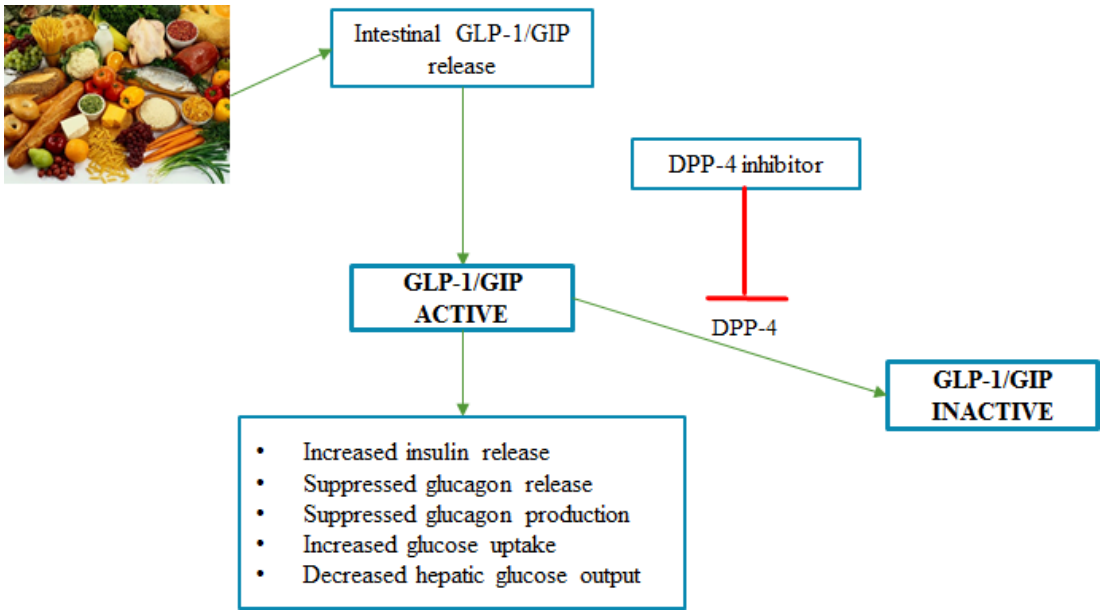

Figure 4.2: Mechanism of action for DPP IV inhibitors. GLP-1/GIP is released following a meal and are subsequently inactivated by DPP IV. Inhibition of DPP IV would thus block the inactivation of these molecules, leading to the increase and/or decrease of key physiological pathways associated with obesity and diabetes.

PTP1b is also being investigated as a target for the treatment of obesity and T2D. It is thought that PTP1b is an important negative regulator of insulin signalling by de-phosphorylating the insulin receptor (IR) and its substrate, insulin receptor substrate-1, (IRS-1). Additionally, PTP1b is a negative regulator of leptin signalling (Cheng *et al.*, 2002; Koren and Fantus, 2007). PTP1b expression and activity has been shown to be increased in obese rodents and in obese, insulin-resistant humans. PTP1b deficient mice show an increase in insulin sensitivity, and neuronal-specific PTP1b knockouts have remarkably reduced weight and adiposity plus increased energy expenditure. Furthermore, PTP1b whole-body knockout mice show resistance to high-fat diet induced obesity (Elchebly *et al.*, 1999). This indicates that PTP1b may be involved in the regulation of body mass and adiposity through effects on the brain (Lantz *et al.*, 2010). Lantz *et al.* hypothesised that fat specific weight loss after administration of an anti-obesity drug (trodusquemine) may be due to the inhibition of PTP1b. They also observed decreased levels of leptin and insulin in the plasma of treated animals.

However, it has proved difficult to find safe and effective inhibitors selective to PTP1b. The active sites of PTP1b are highly conserved thus inhibitors of PTP1b may also inhibit other PTP family members thus causing off-target effects (Vieira *et al.*, 2017). A study by Marrero-Faz and Harvey (2015) showed the potential of natural product extracts in the inhibition of this enzyme. Several aqueous extracts from *Persea Americana* (commonly known as Avocado) a Cuban plant recognised for its nutritional and medicinal properties, effectively inhibited PTP1b in a dose-dependent manner. Many PTP1b inhibitors have progressed to clinical trials, however to date, very few PTP1b inhibitors have successfully passed Phase II.

The inhibition of α-glucosidase has also been investigated as a treatment for T2D and obesity. α-glucosidase is an intestinal cell membrane bound enzyme (Atta-ur-Rahman *et al.*, 2007). It is essential for the degradation of glycogen to glucose leading to postprandial hyperglycaemia. Inhibition of α-glucosidase slows digestion and absorption of carbohydrates, thus delaying the postprandial rise in blood glucose (Dong *et al.*, 2012) and subsequent hyper-insulinaemia. Current therapeutic drugs include acarbose and miglitol (shown in Figure 4.3). Acarbose is the most commonly used inhibitor, however it is reported to be associated with various side effects including abdominal discomfort, diarrhoea and flatulence (Mogale *et al.*, 2011). Of note, acarbose is a natural product produced by fermentation of *Actinoplanes* sp (de Sales *et al.*, 2012). The inhibition of α-glucosidase has also been associated with reduced weight gain following re-feeding of fasted rats. The period of re-feeding is normally associated with increased weight gain without an increase in food intake. However, Kotler *et al.* (1984) demonstrated in rats that acarbose given together with their normal diet, reduced weight gain compared with rats fed a normal diet without acarbose.

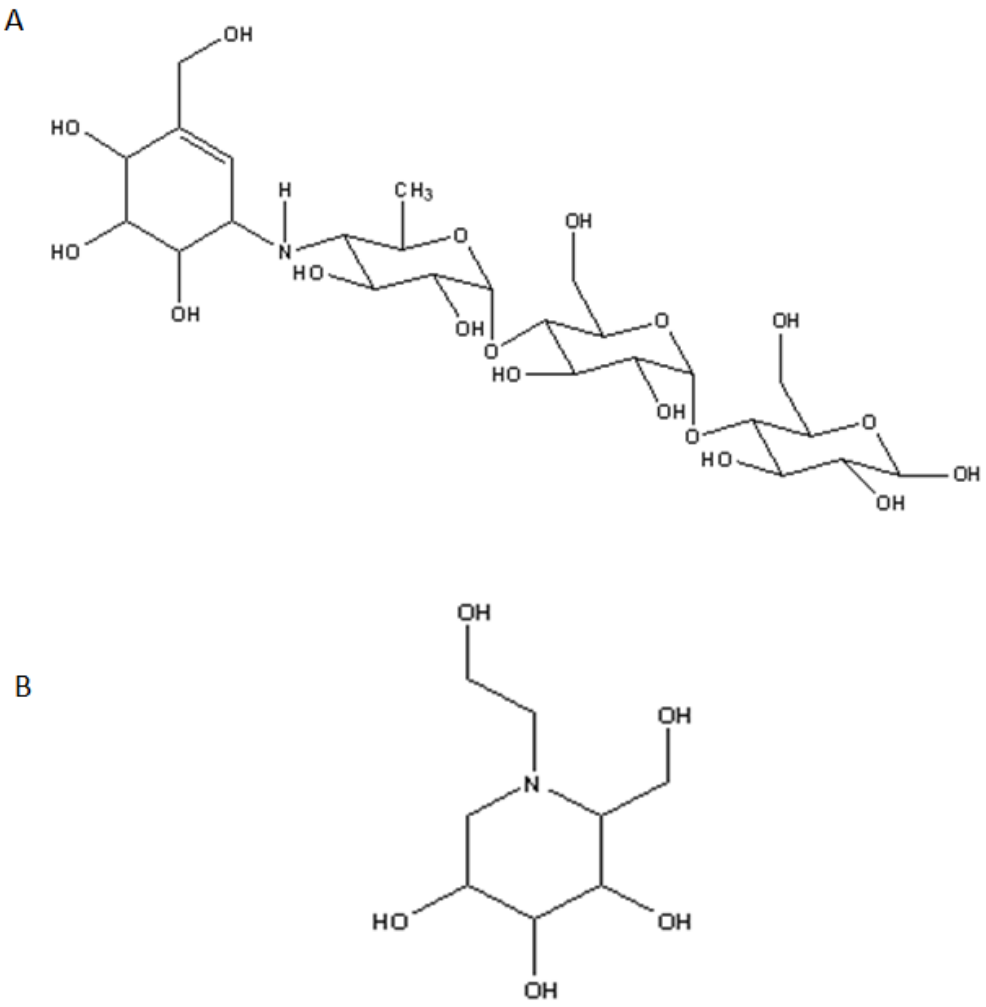

Figure 4.3: Structures of α-glucosidase inhibitors. (A) acarbose and (B) miglitol.

With similarities to α-glucosidase, α-amylase is involved in catalysing the hydrolysis of starch into free sugar molecules, thus adding to the post-prandial glucose spike. Hence, inhibition of this enzyme would significantly reduce the increase in blood glucose and has been investigated as a target enzyme for the treatment of T2D. Acarbose is also an inhibitor of α-amylase. In addition to the anti-diabetic effects of α-amylase inhibitors, some have also been shown to have potential anti-obesity properties. It has been suggested that by blocking α-amylase, there would be a reduction in carbohydrate metabolism, which could potentially mean a decrease in the number of calories absorbed, leading to weight loss. Various studies have looked at the

effect of inhibiting α-amylase on weight loss, however, most examined plant extracts as a whole, specifically from *Phaseolus vulgaris,* rather than specific compounds. Thus, it cannot be concluded that the results are due to inhibition of α-amylase. Such studies have been reviewed by Barrett and Udani (2011).

One of the main target enzymes for the treatment of obesity is pancreatic lipase. Orlistat, a semi-synthetic derivative of the natural product lipstatin, is a US Food and Drug Administration (FDA) approved anti-obesity drug which acts through inhibiting pancreatic lipase (Birari and Bhutani, 2007). Lipases are responsible for the digestion of fats including triacylglycerols and phospholipids. Thus, inhibition of this enzyme would reduce fat digestion. Lipid metabolism is carefully controlled to maintain homeostasis. If this balance is lost, hyperlipidaemia or obesity may occur which can also lead to various other health conditions including diabetes, hypertension, atherosclerosis and stroke. Thus, controlling the metabolism of lipids is crucial. Pancreatic lipase inhibitors are currently being studied for this reason with many natural products from plants being investigated including saponins, terpenes and polyphenolics (Birari and Bhutani, 2007).

In obesity, low-grade inflammation in adipose tissue is thought to be caused as a result of changes in adipokines as well as other cytokines. This state of inflammation increases the development of several secondary diseases such as T2D, metabolic syndrome and hypertension. Tumour necrosis factor–alpha (TNFα) is highly involved in this inflammatory process, thus the effect of the extracts on TNFα release from macrophage-like cells was also investigated. TNFα is known to cause cachexia in cancer patients and patients with severe infections. Romanatto *et al.* (2007) showed that TNFα causes a reduction in food intake (by 25%) 12h post-treatment. Additionally, cytokine induced suppression of appetite has been observed during cytokine immunotherapy in humans and when administered peripherally or in to the brain, cytokines such as TNFα and IL-6 can induce anorexia (Berthold-Losleben and Himmerich, 2008). As TNFα is widely involved in various aspects of the HPA axis and neuroendocrine system, the effect of the tuber crude (cr.) extracts on the release of

cytokine was measured.

Overall, the appetite suppressing capabilities of LL tubers may be a result of one or more of the above mechanisms of actions. The cr. extracts were tested *in vitro* to establish potential biological activity which could then act as a guide for further investigation.

4.2. Materials and methods

4.2.1. Soxhlet Extraction of LL Tuber

A Soxhlet extraction was carried out on 131.9g of dried, ground tuber material (collected by Mark Goff in Reading in September 2014). Before grinding, tubers were washed briefly in H_2O before being air-dried until required. Grinding was carried out using a clean coffee grinder until a homogenous powder was obtained. The powder was then added to cellulose extraction thimbles (single thickness, 123mm) before being topped with a small piece of cotton wool. Soxhlet extraction was started using hexane (LL-Hex) (HPLC Grade) followed by ethyl acetate (LL-EthA) (HPLC Grade), and methanol (LL-M) (HPLC Grade). All solvents were run at approximately 40^{o}C. Anti-bumping granules were added to the extraction flask to prevent the liquid from bumping as it heated. Each solvent ran for approximately 22-24h for hexane and ethyl acetate, and approximately 35h for methanol. The solvents were then evaporated using a rotatory evaporator (set to 40^{o}C), which resulted in the remaining cr. extracts. During evaporation, if crystals or solid particles formed within the solution, these were filtered and kept separate. Thus, for some solvents, there are more than one cr. extract.

LL-Hex-1 resulted from the evaporation of hexane following Soxhlet extraction. While performing rotatory evaporation on this cr. extract, solid particles formed on the sides of the flask. These solid particles were dissolved and collected separately (LL-Hex-2). LL-EthA-2 was obtained as a cr. extract following rotatory evaporation of the ethyl acetate solvent fraction. The solvent fraction was cooled overnight which resulted in the formation of a white, cloudy-like substance forming within the extract

which was separated by filtration and air-died. The filtrate was also retained, however, both cr. extracts were kept separate. A summary of the cr. extracts is outlined in Table 4.1.

Table 4.1: Labels assigned to Crude Extracts

Sample ID	Solvent
LL-Hex-1	Hexane
LL-Hex-2	Hexane
LL-EthA-1	Ethyl Acetate
LL-EthA-2	Ethyl Acetate
LL-M	Methanol

4.2.2. Fractionation of LL-EthA Crude Extracts

VLC was used for the rapid fractionation of ethyl acetate cr. extract, LL-EthA-1. Fractionation of this specific extract was carried out as a result of potential biological activity of this extract (See Chapter 4, Section 4.2.7).

A large vacuum column was prepared using a sintered glass funnel, which was packed with TLC grade silica [Silica gel 60H, gel particle size was less than 45μm] under vacuum. The silica gel was compressed using a glass stopper and filter paper was placed on top. To wet the silica and to ensure uniform packing, 80% (v/v) hexane with 20% (v/v) ethyl acetate was run through the column before adding the sample. The sample in powder form was loaded in a uniform manner onto the top of the silica gel column. The powdered sample was prepared by completely dissolving LL-EthA-1 in minimal solvent (methanol and ethyl acetate) before being added to silica gel and allowed to dry under a fume hood. This was then ground into a fine powder to be used in the VLC column. Gradient elution (using approximately 500 mL of each solvent),

shown in Table 4.2, was used and the column was allowed to dry out following each elution.

Table 4.2: Solvent system used in vacuum liquid chromatography with fraction ID codes

Fraction ID	Solvent System (v/v)
EV1	50% hexane, 50% ethyl acetate
EV2	50% hexane, 50% ethyl acetate
EV3	50% hexane, 50% ethyl acetate
EV4	20% hexane, 80% ethyl acetate
EV5	100% ethyl acetate
EV6	70% ethyl acetate, 30% methanol
EV7	70% ethyl acetate, 30% methanol
EV8	70% ethyl acetate, 30% methanol
EV9	60% ethyl acetate, 40% methanol

The cr. extracts and fractions from chromatography were tested in *in vitro* biological screening assays.

4.2.3. Characterisation of Crude Extracts with NMR and LC-MS

Approximately 30-50mg of each extract was prepared for NMR in a deuterated solvent (for example, D_2O, CDC^{l3}, and DMSO-D_6) before being transferred to borosilicate glass NMR tubes (5mm). NMR spectra were obtained using either a JEOL (JNM LA400) or a 9.4T Bruker UltraShield AV3 400 operating at 400 MHz for ^{1}H and 100MHz for ^{13}C and all spectra obtained were processed using either TopSpin (Bruker) or MestReNova software (version 6.1.0-6224).

^{1}H-NMR was performed on all samples to identify the type and number of compounds present. Further analysis in the form of 2D-NMR was carried out to assist in structure elucidation. These experiments included COSY (COrrelation SpectroscopY), HMBC (Heteronuclear Multiple Bond Coherence) and HSQC (Heteronuclear Single Quantum Coherence). Spatial structural information was obtained using NOESY (Nuclear Overhauser Enhancement SpectroscopY) or TOCSY (Total Correlation SpectroscopY) experiments. 2D-NMR were carried out using an 11.7 T Oxford AV500 operating at 500MHz or an Avance-III 600 operating at 600MHz.

LC-MS was also used to determine the possible molecular weights and molecular formulae of selected cr. extracts. Cr. extracts were ran on a Reverse Phase C18 Column (ACE 3 C18 HICHROM, DV12-7228, 150x4.6mm, 3µM particle size) at a concentration of 0.1mg/mL in acetonitrile/water (see Table 4.3). Liquid chromatographic separation was carried out on an Accela HPLC system interfaced to an Exactive Orbitrap mass spectrometer as detailed in Table 4.4. The mobile phase consisted of 0.1% (v/v) formic acid in water purified by Direct-Q 3 Ultrapure water purification system (Solvent A) and 0.1% (v/v) formic acid in acetonitrile (HPLC Grade) (Solvent B). The solvent method is shown in Figure 4.4. The electrospray ionisation (ESI) interface was operated in a positive/negative dual polarity mode. Full scan data was obtained in the mass-to-charge ratio (m/z) range of 75 to 1500 for both ionisation modes. The resulting data were recorded using the XCalibur 2.1.0 software package.

Table 4.3: Cr. extract sample preparation details for use in LC-MS.

SAMPLE ID	SOLVENTS USED
LL-Hex-1	Acetonitrile/Water (50:50)
LL-Hex-2	Acetonitrile/Water (50:50)
LL-EthA-1	Acetonitrile/Water (50:50)
LL-EthA-2	Acetonitrile/Water (50:50)
LL-M	Water (100%)

Each sample was diluted to 0.1 mg/mL in the solvents detailed below depending on the solubility of the extract.

Table 4.4: Chromatographic method conditions for cr. extract profiling. Details of the column used in LC-MS as well as the experimental conditions.

COLUMN ID	ACE 3 C18 HICHROM, DV12-722
Column length	150x4.6mm
Particle size	3µm
Flow Rate	0.3ml/min
Injection Volume	10µl
Time	40 min
Mass Range	75.00-1500.00

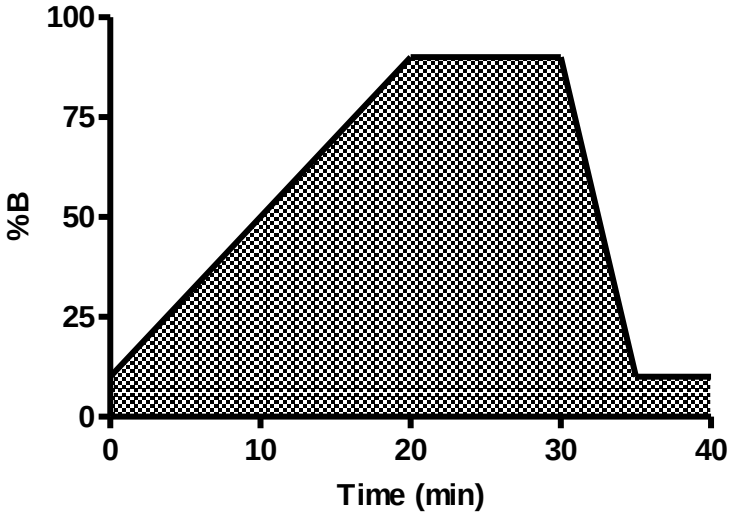

Figure 4.4: Solvent system used for LC-MS profiling of the cr. extracts of LL. %B refers to the percentage of organic solvent used. The solvent system begins with a low percentage of organic solvent and increases in a gradient format for 20 min where it reaches 80% B. The solvent remains at a constant concentration for 10 min where it then decreased over the next 5 min down to 10% B. It then remains at 10% B for the final 5 min.

Data analysis for each crude extract was carried out using MZmine 2.14 software. The extracted ions, and their corresponding m/z values and retention times were processed in an Excel macro, which was prepared in-house. This Excel macro facilitates identification by completing library searches using the DNP. The list of compounds obtained were then analysed manually in comparison to the literature.

4.2.4. Gas Chromatography Mass Spectroscopy (GC-MS)

4.2.4.1. Sample Preparation

LL tuber was dried and ground as in section 1.3.5 before being mixed in ethyl acetate (HPLC Grade) to give a concentration of 100mg/mL. The mixture was allowed to macerate for 3h. TA was prepared in ethyl acetate to give a 10% w/v solution. TA acted as a positive control as it is thought to be one of the active components of the LL tuber

(personal communication with Dr Brian Moffat). A blank sample of ethyl acetate only was also used.

4.2.4.2. GC-MS Method

GC separation was carried out on a Thermo Scientific Focus GC interfaced with a DQS II Mass Spectrometer. The flow rate was 1.5mL/min with nitrogen gas and the temperature gradient ran from 100°C to 350°C at 10°C/min. The electron impact was operated in positive mode and full scan data were obtained in the mass to charge ratio (m/z) range of 50-800.

4.2.5. Cell Culture

All cell lines used were kindly provided by researchers at the University of Strathclyde: 3T3-L1 (mouse embryonic fibroblasts) and U937 (human malignant monocytic cells) cells were provided by Mrs Louise Young; SH-SY5Y (human neuroblastoma cells) were provided by Dr Ben Pickard.

All cell lines were grown in a humidified incubator at 37°C with 5% CO_2. 3T3-L1 cells were cultured in DMEM cell culture medium supplemented with 10% (v/v) new born calf serum (NBS), penicillin/streptomycin (500units/500µg, respectively), and 2mM L-glutamine. SH-SY5Y cells were cultured in DMEM:F12 Hams medium (1:1) supplemented with 10% (v/v) FBS and penicillin/streptomycin (500units/500µg, respectively). U937 cells were cultured in RPMI 1640 cell culture medium supplemented with 10% (v/v) FBS, 2mM L-glutamine, and penicillin/streptomycin (500units/500µg, respectively).

4.2.6. Cytotoxicity

Cytotoxicity tests were carried out with resazurin sodium salt in solution using a modified version of the manufacturer's protocol for the *in vitro* toxicology assay kit (TOX8). The resazurin was purchased on its own and prepared by adding 5mg of

resazurin salt to 50ml deionised water. This was then filter sterilised using a 0.2µm filter. Cr. extracts (samples) were prepared in DMSO to give a stock concentration of 20mg/mL.

All cell lines were grown in 75cm^2 cell culture flasks until approximately 80% confluent before the cells were used in experiments. Adherent cell lines (3T3-L1 and SH-SY5Y), which form a monolayer over the surface of the flask, were dissociated by adding 2ml TripLE Express dissociation reagent to each flask. The cells were then incubated for 3-5 min at 37°C, 5% CO_2. Once fully dissociated, the cells were counted and seeded into clear 96-well cell culture plates at the optimum seeding density for each cell line –3T3-L1 (8x10^3 cells/ml), SH-SH5Y (3x10^5 cells/ml) and U937 (1x10^5 cells/ml). Suspension cells (U937) were counted directly from the cell culture flask (75cm^2) and centrifuged (5 min at 1500g) before plating. The cell plates were then incubated overnight (20-24h) at 37ºC, 5% CO_2 to allow the cells to settle before the samples were added.

Following overnight incubation, samples were prepared on a dilution 96 well microtiter plate in normal cell culture medium depending on the cell line used. For initial testing, samples were added to the cells at a range of different concentrations to determine the IC50 value for each sample. Samples were prepared at 2x the final concentration (200µg/mL) before being diluted 2-fold on the plate which resulted in a serial dilution from 200µg/mL to 1.56µg/mL. One hundred µl of each sample was added to 100µl of the pre-plated cells which consequently halved the concentration of the samples. The final concentrations of DMSO was no higher than 0.5%. See Figure 4.5 for a representative diagram of the 96 well assay plate. Four controls were included on each plate: a final concentration of 10% DMSO (v/v) acted as a cell death control; cell growth control containing cells and cell culture medium; sample solvent control of 0.5% (v/v) DMSO; and a blank control which consisted of medium alone with no cell or samples. Each sample was also tested as a background control to ensure the compounds present did not interfere with the absorbance reading.

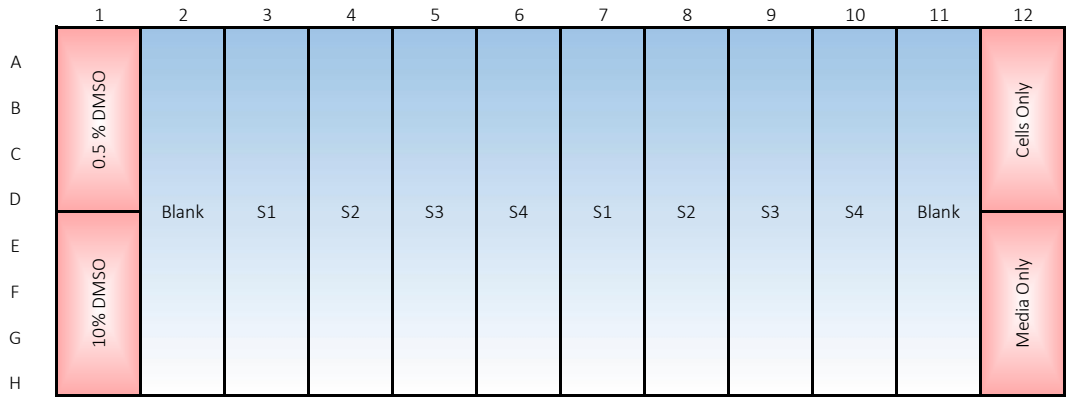

Figure 4.5: Plate map for cytotoxicity testing. Serial dilutions of samples was performed vertically down the plate from row A to row H. Four controls were included on each plate – 0.5% (v/v) DMSO control to represent the highest concentration of DMSO in the samples; 10% (v/v) DMSO; cell only control; and, medium only control.

Following the addition of the samples, the assay plates were incubated for 24 h at 37ºC. Resazurin solution was then added at a final concentration of 10% (v/v). The cell plates were incubated at 37°C in the dark for 4h, 6h and 24h before the fluorescence reading (560nm excitation, 590nm emission) was recorded on a M5 Spectramax Plate Reader (Molecular Devices) using Softmax Pro software. These results were transferred to Microsoft Excel for analysis. Readings after 24h were deemed as optimal. Each sample was tested in triplicate and the results were expressed as percentage cell viability of the cell only control. The equation used to determine the cell viability is shown below:

$$\% \text{ Cell Viability} = \frac{\text{Mean of Sample (OD560-590)}}{\text{Mean of Control (OD560-590)}} \times 100$$

4.2.7. Enzyme Inhibition Assays

Samples were tested at 30µg/mL as a preliminary study. Ten µl of sample or reference standard was added to specific wells on a 96 well half area plate. Following this, 20µl of enzyme was then added to each well. The assay plate was placed on a plate shaker for 1 min before being incubated at 37ºC for 10 min (α-glucosidase), 15 min (pancreatic lipase) or 30 min. The substrate (10µl) was then added to each well before

the plate was placed on the shaker again for another minute. The assay plate was incubated for a second time at 37°C for 10 min (PTP-1b, α-glucosidase), 25 min (pancreatic lipase) or 30 min (DPP IV, α-amylase). Fluorescence was then measured on a plate reader (Wallac Victor) at 355nm/460nm (Excitation/Emission).

4.2.7.1. DPP IV Inhibition Assay

DPP IV inhibitory activity was measured according to Scharp *et al.* (1988) with some modifications. The assay buffer was prepared using 100mM Tris-HCl with bovine serum albumin (BSA) at 0.1mg/mL. The pH of the buffer was adjusted to pH 8 using a pH meter and was stored at 4°C until required. The enzyme buffer consisted of 100mM Tris-HCL at pH8. DPP IV enzyme was prepared in the enzyme buffer to a final concentration of 0.3nM. The enzyme was aliquoted and kept at -20°C until required. Gly-pro-7-amido-4-methylcoumarin hydrobromide was used as the substrate. The final concentration required was 30µM. A stock solution was prepared in distilled water and stored at -20°C until required. Michaelis constant, Km = 22µM. P32/98 (a known DPP IV inhibitor) (BML-PI142-0010, 10mg) was used as a positive control and a standard curve was prepared by diluting the stock solution from 1nM to 3µM.

4.2.7.2. PTP 1b Inhibition Assay

PTP1b inhibitory activity was measured as described by Zhang *et al.* (2006) with some modifications. The PTP1b assay buffer was prepared using 25mM 4-(2-hydroxyethyl)-1-piperazineethanesulfonic acid (HEPES), 50mM sodium chloride, 2mM dithioreitol, 2.5mM ethylene-diamine-tetra-acetic acid (EDTA) and 0.01mg/mL BSA. The solution was adjusted to pH7.2 at 37°C. An amended protocol was also used which consisted of the addition of catalase (0.25mg/mL) to the assay buffer. Due to the addition of dithioreitol, some natural extracts may produce hydrogen peroxide, which can interfere with the assay causing potential false positive results. Therefore, by adding catalase to the buffer, the false positives are minimised. All other procedures and reagents remained the same. The enzyme buffer was prepared using 25mM HEPES 5mM dithioreitol, 1mM EDTA and 0.05% (v/v) NP-40. The enzyme used was protein

tyrosine phostphatase 1b (PTP1b) which was prepared to a final concentration of 1nM on the assay plate and 6,8-difluoro-4-methylumbelliferyl phosphate (DiFMUP) was used as the substrate. The stock was prepared in DMSO and the final concentration on the assay plate was 10µM. Michaelis constant, Km = 6µM. Bis(4-trifluoromethylsulfonamidophenyl)-1,4-diisopropylbenzine (PTP Inhibitor IV, TFMS) was used as a positive control. A serial dilution of TFMS was prepared to produce a final concentration range of 30µM to 100µM.

4.2.7.3. α-Amylase Inhibition Assay

The α-amylase inhibitory activity was measured as described by Funke and Melzig (2005) with slight modifications. The assay buffer consisted of 50mM HEPES in water at pH 7.1. The enzyme used was porcine pancreas α-amylase. A stock concentration was made up in water to 250 units/ml and kept at -20°C until required. A final concentration of 125units/ml was used. 4-nitrophenyl α-D-maltohexaside was used as the substrate. A stock solution was prepared (50mM) in assay buffer and stored at -20°C until required. A final concentration of 1.5mM was used. Acarbose was used as a positive control and a standard curve was prepared to produce a final concentration range from 300nM to 1mM. Michaelis constant, Km = 01.8mM.

4.2.7.4. α-Glucosidase Inhibition Assay

The a-glucosidase inhibitory activity was measured as described by Kwon *et al.* (2008) with slight modifications. The assay buffer was prepared by mixing 25.5ml of 0.2M sodium phosphate monobasic dehydrate with 24.5ml of 0.2M sodium phosphate dibasic heptahydrate. The solution was made up to 100ml using distilled water and was calibrated to pH6.8 using a pH meter. The enzyme used was yeast α-glucosidase. A stock concentration was made up in water to 75 units/ml and kept at -20°C until required. A final concentration of 0.2units/ml was used. P-nitrophenyl-α-D-glucopyranoside was used as the substrate. A stock solution was prepared in phosphate buffer and stored at -20°C until required. A final concentration of 1mM was used. Acarbose was used as a positive control and a standard curve was prepared to produce a final concentration range from 10µM to 25mM. Michaelis constant, Km = 0.83mM

4.2.7.5. Pancreatic Lipase Inhibition Assay

Pancreatic lipase inhibitory activity was measured based on the method used by Zhang *et al.* (2015) with some modifications. The assay buffer used was Tris-HCl (pH 8 at 37ºC) at a concentration of 0.1mM. Pancreatic lipase (type II from porcine pancreas) was utilised as the enzyme. A stock solution of this enzyme was prepared in the assay buffer at a concentration of 50U/ml. The substrate for this assay was 4-methyl umbelliferyl oleate at a final concentration of 250µM. Orlistat, a current drug used in the treatment of obesity, was used as a positive control and a standard curve was prepared to produce a final concentration range from 30µM to 10nM. Michaelis constant, Km = 1mM.

4.2.7.6. Statistical Analysis

Each sample was tested in triplicate and the results are expressed as percent inhibition compared to the control. The control was assumed to have 100% inhibition. The percent inhibition for each cr. extract was calculated as follows:

$$\% \text{ Inhibition} = \frac{\text{Control Reading - Sample Reading}}{\text{Control Reading}} \times 100$$

Statistical analysis was carried out using ANOVA with a Dunnet's post-test using MiniTab 16 and graphs were plotted using GraphPad Prism 4.0. The Ki, the dissociation constant of the enzyme-inhibitor complex, was determined using non-linear regression analysis using GraphPad Prism 4.0.

4.2.8. U937 TNFα Release Assay

U937 cells were differentiated according to Del Bufalo *et al.* (2011) with some modifications. U937 cells were seeded in a 24 well plate (TPP) at $1x10^5$ cells/ml with 60ng/ml phorbol 12-myristate 13-acetate (PMA). The optimal concentration of PMA was determined prior to carrying out the experiment. PMA was dissolved in sterile DMSO to a concentration of 1mg/mL before being diluted in cell culture medium. The cells were incubated with PMA at 37°C, 5% CO_2 and 100% humidity for 48 h before

the medium was changed in each well to complete growth media (see section 3.3.1). The cells were incubated again for 24 h at 37°C, 5% CO_2 and 100% humidity. Following this, each sample was added at a concentration of 30µg/mL. Samples were added with and without lipopolysaccharide (LPS) (1µg/mL, final concentration, dissolved in cell culture medium) before being incubated again for 24h at 37°C, 5% CO_2 and 100% humidity. The supernatant was then removed after 24h and kept at -20°C until required.

A TNF-α ELISA was carried out as per the manufacturer's protocol. Samples were tested in triplicate and data is represented as mean ± SEM. TNF-α was used to prepare a standard curve to determine the level of TNF-α in the supernant after treatment. Samples were diluted before they were added to the ELISA plate to ensure the readings were within the range of the reference standard curve. Therefore, all readings from the standard curve were then multiplied by the dilution factor. Statistical analysis was carried out using ANOVA with a Dunnet's post-test using GraphPad Prism version 4.0.

4.3. Results

4.3.1. Characterisation of Hexane Crude Extracts

The cr. extracts obtained were a mixture of a yellow/orange fatty substance with needle like crystals. LL-Hex-1 was a more oil/fatty texture, whereas LL-Hex-2 appeared to have more needle like crystals present.

4.3.1.1. LL-Hex-1

The ^{1}H NMR spectra for LL-Hex-1 was characteristic of triglyceride molecules with some minor components also visible. Figure 4.6 shows a speculative triglyceride molecule to highlight the peaks observed in ^{1}H NMR.

The olefinic protons (-CH=CH-) of unsaturated fatty acids are seen at 5.27-5.4ppm (a, multiplet). This multiplet is not baseline resolved from the proton signal at 5.25ppm

(b) which can be assigned to the H2 of the glycerol backbone. The H1 and H3 protons of the glycerol resonate at 4.12 and 4.27ppm (c, doublet of doublets). These assignments are interchangeable. Bis-allylic and allylic methylenes of polyunsaturated and unsaturated acyl chains resonate at 2.75ppm (d, multiplet) and 2.02ppm (f, multiplet) respectively. The H2 and H3 protons of acyl moieties in the triglyceride molecules appear at 2.29 (e) and 1.59ppm (g), respectively. Additionally, the protons of the methylene envelope resonate at 1.23ppm (h). The methyl protons of omega-3 polyunsaturated fatty acids are shifted at a higher frequency to 0.91 (I, triplet) compared to the methyl protons of saturated and unsaturated chains, which appear at 0.87 (j, triplet). Triglycerides are well documented throughout scientific literature (Gökhan and Küsefoğlu, 2013; Salinero *et al.*, 2012; Vlahov, 1999) and when comparing the ^{1}H spectra to the literature, it confirmed that the major compounds present in LL-Hex-1 were triglycerides. However, using ^{1}H NMR alone, it was not possible to comment on their exact identity. ^{1}H NMR shows an average spectra based on the compounds present and if more than one triglyceride molecule is present, the peaks will overlap. Additionally, it is possible for the fatty acid chains to be in different positions from the speculative triglyceride shown in Figure 4.6. The triglyceride molecules may be made up of three of the same fatty acid chains, or the three fatty acid chains could be entirely different. For example, it may consist of three oleic acid molecules, or two oleic acid molecules and one palmitic acid, or one oleic acid, one palmitic acid and another entirely different fatty acid. There are numerous possible combinations; thus, in using ^{1}H NMR alone, it is not possible to distinguish between these varying triglyceride molecules.

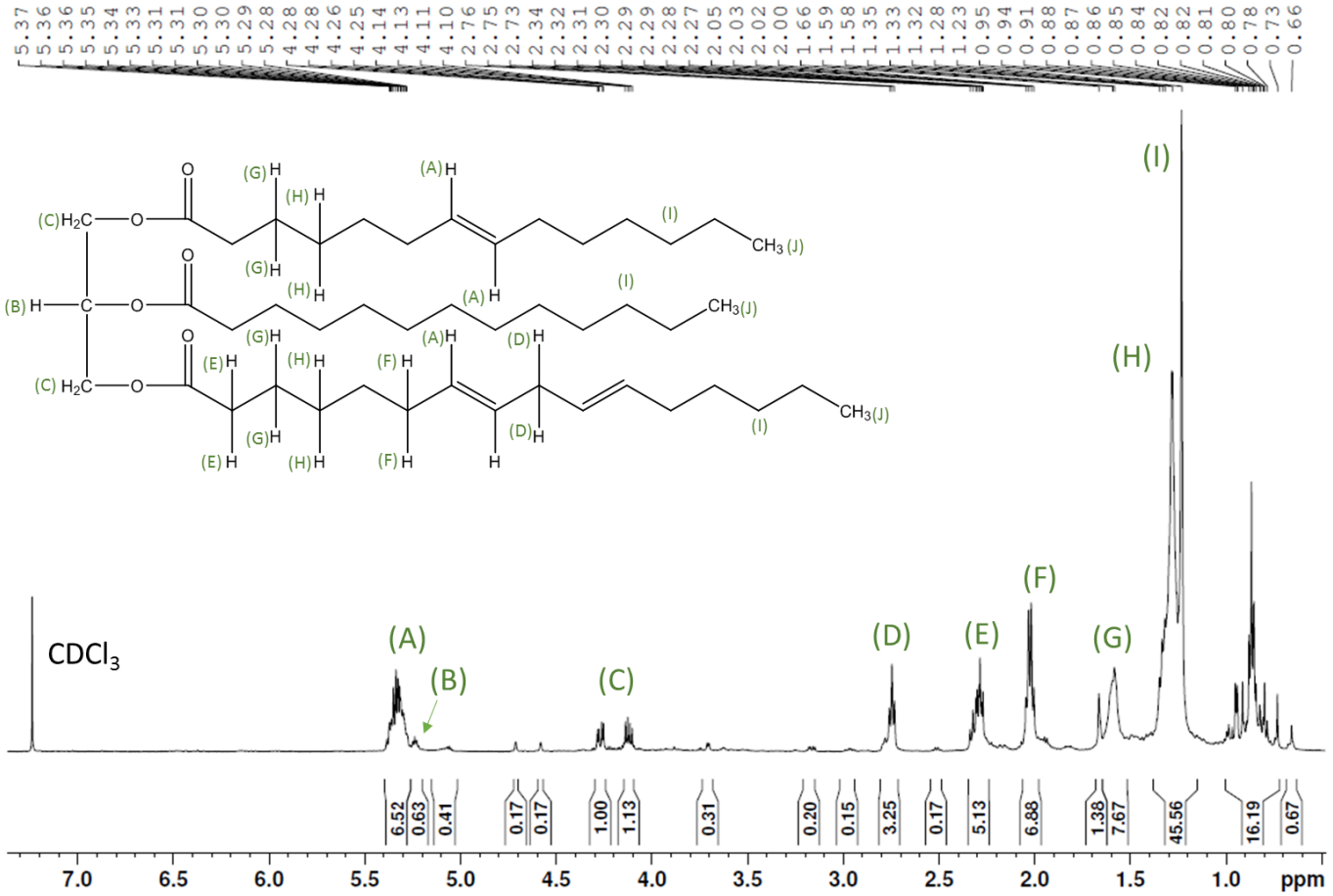

Figure 4.6: 1H NMR (400MHz, CDCl3) of LL-Hex-1. Lettering [(A) to (J)] represents different 1H environments which are detailed above and highlighted on the speculative triglyceride structure at the top left.

4.3.1.2. LL-Hex-2

The major component of LL-Hex-2 is thought to be betulinic acid with some minor components also present. Positive ion mode MS showed a molecular ion [M+H] at *m/z* = 457.36, whilst negative ion mode MS showed a molecular ion [M-H] at *m/z* = 455.35, both of which suggest a molecular formula of $C_{30}H_{48}O_3$. This indicated a double bond equivalent (DBE) of 7 (Williams and Fleming, 2007)

NMR (500MHz, $CDCl_3$, Figures 4.7 to 4.9) shows the presence of five singlet methyls at δ 0.73, 0.80, 0.91, 0.94 and 0.95 (A-E, Figure 4.8), as well as a vinylic methyl at 1.67 ppm (F). Two olefinic protons appeared at δ 4.59 (G) and 4.72 (H) ppm, which is characteristic of exomethylene groups. Signals were also present at δ_H 2.98 ppm (i, 1H, *m*) and 3.17 ppm (j, 1H, *dd*) – see Figure 4.10. The remaining methine and methylene protons were seen between 0.65-2.28ppm. This pattern of protons is typical of lupane-type triterpenes. The J-modulated DEPTq135 ^{13}C NMR indicate thirty carbon atoms, which are listed in Table 4.5 in comparison to Igoli and Gray (2008). These carbons include one carboxylic acid, six methyls, eleven methylenes, six methines and six quaternary carbons. Carbon 17 was not identified in the ^{13}C spectra obtained for this cr. extract, however, it may be due to the concentration of cr. extract used in the experiment, or due to the presence of other compounds in the mixture. In addition to the above, there were no aromatic protons or carbons present, which also supports the fact that the major compound of this extract belongs to the pentacyclic triterpene group. Furthermore, following comparison with data previously reported (Haque *et al.*, 2013; Igoli and Gray, 2008; Uddin *et al.*, 2011) this compound can be tentatively identified as betulinic acid (Figure 4.10).

Following analysis of the NMR spectra for LL-Hex-2, it may be speculated that one of the minor components of LL-Hex-1 could also be betulinic acid due to the similarities in the ^1H NMR spectra. On the other hand, the minor components of LL-Hex-2 may be triglyceride molecules due to the similarities in peaks.

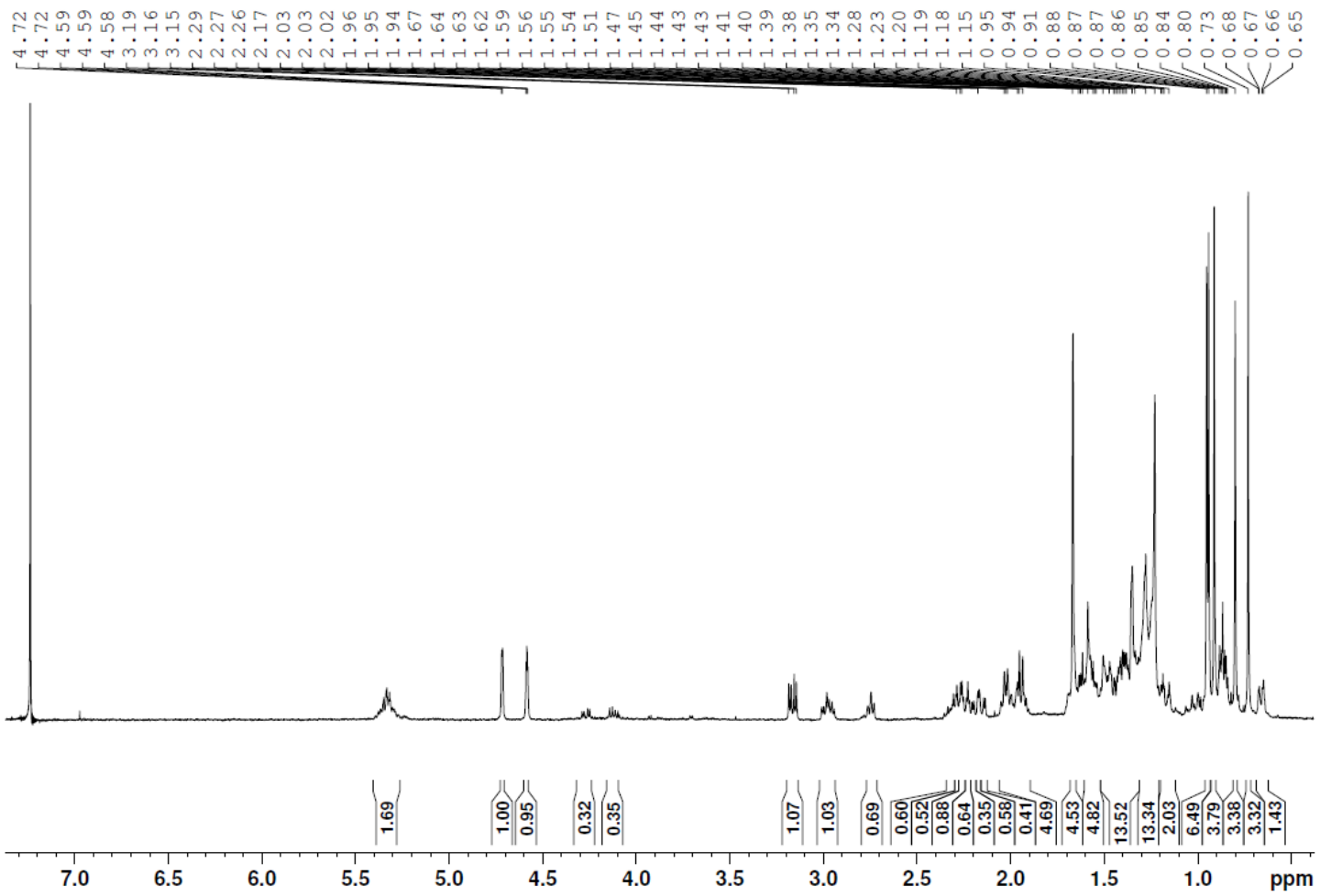

Figure 4.7: LL-Hex 2 Proton NMR. Full ^{1}H NMR spectrum of LL-Hex-2 ($CDCl_3$, 300MHz).

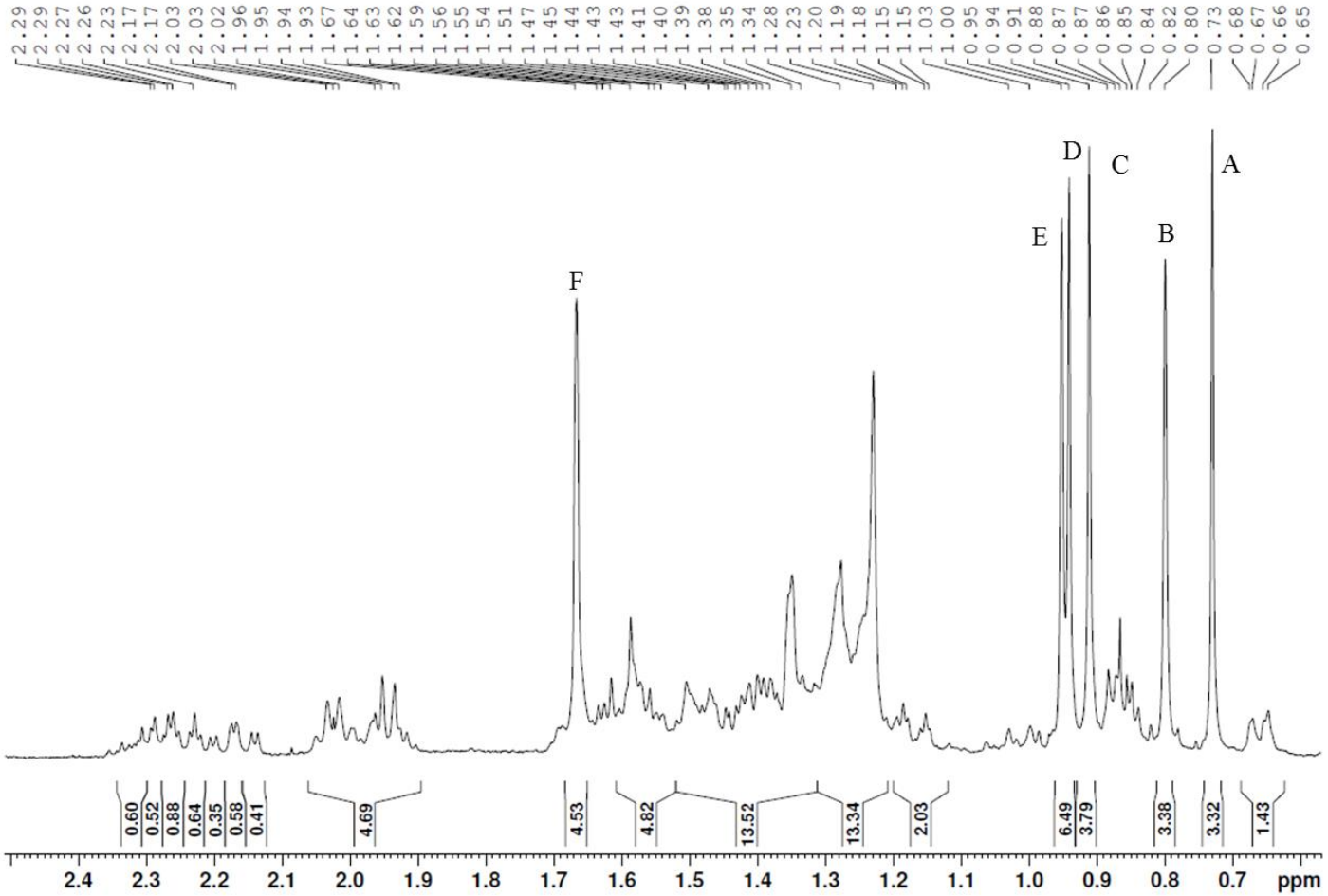

Figure 4.8: LL-Hex 2 Proton NMR. ^{1}H NMR expansion of shielded region from 0ppm to 2.3ppm ($CDCl_3$, 300MHz).

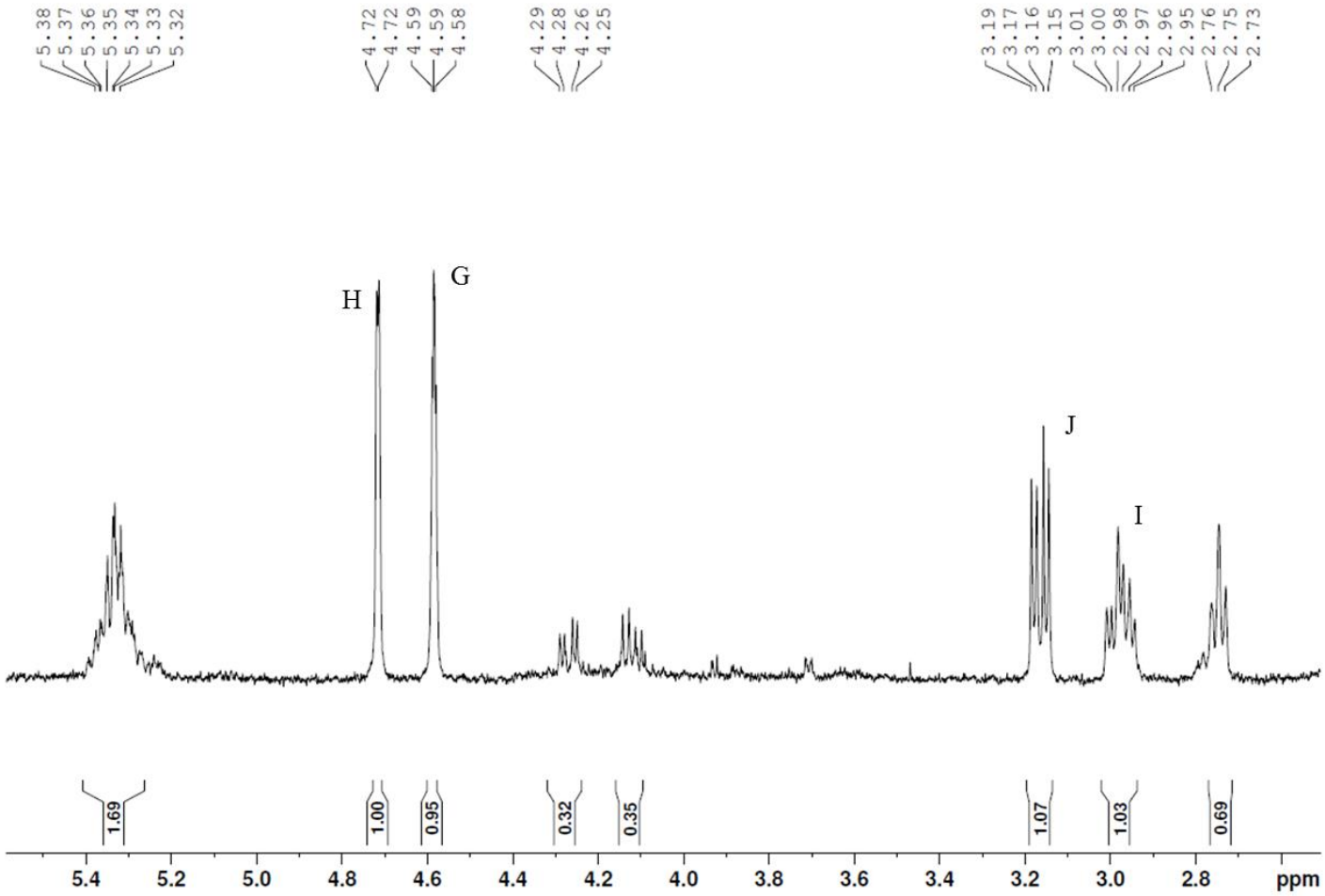

Figure 4.9: LL-Hex 2 Proton NMR. ^{1}H NMR expansion of middle region from 2.7ppm to 5.5ppm ($CDCl_3$, 300MHz).

Table 4.5: LL-Hex 2 Carbon NMR Assignments. ^{13}C chemical shifts (ppm) from LL-Hex-2 in comparison to (Igoli and Gray, 2008). * Solvent used was Pyridine-D_5. *** = unidentified.

CARBON ASSIGNMENT	BETULINIC ACID AS IDENTIFIED BY IGOLI & GRAY (PPM)*	BETULINIC ACID AS IDENTIFIED FROM LL-HEX-2 (PPM)*
1	38.77	38.95
2	27.44	27.64
3	79.05	79.24
4	38.9	39.08
5	55.41	55.58
6	18.33	18.52
7	34.38	34.58
8	40.76	40.93
9	50.58	50.77
10	37.26	37.46
11	20.90	21.00
12	25.56	25.76
13	38.45	38.6
14	42.49	42.66
15	30.61	30.79
16	32.20	32.37
17	57.23	***
18	46.93	47.10
19	49.34	49.50
20	150.41	150.62

21	29.74	29.93
22	37.06	37.26
23	28.02	28.20
24	15.36	15.56
25	16.06	16.24
26	16.15	16.34
27	14.73	14.92
28	180.4	180.29
29	109.71	109.91
30	19.41	19.60

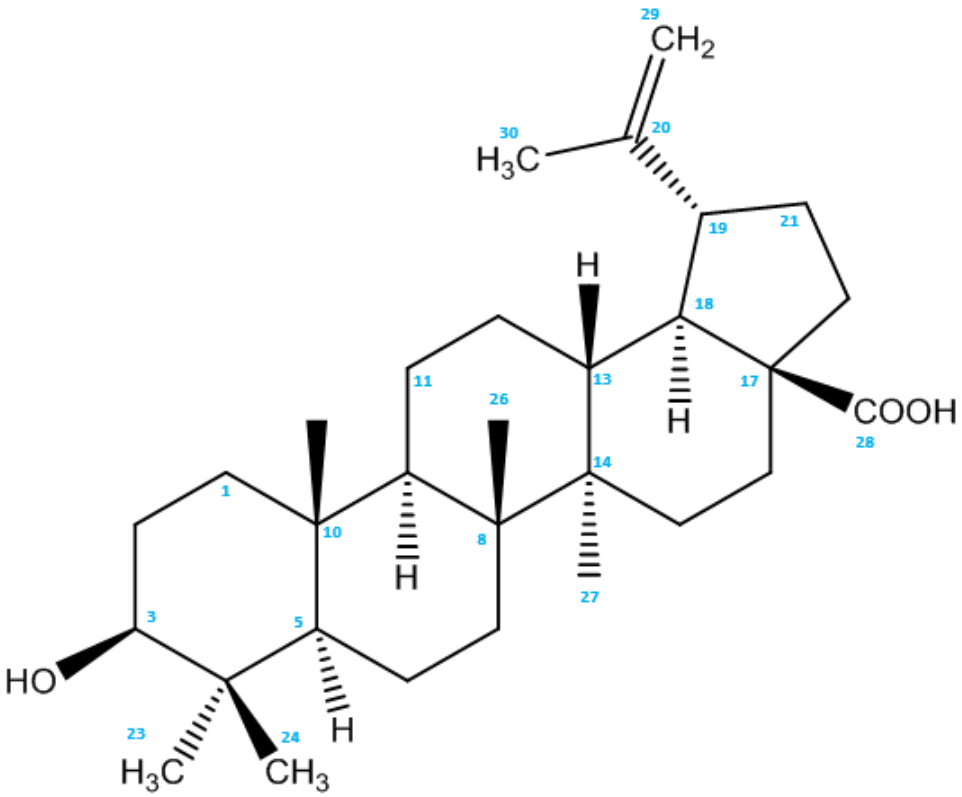

Figure 4.10: Proposed structure of the main compound in LL-Hex-2, betulinic acid. Diagram produced using ChemBioDraw. Structure annotated using numbers (highlighted in blue) which represent carbon atoms.

4.3.2. Characterisation of compounds in the Ethyl Acetate Extracts

4.3.2.1. LL-EthA-2

The major component of LL-EthA-2 was identified as a novel compound, which is a stereoisomer of an azukisapogenol glycoside identified by Pérez *et al.* (2013). The compound was identified as 3-*O*-[-α-L-arabinopyranosyl-(1→2)-β-D-glucuronopyranosyl]-24-hydroxy-12-oleanen-30-oic acid. Positive ion mode MS showed a molecular ion $[M+H]^+$ at *m/z* = 781.44, whilst negative ion mode MS showed a molecular ion [M-H$^-$ at *m/z* = 779.42, both which suggest a molecular formula of $C_{41}H_{64}O_{14}$. This indicated a double bond equivalent (DBE) of 10. There were also other minor components present, which have yet to be elucidated.

NMR (600MHz, Pyridine-d_5) enabled the determination of the triterpenoid glycosidic structure shown in Figure 4.11 (indicated by green numbering) with the ^{1}H and ^{13}C allocations shown in Table 4.6. ^{1}H NMR spectrum (600MHz, pyridine-d_5, see Figures A.5-1, A5-2 and A5-3 in Appendix 5 for ^{1}H NMR Spectra) showed six tertiary methyl groups at δ 0.71, 0.88, 0.89, 1.29, 1.31 and 1.38 for the aglycone moiety, which correlate in the HSQC experiment (see Figures A5-5, A5-6 and A5-7 in Appendix 5 for HSQC NMR Spectra) with the carbon signals at δ 15.92, 28.80, 17.06, 26.45, 22.85 and 29.40, respectively (Figure A5-4). The presence of the signal at 5.45ppm (triplet) is typical of H12 of the oleanene skeleton, which was confirmed by the presence of two olefinic signals in the ^{13}C NMR spectrum at δ 123.03 and 145.35, which were attributed to C12 and C13. C13 was confirmed to be a quaternary carbon due to the absence of any ^{1}H correlations in HSQC experiment. The presence of two carboxylic acid groups was highlighted in the ^{13}C NMR spectrum by the signals at δ 172.75 and 179.94. The signal at 179.94 was assigned to carbon 30 due to the HMBC correlation (see Figure A5-8 and A5-9 in Appendix 5) through three bonds with the methyl group at δ 1.38 (H29). The hydroxymethyl group of the aglycone was identified by the ^{1}H NMR signals at δ 3.40 (d, *J* = 11.31 Hz) and 4.31 (d, *J* = 11.31 Hz). These signals showed a cross peak in the HSQC experiment at δ 63.7, as well as in the HMBC spectrum with carbon signals at δ 22.85 (C23) and 90.78 (C3), which is consistent with data reported in the literature (Pérez *et al.*, 2013) (See Figure 4.12). However, rather

large discrepancies were seen in the chemical shifts of protons and carbons between both compounds around rings D & E which pointed to significant differences especially around C-20 (Table 4.6).

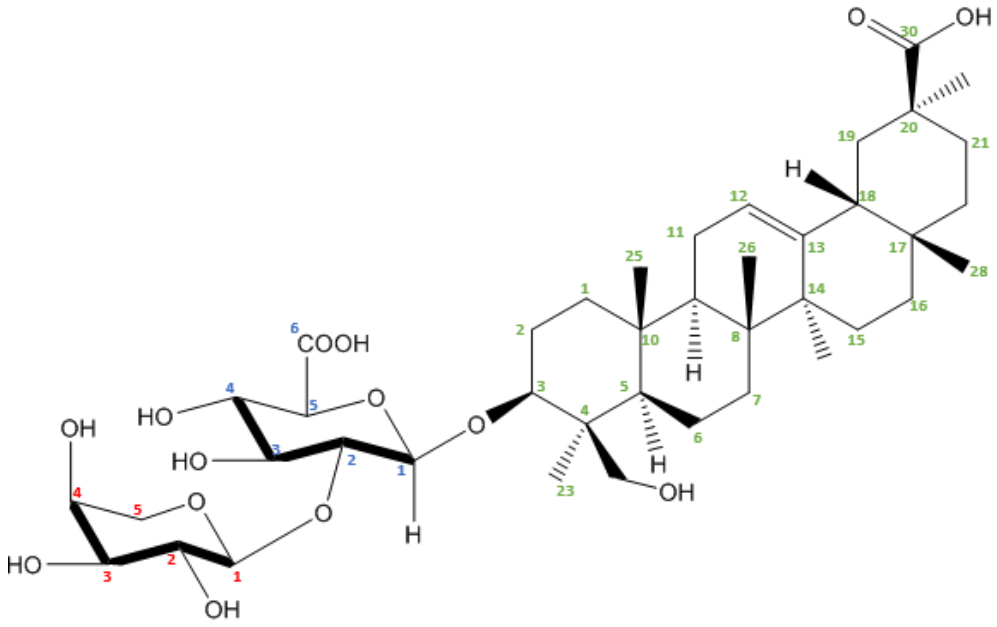

Figure 4.11: Chemical structure of the major component present in LL-EthA-2. Structure drawn using ChemBio Draw. Green numbering represents aglycone carbon atoms, while red and blue numbering represents the two sugars attached.

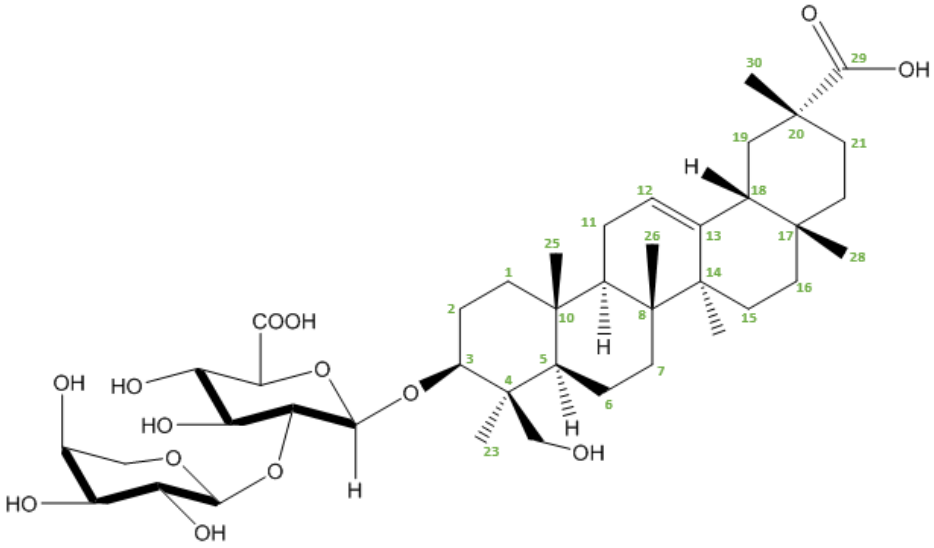

Figure 4.12: Chemical structure of the 3-O-[-β-D-glucuronopyranosyl(1→2)-β-D-glucuronopyranosyl]-29-O-β-D-glucopyranosyl azukisapogenol identified by Perez *et al.* (2013). Structure drawn using ChemBio Draw. Green numbering represents aglycone carbon atoms. This compound is a stereoisomer (at C20) of the compound identified in LL-EthA-2.

Table 4.6: ^{1}H and ^{13}C NMR chemical shift assignments as per the HSQC experiment for the aglycone section of LL-EthA-2 in comparison to a stereoisomer reported by Pereź *et al.* (2013).

Carbon # of acglycone structure	LL-EthA-2		Stereoisomer reported by Pereź *et al.* (2013)	
	^{1}H (ppm)	^{13}C (ppm)	^{1}H (ppm)	^{13}C (ppm)
1	0.76	38.90	0.74	38.60
	1.33		1.30	
2	1.47	39.39	1.91	26.70
	1.77		2.23	
3	3.41	90.78	3.36	90.40
4		44.30		44.00
5	0.84	56.36	0.76	56.00
6*	1.01	18.93	1.28	18.60
	1.58		1.53	
7*	1.76	26.87	1.20	33.00
	2.22		1.35	
8		40.26		40.00
9	1.57	48.01	1.49	47.60
10		36.76		36.50
11	1.78	24.26	1.75	24.00
12	5.45	123.03	5.22	122.90
13		145.35		144.50
14		42.05		41.00
15	0.99	26.96	0.92	26.40
	1.92		1.71	
16	0.91	27.54	0.84	27.20
	2.10		2.13	

17		32.63		32.70
18	2.40	48.88	2.11	46.40
19	1.84	43.81	1.68	41.50
	2.27		2.54	
20		44.64		42.80
21	1.49	32.12	1.7	29.90
	2.28		2.25	
22	1.26	33.37	1.36	36.50
	1.46		1.53	
23	1.31	22.85	1.23	22.50
24	3.39	63.59	3.36	63.30
	4.30		4.29	
25	0.71	15.92	0.71	15.60
26	0.89	17.07	0.88	16.80
27	1.29	26.45	1.22	26.00
28	0.88	28.81	0.91	28.30
29	1.38	29.40		181.2
30		179.94	1.46	19.90

Using NOESY NMR (Appendix 5, Figures A5-10, A5-11 and A5-12) the stereochemistry (shown in Figure 4.13) of this compound was confirmed. The NOE correlations for the aglycone structure are highlighted in Figure 4.14, with three varying angles of the molecule shown in images A, B and C. Using NOESY NMR, it is possible to generate a 3D like structure to visualise the compound identified. The compound identified by Perez *et al.,* (2013) (Figure 4.15) is a stereoisomer of the compound identified in LL-EthA-2, with the difference being the stereochemistry at position 20. Figures 4.14 and 4.15 highlight this difference as C29 correlates to C18 in the compound identified by Perez *et al.* (Figure 4.15)., which is not seen in LL-EthA-2, shown in Figures 4.14(A-C).

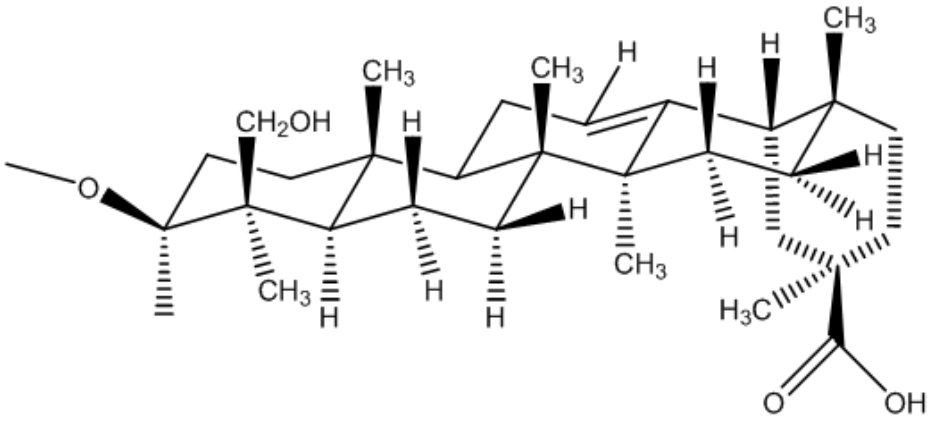

Figure 4.13: Stereochemistry of main compound in LL-EthA-2 based on NOE correlations. Diagram produced using Chem 3D Pro 13.0.

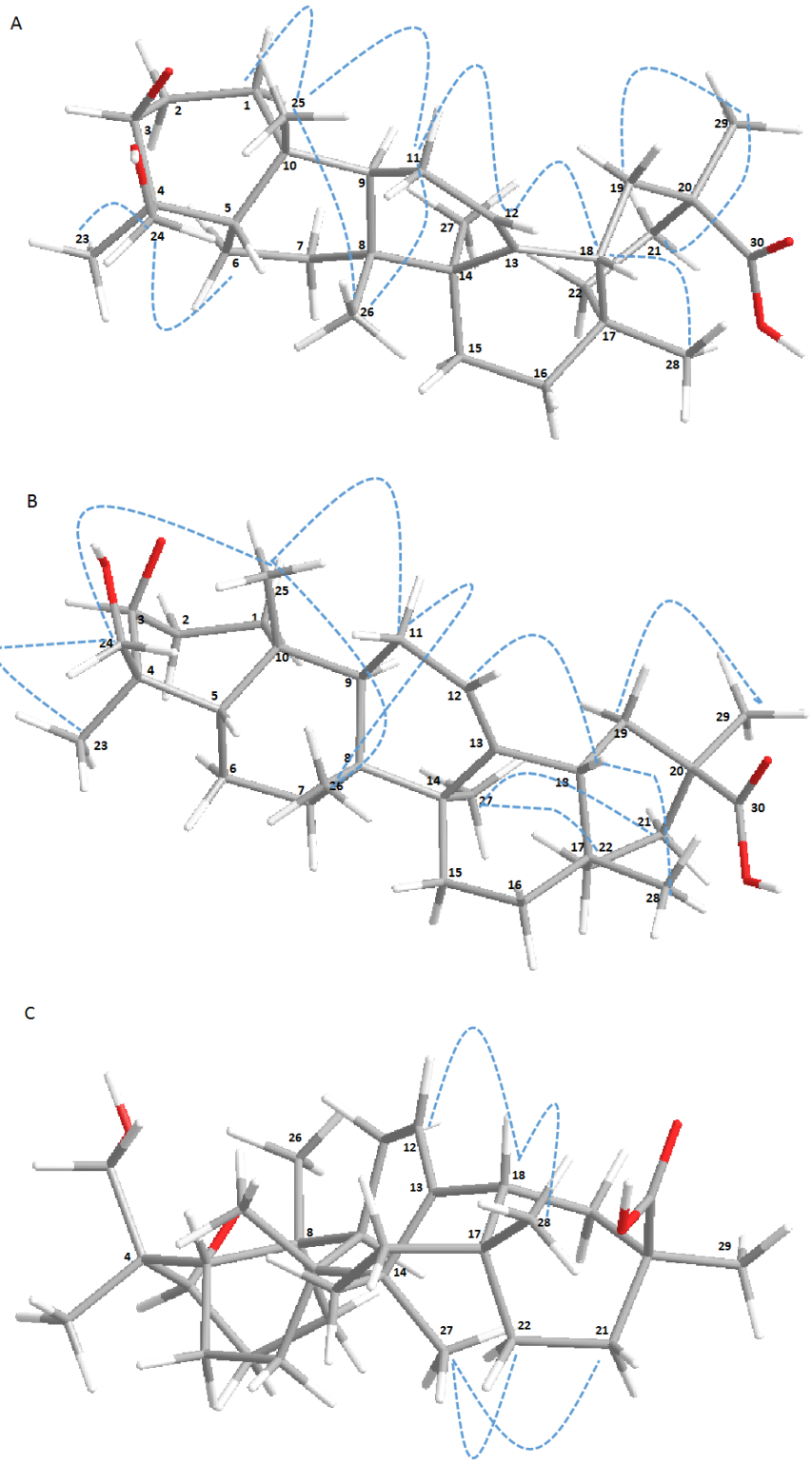

Figure 4.14 (A, B and C): NOE correlations of the main compound in LL-EthA-2. NOE correlations were identified using NOESY NMR (600MHz, Pydridine-D_5). Diagram produced using Chem 3D Pro 13.0. Blue arrows represent proton atoms which show correlations in NOESY NMR.

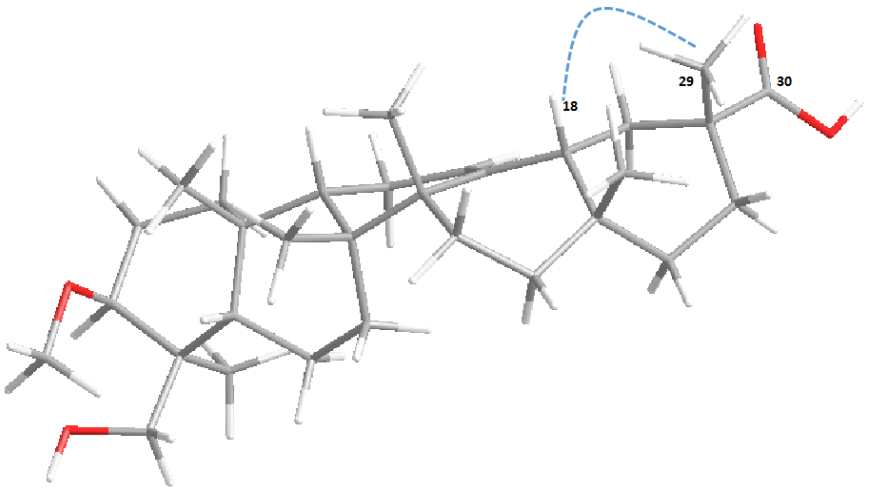

Figure 4.15: NOE correlations of 3-O-[-α-L-arabinopyranosyl-(1→2)]-β-D glucuronopyranosyl azukisapogenol taken from Perez *et al.* (2013). This compound is a stereoisomer of the compound identified in LL-EthA-2. Perez *et al.* identified that the proton on carbon 29 correlated with the proton on carbon 18 using ROESY NMR. This is highlighted with the blue dotted arrow. This correlation is not present in NOESY NMR for the compound identified from LL-EthA-2. Diagram produced using Chem 3D Pro 13.0.

The hydrogen and carbon correlations for the two sugar moieties were identified following analysis of ^{1}H, ^{13}C and HSQC spectra and are shown in Table 4.7. ^{1}H and ^{13}C NMR spectra showed the presence of two anomeric protons at δ 4.96 and 5.47, and carbons at δ 105.53 and 105.17. The individual sugar units were determined using a combination of COSY, HMBC and NOESY experiments (See Appendix 5 for NMR Spectra). The two sugar units were found to be glucuronic acid (GlcA) and arabinose (Ara). The sequence of sugar chains and connection with the aglycone were then determined using HMBC. The anomeric signal at δ 4.93 (H1' of GlcA) showed a long-range coupling to δ 90.8 (C3 of aglycone) indicating that GlcA is directly linked to the triterpenic aglycone at C3. This was confirmed using NOESY where a correlation between δ 4.93 (H1') and δ 3.41 (H3 of aglycone) was identified. The sequence of sugars, Ara (1→2) GlcA, was also shown using HMBC where a clear cross-peak between the signal at δ 5.46 (H1" Ara) and δ 79.21 (C2' GlcA) was observed. This was supported by NOESY correlation between δ 4.39 (H2' GlcA) and δ 5.46 (H1" Ara).

Table 4.7: 1H and 13C NMR chemical shift assignments for LL-EthA-2 sugar moieties. (GlcA is highlighted in Fig. 2.22 using blue numbering, Ara is highlighted using red numbering.) *****Multiplicities: brm = broad multiplet, d = doublet, dd = doublet of doublets, m = multiplet

		^{1}H (ppm)*	^{13}C (ppm)
Glucuronic Acid (GlcA)	1'	4.93 d *J* = 7.8Hz	105.50
	2'	4.39 m	79.21
	3'	4.37 m	78.25
	4'	4.57 dd *J* = 9, 9.6Hz	73.61
	5'	4.60 d *J* = 9Hz	78.05
	6'	N/A	172.75
Arabinose (ARA)	1"	5.46 d,*J* = 7.8Hz	105.12
	2"	4.45 dd *J* = 7.8, 9Hz	73.81
	3"	4.05 dd *J* = 9, 3.6Hz	75.22
	4"	4.15 brm	70.55
	5"	3.68 brd *J* = 12.6Hz	67.78
		4.26 brd *J* = 12.6Hz	

4.3.3. Identification of *trans*-anethole using GC-MS

Following comparison with a standard solution of TA, the presence of *trans*-anethole was confirmed using GC-MS. The largest peak shown in the LL tuber sample was at 148 m/z (shown in Figure 4.16 (A)) which correlates to the TA peak apparent in the chromatogram of the standard (shown in Figure 4.16 (B)). Furthermore, when carrying out a search in the NIST GCMS library in XCalibur, the top result was anethole, thus reiterating the identification of TA.

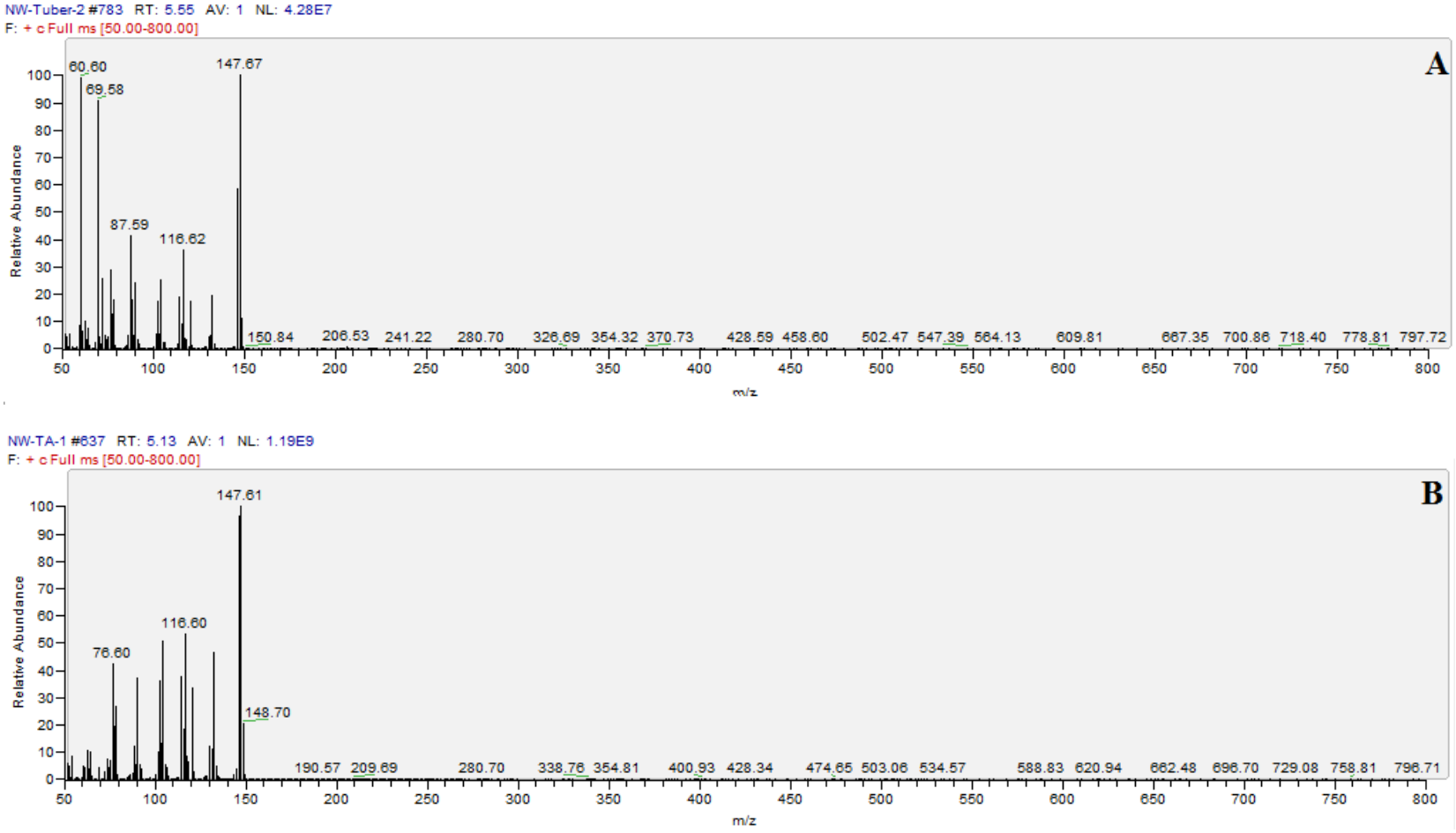

Figure 4.16: GC-MS Chromatogram. (A) shows the chromatogram generated following GC-MS analysis of LL tuber, while (B) shows the *trans*-anethole standard chromatogram. Both samples were ran using the same GC-MS method.

4.3.4. Cytotoxicity

Each crude extract was tested against three cell lines: monocyte-like cells (U937), neuroblastoma cells (SH-SY5Y), and adipocytes (3T3-L1). These cell lines were selected to give an overview of the cytotoxicity of the cr. extracts in an initial screen. Determining the cytotoxicity of natural products is imperative before further analysis is carried out. Of note, cr. extracts contain various compounds which may or may not enhance or subdue the overall biological activity. The cytotoxicity of each compound when pure may be very different.

Figures 4.17 to 4.19 show the effect of each cr. extract on the various cell lines tested. Overall, the cr. extracts of LL were not toxic to the cell lines tested in this study. However, there are a few things to note. Figure 4.19 shows the effect of each extract on SH-SY5Y cells which are neurobalstoma cells. LL-EthA-2, at highest concentration tested, reduced cell viability of SH-SY5Y cells in a dose dependent manner. This was not apparent for the other cell lines, which showed enhanced cell viability at the highest concentration tested. In Figure 4.20, which shows the effect of the cr. extracts on cell viability of 3T3-L1 cells, the two hexane extracts and the methanol extract (LL-Hex-1, LL-Hex-2 and LL-M) increased cell growth by up to 150% of the control at the highest concentration tested (100µg/mL). 3T3-L1 cells are adipocytes, and these extracts contain mainly triglycerides and free fatty acids (hexane extracts) and sugars (methanol extract), which could be enhancing the growth of this cell line. From these results, we can conclude that LL cr. extracts are not toxic when tested *in vitro* using the resazurin cell viability assay.

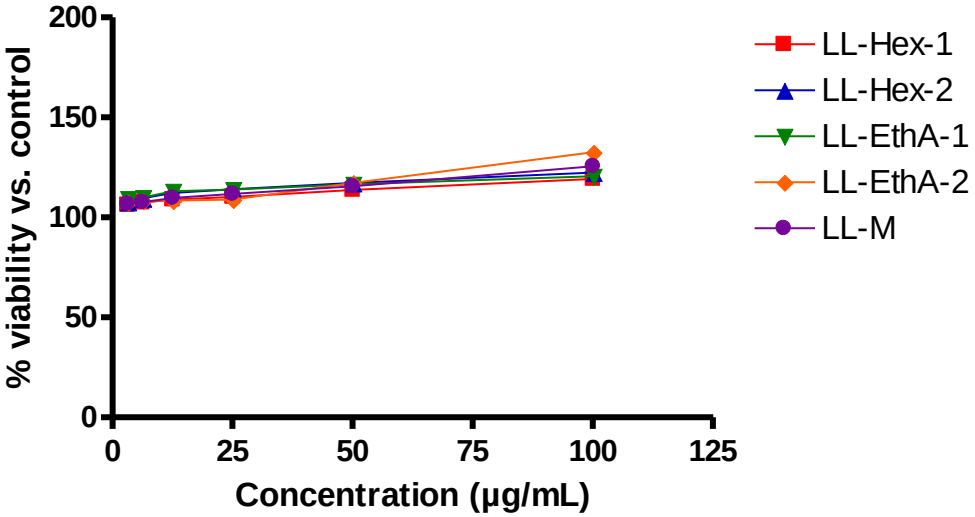

Figure 4.17: The effect of each cr. extract on U937 cells at concentrations from 0.718µg/mL to 100µg/mL. Data represents mean ± SEM, n=3.

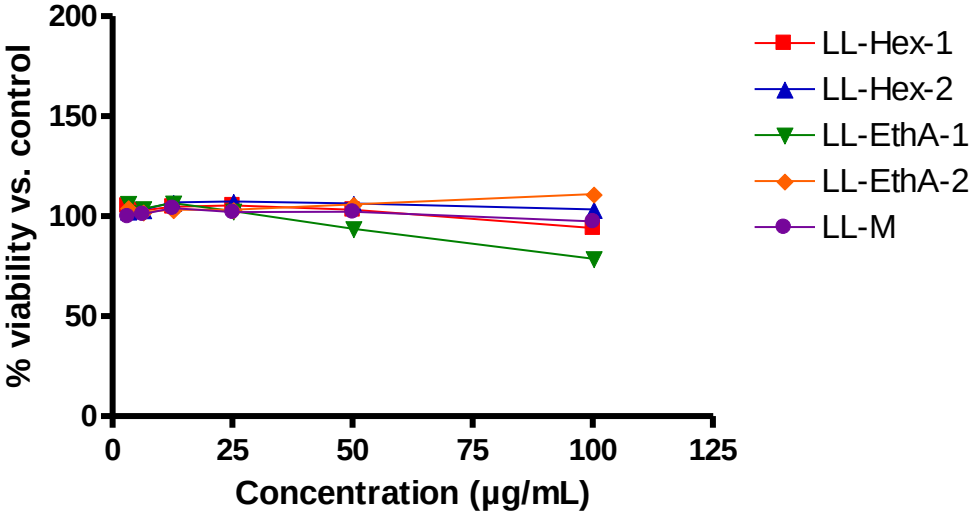

Figure 4.18 The effect of cr. extract on SH-SY5Y cells at concentrations from 0.718µg/mL to 100µg/mL. Data represents mean ± SEM, n=3.

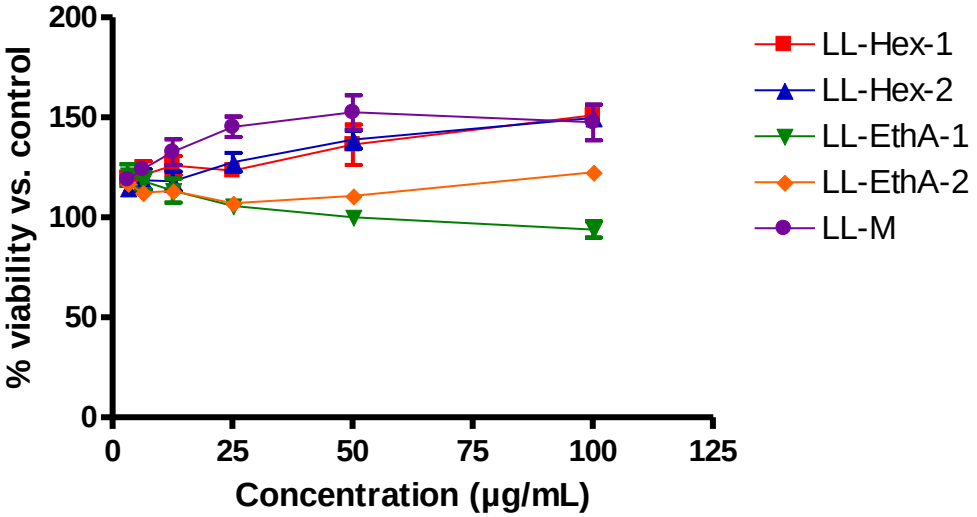

Figure 4.19: The effect of cr. extract on 3T3-L1 cells at concentrations from 0.718µg/mL to 100µg/mL Data represents mean ± SEM, n=3.

4.3.5. Enzyme Inhibition Assays

4.3.5.1. DPP IV

P32/98 is a known inhibitor of DPP IV, thus it was used as a reference standard and positive control. For the initial screen of the cr. extracts, one concentration (30µg/mL) was tested in the enzyme inhibition assays. As seen in Figure 4.20, the LL cr. extracts tested showed minimal inhibitory activity towards DPP IV. The cr. extract which exhibited the highest inhibition against DPP IV was LL-EthA-2 at about 15% inhibition. In comparison to the control, this value is very low and thus would not indicate the need for further investigation.

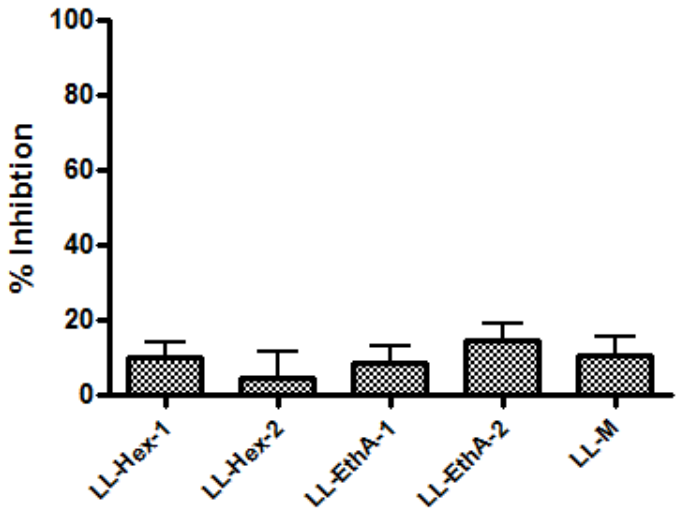

Figure 4.20: Percentage inhibition of LL Cr. extracts (tested at 30µg/mL) on DPP IV enzyme. Results are shown as a percentage of inhibition compared to the positive control (P32/98) at the highest concentration tested. Results represent mean ± SEM, n=4. Data analysed using One-Way ANOVA with a Dunnet Post-Test.

4.3.5.2. PTP1b

All cr. extracts were tested using the PTP1b inhibition assay in comparison with the standard PTP1b inhibitor, TFMS. Figure 4.21 shows the inhibitory effects of the cr. extracts (tested at 30µg/mL) on PTP1b without the addition of catalase. These results were variable between experiments, which could be due to the reactions between the extracts and components of the buffer. Therefore, although some extracts appeared to inhibit the enzyme substantially, these results may be false positives. PTP1b has been shown to be inhibited by H_2O_2 as a result of the formation of reactive oxygen species (ROS) (Bogeski *et al.*, 2006). It is possible that because these samples are cr. extracts which may contain multiple compounds, some of these components may react to form ROS. Thus, to minimise false positives, the assay was carried out again with buffer containing catalase. Figure 4.22 shows the results of this assay with the addition of catalase in the assay buffer with all other conditions remaining the same. From the graph it is evident that extracts no longer show significant inhibition with the highest inhibition value being less than 10%. The inhibition is minimal and did not warrant further investigation.

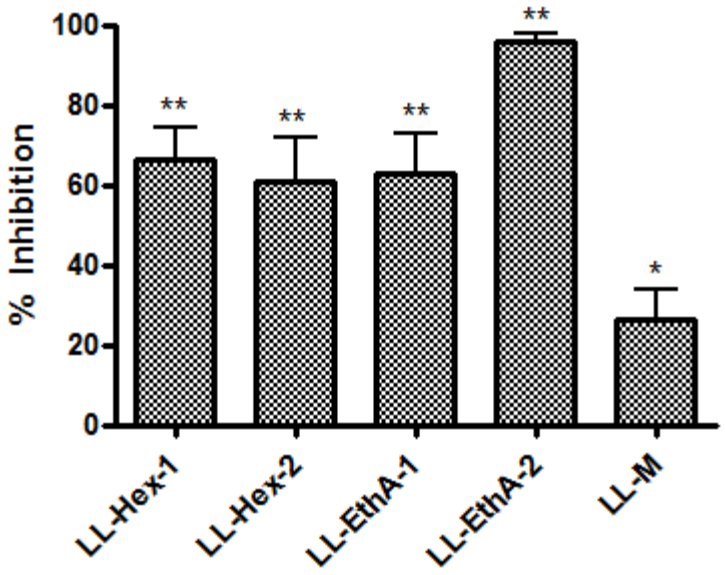

Figure 4.21: Percentage inhibition of PTP1b by LL cr. extracts. The assay buffer did not contain catalase. Data represents mean ± SEM, n=6. Data analysed using One-Way ANOVA with a Dunnet Post-Test. **P<0.01, *P<0.05 vs control.

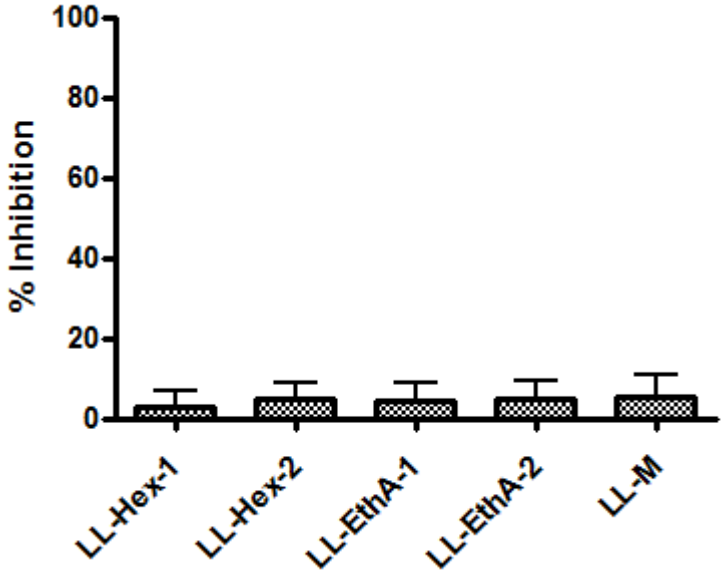

Figure 4.22: Percentage inhibition of PTP1b by the cr. extracts of LL tubers. The assay buffer contained catalase. Data represents mean ± SEM, n=4. Data analysed using One-Way ANOVA with a Dunnet Post-Test.

4.3.5.3. Alpha-amylase

The cr. extracts were tested for α-amylase inhibitiory activity using acarbose as a positive control. The cr extracts were tested at 30µg/mL as a preliminary screen, however, they showed no significant inhibition (Figure 4.23). The highest mean percentage inhibition was for LL-Hex-1 and LL-EthA-2 with values of 8.15% and 7.79% respectively. Thus, the inhibition of α-amylase by these cr. extracts was minimal. As a result, no further investigation in this area was carried out.

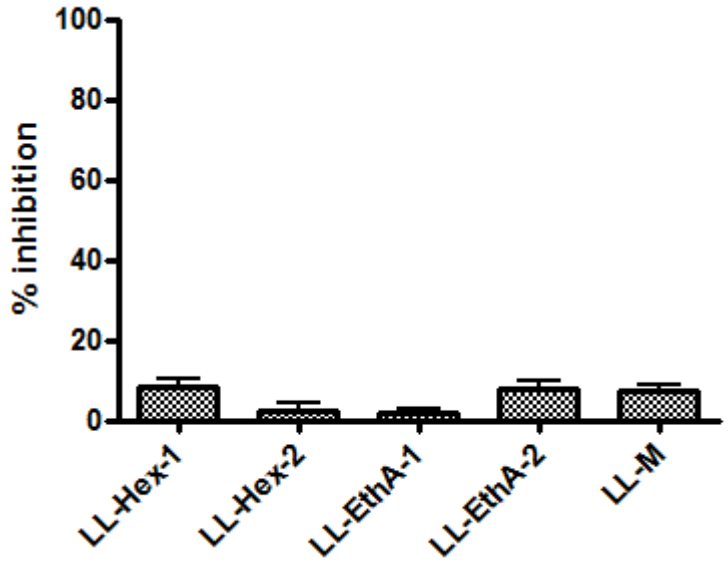

Figure 4.23: Percentage inhibition of α-amylase by LL tuber cr. extracts. Data represents mean ± SEM, n=3. Data analysed using One-Way ANOVA with a Dunnet Post-Test.

4.3.5.4. Alpha-glucosidase

All cr. extracts, at 30µg/mL, were tested in the α-glucosidase inhibition assay using acarbose as a positive control. Two of the five cr. extracts showed significant ($P<0.01$) inhibitory activity against α-glucosidase in comparison to the control (where there was no inhibition of this enzyme) – these extracts were LL-EthA-1 and LL-EthA-2 (Figure 4.24). Both extracts arose from the ethyl acetate extraction, thus may contain similar compounds. The mean inhibition value for LL-EthA-1 was 80.4%, while LL-EthA-2

was 78.7%. As a result of the activity seen when testing the cr. extract, these extracts were fractionated in an attempt to narrow down the activity and isolate specific components. This was achieved using VLC as described in Chapter 4, Section 4.2.2. Each fraction was then tested at 30µg/mL for α-glucosidase inhibitory activity. The results are shown in Figure 4.25. Each fraction showed significant ($P<0.01$) inhibitory activity towards this enzyme, with the lowest inhibition seen when testing EV1 and EV5. Following this, a serial dilution was performed with each fraction to identify the IC50 values. The results are shown in Figure 4.26 and Table 4.8. The most potent inhibition is evident from EV4 and EV3 where the IC50 was 1.59µg/mL and 1.69µg/mL, respectively. As expected, the lowest inhibition was seen for EV1 and EV5 with IC50 values of 36.10µg/mL and 24.47µg/mL, respectively.

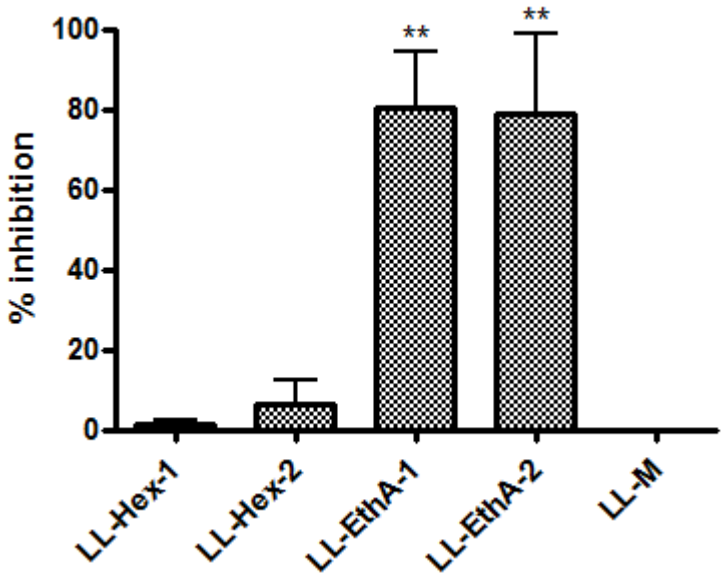

Figure 4.24: Percentage inhibition of α-glucosidase by LL tuber cr. extracts. Data represents mean ± SEM, n=3. Data analysed using One-Way ANOVA with a Dunnet Post-Test. **P<0.01 vs control.

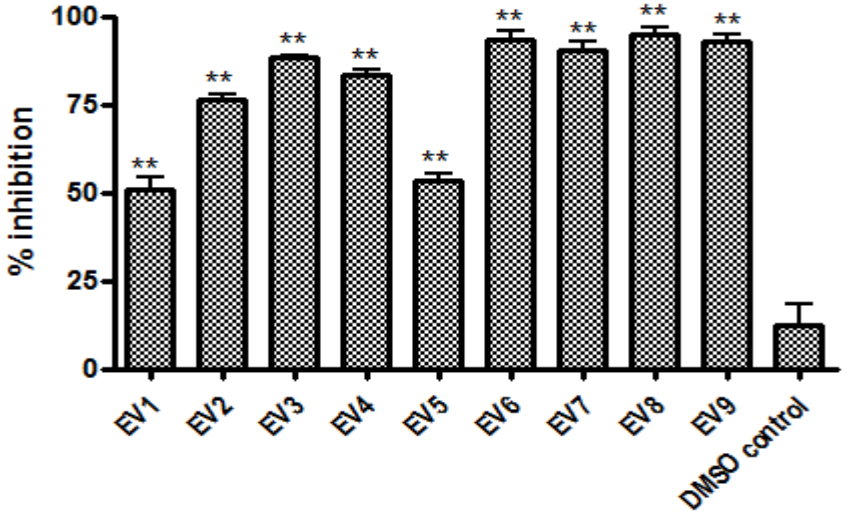

Figure 4.25: Percentage inhibition of α-glucosidase by ethyl acetate fractions from LL tuber cr. extract. Data represents mean ± SEM, n=4. Data analysed using One-Way ANOVA with a Dunnet Post-Test. **P<0.01 vs control.

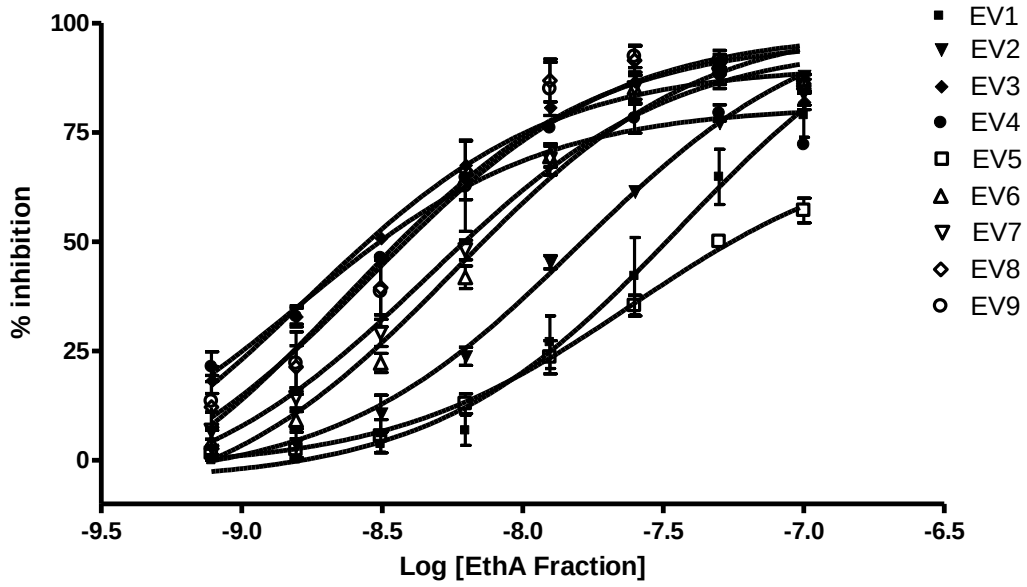

Figure 4.26: Dose response curve of EthA fractions in α-glucosidase inhibition assay. Data represents mean ± SEM, n=3.

Table 4.8: IC50 values of each EthA fraction in α-glucosidase inhibition assay.

FRACTION	IC50 (µg/mL)
EV1	36.10
EV2	15.69
EV3	1.69
EV4	1.59
EV5	24.47
EV6	5.72
EV7	4.61
EV8	2.37
EV9	2.87

4.3.5.5. Pancreatic Lipase

Using Orlistat as the positive control, all cr. extracts were tested in the pancreatic lipase inhibition assay (at 30µg/mL). Figure 4.27 shows the activity of each cr. extract against pancreatic lipase. None of these extracts showed significant inhibitory activity of this enzyme, thus were not investigated further.

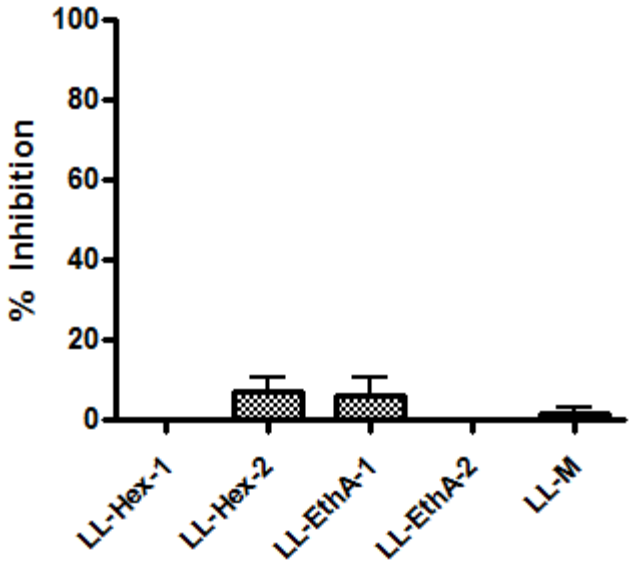

Figure 4.27: Percentage inhibition of pancreatic lipase by LL tuber cr. extracts. Data represents mean ± SEM, n=3. Data analysed using One-Way ANOVA with a Dunnet Post-Test.

4.3.5.6. U937 TNFα release

When LPS was added to differentiated U937 cells, the cells released TNF-α as an immune response to the foreign proteins and antigens present. U937 cells are monocyte-like cells which differentiate into macrophage-like cells. Compared to medium alone (untreated), LPS caused a significant ($P<0.01$) increase in the production of TNF-α in U937 cells. LPS was added to the cells simultaneously with different cr. extracts (30µg/mL) to determine if the extracts could inhibit the production of TNF-α and thus have an anti-inflammatory effect. The cr. extracts (30µg/mL) were also added alone to determine if they could cause the same effect as LPS alone and thus they would be pro-inflammatory. Figure 4.28 shows the concentration of TNF-α released following treatment of cr. extract alone, or crude extracts plus LPS. The crude extracts alone produced a significantly lower concentration of TNF-α when compared to LPS. Therefore, they did not appear to be pro-inflammatory. When added alongside LPS, some cr. extracts significantly ($P<0.01$) enhanced the release of TNF-α from the differentiated U937 cells compared

to the untreated medium control. LL-Hex-1, LL-Hex-2 and LL-EthA-1 significantly ($P<0.01$) increased the release of TNF-α when compared to the LPS control ($P<0.01$). LL-EthA-2 and LL-M did not appear to have any effect in comparison to LPS alone. To conclude, some extracts considerably increased the concentration of TNF-α released which may indicate they can enhance an inflammatory response although they cannot elicit this response on their own.

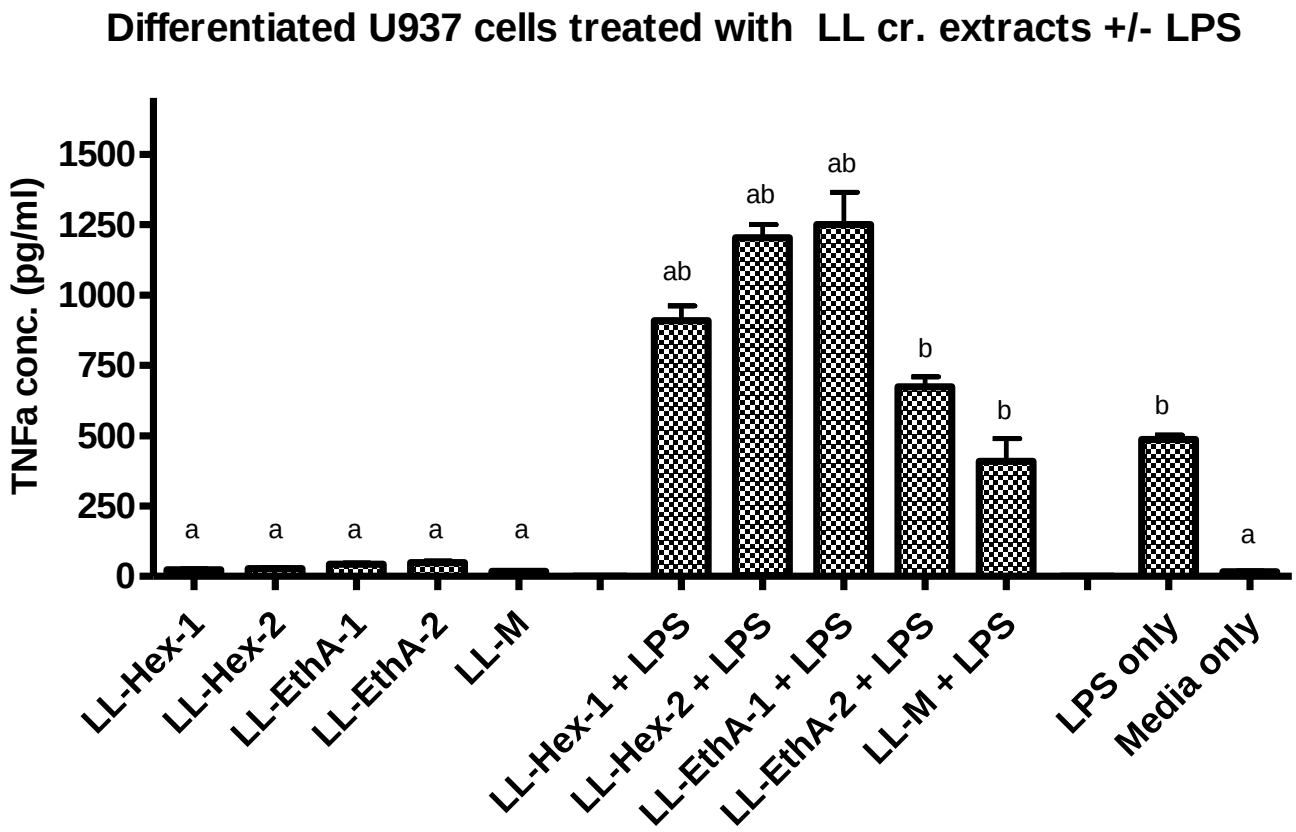

Figure 4.28: Immunomodulatory activity of LL tuber cr. extracts using PMA-differentiated U937 cells. Cr. extracts added either alone, or with LPS (+LPS). Data represents mean ± SEM, n=4, medium alone; n=5, LL-Hex-1, LL-M; n=7 all remaining samples. Data analysed using One-Way ANOVA with a Dunnet Post-Test. [a] $P<0.01$ vs LPS alone, [b] $P<0.01$ vs medium alone.

4.4. Discussion and Conclusion

The investigation of natural products as a source of novel human therapeutics is a widely researched area worldwide. Between 1981 and 2014, around 40% of new chemical entities (NCEs) were either natural products themselves or derived from natural products (Newman and Cragg, 2016). Modern day drug discovery is largely based on the screening of molecules for their ability to bind specific targets. However, natural products, and more specifically cr. extracts (>10 components) and semi-pure extracts (5-10 components) (Koehn and Carter, 2005), may in fact have more than one target or specific site of action. Due to this, and the complexity of natural products, the pharmaceutical industry has shifted to more synthetic libraries for high-throughput screening to obtain lead compounds for drug discovery. However, there is still great potential for natural products in the world of drug discovery today.

Due to the lack of results during the *in vivo* feeding study, an alternative approach was required to investigate the tuber and its components more closely. The purpose of this was to identify possible biologically active compounds which could be causing the appetite suppressing effects in humans. This was achieved using Soxhlet extraction and subsequently subjecting the extracts to *in vitro* bioassays.

Following collection of the LL tubers, they were dried as described in the traditional method, and subjected to extraction. Cr. extracts were obtained via Soxhlet extraction using increasing polarity of solvents. This method is commonly used when extracting natural products from plant material. The process of Soxhlet extraction is continuous, and in using different solvents various types of compounds can be extracted. However, as it involves heating to high temperatures, some compounds may be compromised if they are heat sensitive and/or volatile (Luque de Castro and Priego-Capote, 2010). The purpose of using Soxhlet extraction in this study was to extract as many types of compounds as possible for further analysis. As the traditional method of use did not involve an extraction process before consumption, the method of Soxhlet extraction is deemed appropriate to obtain as many compounds as possible. In other studies on traditional medicines and herbal medicines, it is important to closely mimic the

original extraction process in order to isolate the bioactive constituents. There are no prior extraction processes documented in the literature for LL tubers, thus the method of extraction was solely used to extract as many compounds as possible for initial analysis.

Three solvents of increasing polarity were used in the Soxhlet extraction – hexane, ethyl acetate and methanol. The major compounds extracted from the hexane extracts were triglycerides and betulinic acid. Triglycerides have been the focus of many scientific studies as researchers look into the benefits and bioactivity of different fatty acids. In this study, the exact nature of the triglycerides was not identified. Identification of the exact fatty acids attached would involve esterification of the fatty acids. Subsequently, the samples could have been analysed using LC-MS with known standards. However, even using this method, the nature of the whole triglyceride molecule could not be determined in terms of the position of each fatty acids on the triglyceride molecule. This experiment could be conducted in future work for this project to confirm the extact nature of the triglycerides and fatty acids present. Fatty acids, particularly omega-3 fatty acids are known to have health promoting benefits and have shown some bioactivity *in vitro* as well as *in vivo* (Cazzola *et al.*, 2007; Sneddon *et al.*, 2008; Wahle *et al.*, 2004, 2003).

Betulinic acid has also been shown to have bioactive properties. In the 1990s, betulinic acid was selected in the NCI Rapid Access to Intervention Development programme as one of the most promising anti-cancer agents in a screen of over 2500 plant extracts. In addition to this, betulinic acid is thought to have anti-bacterial, anti-malarial, anti-HIV (Cichewicz and Kouzi, 2004) and anti-inflammatory activities (Moghaddam *et al.*, 2012). Betulinic acid has been isolated from many taxonomically diverse plant species with the birch tree (*Betula spp.*) being a major source (Cichewicz and Kouzi, 2004). Various mechanisms of action have been reported for betulinic acid. In regards to the anti-cancer activities, it is thought to trigger apoptosis via the mitochondrial pathway in cancer cells (Fulda, 2008) as well as to modulate the activity of the transcription factor nuclear factor-κB (NKκB). The modulation of NKκB could also

be responsible for the anti-inflammatory activities of NFκB plays an important role in the induction of pro-inflammatory genes (Tak *et al.*, 2001).

LL-EthA-2 has been identified as a novel compound, which we have named lathyrosaponin-A, (3-*O*-[-α-L-arabinopyranosyl-(1→2)-β-D-glucuronopyranosyl]-24-hydroxy-12-oleanen-30-oic acid) and to our knowledge has not been identified before in any plant species. However, it has similarities to previously identified compounds. Yoshikawa *et al.* (2002) identified a similar compound which they referred to as albiziasaponin B. This compound was isolated from *Albizia myriophylla* (AM) stems. LL and AM are both from the same plant family, Fabaceae, however they have different subfamilies with LL belonging to Faboideae and AM belonging to Mimosoideae. Lathyrosaponin-A is similar to albiziasaponin B in that the aglycone structure is the same, however, albiziasaponin B has three sugar molecules attached at C3 whereas Lathyrosaponin-A only has two sugar molecules. The taste of the LL tubers has been described as being similar to sweet liquorice. A similar compound has been isolated from Chinese liquorice (*Glycyrrhiza uralensis)*. Licoricesaponin J2, which has two glucuronic acid residues attached to C-3 of the same aglycone as albiziasaponin B (Kitagawa *et al.*, 1991). Yoshikawa *et al.* determined that the carboxylic acid at position 30 on albiziasaponin B gave rise to potent sweetness of this molecule, which they determined to be 600 times sweeter than sucrose. Thus, it is possible that this compound contributes to the sweetness of the LL tubers. Additionally, Perez *et al.* (2013) reported the isolation and identification of another compound similar to Lathyrosaponin-A, which they referred to as 3-O-[-α-L-arabinopyranosyl(1→2)]-β-D glucuronopyranosyl azukisapogenol (compound 1). This compound was isolated from the aerial parts of *Trifolium hybridum* L. which is also from the plant family Fabaceae, with the sub-family being the same as Lathyrosaponin-A – Faboideae. However, *T. hybridum* L is from the Trifolieae tribe while LL is from Vicieae. The stereochemistry of compound 1 is different to Lathyrosaponin-A as the carboxylic acid is in position 29 for compound 1, but at position 30 for Lathyrosaponin-A, i.e. the stereochemistry at carbon 20 is opposite (Table 2.14). In NOESY NMR of compound 1, it was identified that the C30 methyl group correlates with H18. However, in the case of Lathyrosaponin-A, there is no

correlation between these protons and therefore the stereochemistry must be different for both compounds (see Appendix 5, Figure A5-10). The sugars attached at position C3 appear to be identical, where there is a glucuronic acid attached to an arabinose (2→1) (see Appendix 5, Figure 5-12). Compound 1 was identified for the first time in *T. hybridum* L., however, it had been identified before in other species (*Vigna angulariz, Oxytropis glabra, and O. myriophylla*). The two studies described above used acid hydrolysis to aid in the identification of the sugar moieties, thus this could be conducted in future work for LL. Lathyrosaponin-A is also very similar in structure to glycyrrhizin (Figure 4.30) – a saponin found in the root of *G. glabra* (liquorice). Glycyrrhizin (glycyrrhizic acid) gives rise to the sweet taste of the root (30-50 times sweeter than sucrose (Kao *et al.*, 2013) and has been associated with various biological activities including the reduction of serum testosterone levels (Armanini *et al.*, 2004) and protection of the liver bile-acid induced cytotoxicity (Kao *et al.*, 2013). Moreover, it has been reported that glycyrrhizic acid has beneficial effects on hepatitis by reducing serum alanine transaminase (ALT) levels, as well as necro-inflammation and fibrosis in the liver (Kao *et al.*, 2013). Glycyrrhizin is also associated with adverse side-effects such as increased blood pressure, hypernatraemia (high blood sodium levels) and hypokalaemia (low blood potassium levels). Following hydrolysis by intestinal bacteria (Omar *et al.*, 2012), glycyrrhizin can block the activity of the enzyme (11-β-hydroxysteroid dehydrogenase type 2) which converts cortisol to inactive cortisone. Subsequently, cortisol binds to mineralocorticoid receptors (MR) which promote sodium reabsorption, excretion of potassium and hypertension. This leads to the clinical state of liquorice-induced pseudoaldosteronism (Sonita *et al.*, 2008). Blockage of this enzyme also leads to immunomodulatory activities. Additionally, glycyrrhizin can cause water retention, with subsequent oedema formation. There are minimal differences between glycyrrhizin and Lathyrosaponin-A. Firstly the ketone group at C11 is present in glycyrrhizin but not in Lathyrosaponin-A. Additionally, Lathyrosaponin-A has a hydroxyl group at C24 instead of a methyl group, and arabinose attached to a glucuronic acid on carbon 3 of the aglycone. It is thought that the properties of glycyrrhizin are attributed to its steroid-like aglycone structure. Thus, the properties of both glycyrrhizin and Lathyrosaponin-A could be similar, although the differences in functional groups may influence this.

Lathyrosaponin-A was obtained as a crude fraction, therefore there are also minor components present within this extract. Future work could involve purification and further structure confirmation experiments such as X-ray crystallography. Similar compounds have also been identified in other *Lathyrus* species. Lathyrus saponin, isolated from *L. japonicus* (Sam Sik *et al.*, 1998) lacks the carboxylic acid at position 24, and has a hydroxyl group at position 22. Additionally, the sugar moieties attached at position 3 are different. Kang *et al.* also identified two azukisaponins in this plant.

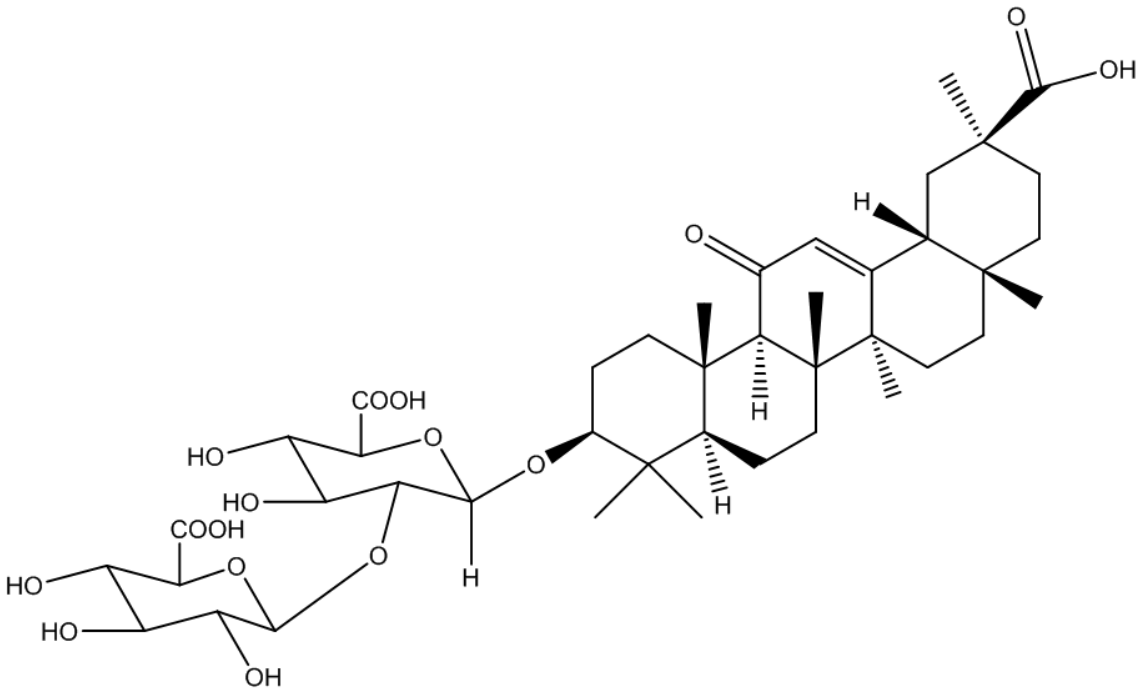

Figure 4.29: Structure of glycyrrhizinic acid. Diagram generated using ChemBio Draw 13.0. Glycyrrhizinic acid is very similar in structure to LL-EthA-2 with the exception of a ketone at carbon 11, two glucuronic acid molecules attached to carbon 3 rather than glucuronic acid and an arabinose, and a methyl group at carbon 24 rather than a hydroxyl group.

Dr Moffat speculated that a potential active constituent of the LL tubers is TA (structure shown in Figure 4.30). The presence of TA in the tuber was confirmed for the first time using GC-MS. TA is widely found in many essential oils extracted from

plants including anise (*Pimpinella anisum*), star anise (*Illicium verum*) and fennel (*Foeniculum vulgare*). It is widely used as a flavouring substance in baked goods, chewing gum, alcoholic beverages and ice cream. As a result of its extensive use as a flavouring agent, many studies have been carried out to determine the toxicity of this compound and to identify any carcinogenic effects. The toxicity has generally been shown to be of low order, however, one study did show TA to have a very weak hepatocarcinogenic effect in female Sprague dawley rats, but not males (Truhaut *et al.*, 1989).

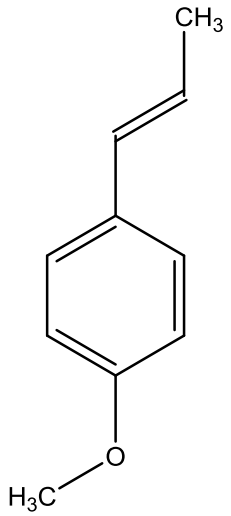

Figure 4.30: Structure of *trans*-anethole.

Furthermore, to understand the fate of TA *in vivo*, Bounds and Caldwell (1996) studied the metabolism of this compound in rats and mice at a dose of 250mg/kg BW. They found that TA is metabolised within the rat, with 95% of the dose being recovered in the urine within 24h. Additionally, they identified that it undergoes various oxidation reactions to produce a variety of metabolites. Details of the metabolites and the primary pathways are noted in their publication (Bounds and Caldwell, 1996). Furthermore, Rompleberg *et al.* (1993) studied the effect of TA on drug-metabolising enzymes within the rat liver using a dose of 125 or 250mg/kg BW. The aim of this study was to identify if TA had any cancer modulatory effects following oral administration. They identified a dose-dependent decrease in BW following treatment

with TA, however the results were not significant. Additionally, they noted that there was no effect on haematological parameters such as number of erythrocytes, leucocytes and platelets. Lastly, they concluded that TA has a larger effect on the induction of phase-II enzymes (which generally serve as a detoxifying step in the metabolism of drugs) and could have potential cancer preventative properties. The dose of TA used in the above experiments are approximately 3-6 times higher, respectively, than the dose of tuber administered in the *in vivo* study (42mg/kg BW) discussed in Chapter 3. The final dose given (210mg/kg BW) was comparable to the above, however, the concentration of TA in the tuber is unknown therefore it could be much lower.

Fennel, one of the most common natural sources of TA, is widely known for its biological properties including antioxidant, anti-inflammatory, anti-cancer and anti-genotoxic activities (Sheikh *et al.*, 2015). Treatment of streptozotocin-induced diabetic mice with a petroleum extract of fennel improved their blood glucose levels and lipid profile, which could potentially be due to the presence of TA. Sheikh *et al.* (2015) recently showed that administration of TA (80mg/kg BW) to diabetic rats significantly decreased plasma glucose levels and increased plasma insulin levels in a dose-dependent manner compared to untreated diabetic controls. Administration of TA to normal rats resulted in no significant changes in terms of plasma glucose or plasma insulin levels. The glucose lowering effect of TA to the diabetic rats was very similar to the effect seen when administering glibenclamide (an anti-diabetic drug in the sulfonylurea class) compared to rats receiving no treatment. This group also showed that treatment with TA restored levels of haemoglobin (Hb) in diabetic rats to the level of normal untreated rats, while also decreasing levels of haemoglobin A1c (HbA1c) significantly compared to diabetic controls. HbA1c is commonly used to identify the average plasma glucose levels over a prolonged period of time. Again, normal rats treated with the same dose showed no significant changes compared to the control.

Moreover, Sheikh *et al.* (2015) examined the effect of TA treatment on carbohydrate metabolic enzymes – hexokinase, glucose-6-phosphate dehydrogenase, glucose-6-

phosphatase and fructose-1,6-biphosphatase. When induced with diabetes, the rats showed a significant increase in the activities of hexokinase and glucose-6-phosphate dehydrogenase while also producing a significant decrease in the activities of glucose-6-phosphatase and fructose-1,6-biphosphatase. When treated with TA, the enzyme activities reverted back to near normal and again the results were similar to that of glibenclamide. These findings indicate a potential use of TA in the treatment and prevention of diabetes. A follow up *in vivo* study could examine the effect of the tuber on the parameters above to give an indication of the potential anti-diabetic effects of the tuber.

This is the first time it has been confirmed to be present in the tubers of LL. TA has a wide variety of applications in the food industry, as well as being used as a precursor in the pharmaceutical industry and cosmetic industry (Wiirzler *et al.*, 2015). Moreover, essential oils containing TA have been shown to have various biological activities including wound-healing (Malveira Cavalcanti *et al.*, 2012), immunomodulation (Wiirzler *et al.*, 2015), antioxidant (Sheikh *et al.*, 2015), a hypoglycaemic (Sheikh *et al.*, 2015), gastro-protective (Coelho-de-Souza *et al.*, 2013), and an anti-microbial (Senatore *et al.*, 2013). During the metabolism of TA in humans, *trans*-aminase enzymes - such as aspartate transaminase (AST) and ALT – can potentially add an amine group at the double bond position thus converting TA to amphetamine-like compounds. A similar pathway can also occur in plants with use of transaminase enzymes. It is thought that the pathway from L-phenylalanine to amphetamine-type alkaloids in khat and *E. sinica* consists of at least two transaminase steps (Groves *et al.*, 2015). Amphetamine-like compounds, such as cathinone present in khat and pseudoephedrine and (1R,2S)-ephedrine in *E. sinica,* can result in reduced appetite and hunger through various mechanisms in the brain including activation of catecholaminergic neurotransmission (Hsieh *et al.*, 2005). Thus, it is possible that the metabolism of TA to an amphetamine-like compound is the cause of appetite suppressing properties of LL tuber.

Following extraction, preliminary *in vitro* assays were carried out to assess potential

biological activity. In this study, the cr. extracts of the tubers were not toxic to various cell lines at concentrations between 100 µg/mL to 0.718 µg/mL. These results allowed further investigation into the actions of the tuber. However, they do not indicate if there is any long-term toxicity or accumulative toxicity. Although there was no cytotoxicity evident, the hexane and methanol extracts (LL-Hex-1, LL-Hex-2, and LL-M) appear to increase the viability by up to 50% in comparison to the control. The viability increases with concentration of the extracts thus showing a dose-dependent effect. There may be multiple reasons for this. Firstly, the cells could be growing at a faster rate, with an increased doubling time due to the presence of fatty acids and sugars in the extracts. However, it is also possible that the extracts have increased the metabolism of the cells, rather than the growth. These cells may metabolise the resazurin at a quicker rate, thus giving the same result. To establish the exact cause, further investigation would be required.

Due to the traditional usage of LL tubers as an appetite suppressant, several enzymatic assays were selected which involve enzymes implicated in various aspects of obesity as well as diabetes. These disease states involve complex signalling pathways, of which some also involve the control and regulation of appetite and food intake. The enzymes included DPP IV, PTP1b, α-amylase, α-glucosidase and pancreatic lipase. When testing the cr. extracts for inhibitory activity against these enzymes, it was found that the extracts did not inhibit DPP IV, PTP1b, α-amylase or pancreatic lipase. Due to this, no further investigation was carried out involving these enzymes. Contrary to this, the ethyl acetate cr. extracts and fractions significantly inhibited the actions of α-glucosidase, with many fractions eliciting a potent inhibition. This extract may consist of several different compounds, all of which could have an effect on the α-glucosidase inhibitory activity. Betulinic acid, identified in the hexane extracts, has previously been shown to inhibit α-glucosidase (Kumar *et al.*, 2013). However, these extracts did not show any inhibition in this study. This may be due to the cr. extracts being a mix of more than one compound, thus other compounds present may be blocking this effect. Additionally, betulinic acid was tested by Kumar *et al.* at 50µg/mL, whereas the cr. extracts in this study were screened at 30µg/mL, thus the concentration of betulinic acid would be less than 30µg/mL. α-glucosidase is involved in the breakdown of

carbohydrates following a meal, thus inhibition of this enzyme reduces the post-prandial blood glucose spike. Various types of compounds have been shown to elicit similar responses against α-glucosidase. Yilmaza-Musa *et al.* (2012) showed that green tea extract, white tea extract and grape seed extracts were able to inhibit α-glucosidase activity. They hypothesised that these actions are due to the large volume of flavonoids present, particularly flavan-3-ols. Additionally, green and white tea extracts are abundant in catechins while grape seed extracts are abundant in procyanidins. It is possible that the combination of these compounds gives rises to differing inhibitory activities of each extract. Moreover, Hou *et al.* (2008) identified triterpene acids from the ethyl acetate fraction of *Lagerstroemia speciose* leaves as potent inhibitors of α-glucosidase. They isolated six compounds including oleanolic acid, corosolic acid, arjunolic acid, asiatic acid, maslinic acid and 23-hydroxyursolic acid, each of which had different IC50 values for this enzyme. It is possible that the ethyl acetate extract from LL tubers (LL-EthA-1 and LL-EthA-2) contain multiple compounds which may act synergistically to elicit a strong response to α-glucosidase. The main component of LL-EthA-2 was identified as a novel compound (3-*O*-[-α-L-arabinopyranosyl-(1→2)-β-D-glucuronopyranosyl]-24-hydroxy-12-oleanen-30-oic acid; see Chapter 4), with similarities to glycyrrhizin and albiziasaponin B (Yoshikawa *et al.*, 2002). There is no scientific literature indicating the ability of albiziasaponin B or glycyrrhizin to inhibit α-glucosidase. However, many α-glucosidase inhibitors have been shown to contain similar sugar moieties which act as competitive inhibitors of the enzyme. Thus, it is possible that the major compound in LL-EthA-2 is an inhibitor of α-glucosidase. To confirm this, purification of this crude extract needs to be carried out followed by further α-glucosidase inhibition assays for confirmation. One of the most common inhibitors of α-glucosidase is miglitol. As with other α-glucosidase inhibitors, miglitol induces malabsorption by preventing or slowing down the absorption and metabolism of carbohydrates to glucose. This happens in the proximal small intestine. Subsequently, the absorption of complex carbohydrates moves further down to the distal portion of the intestine. In some clinical trials where α-glucosidase inhibitors have been given to volunteers with a high carbohydrate meal, an enhancement of peptides associated with satiety has been reported alongside a decrease in the rate of gastric emptying. Such peptides include GLP-1, secreted predominately from the ileal

endocrine L-cells (Shin *et al.*, 2015). Moreover, activation of the ileal brake (Spiller *et al.*, 1984) has been shown to have profound effects on food intake as well as satiety (Maljaars *et al.*, 2010). The ileal brake is an inhibitory feedback mechanism which controls the movement of foodstuffs through the GIT for the purpose of optimising nutrient absorption. When nutrients have not been metabolised appropriately, and subsequently reach the hind gut causing an unusually high intraluminal nutrient content, the ileal brake is activated (Shin *et al.*, 2013). Activation of this feedback mechanism has been shown to result in a reduction in food intake and inhibition of hunger (Shin *et al.*, 2013). Therefore, in inhibiting α-glucosidase, the compounds present in the LL tubers may be promoting satiety and thus reducing food intake via the ileal brake mechanism. Thus the findings above may provide a possible mechanism of appetite or hunger suppression by the LL tubers. Current drugs for the inhibition of α-glucosidase, such as acarbose, are effective, but can cause severe side effects. Therefore, there is great interest in discovering new inhibitors with fewer side effects.

In addition to investigating the inhibitory effect of each extract on various enzymes, a further screening study was carried out to determine the effect of the extracts on TNFα release from differentiated U937 cells. TNFα is known to be a mediator of anorexigenic and pro-catabolic events, which result in severe inflammatory diseases and cachexia (weight and appetite loss) in cancer (Ebadi and Mazurak, 2015). It has also been shown to be over expressed in obese individuals and rodent models of obesity (Sethi and Hotamisligil, 1999) and has been implicated in insulin resistance in diabetes. TNFα is also thought to be involved in the regulation of leptin (Kirchgessner *et al.*, 1997) which influences appetite. Although TNFα is known to cause an inflammatory response, it is also thought to increase metabolism and therefore is associated with weight loss. Romanatto *et al.* (2007) showed that intracerebroventricular (ICV) administration of TNFα (10^{-8} M) to male Wistar rats causes significant increases in body temperature and respiratory quotient and while there was a decrease in oxygen consumption. Administration of leptin and insulin did not produce these changes, neither did a lower dose of TNFα (10^{-12} M). These changes suggest an increase in metabolism associated with TNFα which appears to be dose-dependent.

In this study, all of the extracts significantly increase TNFα in comparison to the control containing medium alone. However, when comparing these results to treatment of LPS alone, the increase is very minimal. When added alongside LPS, LL-Hex-1, LL-Hex-2 and LL-EthA-1 significantly increase TNFα release in comparison to LPS alone. The U937 cells were differentiated, using PMA, to macrophages which resemble inflammatory macrophages, previously characterised by Verhoeckx *et al.* (2004). Macrophages share signalling pathways and molecules with cells associated with metabolism such as adipocytes and hepatocytes. For example, both macrophages and adipocytes express toll-like receptors such as TLR2 and TLR4 which recognise LPS in bacterial cells walls, but also nutritional signals such as fatty acids (Tornatore *et al.*, 2012). The results shown in this study may indicate the presence of compounds which may bind to receptors in the cells to induce a larger inflammatory response via the release of TNFα – these could be saturated fatty acids or other biologically active compounds. The major components of the hexane extracts were identified as triglycerides and fatty acids, and betulinic acid, respectively. Thus, it is possible that the fatty acids present are causing the enhancement of TNFα. Moreover, glycyrrhizin has also been shown to have immunomodulatory effects (Kao *et al.*, 2013). LL-EthA-2 has structural similarities to glycyrrhizin therefore, the activity seen from the ethyl acetate cr. extracts may be due to the presence of similar compounds.

Previous research carried out in 1980 by Robeson and Harborne indicated the presence of anti-inflammatory compounds in leaf/cotyledon samples of LL. However, no anti-inflammatory effects were found from the extracts of the tuber. This may be due to their presence in trace amounts which may be unable to show any effect, or due to their absence within the tuber. Furthermore, the extracts may influence intracellular components. Thapsigargin, a sesquiterpene lactone isolated from *Thapsia garganica* is a non-competitive inhibitor of sacro/endoplasmic reticulum Ca^{2+} ATPase. This compound raises intracellular Ca^{2+} concentrations and has been found to amplify the release of TNFα in macrophages after the addition of LPS but not on its own (Chen *et al.*, 2001).

The biological activity of the tuber constituents may depend on their bioavailability and also on where they are within the body. Some compounds may be able to cross the BBB and act upon the hypothalamus. Other compounds may not be able to act in this way and may exert their effects in adipocytes or various other cells within the body such as the gastrointestinal tract (GIT). Moreover, some components of the cr. extracts may act as "pro-drugs", for example, glycosides, which must be metabolised within the body before they become "biologically active". Thus, when testing such compounds in an *in vitro* setting, the full potential and activity of the compound is not experienced (David *et al.*, 2014).

To conclude, there is some evidence to support the hypothesis that the LL tubers contain compounds which could influence appetite and food intake which corresponds to the traditional usage of the plant. However, the actions of the LL tubers may not be the result of one or more specific compounds acting individually. The biological effects may be due to the metabolism of the whole tuber, thus we would not see such results using *in vitro* experiments. Based on these results, a further *in vivo* study could look at blood serum and urine metabolomics following tuber consumption. Additionally, looking at enzyme activity and protein expression within specific tissues would be beneficial.

5. CHAPTER 5, RNA SEQUENCING OF HYPOTHALAMIC TISSUE

5.1. Introduction

Appetite is an extremely complex process, which is regulated and influenced by various hormones, peptides and signalling molecules within the body (Chapter 1 Introduction, Section 1.5). Identifying one single compound which has significant influence on appetite may be extremely difficult, thus a combination of poly-pharmacology and a systems level approach may be better (Anighoro *et al.*, 2014; Boran and Iyengar, 2010). The poly-pharmacology phenomena is defined as single drugs acting upon multiple sites of a disease pathway, but may also include several drugs acting upon multiple sites, which regulate a physiological response. Moreover, a systems level approach looks at multiple modulators of physiological pathways which make up a complex network of signals (Boran and Iyengar, 2010).

As identified in Chapter 4, LL tubers contain a wide variety of compounds, some of which may show physiologically relevant biological activity.

As the initial results from the *in vivo* feeding study (Chapter 3) lacked any indication of appetite suppression, the next best approach to identify mechanisms of action of these tubers was to use a poly-pharmacological approach in the hope of identifying multiple sites of action and/or multiple signalling networks involved. A similar approach was utilised by Kim *et al.,* (2016) when investigating the effects of metformin. Metformin is an established anti-diabetes drug. However, it has also been associated with anorectic effects, thus it has numerous mechanisms of action. Kim *et al.* (2016) found that metformin was able to activate neurons in multiple sites within the brain, not only regions involved in appetite regulation. However, they did not conclude what sites within the brain are responsible for the anorectic effects of metformin, thus highlighting the complexity of its mechanism.

The hypothalamus is the main site of appetite control and regulation. Central neural

circuits and target peripheral tissues regulate appetite, energy regulation and BW in a coordinated way. There are various modulators which act upon hypothalamic nuclei to elicit a physiological response. These nuclei include ARC, LHA, VHM, PVN and DMH as described in Section 1.5 (Introduction). Each of the nuclei interact with each other and can span various regions of the brain, thus creating a large and complex signalling network (Wang *et al.*, 2015). As a result, this area is widely researched in an attempt to dissect the processes involved. Many studies have focused on the hypothalamus to understand the process of energy regulation in the hope of subsequently developing therapies for disorders related to over- and/or under- eating i.e. obesity and anorexia. Thus, due to the potential of LL tubers to influence appetite and/or hunger, this area is of great interest as it may give insight into the mechanisms of action of the tuber as well as insight into the control and regulation of appetite.

One of the most recent discoveries in relation to energy regulation and appetite control is the potential involvement of a protein called Kisspeptin. Kisspeptin is generally associated with the regulation of reproduction through its interaction with the G-protein coupled receptor, GPR54 (Kisspeptin receptor). Hypothalamic kisspeptin directly stimulates gonadotropin-releasing hormone (GnRH) neurons, which expres Kisspeptin receptor, and it was identified that patients with idiopathic forms of hypogonadotropic hypogonadism (characterised by an impaired secretion of gonadotropins such as follicle-stimulating hormone (FSH) and luteinising hormone (LH)) had inactivating mutations in *KISS1R*. These finding were replicated in mice with mutations in both *Kiss1* and *Kiss1r* causing a similar condition (Seminara *et al.*, 2003). *Kiss1* and *Kiss1r* are not only expressed in the hypothalamus, they have also been found to be expressed in peripheral tissue including the pancreas, liver and adipose tissue, suggesting a role in metabolic function and or energy balance (De Bond *et al.*, 2016).

Quennell *et al.* (2011) demonstrated that leptin deficiency and diet-induced obesity in mice reduced *Kiss1* expression in the hypothalamus. These results correlate with the idea that decreased energy status negatively affects fertility, thus a reduction in leptin,

a hormone which controls food intake, would have a negative effect on fertility. Moreover, increased leptin levels increase *Kiss1* gene expression (Fu and van den Pol, 2010). Fu and van den Pol (2010) demonstrated that Kisspeptin directly interacts with anorexigenic POMC neurons in the ARC due to the presence of Kisspeptin receptor on the POMC neurons. Additionally, they showed that Kisspeptin inhibits NPY neurons in the ARC. These results indicate that Kisspeptin may modulate energy homeostasis and appetite. Furthermore, Tolson *et al.* (2014) demonstrated that *Kiss1r* knockout female mice developed an obese and diabetic phenotype, with increased bodyweight, leptin levels, adiposity and impaired glucose tolerance. The reason for this phenotype development remains unclear as De Bond *et al.* (2016) subsequently showed that despite this obese and diabetic phenotype development, hypothalamic gene expression remained unaltered. Thus, these changes may be the result of peripheral rather than central influences. Dudek *et al.* (2016) investigated the peripheral mRNA expression of *Kiss1* and *Kiss1r* in diet-induced obese and diabetic male rats. The results of this study indicate that diabetic, but not obese, rats have altered *Kiss1* and/or *Kiss1r* expression in the HPG axis. Furthermore, there was also altered expression in peripheral tissues including adipose tissue, pancreas and liver. Cockwell *et al.* (2013) showed the effects of fed and fasting states, in male and female rats, on *Kiss1* expression in adipose tissue and the hypothalamus. In male rats, fasting caused a significant increase in *Kiss1* in adipose tissue, but no significant effect in the hypothalamus. On the other hand, fasting in female rats caused a significant increase of *Kiss1* in adipose tissue, while there was a significant reduction in the hypothalamus. These results could indicate the involvement of changes in sex hormones as a result of fasting. The above research highlights again the complexity of appetite regulation and the maintenance of energy balance. Figure 5.1 shows a potential link between Kisspeptin, Kisspeptin receptor, POMC, NPY, and the HPG axis.

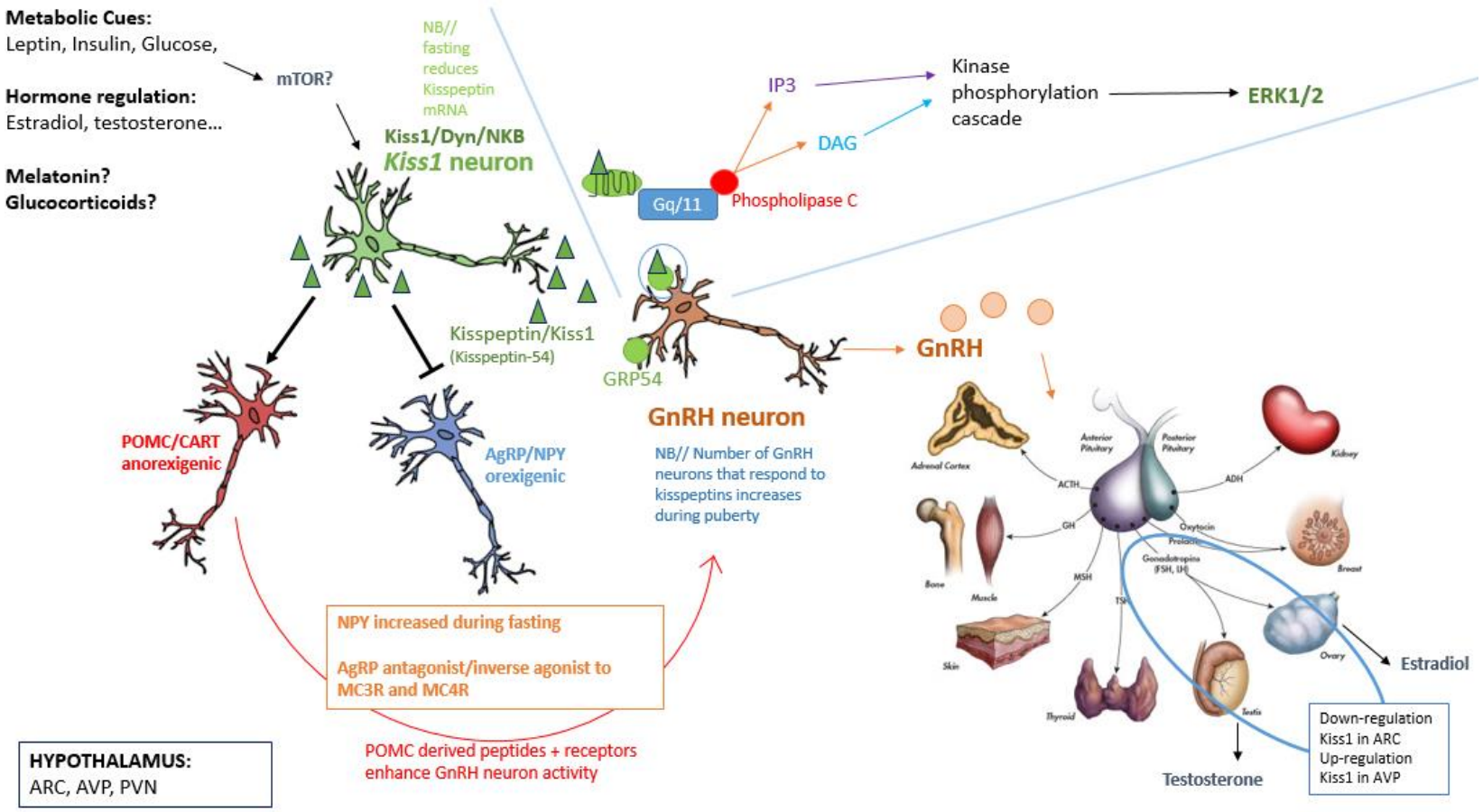

Figure 5.1: Schematic diagram showing potential links between Kisspeptin, Kisspeptin receptor, POMC, NPY and the HPG axis.

There are also several other genes and proteins of interest in the area of energy regulation and appetite control which have been studied extensively such as leptin, ghrelin, adiponectin, resistin, NPY, CCK to name a few (Ahima and Antwi, 2008; Ahima and Lazar, 2008; Archer *et al.*, 2005; Hsieh *et al.*, 2015; Ibars *et al.*, 2016; Lau and Herzog, 2014; Neary *et al.*, 2004; Sone *et al.*, 2016; Walewski *et al.*, 2014; Yu and Kim, 2012).

Henry *et al.* (2015) demonstrated the potential of a systems level approach using RNA Sequencing (RNASeq) technology. RNASeq is a next generation, ultra-high throughput method for transcriptome analysis (Wold and Myers, 2007). Using this technique, Henry *et al.* investigated neuronal responses to weight loss by examining differential gene expression following fed and fasted states in mice. Specifically, they looked at transcriptomics of single neuronal cell types including AgRP and POMC. This approach allows a very broad range of genes to be analysed, thus allowing dissection of complex signalling pathways. Similarly, Resnyk *et al.* (2015) carried out a transcriptomics study using RNASeq analysis to identify genes associated with increased adiposity in chickens with an additional aim to understand more about human metabolic diseases. The animal model utilised was developed originally to study the mechanisms involved in abdominal fat accumulation, which is a complex polygenic trait involving interactions of multiple genes in the endocrine and metabolic pathways. Thus, in using RNASeq technology, Resnyk *et al.* were able to understand the molecular mechanisms involved. Furthermore, Meng *et al.,* (2016) studied a non-obese type 2 diabetic rat model (the Goto-Kakizaki (GK) rat) using RNASeq technology. These rats exhibit hyperglycaemia, β cell defects and insulin resistance, in addition to hyperphagia. Using RNASeq, Meng *et al.* were able to study several important pathways involved in the pathogenesis of T2D within the hypothalamus including the melanocortin pathway and glucose sensing pathway.

These studies highlight the immense potential of RNASeq technology in poly-pharmacology and systems level approaches which may be the key to understanding the biological activity of natural products.

The aim of this chapter was to use next generating sequencing to identify gene expression changes within the hypothalamus as a result of treatment with LL tuber and TA.

5.2. Materials and Methods

5.2.1. RNA Extraction and Quality Control

RNA was extracted using either a Qiagen RNeasy Midi Kit (50mg-150mg) or a RNeasy Mini Kit (<50mg). The quality and integrity of the RNA was confirmed using a Nanodrop™ Spectrophotometer and Experion™ RNA StdSens Analysis kit, respectively. The Experion™ RNA StdSens kit was used as per the manufacturer's instructions. Hypothalamic tissue from two animals in each treatment group were initially used for RNA extraction – each animal was numbered 1-6 with the pre-fix referring to the treatment group they were allocated to. For example, the first animal in the control group would be referred to as 1.1, while the second would be 1.2. Similarly, the first animal from the tuber group is 2.1, and the second is 2.2. Lastly, the first animal from the TA group is 3.1, and the second sample is 3.2. Tissue used for RNA extraction were from animals 1 and 2 from each treatment group hence, 1.1, 1.2, 2.1, 2.2, 3.1 and 3.2. RNA extraction was performed individually on each tissue before pooling RNA from the two animals within each group.

5.2.2. RNASequencing (RNASeq) Analysis

The two RNA samples of each group were pooled and submitted to BGI-Tech (Shenzhen, China) for RNASeq Analysis (Illuminia HiSeq technology, 20Mb clean reads) – thus three samples were submitted, one for each treatment group. Pairwise comparisons were carried out on the three experimental groups – (1) Control *versus* Tuber treated; (2) Control *versus* TA treated; and, (3) Tuber treated *versus* TA Treated. Correlation heat maps were generated which indicate differences between each pairwise comparison at a high level. The experimental process at BGI-Tech is shown in Figure 5.2.

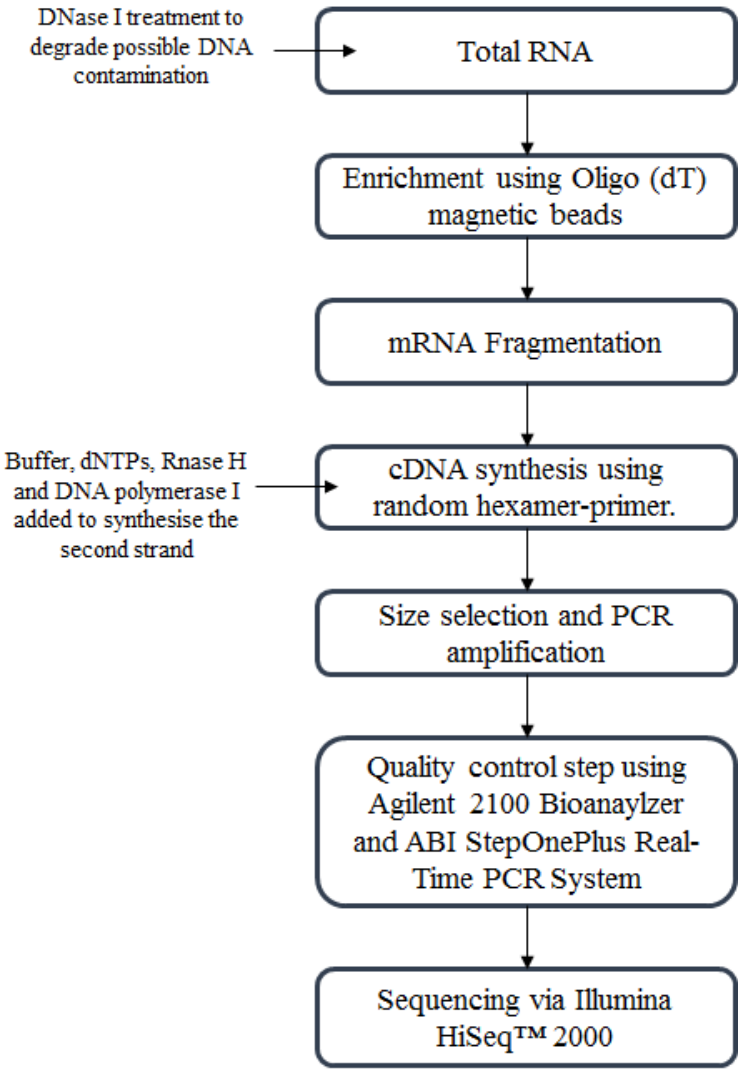

Figure 5.2: Experimental process of RNASeq as provided by BGI-Tech. Three RNA samples were submitted to BGI-Tech for RNASeq following quality control checks in-house. QC checks were also carried out at BGI-Tech before the samples were sequenced.

The primary sequencing data generated was subjected to quality control and filtering into clean reads by BGI-Tech. The clean reads were then aligned to the reference genome (*Rattus;* genome version rn6*;* University of California Santa Cruz (UCSC) which is again subjected to quality control analysis by BGI-Tech. Subsequently, BGI-Tech then performed differential gene expression analysis which was utilised in downstream analysis.

5.2.2.1. Pathway Enrichment Analysis

To understand the biological relevance of differentially expressed genes, pathway enrichment analysis was performed using Cytoscape software (version 3.3.0) (Shannon *et al.*, 2005) and the ClueGO plugin (version 2.2.4) (Lotia *et al.*, 2013). ClueGo software allows visualisation of functionally related genes, which are displayed in a clustered network. The statistical test used in the enrichment analysis was based on a two-sided hypergeometric option with Benjamini-Hochberg correction. The following settings were used in the ClueGO analysis: significant KEGG pathway enrichment ($P<0.05$), a kappa score of 0.3, GO Term/Pathway Selection (3/4%), medium network specificity, and GO Term grouping. Differentially expressed genes, which were shown to be up- or down-regulated by 2-fold or more were considered in the analysis. Using DAVID Bioinformatics Resources 6.8 (Huang *et al.*, 2009a, 2009b), genes associated with significant KEGG pathways were identified.

5.2.3. Identification of Genes associated with Appetite, Food Intake and Energy Metabolism and Regulation

Using the preliminary analysis provided by BGI-Tech as well as the raw data, a more thorough analysis was carried out in-house using various enrichment analysis software as well as comprehensive searches of current literature. The in-house analysis was specifically focused on energy balance and regulation, the regulation of food intake and appetite, satiety regulation, and neuronal and peripheral modulators of energy balance and food intake. An internal database was produced based on the above research which was then used in analysis of the RNASeq raw data and differential gene expression profiles provided by BGI-Tech. The internal database was then cross-

referenced to the RNASeq data for both the tuber vs. control data and TA vs. control data.

5.2.4. Real Time Quantitative PCR (RT-qPCR)

RT-qPCR was used to determine the expression of specific genes in all hypothalamic RNA samples from each treatment group. This information was utilised to determine variability within treatment groups, as well as to validate the RNASeq results. Specific appetite-related genes, identified during RNASeq analysis, were selected for RT-qPCR.

5.2.4.1. cDNA Synthesis

RT-qPCR requires DNA, thus cDNA was synthesised from each hypothalamic RNA sample in all three treatments groups. To synthesise cDNA from the extracted RNA, a Tetro cDNA Synthesis Kit (Bioline, London, UK) was used. Briefly, a master mix was prepared on ice which included the following: 1µg of RNA, 1µl Oligo $(dT)_{18}$, 1µl 10mM dNTP mix, 4µl 5x RT Buffer, and 1µl Ribosafe RNase Inhibitor. Samples were prepared in duplicate either with or without reverse transcriptase (RT). Samples which included 1µl Tetro Reverse Transcriptase (200u/ µl) were referred to as RT(+) samples. Minus-reverse transcriptase control samples were prepared in parallel using 1µl of DEPC-treated water in place of the RT. These samples were referred to as RT(-). All samples were made up to a total volume of 20µl with DEPC-treated water. Additionally, a no-template control (NTC) sample was prepared, without RNA, again with and without RT. Following sample preparation, each sample was incubated for 30 min at 45ºC, followed by 5 min at 85ºC. Samples were then cooled on ice and either used immediately or stored at -20ºC until required.

5.2.4.2. Reference Gene Optimisation

Reference gene PCR primers were designed based on MIQE guidelines (Bustin *et al.*, 2009) where possible. Gene Runner v.3.05 (www.generunner.net) was used for primer design followed by Primer-BLAST search (NCBI, (Ye *et al.*, 2012)) to ensure primers

were specific to the gene of interest and would not amplify genomic DNA. As the primers were intended for use with SYBR-green real-time PCR chemistry, all of the amplicons generated by the primer sets were approximately the same length and less than 150bp. Details of each primer are detailed in Table 5.1. All primer couples were designed to have a maximum Tm difference of 2-3ºC.

Table 5.1: Reference Gene Primer Design for qRT-PCR. Primers were designed using Gene Runner v3.05 followed by Primer-BLAST.

Ref. Gene ID	GenBank Accession Number	Primer Sequence (5' – 3')	Tm	Amplicon Size
HPRT For	NM_012583	CTCATGGACTGATTATGGACAGGAC	61.7	123
HPRT Rev		GCAGGTCAGCAAAGAACTTATAGCC	62.4	
B2M For	NM_012512	CTTGTCTCTCTGGCCGTCGTGC	62.2	131
B2M Rev		ATTTGAGGTGGGTGGAACTGAGACAC	60.6	
PGK1 For	NM_053291	AGCGGCTGGGACTGTCATCCTC	63.4	135
PGK1 Rev		TTGGACAGGGAGGCTCGGAAAG	61.2	
Tbp For	NM_001004198	TGGGATTGTACCACAGCTCCA	62.2	131
Tbp Rev		CTCATGATGACTGCAGCAAACC	61.5	

5.2.4.3. Reference Gene Stability Analysis

The stability of each reference gene was ranked using RefFinder [http://fulxie.0fees.us/; (Xie *et al.*, 2012)]. RefFinder integrates various computational programmes (GeNorm, Normfinder, BestKeeper, and the comparative ΔΔ-Ct method) to compare and rank tested candidate reference genes for stability under experimental conditions.

5.2.4.4. Target Gene Primer Design

Target gene primers were designed as above (Methods Section 4.3.10.2). Genes were chosen based on current literature which looked at genes involved in energy metabolism, the regulation of appetite and satiety and the regulation of food intake cross referenced with the database prepared from the RNASeq data. The genes chosen for RT-qPCR are highlighted in Table 5.2.

Table 5.2: Primer sequences of the selected target genes used for RT-qPCR.

TARGET GENE	GenBank Accession number	FORward PRIMER	FOR TM	REVerse PRIMER	REV TM	Amplicon size
Agrp	NM_033650	AGAAGGTCTGACCAGGCCCTGTTC	60.7	TCTAGCACCTCTGCCAAAGCTTCTG	60.0	120
Cck	NM_012829	CTAGCCCGATACATCCAGCAGGTC	59.9	CCCATGTAGTCCCGGTCACTTATCC	60.5	113
Cart	NM_017110	GGCGCTGTGTTGCAGATTGAAG	59.4	ACTGCTCTCCAGCGTCACACATG	58.9	118
Goat	NM_001107317	CCACCTGGGTCTTCACTACAAGGAG	59.0	ATGTCCAGGGAGAGAGACGTGACTC	58.7	120
Ghsr	NM_032075	AGATGCTTGCTGTGGTGGTGTTTG	59.9	TGGCTGATCTGAGCGATCTCCAG	60.3	118
Npy	NM_012614	TCATCACCAGACAGAGATATGGCAAGAG	60.7	CACCACATGGAAGGGTCTTCAAGC	60.5	116
Ntrk3	NM_001270655	CCAGCATCAACATCACGGACATC	58.8	AGCTTCTGGAGTCCCGTGTAGAGC	59.0	118
Pyy	NM_001034080	AGCTTCTCCTGCCTTCCATCTCC	58.9	CGAGCAGGACAAGCAGCATTG	58.2	115
Pomc	NM_139326	AACATCTTCGTCCTCAGAGAGCTGC	59.1	GTCTATGGAGGTCTGAAGCAGGAGG	58.4	125
Kiss1	NM_181692	GGCACCTGTGGTGAACCCTGAAC	61.3	CCCCAGGCTTGCTCTCTGCATAC	60.9	102

5.2.4.5. SYBR-Green RT-qPCR

PowerUp™ SYBR™ Green Master Mix was used according to the manufacturer's instructions. Using MicroAmp® Fast Optical 96-well reaction plates, three replicates of each reaction were carried out in addition to no-template controls (NTCs), and RT(-) controls. A total volume of 20µl was used consisting of 10µl 2x PowerUp™ SYBR™ Green Master Mix, 0.8µl of each primer (forward and reverse, 10µM), 1µl cDNA and 7.4µl Nuclease-free water. RT-qPCR was performed within 24h of the reactions being set up. Reactions were stored at room temperature until loaded into real-time PCR system as per the PowerUp™ instructions. All reactions were ran on an ABI StepOne Plus Real-Time PCR System using fast cycle conditions outlined in Table 5.3. The settings applied to the instrument were as follows: Experiment type: standard curve; Reagent: SYBR™ Green reagents; Reporter: SYBR™; Quencher: None; Passive reference dye: ROX; Ramp Speed: fast; Melt curve ramp increments: continuous.

Table 5.3: Fast cycle RT-qPCR conditions.

Step	Temperature	Duration	Cycles
UDG Activation	50ºC	2 min	Hold
Dual-Lock™ DNA Polymerase	95ºC	2 min	Hold
Denature	95ºC	3 sec	40
Anneal/Extend	60ºC	30 sec	

5.2.5. *Kiss1r* Transcript Identification

Following identification of two rat *Kiss1r* transcripts and their differential expression in their hypothalamus in response to treatment the RNASeq analysis, melting curve analysis was carried out to identify the two transcripts in each sample as confirmation.

5.2.5.1. Melting Curve Analysis

Melting curve analysis was used in an attempt to identify which *Kiss1r* transcript

variant is present in each cDNA sample as two *Kiss1r* transcripts, transcript variant 1 (*Kiss1r1*) and transcript variant 2 (*Kiss1r2*), have been recorded as present in the *Rattus* genus with GenBank accession numbers NM_023992 and NM_001301151, respectively. The RP-qPCR melting curve conditions are presented in Table 5.4. The primers, outlined in Table 5.5, were designed to identify both individual *Kiss1r* transcripts through analysing the melting curve generated following RT-qPCR. If *Kiss1r1* is present, the product size will be 70 base pairs (bp), whereas if *Kiss1r2* is present, the product size will be 64bp. This is due to a deletion in *Kiss1r2* of 6bp (coding for two amino acids in the protein) in comparison to *Kiss1r1* (see Figure 5.3). Depending on the size and sequence of the product generated, the melting curve temperature will differ as this correlates with the number of bp present and sequence of the product. The two samples which were pooled for RNASeq were tested individually for each group then the mean melting temperature was calculated. This was to give an accurate representation of the samples submitted for RNASeq.

Table 5.4: RT-qPCR melt curve conditions.

Step	Ramp rate	Temperature	Time
1	1.6ºC/sec	95ºC	15 sec
2	1.6ºC/sec	60ºC	1 min
3	0.10ºC/sec	95ºC	15 sec

Table 5.5: Primers designed for Melting Curve Analysis. Primers were designed flank the site of variation between the two transcript variants of *Kiss1r*.

Gene ID	Primer Sequence (5' – 3')	Tm
rKiss1r12_HRMFor	CCCCGCACCCACTGATGG	61.6
rKiss1r12_HRMRev	CTTGGTGCGCACTGCTCCAG	61.6

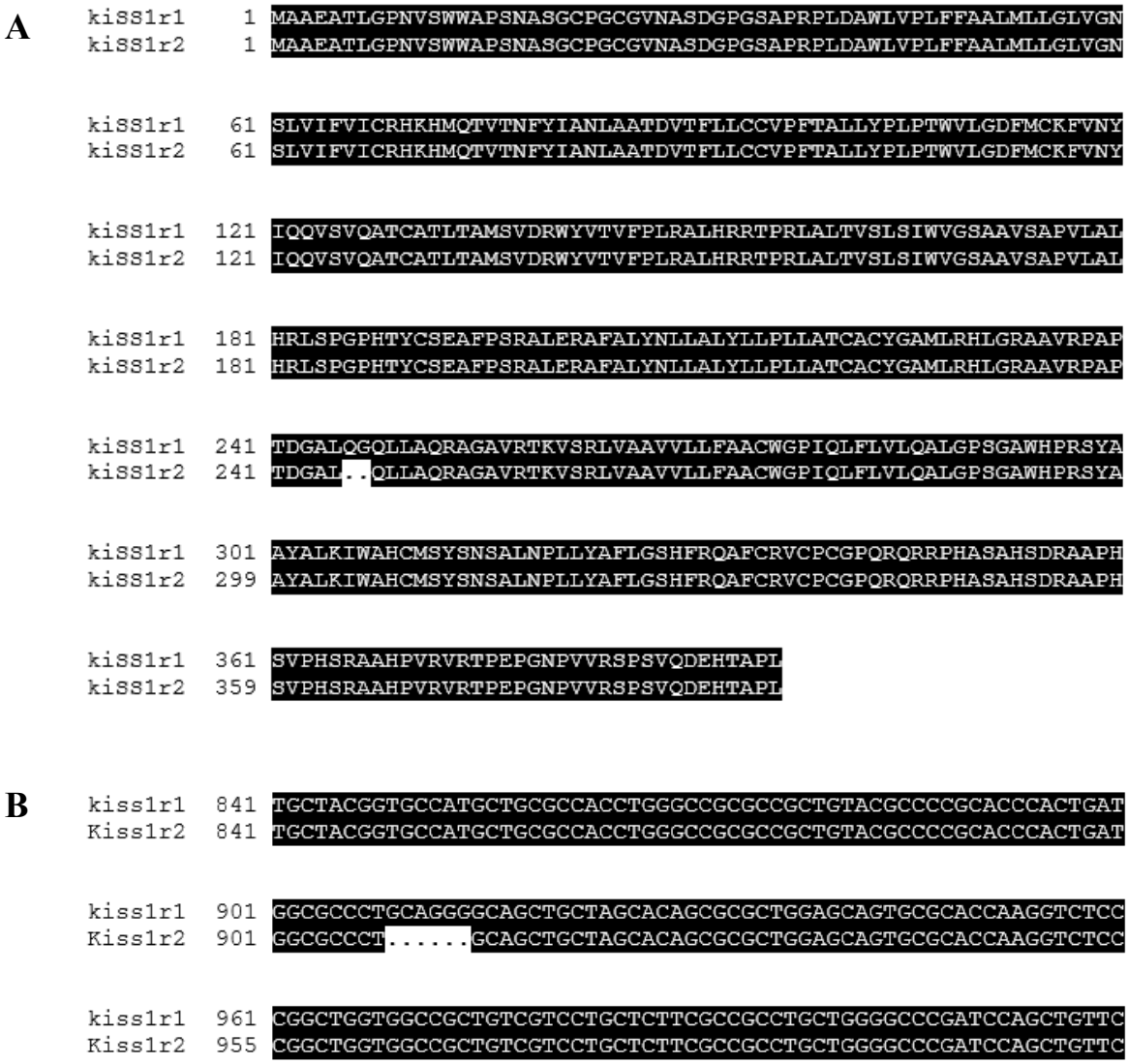

Figure 5.3: Comparison of amino acid sequence (A) and DNA sequence (B) between *Kiss1r1* and *Kiss1r2*. Amino acid and DNA sequences were compared using GeneRunner (www.generunner.net; v6.0.28 beta). White gap with two black dots (A) and 6 black dots (B) represents two missing amino acids, equivalent to 6 base pairs) in *Kiss1r2* (see sequence starting at number 241 for amino acid sequence and 901 for the DNA sequence).

5.3. Results

5.3.1. RNA Extraction and Quality Control

5.3.1.1. Nanodrop Analysis

Each RNA sample was assessed based on quality and quantity before being submitted to BGI-Tech for RNASeq. BGI-Tech sample requirements include sample quantity more than 200ng; sample concentration more than 20 ng/μL; and, sample purity - RNA Integrity Number (RIN) more than 7.0, and 28S/18S more than 1.

The ratio of absorbance at 260nm and 280nm is used to assess the purity of RNA, with values close to 2.0 being optimal. Additionally, the ratio of absorbance at 260nm and 230nm is used as a secondary measure to assess the quality of nucleic acids. The 260:230 ratio also indicates reagent carryover from the extraction process which may contaminate the sample. Values between 2.0 and 2.2 are optimal for a high purity sample. As seen in Table 5.6, the quality of each sample is very high and thus they were deemed acceptable to be used in RNASeq.

Table 5.6: Nanodrop results showing 260:280 and 260:230 ratios for each RNA sample. Sample I.D. refer to group allocations detailed in Section 4.3.1.2.

Sample I.D.	Sample Info	260:280	260:230	Concentration (ng/mL)
G1.1	Control	2.06	2.13	404.4
G1.2	Control	2.06	2.22	284.1
G2.1	Tuber treated	2.05	2.10	354.4
G2.2	Tuber treated	2.05	2.21	287.1
G3.1	TA treated	2.07	2.20	487.1
G3.2	TA treated	2.05	2.21	240.6

5.3.1.2. Experion™ RNA StdSens Analysis

The Experion™ RNA StdSens Analysis kit provides accurate measurement of RNA quality by assessing the RNA quality indicator (RQI) number and 28S:18S ratio. RQI and RIN are comparable with 1 indicating highly degraded RNA and 10 indicating intact RNA. Samples with an RIN number over 7 and a 28S/26S ratio more than 1.0 are the minimal requirements for BGI-Tech RNASeq analysis.

Ribosomal RNA (rRNA) makes up 80% of total RNA in samples, with the majority of that consisting of 28S and 18S rRNA. Mammalian 28S and 18S rRNA are approximately 5kb and 2kb in size, thus the theoretical ratio is approximately 2.7:1. A ratio of 2:1 is widely accepted as a benchmark for intact RNA, although values more than 1.0 are suitable for the majority of down-stream applications. Using Experion™ RNA StdSens kit, the 28S:18S ratio was examined. A virtual gel report was obtained following the Experion™ RNA StdSens experiment and is shown in Figure 5.4. Experion™ software subsequently uses the data generated to calculate the 28S:18S ratio which is shown in Table 5.7. This ratio is based upon the peak area of both the 18S and 28S rRNA bands. The 28S:18S ratio is lower than the expected theoretical 2:1 ratio for all samples. However, each sample has a 28S/18S ratio of more than 1.0, all samples meet the minimum requirements for BGI-Tech. The lower ratios may be due to the instability of 28S rRNA compared to 18S rRNA. Furthermore, rRNA ratio measurements are reliant upon specific start and end points when measuring the peak area which can be highly variable between users and software. Due to this, rRNA ratios are relatively difficult to reproduce, thus RQI/RIN numbers are frequently used to assess RNA integrity. Experion software is able to generate the RQI giving an unbiased and reproducible result. THE RQI values, shown in Table 4.8, are all above 9 which indicates very high quality RNA. The only exception is sample #4 where the RQI value was not determined. This was due to low signal from the ladder during the Experion™ electrophoresis, thus meaning the RQI value could not be calculated. However, as the 28S/18S value was within the acceptable range, as well as the 260/280 ratio, this was not deemed to be an issue and the samples were thus submitted to BGI-Tech for RNASeq analysis.

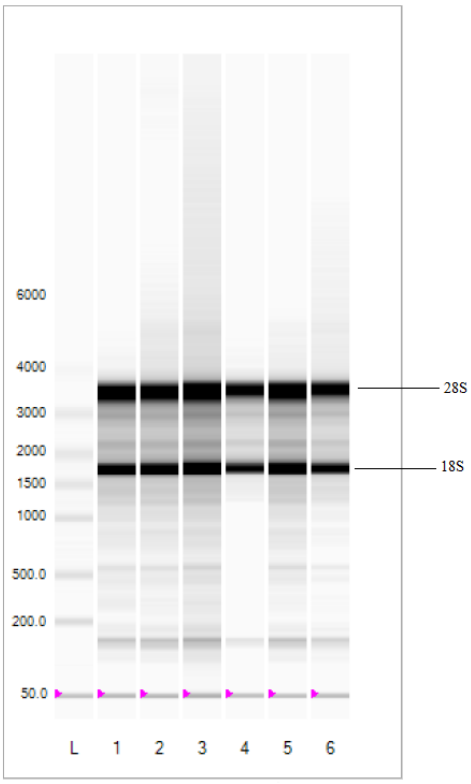

Figure 5.4: Experion™ RNA Std Sens virtual gel report showing bands for 18S and 28S. L: ladder; 1-6 refer to samples tested: 1 – Control 1.1; 2 – Control 1.2; 3 – Tuber treated 2.1; 4 – Tuber treated 2.2; 5 – TA treated 3.1; and, 6 – TA treated 3.2.

Table 5.7: Experion™ results of 28S:18S ratio and RQI for each sample. * No RQI reported for this sample

Sample #	ID	28S:18S ratio	RQI
1	Control 1.1	1.40	9.3
2	Control 1.2	1.36	9.2
3	Tuber 2.1	1.37	9.1
4	Tuber 2.2	1.39	N/A*
5	TA 3.1	1.41	9.3
6	TA 3.2	1.41	9.7

5.3.2. RNASeq

Three samples were sequenced by RNASeq on the Illimnia HiSeq™ 2000 which generated an average of 13,126,353 raw sequence reads and subsequently 13,008,619 clean reads following filtering. Table 5.8 shows the alignment statistics of the reads to the reference genome. Filtering included the removal of 'dirty' reads such as reads with adaptors, reads with a high content of unknown bases and low quality reads. This process was performed at BGI-Tech. BGI-Tech additionally provided information of reads mapping where Bowtie 2 (Langmead *et al.*, 2009) was utilised to map the clean reads to the reference genome.

Table 5.8: RNASeq alignment statistics provided by BGI-Tech.

Sample	Total Reads	Total Bases	Total Mapped Reads (%)	Perfect Match (%)	Mis-match (%)	Total Unmapped Reads (%)
Control	13,073,582	640,605,518	84.07	71.14	12.93	15.93
TA treated	12,891,057	631,661,793	84.21	71.34	12.87	15.79
Tuber treated	13,061,219	639,999,731	84.14	71.18	12.96	15.86

5.3.2.1. RNASeq Analysis

5.3.2.1.1. Correlation Heat map

The correlation heat map shown in Figure 5.5 shows the relationship between each group based on gene expression changes. Values close to 1 represent samples which are very similar. In comparison to the control group, the TA group is most similar as it shows a coefficient value of 0.978067. The tuber treated group is also similar to the control group, but not to the same extent as the TA treated group as the correlation coefficient value is lower at 0.936589. Moreover, the TA treated group and tuber treated group are similar with a coefficient value of 0.936909. The differences between each group indicate the effects of both the tuber and TA on hypothalamic gene expression.

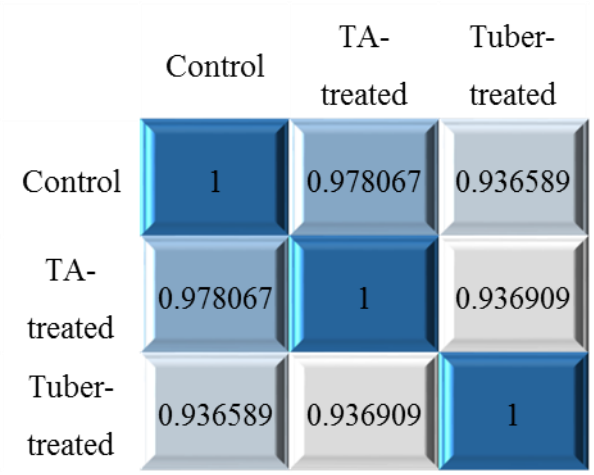

Figure 5.5: Heat map of correlation coefficient values across samples as provided by BGI-Tech. If one sample is highly similar with another one, the correlation value between them is very close to 1.

5.3.2.1.2. Differential Gene Expression

After confirming that there were differences in gene expression between each group by looking at the correlation coefficients, the next step was to identify the number of genes expressed in each group and, subsequently, the number of differentially expressed genes between each pairwise comparison. The total number of genes expressed is shown in Figure 5.6. Using RNASeq, around 79% of genes from the reference database were identified in each of the samples submitted. When reads are mapped against a transcriptome, it is expected that some unannotated transcripts will be lost, thus giving a lower percentage of total reads mapped. Values between 70-90% are expected, thus 79% suggests adequate gene mapping to the reference transcriptome. Subsequently, differential gene expression (DEG) analysis was carried out to determine the number of genes which were affected by each treatment, as well as the comparison between treatment groups. Figure 5.7 shows the DEGs (≥ 1.0 and ≤ -1.0 log2 ratio) of each pairwise comparison – Control vs. Tuber, Control vs. TA and, TA vs Tuber. TA appears to up-regulate more genes than the control group in comparison to the tuber group. On the other hand, both the tuber group and TA group down-regulated a similar number of genes in comparison to the control. Following on from this, Figure 5.8 emphasises the similarities and differences between each pairwise

comparison. Using Java TreeView (version 1.1.6r2), the DEG analysis can be visualised as a heat map, with green showing downregulated genes and red showing up regulated genes. It is evident that the two treatment (tuber and TA) groups cause numerous effects on gene expression in both directions. Clustering analysis, based on the gene expression patterns, was conducted before generating the heat map thus genes clustered together may have similar functionalities.

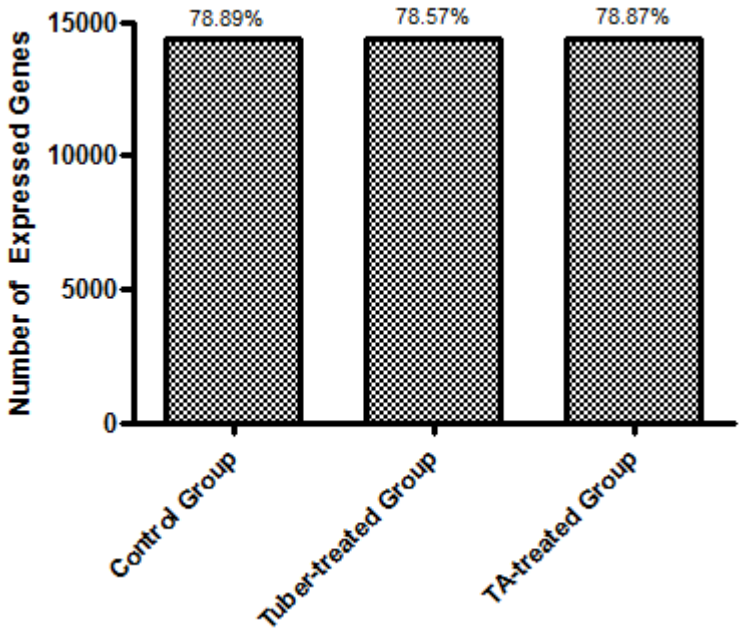

Figure 5.6: Number of DEGs following RNASeq in each experimental group. Total number of genes expressed in the reference database was 18,258. The percentage of total genes in the database is shown above each bar.

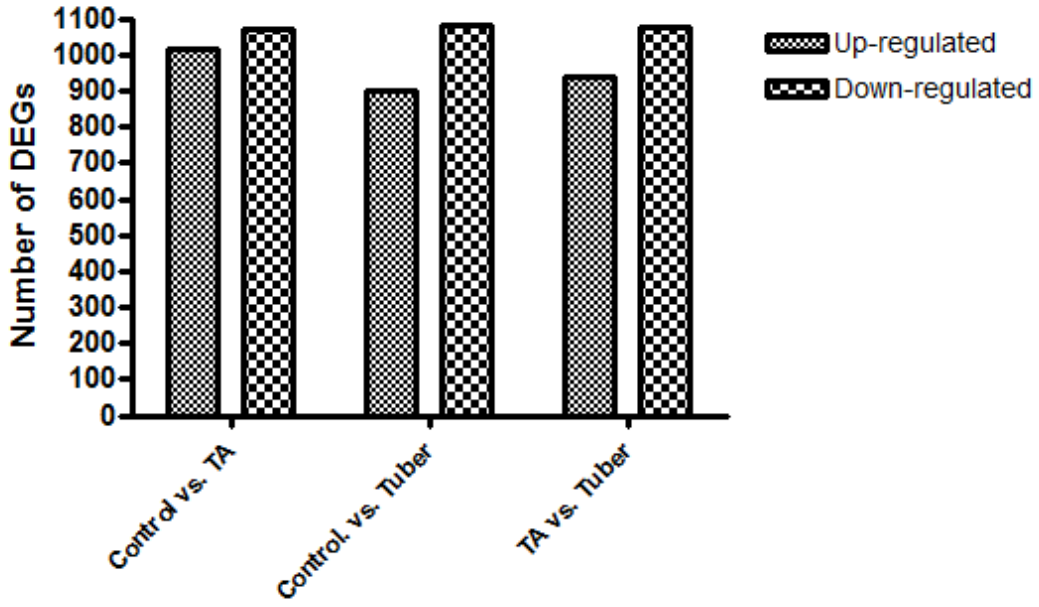

Figure 5.7: Differential gene expression in each pairwise comparison. Data shown represents the number of differentially expressed genes in the second named group compared to the first named group.

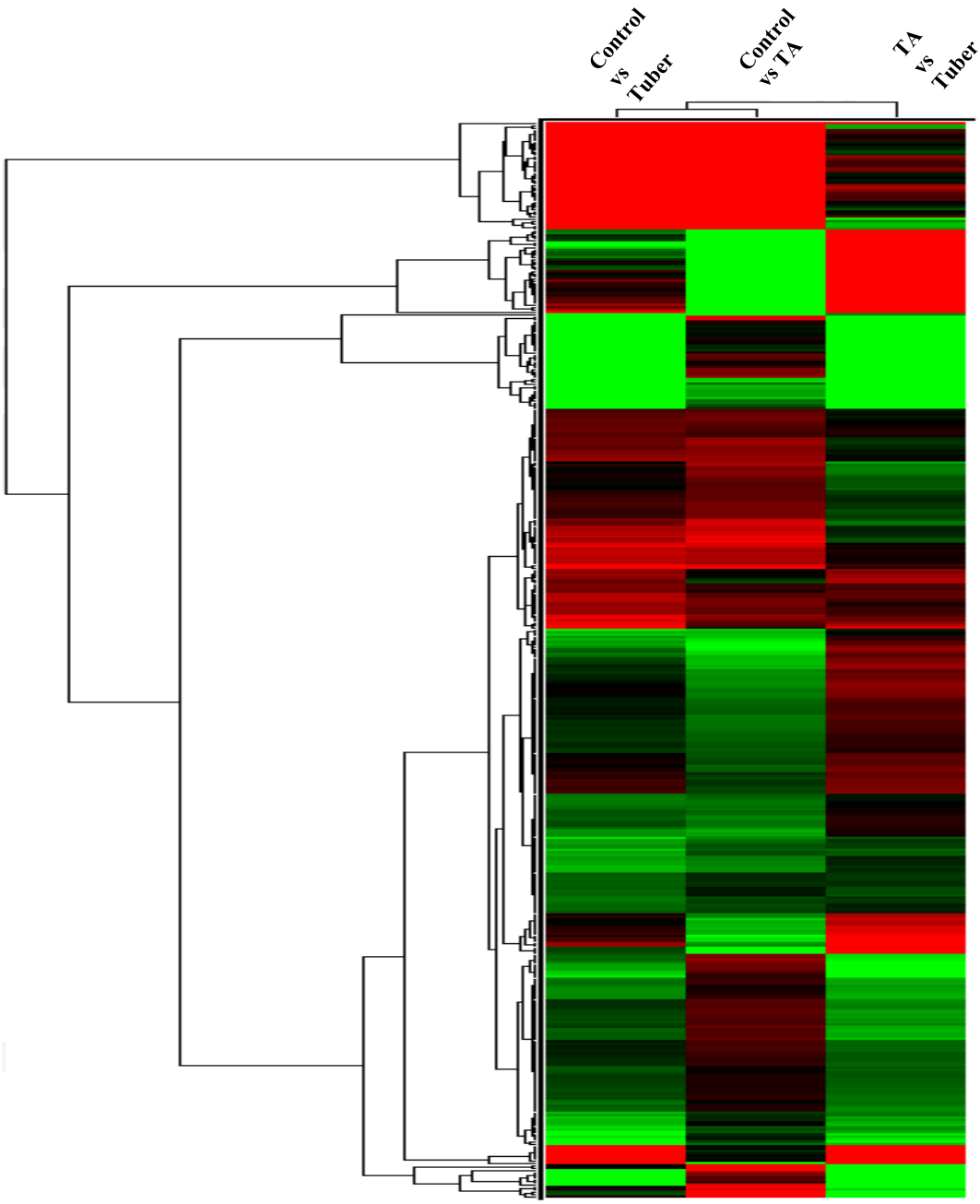

Figure 5.8: Differential gene analysis heat map generated using TreeView (Java, version 1.1.6r2). Red represents upregulated genes; Green represents downregulated genes; Black represents no change. Each row represents a differentially expressed gene, while each column represents a pairwise comparison. Genes are clustered based on the expression patterns, which can occasionally be correlated to the functional classification of the genes. Branches at the left of the diagram indicates gene clusters.

5.3.2.1.3. Pathway Enrichment Analysis

Pathway enrichment analysis was carried out using Cytoscape and the ClueGO plugin. Overall, there were 19 GO terms associated with up-regulated genes in the tuber sample, whereas there were 25 GO terms associated with up-regulated genes in the TA sample. Contrastingly, only 8 GO terms were associated with down-regulated genes associated with the tuber sample, and 16 GO terms associated with down-regulated genes associated with the TA sample. All analysis was performed in comparison to the control group. The most significantly enriched terms for each are shown in Figures 5.9 and 5.10 and were as follows: Tuber up-regulated genes – graft-*vs*.-host disease, type I diabetes mellitus, and neuroactive ligand-receptor interaction; Tuber down-regulated genes – phototransduction and cell adhesion molecules (CAMs); TA up-regulated genes – retinol metabolism, starch and sucrose metabolism; TA down-regulated genes – cytokine-cytokine receptor interactions, CAMs and maturity onset diabetes of the young. Following ClueGO analysis, DAVID bioinformatics platform was used to identify specific genes associated with the most significant GO terms.

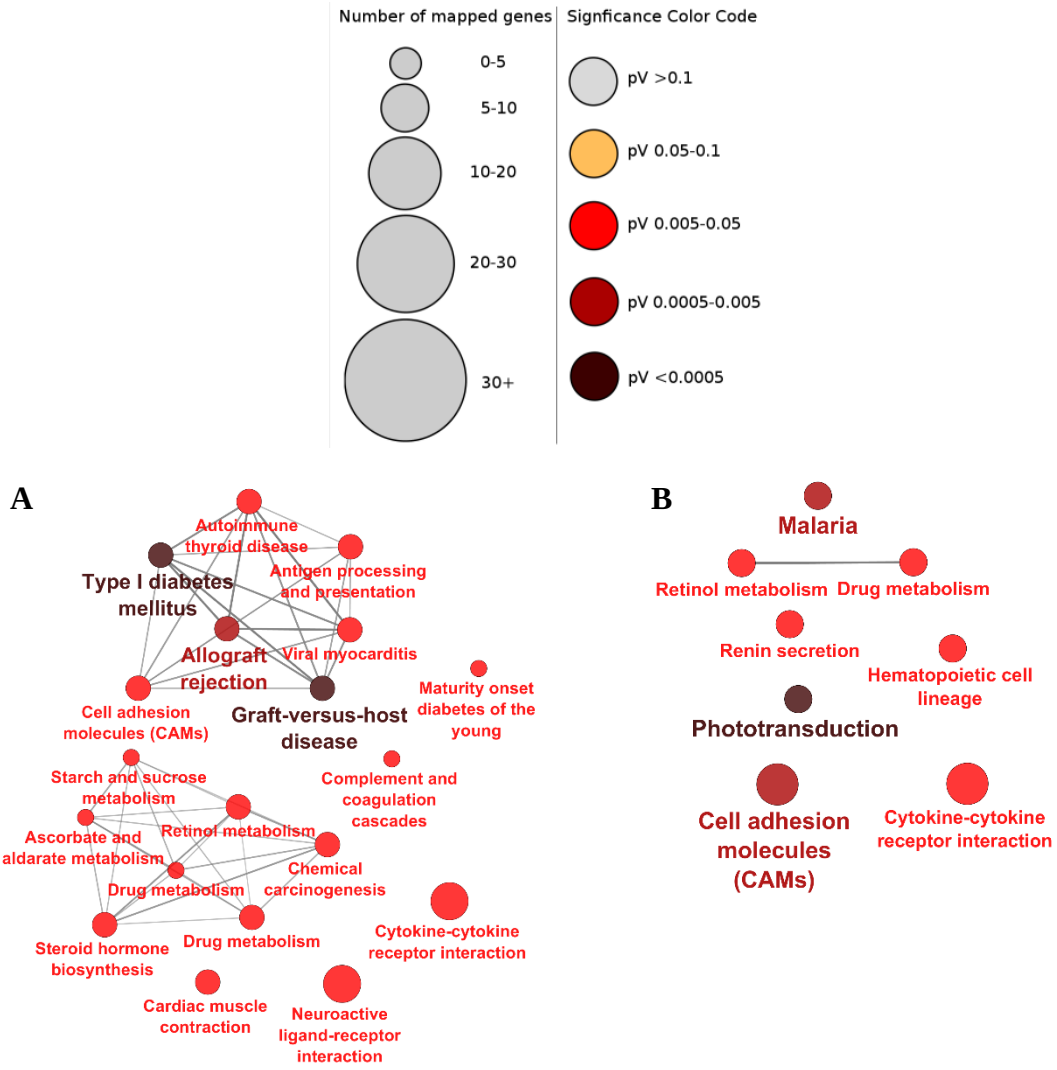

Figure 5.9: Cytoscape ClueGO cluster results using differentially expressed genes in the tuber sample vs. control. ClueGO legend (shown at the top of the figure) – circle size represent the number of genes associated with the GO term, colours represent the significance; A, significantly enriched KEGG pathways associated with all genes up-regulated by more than 2-fold; B, significantly enriched KEGG pathways associated with all genes down-regulated by more than 2-fold.

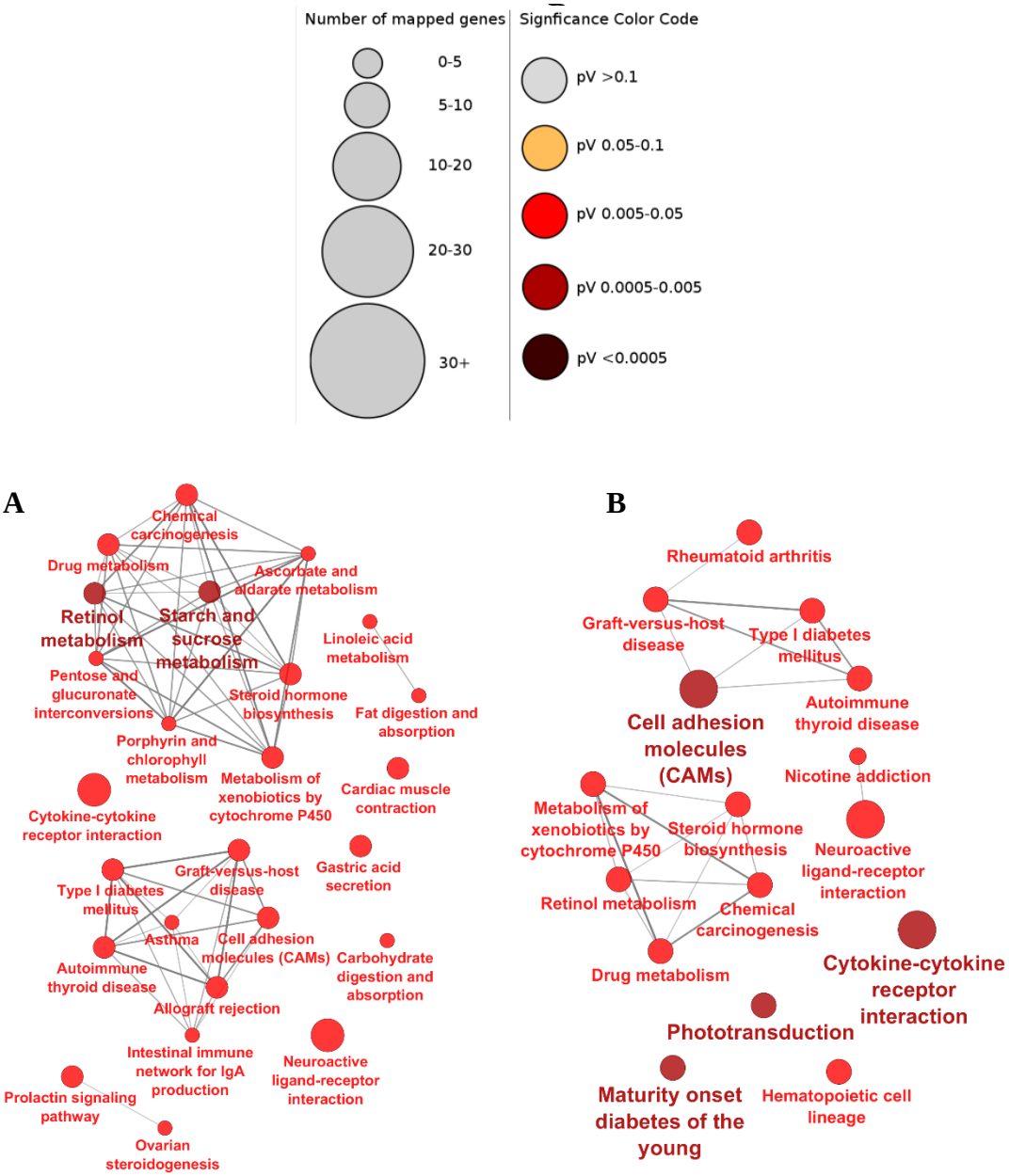

Figure 5.10: Cytoscape ClueGO cluster results using differentially expressed genes in the TA sample vs. control. ClueGO legend (shown at the top of the figure) – circle size represents the number of genes associated with the GO term, colours represent the significance; A, significantly enriched KEGG pathways associated with all genes up-regulated by more than 2-fold; B, significantly enriched KEGG pathways associated with all genes down-regulated by more than 2-fold.

The genes identified from each GO term cluster are shown in Tables 5.9 and 5.10. The neuroactive ligand receptor interaction pathway was significantly upregulated in both the tuber-treated group and the TA-treated group. The specific genes and their Log2 ratio according to the RNASeq data are shown in Figures 5.11 and 5.12 for the tuber-treated group and TA-treated group, respectively.

For the group treated with LL tuber, the three most up-regulated genes are *Kiss1r* (Kisspeptin receptor, GPR54), *Bdkrb2* (Bradykinin receptor B2) and *Hrh3 isoform H3C* (Histamine receptor H3). The TA treated group also shows a significant upregulation of *Kiss1r,* as well as *Adcyap1r1* (adenylate cyclase-activating polypeptide type I receptor) and *Hrh3 isoform H3B* (Histamine receptor H3). Each of these receptors are part of Class I (*Kiss1r, Bdkrb2, Hrh3*) or Class II (Adcyap1r1) G-protein coupled receptor (GPCR) families. G-protein coupled receptors are important signalling proteins of which many are key players in the postprandial control of food intake and metabolism, particularly GPRCs in the gut-brain-pancreatic axis.

In addition to the up-regulation of neuronal GPRCs, treatment with LL tuber appeared to cause an up-regulation of genes associated with immune function such as Interleukin-1β (IL-1β) and tumour necrosis factor (TNF), while treatment with TA caused an upregulation of metabolic enzymes including α-amylase (AmyA) and glucokinase (Gck).

The most significantly down-regulated pathway, following treatment with LL tuber compared to the control, was the CAMs pathway, whereas in the TA *vs*. control analysis, the cytokine-cytokine receptor interaction pathway was the most significantly down-regulated. However, the genes associated with these pathways at this time are not thought to relate to the control of appetite, food intake or energy regulation. Thus no further analysis was carried out.

Table 5.9: Most significant genes associated with treatment of LL tuber. Associated genes identified using DAVID Bioinformatics analysis and ClueGO KEGG pathway enrichment analysis. No.: Number of genes from list submitted; %: percentage of genes found from the total number of associated genes.

KEGG Pathway	No.	%	P-value	Associated Genes Found
Up-Regulated				
Graft *vs*. Host Disease	9	1.6	0.00016	*Cd28, Cd80, RT1-M1-4, RT1-M6-1, RT1-N1, RT1-T18, Il1b, Prf1, Tnf*
Type I Diabetes Mellitus	9	1.6	0.00042	*Cd28, Cd80, RT1-M1-4, RT1-M6-1, RT1-N1, RT1-T18, Il1b, Prf1, Tnf*
Neuroactive ligand receptor interaction	18	3.3	0.00056	*Gpr35, Kiss1r, Adcyap1r1, Bdkrb2, Chrna10, F2rl2, Cysltr2, Grpr, Grik1, Grm1, Hrh3, Lhcgr, Mtnr1b, Npy4r, Oprd1, Prl, Sctr, Sstr5*
Down-Regulated				
Phototransduction	7	1.1	0.000096	*Gnat1, Grk1, Calml3, Cnga1, Gucy2f, Guca1a, Rho*
Cell Adhesion Molecules	15	2.4	0.00098	*Cd226, Cd8b, RT1-CE5, RT1-N2, Cldn14, Cldn2, Cldn20, Cldn3, Itgb7, Nfasc, Ptpr, Sell, Selp, CD43*

Table 5.10: Most significant genes associated with treatment of TA. Associated genes identified using DAVID Bioinformatics analysis and ClueGO KEGG pathway enrichment analysis. No.: Number of genes from list submitted; %: percentage of genes found from the total number of associated genes.

KEGG Pathway	No.	%	P-value	Associated Genes Found
Up-Regulated				
Retinol Metabolism	9	1.6	0.0017	*Ugt2b10, Ugt2b17, Ugt2b35, Ugt1a1, Cyp1a1, Cyp2a3, Cyp2c12, Cyp3a2, Rdh7*
Neuroactive ligand receptor interaction	18	3.3	0.0023	*F2rl3, Gpr35, Kiss1r, Adcyap1r1, Chrna10, Cysltr1, Cystlr2, Grin1, Grik1, Ghrhr, Hrh3, Lhb, Mtnr1b, Oprm1, Plg, Prl, Ptgdr, P2rx1*
Starch and sucrose metabolism	4	0.7	0.052	*Amya23, Gck, Si, Treh*
Down-Regulated				
Maturity onset diabetes of the young	7	1.1	0.00014	*Hnf1a, Foxa2, Foxa3, Hnf4a, Ins1, Pax4, Slc2a2*
Cytokine-cytokine receptor interaction	18	2.8	0.00033	*Ccl2, Ccl4, Ccr7, Cxcl11, Cxcr1, Cxcr2, Faslg, Kitlg, Tnfrsf17, Epo, Ifna4, Il20rb, Il6, Il7, Ilr, Osm, Tnfsf4, Vegfa*
Cell Adhesion Molecules	15	2.2	0.0008	*Cd8b, RT1-CE5, RT1-M6-1, RT1-Bb, RT1-Doa, RT1-N2, Cldn1, Cldn2, Cldn20, Cldn6, Cldn7, Ctla4, Glycam1, Ptprc, Vcan*

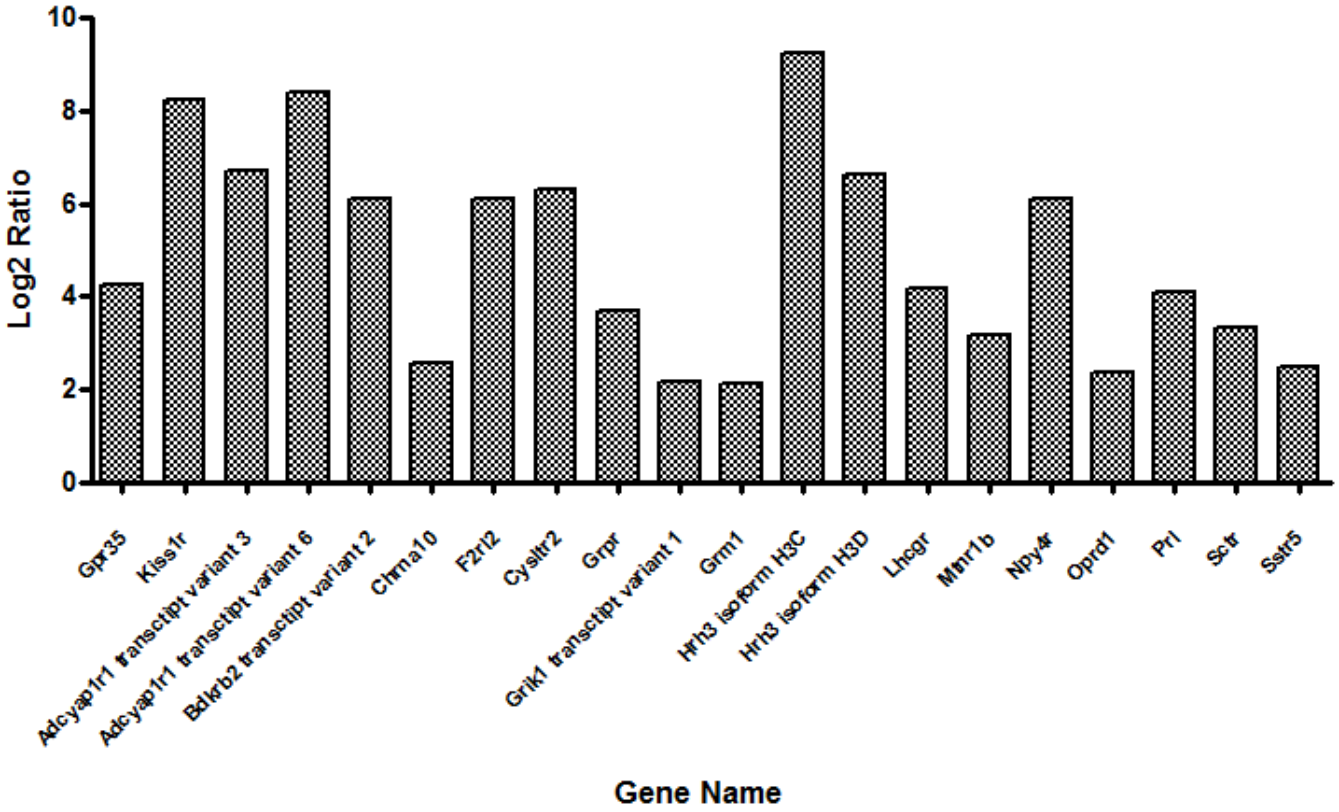

Figure 5.11: Log2 ratio of genes identified in the neuroactive ligand receptor interaction pathway. Data represents tuber *vs*. control, n=1 [representative of two pooled samples from each treatment group].

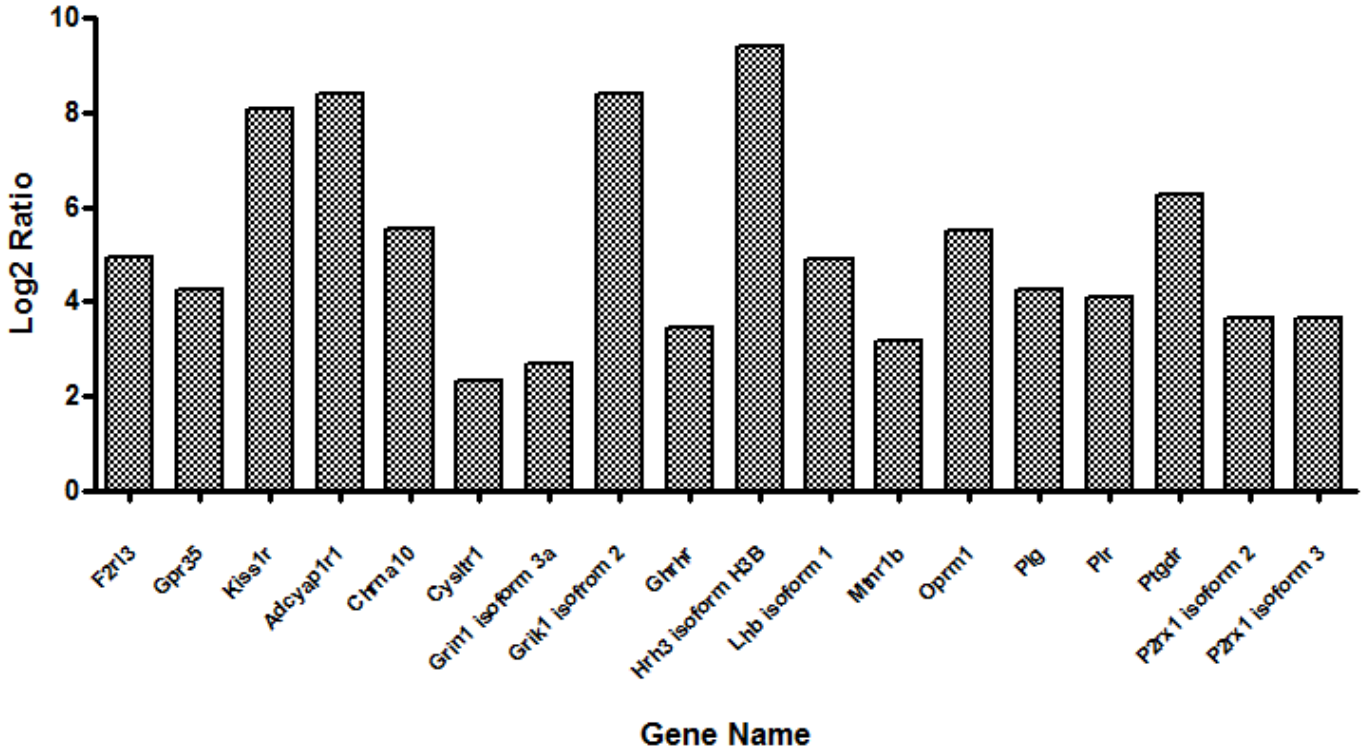

Figure 5.12: Log2 ratio of genes identified in the neuroactive ligand receptor interaction pathway. Data represents TA *vs*. control, n=1 [representative of two pooled samples from each treatment group].

5.3.2.2. Identification of Genes associated with Appetite, Food Intake and Energy Metabolism and Regulation

As mentioned in Section 5.2.3, an internal database was established and was cross-referenced with RNASeq data to investigate the effect of LL tuber and TA treatments on genes specifically related to appetite, food intake and energy metabolism and regulation both in the central neuronal system and peripheral system. Figure 5.13 shows the most relevant genes identified alongside the Log2 ratios for each treatment in comparison to the control group. The results for both treatments are relatively similar, suggesting that the presence of TA in LL tubers may be causing several of the changes.

The main neurons within the hypothalamus which are associated with appetite and food intake include POMC/CART neurons and AgRP/NPY neurons. The RNASeq results in Figure 4.14 indicate that there are minimal changes (less than 2-fold) in the gene expression of *Pomc, Cart, Agrp* and *Npy*. Despite this, there are various changes in genes associated with these neurons which form a complex signalling network. The largest changes in gene expression include the down regulation of adiponectin precursor protein, BDNFv10, GH, and the up-regulation of BDNFv3, gastrin-releasing peptide receptor, glucocorticoid-regulated kinase 1, Histamine receptor (H3B for tuber and H3C for TA), Kiss1r, NTKR3, NPY receptors, PYY, prolactin (PRL) and PTP receptor c. Ghrelin and its receptor, growth hormone secretagogue receptor (GHSR), show minimal change, while leptin was not identified within the RNASeq data.

Of note, both treatments changed the expression of different isoforms of *Kiss1r* – LL tuber caused an increase in *Kiss1r* isoform 2 by 8.2-fold, whereas TA caused an increase in *Kiss1r* isoform 1 by 8-fold. Similarly, two transcripts of *Bdnf* were also noted – transcript variant 3 and 10.

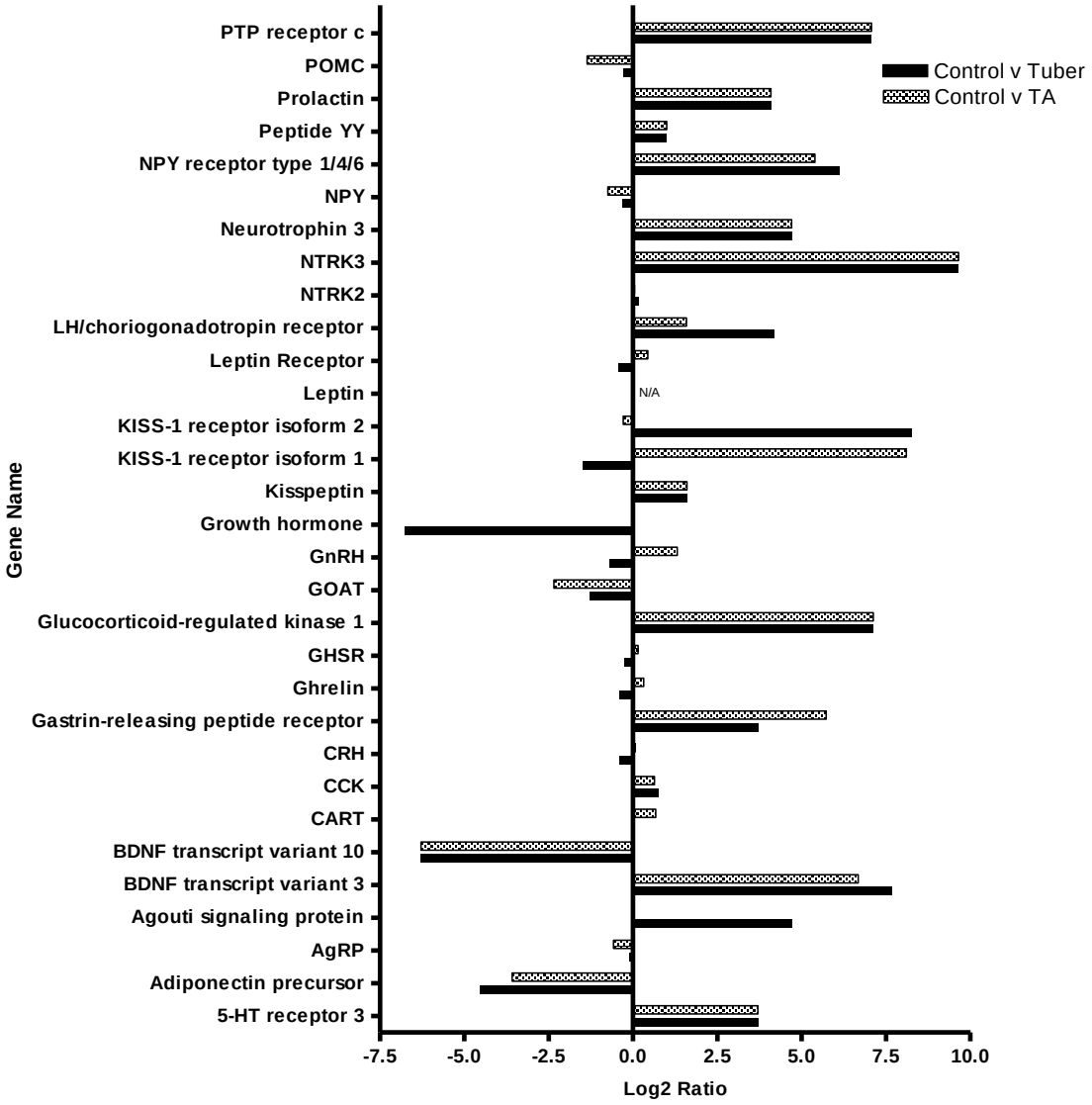

Figure 5.13: RNASeq gene expression changes (Log2 ratio) as a result of treatment with LL Tuber or TA. Log2 ratio calculated in comparison to the control. Solid bars represent changes as a result of LL Tuber, while patterned bars represent changes as a result of TA. Positive values represent up-regulation, negative values represent down-regulation. n=1.

5.3.3. RT-qPCR

5.3.3.1. Reference Gene Stability

In order to select the optimum reference gene for RT-qPCR, four different genes were investigated to identify their expression stability in the hypothalamus following treatment. Using an online gene stability tool (RefFinder), the expression of each candidate reference gene in the control and treated hypothalamus was analysed in comparison to one another. Figure 5.14 highlights the most and least stable genes. Each sample was tested with (RT+) and without (RT-) reverse transcriptase alongside a no-template control (NTC). No amplifications were observed in RT- or NTC samples. B2M was identified as being the most stable reference gene in the hypothalamus tissue used, whereas PGK1 was identified as being the least stable. Thus, B2M was used as the reference gene in subsequent RT-qPCR experiments using the hypothalamus tissue.

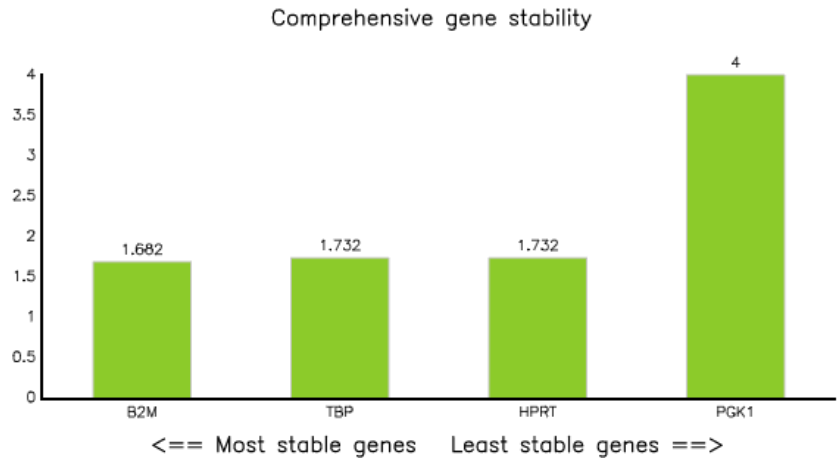

Figure 5.14: Stability of Reference Genes analysed using RefFinder. Most stable genes are towards the left hand side of the graph while least stable genes are shown to the right hand side of the graph.

5.3.3.2. Gene Expression Analysis (2^-ΔΔC$_T$)

Using the results shown in Section 5.3.2.2 and Figure 5.13, several genes were selected for validation of the RNASeq data. Gene expression analysis was carried out to confirm the direction and magnitude of the gene expression changes identified in RNASeq. All samples were tested with (RT+) and without (RT-) reverse transcriptase alongside a no-template control (NTC). No amplifications were observed in RT- or NTC samples thus no genomic DNA acted as template for the amplifications and no false positive signals affecting the results. ΔΔC$_T$ was calculated from raw data following RT-qPCR. Subsequently, the fold-change for each gene was calculated using the equation below:

$$\text{Fold Change} = 2^{-\Delta\Delta CT}$$

The direction of the gene expression changes match for several of the genes shown in Figure 5.13 and Figure 5.15. Specifically, POMC, and NPY are both shown to be down-regulated while CCK, NTKR3 and PYY are shown to be up-regulated. There are some discrepancies where the direction of the change does not correlate. In the RNASeq data, *Kiss1* (Kisspeptin) is up-regulated, however, when investigated using RT-qPCR, *Kiss1* is shown to be down-regulated in both LL tuber and TA samples. Similarly, the data for *GOAT, GHSR* and *Agrp* do not correlate with each other.

In terms of the magnitude of the changes, there are further discrepancies between the two methods, even when the direction of the change correlates. *Pomc* is shown to be down-regulated by 1.5-fold and 1.2-fold in the tuber and TA sample respectively using RT-qPCR. However, in the RNASeq data, the down-regulation for the tuber sample is much lower at 0.3-fold, while the TA sample shows a down-regulation of 1.4-fold. Moreover, NPY is shown to be down-regulated by 1.2-fold in the tuber sample and 1.1-fold in the TA sample using RT-qPCR. However, RNASeq shows the down-regulation to be 0.3-fold in the tuber sample, and 0.7-fold in the TA sample. CCK is shown to be up-regulated by 1.2-fold in the tuber sample and 1.4-fold in the TA sample using RT-qPCR.

On the other hand, using RNASeq, the up-regulation is shown to be 0.8-fold and 0.6-fold for tuber and TA samples, respectively. The largest discrepancy is evident in the analysis of *Ntrk3* – RT-qPCR shown an up-regulation of 1-fold and 1.5-fold for tuber and TA samples, respectively, while RNASeq shows the up-regulation to be 9.7-fold for both tuber and TA samples. Lastly, *Pyy* is shown to be up-regulated by 1.3-fold and 2.2-fold for tuber and TA samples respectively, while RNASeq data shown that the up-regulation is 1-fold for both tuber and TA samples.

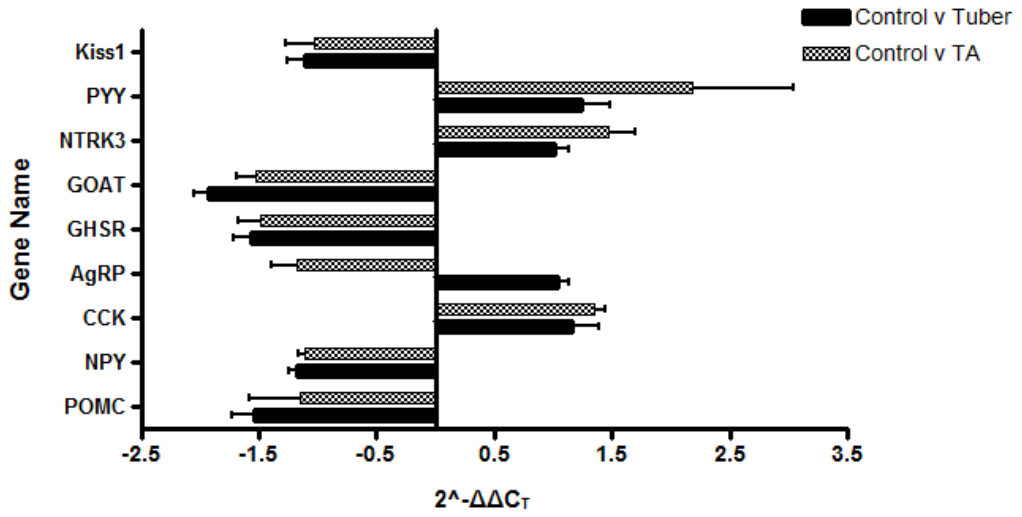

Figure 5.15: RT-qPCR gene expression changes in various genes of interest in the Tuber and TA treated groups in comparison to the control. Solid bars represent changes as a result of LL Tuber, while patterned bars represent changes as a result of TA. Positive values represent up-regulation, negative values represent down-regulation. Data represents mean ± SEM. n=6.

5.3.4. *Kiss1r* Transcript Identification

Upon further analysis of the raw data from RNASeq, it was noted that there were differences in gene expression between each of the RNA samples. Looking at *Kiss1r* in particular, it is apparent that the RNA from the control group showed only the presence of *Kiss1r1* transcript variant 2, while the RNA from the TA group showed only the presence of *Kiss1r1* transcript variant 1 (Table 5.11). On the other hand, the RNA from the Tuber group showed the presence of both variants of Kisspeptin receptor. To confirm this data, melting curve analysis was carried out to distinguish between the presence of both variants in the samples.

Table 5.11: FPKM (Fragments Per Kilobase of transcript per Million mapped reads) data for *Kiss1r* isoform 1 and *Kiss1r* isoform 2. FPKM relates to the abundance of each transcript within one sample. The value is proportional to the number of cDNA fragments that originate from the transcript during RNASeq. FPKM values cannot be compared due to differences in total reads (Table 4.9).

Accession #	Control FPKM	TA FPKM	Tuber FPKM	Transcript Variant
NM_001301151	0	3.71	3.03	Kiss1r variant 2
NM_023992	7.71	0	2.74	Kiss1r variant 1

5.3.4.1. Melting Curve Analysis

To differentiate between the products of RT-qPCR, melting curve analysis was utilised. Melting curves are representative of G-C content, length and sequence of the PCR product and these variations within the products can be determined. *Kiss1r1* and *Kiss1r2* differ in length (basepairs, bp) and the primers used were designed to highlight this difference. As identified in Section 5.3.4 (Table 5.11), the control RNA sample shows only *Kiss1r1* being present, whereas the TA-treated hypothalamus RNA sample shows *Kiss1r2* being present. The only sample with both *Kiss1r1* and *Kiss1r2* present is that from the tuber-treated hypothalamus samples. Figure 5.16 highlights this difference. The melting temperature of the control sample amplicon using the primers stated in Table 5.5 (Section 5.2.4.1) was 88.07°C where the longer variant is present, whereas the TA sample showed a lower melting temperature of 87.79°C where the shorter variant is present. The melting curve temperature for the tuber sample is 87.90°C, which equates to the average of both the control and TA amplicon melting temperatures. This indicates the presence of one of each variant and confirms the RNASeq data.

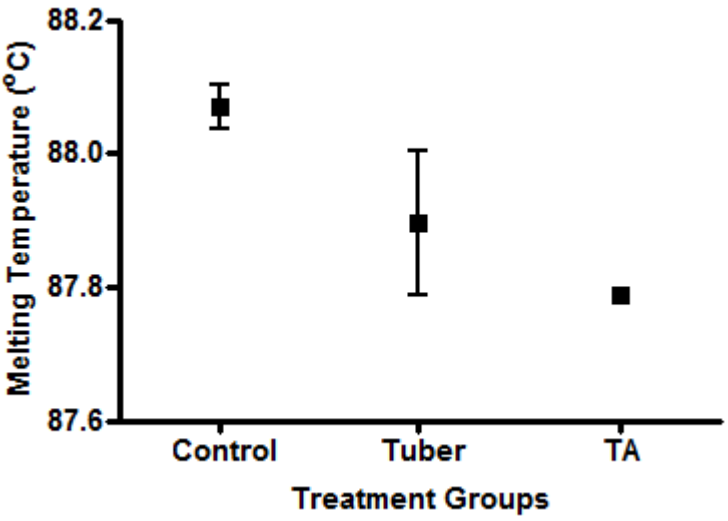

Figure 5.16: Melting curve analysis to identify *Kiss1r1* and *Kiss1r2*. Two primer sets were used (shown in Table 4.5) to identify differences in the amplicon melting temperatures from each RNA sample. RNA samples used were identical to those submitted for RNASeq. Data shown represents mean ± SEM, n=2.

5.4. Discussion and Conclusions

Over the past 20 years, the primary tool for assessing gene expression between disease states and biological conditions was the microarray. However, in recent years, RNASeq has become more popular. RNASeq is a cutting edge, next generation sequencing technique which reveals the presence and quantity of RNA transcripts in a sample at a given time. In order to gain a broad insight into the potential mechanisms of action of LL tuber, RNASeq was carried out using hypothalamus tissue to compare the treatments of tuber and TA to the control group. RNASeq is gaining much interest as it can overcome some of the limitations of the microarray. For example, *de novo* transcripts can be discovered since no reference genome is used to generate reads. Moreover, RNASeq avoids problems caused due to cross hybridisation. It has also been suggested that RNASeq is more sensitive and robust in comparison to microarray technology (McIntyre *et al.*, 2011).

The RNASeq data shows the complexity of the effects of LL tuber and TA on hypothalamic gene expression. Several genes identified are associated with appetite, energy regulation and metabolism and food intake which suggests that the LL tuber may had some effect on appetite, as suggested in mediaeval literature. Due to the size of the dataset generated, specific searches were carried out to identify appetite-related genes with the aim of creating a broad database for gene expression analysis. Thus, there may also be various other pathways and physiological processes affected by each treatment which are not discussed in this thesis.

The hypothalamus is an integral part of the central circuit controlling energy intake and expenditure. In particular, the ARC is highly involved in neuropeptide signalling between various orexigenic and anorexigenic neurons in the brain as well as peripheral tissues (Lopaschuk *et al.*, 2010). NPY/AgRP neurons are primarily orexigenic neurons which are associated with an increase in food intake. On the other hand, anorexigenic neurons POMC/CART are associated with decreases in food intake through complex signalling pathways. *Npy* and *Pomc* were down-regulated in the RNASeq data as well as the RT-PCR in this study for both the tuber and TA treatments. Various factors may

have influenced this including changes in signalling proteins throughout the body as a result of the different treatments. Leptin and resistin, from adipose tissue, and insulin (pancreas) inhibit NPY/AgRP neurons, whereas adiponectin (adipose tissue) and ghrelin (GIT) stimulate NPY/AgRP neurons. Additionally, leptin and insulin can stimulate POMC/CART neurons, while adiponectin inhibits POMC/CART neurons (Lopaschuk *et al.*, 2010).

The NPY system is thought to be one of the most important regulators in terms of feeding behaviour and energy homeostasis. This system consists of various neuropeptides and receptors including NPY, PYY and PP as well as Y1, Y2, Y4, Y5 and Y6 receptors. NPY, an orexigenic neuropeptide, is one of the most abundant peptides in the brain. The levels of NPY within the hypothalamus are suggested to be indicative of nutritional status. During fasting, NPY levels increase whereas NPY levels decrease following feeding. *Npy* levels in the tuber- and TA- treated samples are down-regulated both in the RNASeq and RT-qPCR data, thus suggesting the subjects had high nutritional status despite being fasted. This may also indicate lack of hunger although this is speculative. *Pyy*, an anorexigenic neuropeptide, is upregulated in the tuber and TA samples, shown in both RNASeq and RT-qPCR data. As mentioned above, PYY has been shown to reduce food intake in rats. Taken together, the downregulation of *Npy* and up regulation of *Pyy* could suggest appetite-suppressing properties of the treatments. Furthermore, NPY receptors appear to be highly upregulated in the RNASeq data. NPY receptors have been studied widely as potential targets for anti-obesity drug development (Yulyaningsih *et al.*, 2011).

Another physiological system which was highlighted to be affected by the treatments was the HPA axis. The HPA axis is a major neuroendocrine system which is involved in energy metabolism, reproduction and stress response (Sominsky and Spencer, 2014). Various peptides and receptors involved in the HPA axis are also related to food intake such as CRH, luteinising hormone/chroiogonadotropin receptor (LH/CG), PRL, GH, GnRH, BDNF, Kisspeptin and Kisspeptin receptor.

Following acute stress, CRH is released from the PVN in the hypothalamus and subsequently inhibits appetite (Sominsky and Spencer, 2014). However, it has been suggested that this only occurs during stress responses. George *et al.* (2010) determined that CRH administration in healthy, non-obese humans resulted in an increase in food intake 1h after peripheral administration, and that the amount of food consumed correlated with the dose of CRH given. Thus, in a non-stressful environment, CRH has the opposite effect. The RNASeq data indicates minimal effect of the tuber and TA on *Crh* expression in the hypothalamus (< 0.5-fold, p=0.8892 (n.s.) (Tuber); p=0.2646 (n.s.) (TA)). Contrary to this, there was a larger effect on LH/CG, PRL and GH as a result of both treatments. LH/CG appears to be upregulated to a larger extent in the tuber sample (4-fold, p=0.1246 (n.s.))) than in the TA sample (1.6-fold, p=0.3761 (n.s.)). PRL was also upregulated (4-fold, p=0.4992 (n.s.) (Tuber); p=0.5009 (n.s.) (TA)) in both samples, while GH appears to be down regulated in the tuber (6-fold, p=0.0314 (n.s.)) and unidentified in the TA sample.

PRL is a critical hormone involved in reproduction, but is also involved in growth and development, endocrinology and metabolism, immune regulation and the brain and behaviour (Grattan, 2015). PRL is thought to modulate energy balance through acting within the brain to increase food intake (Naef and Woodside, 2007). Naef *et al.*, (2007) showed that PRL was able to decrease food intake in a dose dependent manner, although there was no effect on BW. Moreover, PRL is involved in pancreatic and adipose development, and plays an essential role in adipogenesis, adipocyte differentiation and lipid metabolism (Grattan, 2015). In addition to this, PRL regulates several adipokines including leptin and adiponectin. Adiponectin precursor protein is down regulated in both the tuber and TA samples by 4.5-fold (p=0.2506 (n.s.)) and 3.5-fold (p=0.4991 (n.s.)), respectively. GH levels are high under conditions of nutritional restriction (Nass *et al.*, 2010). Zhao *et al.* (2010) concluded that GH is essential in preserving blood glucose levels in mice during sever calorie restriction. However, the RNASeq data shows a large down-regulation of GH. Additionally, GH release is stimulated by ghrelin, which is regulated by leptin. Thus, it is possible that increasing leptin levels would reduce ghrelin and thus GH, although this was not confirmed. Moreover, ghrelin O-acyl transferase (GOAT) was down-regulated in both the tuber

and TA sample by 1.3-fold (p=0.2901 (n.s.)) and 0.3-fold (p=0.6263 (n.s.)), respectively. GOAT is an enzyme involved in the modification of ghrelin to its acylated form, which is essential for the binding of ghrelin to its receptor (growth hormone secretagogue receptor, GHSR).

Leptin is an anorexigenic peptide, which decreases appetite and is highly involved in energy regulation as well as reproduction (Naef and Woodside, 2007; Woods and D'Alessio, 2008). Leptin and ghrelin form part of both the neuronal circuit regulating appetite, as well as the peripheral circuit and their mechanisms have been extensively researched and reviewed by many others (Aragonès *et al.*, 2016; Heppner and Tong, 2014; Iqbal *et al.*, 2006; Iwasa *et al.*, 2011; Klok *et al.*, 2007; Morrison, 2009; Siegrist-Kaiser *et al.*, 1997; Zigman *et al.*, 2016). Leptin was not identified in the RNASeq data, while ghrelin was minimally down-regulated in the tuber sample and up regulated in the TA sample [<0.5-fold for both, p=0.4077 (n.s.) (Tuber); p=0.5749 (n.s.) (TA)]. Other peripheral proteins and hormones identified to be affected by the treatments include CCK and gastrin-releasing peptide. CCK (up regulated 0.7-fold in the tuber sample (p<0.01), and 0.6-fold in the TA sample (p=0.1683 (n.s.)) is released from the small intestine and acts upon receptors resulting in a satiating effect in humans and animals, while gastrin-releasing peptide receptor (up regulated 3.7-fold (p=0.4992) (n.s.) and 5.7-fold (p=0.2179) (n.s.) in the tuber and TA samples, respectively) is a neuropeptide which stimulates the release of gastrin from the stomach. Recently, Mhalhal *et al.* (2017) showed that administration of exogenous CCK, exogenous gastrin-releasing peptide, and the combination of both, was able to reduce BW, if injected near their site of action in obese rats. Thus, changes in these genes may add to the appetite regulating effects of the tuber.

5-HT is known to decrease food intake and various anti-obesity drugs, including sibutramine and dexfenfluramine, act to increase signalling from serotonin receptors. Serotonin receptor 3 is up regulated 3.7-fold in both the tuber (p=0.499 (n.s.)) and TA samples (p=0.500 (n.s.)). Moreover, knockout models of the serotonin receptor resulted in an increase of food intake and BW (Schwartz *et al.*, 2000). Thus, this may

add to the possible mechanisms of action of the treatments to decrease appetite.

BDNF, of which transcript 3 is up-regulated 7.6-fold and 6.7-fold in tuber ($p<0.01$) and TA ($p<0.05$) samples, respectively, is also able to regulate appetite and food intake through acting upon the hypothalamic neurons. In addition to this, BDNF is involved in learning, depression and energy metabolism. Through intracerebroventricular (icv) administration, Toriya *et al.* (2010) showed that BDNF is able to decrease food intake and bodyweight. Additionally, administration of BDNF upregulated CRH mRNA expression in the paraventricular nucleus. They concluded that the reduction in food due to BDNF administration is mediated through CRH signalling. BDNF also suppresses appetite through downstream regulation of the melanocortin signalling pathway in the hypothalamus. Furthermore, Urabe *et al.* (2013) showed that haematopoietic cells, which produce BDNF, can control appetite and energy balance as they can migrate to the hypothalamus. The main receptor for BDNF is neurotrophic tyrosine kinase receptor 2 (NTRK2) (Ozek *et al.*, 2015). Mutations in either BDNF or NTRK2 in humans has been shown to be associated with obesity and hyperphagia (Ozek *et al.*, 2015). However, there is minimal change in expression of this receptor following treatment of the tuber or TA. Despite this, there is a large up regulation of NTRK3 (9.7-fold in both samples ($p<0.01$ in tuber and TA), the major binding site for neurotrophin 3 [(also up regulated in both samples by 4.7-fold ($p=0.2494$ (n.s.), tuber; $p=0.2506$ (n.s.), TA)].

Further to this, Kisspeptin and Kisspeptin receptor are also associated with the HPG axis, and subsequently may be involved in feeding behaviour and energy regulation. KISS1 has been identified in the ARC and has been shown to regulate the release of GnRH in the hypothalamus. It is also thought to regulate NPY expression and POMC expression, as well as GH, PRL and LH, thus highlighting the complexity of the HPG system (Bond and Smith, 2014; Daniel *et al.*, 2015). Furthermore, kisspeptin is regulated by leptin, insulin and ghrelin, all of which are highly involved in the regulation of food intake and energy regulation (Bond and Smith, 2014). Kisspeptin was up regulated by 1.6-fold by both the tuber ($p=0.3740$ (n.s.)) and TA treatments

(p=0.3761 (n.s.)). *Kiss1r* was also up regulated, however, each treatment affected a different transcript variant of *Kiss1r1* – specifically, the tuber upregulated *Kiss1r2* by 8.2-fold ($p<0.01$), while TA up regulated *Kiss1r1* by 8-fold ($p<0.01$). The different variants were confirmed in each sample though RT-qPCR melting curve analysis. The variants have a difference of 2 amino acids, however, there is no indication of a difference in their function. RNASeq data showed only the presence of one transcript in the control sample, and TA sample, but both in the tuber sample. These results highlight the need for a larger sample size as it appears the animals express different forms of this receptor. Furthermore, the two transcript variants identified are only present in the *Rattus* genus, and not in human. This may potentially cause large implications in studies examining the Kisspeptin pathway as looking at only one transcript variant may obscure the true data. As seen in this instance, looking at only one transcript for each treatment group would give contrasting results.

Taking all of the above together, it is evident that both the tuber and TA treatments had significant effects on the NPY system as well as at various points in the HPG axis, both of which are highly involved in the control of food intake and energy metabolism. Moreover, as some of the results are similar in the tuber and TA analysis, it suggests that the TA in the tuber may be causing some of the gene expression changes identified. However, as the tuber was administered whole, there are also many other compounds which could be attributing to the results. It also highlights the complexity of the neuronal and peripheral circuits which control appetite. There are some discrepancies between the RNASeq data and RT-qPCR which highlight the need for larger sample size in RNASeq. In this study, two samples from each treatment group were pooled to give an n=1 for each group. Pooling of samples gives a more accurate representation of the group as a whole, but can also result in a loss of information between individual samples. Furthermore, pooling samples prevents statistical analysis being carried out between groups and thus determine animal variation within the experiment. Additionally, the opportunity to relate transcript expression changes to the individual animal phenotype, which can often vary within a group, is lost. However, the benefit of pooling samples is that it reduces costs dramatically while giving an overview of transcript changes within each treatment group. Thus the reason for the mismatch in

RNASeq and RT-qPCR results in this study could be due to pooling of the samples. Jolly *et al.* (2005) investigated the use of pooled samples compared to individual samples, from the same experiment, in a microarray experiment. They found that only 30% of the probes analysed gave similar results for both datasets. The majority of the changes identified in the pooled group were also identified in the individual sample group. However, there was a large percentage of changes (49-67%) identified in the individual sample group that were not found in the pooled data. Additionally, they carried out RT-qPCR to confirm the magnitude and direction of the microarray results. Only the results obtained from the individual sample analysis were verified using RT-qPCR, suggesting that the rate of false positive in the pooled data is higher. Peng *et al.,* (2003) suggest that some 'pooling schemes' can actually provide adequate efficiency while still being cost-effective, for example, multiple animals within a group are pooled into multiple, evenly spread, groups. This helps to decrease variability whilst also reducing the number of experiments. In this instance, more biological repeats may also be required. Although the above studies focus on microarrays, the points are also valid for RNASeq experiments. Thus, it is possible this is the reason for being unable to validate the RNASeq using RT-qPCR in this study. Although a number of genes involved in appetite control and energy metabolism appear to alter expression following treatment, further work needs to be carried out to correlate these results with protein expression within the tissue. RNASeq allows identification of the gene transcripts however, changes in gene expression does not always result in changes in protein expression (Wolf, 2013). Additionally, analysis of specific appetite-regulating genes in peripheral tissues such as adipose tissue and skeletal muscle would be beneficial.

To conclude, the above study has confirmed that tubers of LL influence genes which control and regulate appetite and energy metabolism. These results correlate with traditional usage of this plant, although the exact mechanism of action is still not fully understood. Future work in this area would include a repeat of the feeding study with higher doses of the tuber, and possibly at more time-points. Following this, the gene expression changes could be examined again in the hypothalamus using a larger sample size to increase the reliability and accuracy of the results. The results described

above are representative of n=1 from two pooled samples. Thus increasing the sample size and looking at individual samples may give a clearer insight into the pathways involved. Additionally, peripheral tissues could also be examined.

6. CHAPTER 6, GENERAL DISCUSSION AND FUTURE WORK

The objectives of this thesis, outlined in Chapter 1, were to investigate the traditional usage of LL tubers as an appetite suppressant. LL tubers were used in mediaeval times (ca. 1700s) to prevent hunger and thirst and provide an energy boost in times of war and famine. During an excavation of an old mediaeval hospital at Soutra Aisle, Dr Brian Moffat found remnants of LL tuber in the waste drains and subsequently began researching the historical usage of such tubers in addition to many other plant species identified. A supply of the tubers was established with the founder of 'Bitter Vetch', Mr Mark Goff, to allow investigation into the potential mechanisms of action. Dr Moffat and Mr Goff both consume the tubers and have confirmed reduced appetite following consumption as well as heightened alertness. Thus, based on this, and the mediaeval literature, this project focused on investigating the potential biological activity using both *in vitro* and *in vivo* methods.

The starting point was to collect and correctly identify the tubers of LL. In 2006, a company called Heath Pea Ltd was established to develop a new 'slimming aid' using LL tubers. The success of this company is unknown, however due to recent lack of literature and publicity around this plant, it is assumed they were not successful in identifying active compounds or their mechanisms of action. Commercialisation of such a product would need correct identification of the tuber, thus the starting point of this thesis was to develop a method to confirm the identity of LL using ISSR-PCR and Experion DNA™ analysis. This method would prove useful in future batch testing of different collections of the tuber. These results are discussed in Chapter 2. Further work in this area could include investigating a larger number of ISSR primers, as well as a wider range of plant species. Moreover, the tuber morphology was characterised using different histological stains. Various distinctive features were noted including large starch grains and an orange periderm/skin. Additionally, when stained with toludine blue, a pink/purple colour is evident. The novel compound identified in the cr. extract LL-EthA-2, contains two carboxylic acid groups. This compound could

potentially cause the pink/purple staining of the tuber slices. Numerous other compounds present within the tuber could also influence the staining depending on the functional groups present. A method of confirming this involves matrix-assisted laser desorption/ionisation-time of flight (MALDI-TOF) analysis of the tuber slices. Bjarnjolt *et al.* (2014) discusses the principles of this technique in imaging metabolites present in plant tissues. MALDI-TOF could be coupled with traditional staining techniques to profile the location of active compounds. For example, the defence compounds found in barley (*Hordeum vulgare)* such as hydroxynitrile glucosides, are found in a single layer of cells in the epidermis. The down-side of this technique is that one would need to know the exact compound to be identified, thus it is not used in the discovery process. However, it could be used to characterise the tubers, and as quality control to identify active components in tubers from various locations. This method was initially attempted to examine the presence of TA in the tuber. However, due to the volatility of TA under high vacuum conditions, the method was not optimised within the time available and thus no results were obtained.

Following this, a "look-see" investigation into the effect of the whole tuber on BW, food intake and water intake was conducted *in vivo.* Sprague Dawley rats were treated with either a sham control (0.9% v/v saline) or one of two treatments – LL tuber, and TA. The aim of this study was to mimic the traditional usage of the tuber and observe any subsequent effects based on symptoms described by Dr Brian Moffat. Dr Moffat described reduced hunger and thirst, as well as increased energy and heightened alertness, therefore various physical aspects were monitored post-treatment including food intake, water intake, body weight and physical activity. However, there were no significant differences at any time-point between each group. Additionally, the effect of the tuber on serum testosterone levels was examined. At a dose of 210mg/kg BW, the tuber significantly decreased testosterone levels. This decrease was not evident at a dose of 42mg/kg BW. The reduction in testosterone may be due to the presence of the glycyrrhizin-like compound identified in the tuber extracts (see Chapter 3). Glycyrrhizin, found in liquorice, has been shown to reduce testosterone levels in healthy women and men through the inhibition of two enzymes, 17-hydroxysteroid dehydrogenase (HSD) and 17-20 lyase (Armanini *et al.*, 2004, 1999; Omar *et al.*,

2012). It is possible that the aglycone structure of the compound found in the tubers has properties which are similar to glycyrrhizin.

Due to the lack of results in this investigation in terms of the appetite suppressing properties, the tuber itself was subsequently investigated. To do this, a Soxhlet extraction was carried out which produced cr. extracts. Using NMR, LC-MS and GC-MS, the extract components were studied with the aim of identifying possible active compounds present in the tuber. These extracts were screened for potential biological activity using methods such as cytotoxicity and enzyme inhibition assays as well as being investigated for their effect on TNFα release in U937 cells. These results are discussed in Chapter 4.

The main finding was the identification of a novel compound in one of the ethyl acetate crude extracts (LL-EthA-2). This compound was identified as 3-O-[-α-L-arabinopyranosyl-(1→2)-β-D-glucuronopyranosyl]-24-hydroxy-12-oleanen-30-oic acid, designated lathyrosaponin A. In addition to this, the hexane extracts (LL-Hex-1 and LL-Hex-2) were found to contain fatty acids and triglycerides, which could explain the enhancement of TNFα observed in the *in vitro* study. Fatty acids can interact with toll-like receptor 4 (TLR4) which subsequently activates the NFkB pathway, initiating the release of TNFα. Betulinic acid was also identified in these two extracts, with LL-Hex-2 showing this as the major compound while LL-Hex-1 only had minor levels. Based on information provided by Dr Moffat, the presence of TA was confirmed using GC-MS. As a result of this, TA was also used as a control in the *in vivo* study discussed in Chapter 3. Based on these findings, future work would include further separation of the cr. extracts, and purification of each compound. Additionally, x-ray crystallography of the compound identified in LL-EthA-2 would confirm the stereochemistry and structure of this compound. Following purification, further *in vitro* bioassays could be conducted to identify the bioactivity of the pure compounds in comparison to the cr. extracts. The crude extracts were deemed as not toxic against three cell lines, 3T3-L1, SH-SY5Y and U937, at concentrations up to 100µg/mL. Additionally, the enzyme inhibition potential was investigated using enzymes including DPPIV, PTP1b, α-amylase, α-glucosidase and pancreatic lipase.

Enzymes were selected on the basis of their association with appetite-related signalling pathways. No inhibitory activity was observed for any of the cr. extracts against DPPIV, PTP1b, α-amylase or pancreatic lipase. Contrastingly, the ethyl acetate extracts (LL-EthA-1 and LL-EthA-2) showed significant ($p<0.01$) inhibition of α-glucosidase. These extracts were further fractionated using VLC and the fractions were tested in this assay again to focus the investigation to one or two fractions. However, all fractions showed inhibitory activity. Future work would be to identify all possible compounds present in these fractions. It is possible that similar compounds are present in each fraction giving rise to this inhibitory potential. Three of the cr. extracts (LL-Hex-1, LL-Hex-2 and LL-EthA-1) also show significant enhancement of TNFα in the presence of LPS. U937 cells were differentiated into inflammatory-like macrophages, and subsequently stimulated with the samples in the presence or absence of LPS. LPS is known to cause TNFα release from these cells, thus the aim was to identify whether the samples reduce or increase the release of TNFα, or if they can cause this release when added alone. LL-Hex-1, LL-Hex-2 and Ll-EthA-1 were able to enhance the release of TNFα in the presence of LPS however they did not significantly increase the release of TNFα on their own in comparison to LPS. These extracts have been shown to contain various compounds including fatty acids and triglycerides which can act upon the same receptor as LPS (toll-like receptor 4) to activate inflammatory signalling pathways. It was not possible to confirm the exact nature of these fatty acids and triglycerides or the concentration present in the extracts. Future work would involve identifying each individual compound present and assessing their individual activity. This would allow further investigation of the mechanism of action of TNFα release.

Using tissues isolated during the *in vivo* study, the effect of LL tuber was investigated on a larger scale by conducting RNASeq using hypothalamic tissue. Although no effect was observed on BW, food intake, water intake or physical activity, there were numerous changes in gene expression within the hypothalamus. The hypothalamus is one of the main control sites for appetite regulation and energy regulation and metabolism. Specifically, many genes associated with appetite regulating pathways, including the melanocortin pathways, NPY signalling pathways, leptin pathway etc.,

have been affected by treatment with the tuber and TA. These results highlight the need for a systems level approach to natural product drug discovery. Another main finding of this study was the expression of two different *Kiss1r* transcripts, of which one was upregulated by treatment with the tuber, and the other by treatment with TA. The implications of this finding are large, as when using RT-qPCR, primers are designed upon known genes, therefore, designing a primer to only show one of these transcripts could mean changes in this gene expression may be missed. It may also raise questions as to the correct animal model to use when looking at kisspeptin signalling. Humans only express one transcript, therefore the Sprague Dawley rat may not represent the best animal model due to the expression of two transcripts. There are several other experiments which would add to the data obtained in this study. Firstly, determining the effect on protein expression would give more insight into the physiological effects of the tuber. Secondly, looking at gene expression and protein expression in peripheral organs would allow the results to be examined in a broader context. The results above represent n=1, therefore repeating this study for each individual biological replicate would enhance the reliability and accuracy of the results. Metabolomic analysis of blood serum samples would also give insight into the effect of the treatments on circulating proteins.

6.1. Conclusions

Going backwards to investigate the historical use of LL tubers fuelled the investigation of their potential biological activity and mechanisms of action. Using a broad range of techniques, including Next Generation Sequencing (RNASeq), it was confirmed that the tuber influences various pathways in the hypothalamus associated with appetite, food intake, energy regulation and reproduction. Going forwards, it is possible that isolated compounds, which are shown to be responsible for such effects, or the tuber as a whole, could be used to regulate hunger. With worldwide problems of obesity as well as undernourishment, there is a need to develop therapies which can regulate hunger and potential help in both cases. With further work and development, LL tubers could be the key to this.

7. REFERENCES

Ahima, R.S., Antwi, D. a., 2008. Brain Regulation of Appetite and Satiety. Endocrinol. Metab. Clin. North Am. 37, 811–823.

Ahima, R.S., Lazar, M. a, 2008. Adipokines and the peripheral and neural control of energy balance. Mol. Endocrinol. 22, 1023–1031.

Ahrén, B., 2007. DPP-4 inhibitors. Best Pract. Res. Clin. Endocrinol. Metab. 21, 517–533.

Ajmal Ali, M., Gyulai, G., Hidvégi, N., Kerti, B., Al Hemaid, F.M.A., Pandey, A.K., Lee, J., 2014. The changing epitome of species identification - DNA barcoding. Saudi J. Biol. Sci. 21, 204–231.

Albrecht, U., 2017. The circadian clock, metabolism and obesity. Obes. Rev. 18, 25–33.

Allkin, R., Gyder, D., Bisby, F., White, R., 1986. Names and synonyms of species and subspecies in the Viciea. Vicieae Database Poject, Southampt. Univ. Southampton, UK.

Anighoro, A., Bajorath, J., Rastelli, G., 2014. Polypharmacology: Challenges and opportunities in drug discovery. J. Med. Chem. 57, 7874–7887.

Aragonès, G., Ardid-Ruiz, A., Ibars, M., Suárez, M., Bladé, C., 2016. Modulation of leptin resistance by food compounds. Mol. Nutr. Food Res. in press, 1–42.

Archer, Z.A., Rayner, D. V., Barrett, P., Balik, A., Duncan, J.S., Moar, K.M., Mercer, J.G., 2005. Hypothalamic energy balance gene responses in the Sprague-Dawley rat to supplementation of high-energy diet with liquid ensure and subsequent transfer to chow. J. Neuroendocrinol. 17, 711–719.

Armanini, D., Bonanni, G., Palermo, M., 1999. Reduction of serum testosterone in men by licorice. N. Engl. J. Med. 341, 1158.

Armanini, D., Mattarello, M.J., Fiore, C., Bonanni, G., Scaroni, C., Sartorato, P., Palermo, M., 2004. Licorice reduces serum testosterone in healthy women. Steroids 69, 763–766.

Arnau, G., Lallemand, J., Bourgoin, M., 2002. Fast and reliable strawberry cultivar identication using inter simple sequence repeat (ISSR) amplication. Euphytica 129, 69–79.

Astell, K.J., Mathai, M.L., Su, X.Q., 2013. A Review on Botanical Species and Chemical Compounds with Appetite Suppressing Properties for Body Weight Control. Plant Foods Hum. Nutr. 68, 213–221.

Ata, A., Naz, S., Elias, E.M., 2011. Naturally occurring enzyme inhibitors and their pharmaceutical applications. Pure Appl. Chem. 83, 1741–1749.

Atanasov, A.G., Waltenberger, B., Pferschy-Wenzig, E.M., Linder, T., Wawrosch, C., Uhrin, P., Temml, V., Wang, L., Schwaiger, S., Heiss, E.H., Rollinger, J.M., Schuster, D., Breuss, J.M., Bochkov, V., Mihovilovic, M.D., Kopp, B., Bauer, R., Dirsch, V.M., Stuppner, H., 2015. Discovery and resupply of pharmacologically active plant-derived natural products: A review. Biotechnol. Adv. 33, 1582–1614.

Atta-ur-Rahman, Choudhary, M.I., Basha, F.Z., Abbas, G., Khan, S.N., Ali Shah, S.A., 2007. Science at the interface of chemistry and biology: Discoveries of α-glucosidase inhibitors and

antiglycation agents. Pure Appl. Chem. 79, 2263–2268.

Azmir, J., Zaidul, I.S.M., Rahman, M.M., Sharif, K.M., Mohamed, A., Sahena, F., Jahurul, M.H. a., Ghafoor, K., Norulaini, N. a. N., Omar, A.K.M., 2013. Techniques for extraction of bioactive compounds from plant materials: A review. J. Food Eng. 117, 426–436.

Bado, A., Levasseur, S., Attoub, S., Kermorgant, S., Laigneau, J.P., Bortoluzzi, M.N., Moizo, L., Lehy, T., Guerre-Millo, M., Le Marchand-Brustel, Y., Lewin, M.J., 1998. The stomach is a source of leptin. Nature 394, 790–793.

Baines, E., 1836. History of The County Palatine and Duchy of Lancaster.

Baker, D.D., Chu, M., Oza, U., Rajgarhia, V., 2007. The value of natural products to future pharmaceutical discovery. Nat. Prod. Rep. 24, 1225–44.

Barrett, M.L., Udani, J.K., 2011. A proprietary alpha-amylase inhibitor from white bean *(Phaseolus vulgaris)* : A review of clinical studies on weight loss and glycemic control. Nutr. J. 10, 24.

Batterham, R.L., Cohen, M. a, Ellis, S.M., Le Roux, C.W., Withers, D.J., Frost, G.S., Ghatei, M. a, Bloom, S.R., 2003. Inhibition of food intake in obese subjects by peptide YY3-36. N. Engl. J. Med. 349, 941–948.

Begg, D.P., Woods, S.C., 2013. The endocrinology of food intake. Nat Rev Endocrinol 9, 584–597.

Beiroa, D., Imbernon, M., Gallego, R., Senra, A., Herranz, D., Villaroya, F., Serrano, M., Fernø, J., Salvador, J., Escalada, J., Dieguez, C., Lopez, M., Frühbeck, G., Nogueiras, R., 2014. GLP-1 Agonism Stimulates Brown Adipose Tissue Thermogenesis and Browning Through Hypothalamic AMPK. Diabetes 1–13.

Benoit, S.C., Schwartz, M.W., Lachey, J.L., Hagan, M.M., Rushing, P.A., Blake, K.A., Yagaloff, K.A., Kurylko, G., Franco, L., Danhoo, W., Seeley, R.J., 2000. A novel selective melanocortin-4 receptor agonist reduces food intake in rats and mice without producing aversive consequences. J. Neurosci. 20, 3442–3448.

Berthold-Losleben, M., Himmerich, H., 2008. The TNF-alpha system: functional aspects in depression, narcolepsy and psychopharmacology. Curr. Neuropharmacol. 6, 193–202.

Birari, R.B., Bhutani, K.K., 2007. Pancreatic lipase inhibitors from natural sources: unexplored potential. Drug Discov. Today 12, 879–889.

Bjarnholt, N., Li, B., D'Alvise, J., Janfelt, C., 2014. Mass spectrometry imaging of plant metabolites – principles and possibilities. Nat. Prod. Rep. 31, 818–837.

Blouin, K., Boivin, A., Tchernof, A., 2008. Androgens and body fat distribution. J. Steroid Biochem. Mol. Biol. 108, 272–280.

Bogeski, I., Bozem, M., Sternfeld, L., Hofer, H.W., Schulz, I., 2006. Inhibition of protein tyrosine phosphatase 1B by reactive oxygen species leads to maintenance of Ca2+ influx following store depletion in HEK 293 cells. Cell Calcium 40, 1–10.

Boncler, M., Rózalski, M., Krajewska, U., Podswdek, A., Watala, C., 2014. Comparison of PrestoBlue and MTT assays of cellular viability in the assessment of anti-proliferative effects of plant extracts on human endothelial cells. J. Pharmacol. Toxicol. Methods 69, 9–16.

Bond, J.P. De, Smith, J.T., 2014. Kisspeptin and energy balance in reproduction. Reproduction 147,

53–63.

Boran, A.D.W., Iyengar, R., 2010. Systems approaches to polypharmacology and drug discovery. Curr. Opin. Drug Discov. Dev. 13, 297–309.

Bornstein, S.R., Schuppenies, A., Wong, M.L., Licinio, J., 2006. Approaching the shared biology of obesity and depression: the stress axis as the locus of gene-environment interactions. Mol Psychiatry 11, 892–902.

Bounds, S. V, Caldwell, J., 1996. Pathways of metabolism of [1'-14C]-trans-anethole in the rat and mouse. Drug Metab. Dispos. 24, 717–724.

Bustin, S.A., Benes, V., Garson, J.A., Hellemans, J., Huggett, J., Kubista, M., Mueller, R., Nolan, T., Pfaffl, M.W., Shipley, G., Vandesompele, J., Wittwer, C.T., 2009. The MIQE Guidelines: *M*inimum *I*nformation for Publication of *Q*uantitative Real-Time PCR *E*xperiments. Clin. Chem. 55, 611–622.

Cazzola, R., Russo-Volpe, S., Miles, E.A., Rees, D., Banerjee, T., Roynette, C.E., Wells, S.J., Goua, M., Wahle, K.W.J., Calder, P.C., Cestaro, B., 2007. Age- and dose-dependent effects of an eicosapentaenoic acid-rich oil on cardiovascular risk factors in healthy male subjects. Atherosclerosis 193, 159–167.

Chang, C.-J., Lin, C.-S., Lu, C.-C., Martel, J., Ko, Y.-F., Ojcius, D.M., Tseng, S.-F., Wu, T.-R., Chen, Y.-Y.M., Young, J.D., Lai, H.-C., 2015. *Ganoderma lucidum* reduces obesity in mice by modulating the composition of the gut microbiota. Nat. Commun. 6, 7489.

Charaux, C., Rabate, J., 1939. Constitution chimique de l'orobol. Bull. Soc. Chim. Biol 12, 1330–1333.

Chavan, U.D., McKenzie, D.B., Amarowicz, R., Shahidi, F., 2003. Phytochemical components of beach pea (*Lathyrus maritimus* L.). Food Chem. 81, 61–71.

Chen, B.C., Hsieh, S.L., Lin, W.W., 2001. Involvement of protein kinases in the potentiation of lipopolysaccharide-induced inflammatory mediator formation by thapsigargin in peritoneal macrophages. J. Leukoc. Biol. 69, 280–288.

Chen, F., Wen, Q., Jiang, J., Li, H.L., Tan, Y.F., Li, Y.H., Zeng, N.K., 2016. Could the gut microbiota reconcile the oral bioavailability conundrum of traditional herbs? J. Ethnopharmacol. 179, 253–264.

Cheng, A., Uetani, N., Simoncic, P.D., Chaubey, V.P., Lee-Loy, A., McGlade, C.J., Kennedy, B.P., Tremblay, M.L., 2002. Attenuation of leptin action and regulation of obesity by protein tyrosine phosphatase 1B. Dev. Cell 2, 497–503.

Chinsembu, K.C., Hedimbi, M., 2010. Ethnomedicinal plants and other natural products with anti-HIV active compounds and their putative modes of action. Mol. Biol. 1, 74–91.

Chiu, T.H., Kuo, C.W., Lin, H.C., Huang, D.S., Wu, P.L., 2015. Genetic diversity of ivory shell (*Babylonia areolata*) in Taiwan and identification of species using DNA-based assays. Food Control 48, 108–116.

Choi, H.J., Bae, E.Y., Song, J.H., Baek, S.H., Kwon, D.H., 2010. Inhibitory effects of orobol 7-O-d-glucoside from banaba (*Lagerstroemia speciosa* L.) on human rhinoviruses replication. Lett.

Appl. Microbiol. 51, 1–5.

Cichewicz, R.H., Kouzi, S.A., 2004. Chemistry, Biological Activity, and Chemotherapeutic Potential of Betulinic Acid for the Prevention and Treatment of Cancer and HIV Infection. Med. Res. Rev. 24, 90–114.

Cockwell, H., Wilkinson, D.A., Bouzayen, R., Imran, S.A., Brown, R., Wilkinson, M., 2013. KISS1 expression in human female adipose tissue. Arch. Gynecol. Obstet. 287, 143–147.

Coelho-de-Souza, A.N., Lahlou, S., Barreto, J.E.F., Yum, M.E.M., Oliveira, A.C., Oliveira, H.D., Celedônio, N.R., Feitosa, R.G.F., Duarte, G.P., Santos, C.F., De Albuquerque, A.A.C., Leal-Cardoso, J.H., 2013. Essential oil of *Croton zehntneri* and its major constituent anethole display gastroprotective effect by increasing the surface mucous layer. Fundam. Clin. Pharmacol. 27, 288–298.

Cohen, M.A., Ellis, S.M., Le Roux, C.W., Batterham, R.L., Park, A., Patterson, M., Frost, G.S., Ghatei, M.A., Bloom, S.R., 2003. Oxyntomodulin Suppresses Appetite and Reduces Food Intake in Humans. J. Clin. Endocrinol. Metab. 88, 4696–4701.

Cox, P.A., Balick, M.J., 1994. The Ethnobotanical Approach to Drug Discovery. Sci. Am. 270, 60–65.

Cullen, K.J., 2010. Famine in Scotland: The "Ill Years" of the 1690s.

Dailey, M.J., Moran, T.H., 2013. Glucagon-like peptide 1 and appetite. Trends Endocrinol. Metab. 24, 85–91.

Daniel, J., Foradori, C., Whitlock, B., Sartin, J., 2015. Reproduction and beyond, kisspeptin in ruminants. J Anim Sci Biotechnol 6, 23.

Dasmahapatra, K.K., Mallet, J., 2006. Taxonomy: DNA barcodes: recent successes and future prospects. Heredity (Edinb). 97, 254–255.

David, J., Wolfender, J., Dias, D.A., 2014. The pharmaceutical industry and natural products: historical status and new trends. Phytochem. Rev. 14, 299–315.

De Bond, J.-A.P., Tolson, K.P., Nasamran, C., Kauffman, A.S., Smith, J.T., 2016. Unaltered hypothalamic metabolic gene expression in *Kiss1r* KO mice despite obesity and reduced energy expenditure. J. Neuroendocrinol. 1–10.

de Sales, P.M., de Souza, P.M., Simeoni, L.A., Magalhães, P.D.O., 2012. α -Amylase Inhibitors : A Review of Raw Material and Isolated Compounds from Plant Source. J Pharm Pharmaceur Sci 15, 141–183.

Debnath, S.C., Khanizadeh, S., Jamieson, A.R., Kempler, C., 2008. Inter Simple Sequence Repeat (ISSR) markers to assess genetic diversity and relatedness within strawberry genotypes. Can. J. Plant Sci. 88, 313–322.

Del Bufalo, A., Bernad, J., Dardenne, C., Verda, D., Meunier, J.R., Rousset, F., Martinozzi-Teissier, S., Pipy, B., 2011. Contact sensitizers modulate the arachidonic acid metabolism of PMA-differentiated U-937 monocytic cells activated by LPS. Toxicol. Appl. Pharmacol. 256, 35–43.

Dong, H.Q., Li, M., Zhu, F., Liu, F.L., Huang, J.B., 2012. Inhibitory potential of trilobatin from *Lithocarpus polystachyus* Rehd against a-glucosidase and a-amylase linked to type 2 diabetes.

Food Chem. 130, 261–266.

Dudek, M., Kołodziejski, P.A., Pruszyńska-Oszmałek, E., Sassek, M., Ziarniak, K., Nowak, K.W., Sliwowska, J.H., 2016. Effects of high-fat diet-induced obesity and diabetes on Kiss1 and GPR54 expression in the hypothalamic–pituitary–gonadal (HPG) axis and peripheral organs (fat, pancreas and liver) in male rats. Neuropeptides 2, 1–9.

Dwarkasing, J.., Marks, D.L., Witkamp, R.., van Norren, K., 2015. Hypothalamic inflammation and food intake regulation during chronic illness. Peptides.

Ebadi, M., Mazurak, V.C., 2015. Potential Biomarkers of Fat Loss as a Feature of Cancer Cachexia.

Elchebly, M., Payette, P., Michaliszyn, E., Cromlish, W., Collins, S., Loy, A.L., Normandin, D., Cheng, A., Himms-hagen, J., Chan, C., Ramachandran, C., Gresser, M.J., Tremblay, M.L., Kennedy, B.P., 1999. Increased Insulin Sensitivity and Obesity Resistance in Mice Lacking the Protein Tyrosine. Science (80-.). 283, 1544–1548.

Escrig, V., Ubeda, a, Ferrandiz, M.L., Darias, J., Sanchez, J.M., Alcaraz, M.J., Paya, M., 1997. Variabilin: a dual inhibitor of human secretory and cytosolic phospholipase A2 with anti-inflammatory activity. J. Pharmacol. Exp. Ther. 282, 123–131.

Fabricant, D.S., Farnsworth, N.R., 2001. The value of plants used in traditional medicine for drug discovery. Environ. Health Perspect. 109, 69–75.

Fang, X.L., Shu, G., Yu, J.J., Wang, L.N., Yang, J., Zeng, Q.J., Cheng, X., Zhang, Z.Q., Wang, S.B., Gao, P., Zhu, X.T., Xi, Q.Y., Zhang, Y.L., Jiang, Q.Y., 2013. The Anorexigenic Effect of Serotonin Is Mediated by the Generation of NADPH Oxidase-Dependent ROS. PLoS One 8, 1–8.

Fratianni, F., Cardinale, F., Cozzolino, A., Granese, T., Albanese, D., Di Matteo, M., Zaccardelli, M., Coppola, R., Nazzaro, F., 2014. Polyphenol composition and antioxidant activity of different grass pea *(Lathyrus sativus*), lentils *(Lens culinaris*), and chickpea (*Cicer arietinum*) ecotypes of the Campania region (Southern Italy). J. Funct. Foods 7, 551–557.

Friedman, J.M., 2002. The function of leptin in nutrition, weight, and physiology. Nutr. Rev. 60, S1–S14.

Fu, L.-Y., van den Pol, A.N., 2010. Kisspeptin directly excites anorexigenic proopiomelanocortin neurons but inhibits orexigenic neuropeptide Y cells by an indirect synaptic mechanism. J. Neurosci. 30, 10205–10219.

Fuchs, A., De Vries, F., Landheer, C., Van Veldhuizen, A., 1984. Odoratol and methylodoratol, two alpha-hydroxydihydrochalcone stress metabolites from *lathyrus odoratus*. Phytochemistry 23, 2199–2201.

Fulda, S., 2008. Betulinic acid for cancer treatment and prevention. Int. J. Mol. Sci. 9, 1096–1107.

Funke, I., Melzig, M.F., 2005. Effect of different phenolic compounds on a-amylase activity: Screening by microplate-reader based kinetic assay. Pharmazie 60, 796–797.

George, S.A., S, K., Briggs, H., Abelson, J., 2010. CRH-stimulated cortisol release and food intake in healthy, non obese adults. Psychoneuroendocrinology2 35, 607–612.

Ghorbel, M., Marghali, S., Tri, N., Chtourou-ghorbel, N., 2014. Phylogeny of Mediterranean *Lathyrus*

species using Inter Simple Sequence Repeats markers 161, 91–98.

Ghosh, B., Mitra, J., Chakraborty, S., Bhattacharyya, J., Chakraborty, A., Sen, S.K., Neerathilingam, M., 2015. Simple detection methods for antinutritive factor β-ODAP present in *Lathyrus sativus* L. by high pressure liquid chromatography and thin layer chromatography. PLoS One 10, 1–14.

Glossmann, H., Presek, P., Eigenbrodt, E., 1981. Querceyin Inhibits Tyrosine Phosphorylation by the Cyclic Nucleotide-Independent, Transforming Protein Kinase, pp60. Arch. Pharmacol. 317, 100–102.

Gökhan, Ç., Küsefoğlu, S., 2013. A Simple One-Step Synthesis and Polymerisation of Plant Oil Triglyceride Iodo Isocyanates. J. Appl. Polym. Sci. 116, 2433–2440.

Grattan, D.R., 2015. The hypothalamo-prolactin axis. J. Endocrinol. 226, T101–T122.

Green, B.D., Flatt, P.R., Bailey, C.J., 2006. Dipeptidyl peptidase IV (DPP IV) inhibitors: A newly emerging drug class for the treatment of type 2 diabetes. Diab. Vasc. Dis. Res. 3, 159–165.

Greenwood, M.R., Cleary, M.P., Gruen, R., Blase, D., Stern, J.S., Triscari, J., Sullivan, a C., 1981. Effect of (-)-hydroxycitrate on development of obesity in the Zucker obese rat. Am. J. Physiol. 240, E72–E78.

Groves, R.A., Hagel, J.M., Zhang, Y., Kilpatrick, K., Levy, A., Marsolais, F., Lewinsohn, E., Sensen, C.W., Facchini, P.J., 2015. Transcriptome profiling of khat (*Catha edulis*) and *Ephedra sinica* reveals gene candidates potentially involved in amphetamine-type alkaloid biosynthesis. PLoS One 10.

Halaas, J.L., Boozer, C., Blair-West, J., Fidahusein, N., Denton, D.A., Friedman, J.M., 1997. Physiological response to long-term peripheral and central leptin infusion in lean and obese mice. Physiology 94, 8878–8883.

Halaas, J.L., Gajiwala, K.S., Maffei, M., Cohen, S.L., Chait, B.T., Rabinowitz, D., Lallone, R.L., Burley, S.K., Friedman, J.M., 1995. Weight-reducing effects of the plasma protein encoded by the obese gene. Science 269, 543–546.

Halatchev, I.G., Ellacott, K.L.J., Fan, W., Cone, R.D., 2004. Peptide YY3-36 inhibits food intake in mice through a melanocortin-4 receptor-independent mechanism. Endocrinology 145, 2585–2590.

Halford, J.C.G., Harrold, J. a., 2012. Satiety-enhancing products for appetite control: science and regulation of functional foods for weight management. Proc. Nutr. Soc. 71, 350–362.

Hamid, R., Rotshteyn, Y., Rabadi, L., Parikh, R., Bullock, P., 2004. Comparison of alamar blue and MTT assays for high through-put screening. Toxicol. Vitr. 18, 703–710.

Haque, A., Siddiqi, M.M.A., Rahman, A.F.M.M., Hasan, C.M., 2013. Isolation of Betulinic Acid and 2 , 3-Dihydroxyolean-12-en-28-oic Acid from the leaves of *Callistemon linearis*. Dhaka Univ J Sci 61, 211–212.

Henry, F.E., Sugino, K., Tozer, A., Branco, T., Sternson, S.M., 2015. Cell type-specific transcriptomics of hypothalamic energy-sensing neuron responses to weight-loss. Elife 4, 1–30.

Heppner, K.M., Tong, J., 2014. Mechanisms in endocrinology: regulation of glucose metabolism by the ghrelin system: multiple players and multiple actions. Eur. J. Endocrinol. 171, 21–32.

Hill, J.W., 2010. Gene Expression and the Control of Food Intake by Hypothalamic POMC/CART Neurons. Open Neuroendocrinol. J. 3, 21–27.

Hooker, W.J., 1821. Flora Scotia: A Description of Scottish Plans, arranged both according to the artificial and natural methods. Volume 2.

Hou, W., Li, Y., Zhang, Q., Wei, X., Peng, A., Chen, L., Wei, Y., 2008. Triterpene Acids Isolated from *Lagerstroemia speciosa* Leaves as α-Glucosidase Inhibitors. Zhongguo Zhong Yao Za Zhi 614–618.

Hsieh, Y.S., Chen, P.N., Yu, C.H., Chen, C.H., Tsai, T.T., Kuo, D.Y., 2015. Involvement of oxidative stress in the regulation of NPY/CART-mediated appetite control in amphetamine-treated rats. Neurotoxicology 48, 131–141.

Hsieh, Y.S., Yang, S.F., Kuo, D.Y., 2005. Amphetamine, an appetite suppressant, decreases neuropeptide Y immunoreactivity in rat hypothalamic paraventriculum. Regul. Pept. 127, 169–176.

Huang, W., Sherman, B.T., Lempicki, R.A., 2009a. Systematic and integrative analysis of large gene lists using DAVID bioinformatics resources. Nat. Protoc. 4, 44–57.

Huang, W., Sherman, B.T., Lempicki, R.A., 2009b. Bioinformatics enrichment tools: paths toward the comprehensive functional analysis of large gene lists. Nucleic Acids Res. 37, 1–13.

Huszar, D., Lynch, C.A., Fairchild-Huntress, V., Dunmore, J.H., Fang, Q., Berkemeier, L.R., Gu, W., Kesterson, R.A., Boston, B.A., Cone, R.D., Smith, F.J., Campfield, L.A., Burn, P., Lee, F., 1997. Targeted Disruption of the Melanocortin-4 Receptor Results in Obesity in Mice. Cell 88, 131–141.

Ibars, M., Ardid-Ruiz, A., Suárez, M., Muguerza, B., Bladé, C., Aragonès, G., 2016. Proanthocyanidins potentiate hypothalamic leptin/STAT3 signalling and Pomc gene expression in rats with diet-induced obesity signalling. Int. J. Obes. (Lond). 1–8.

Igoli, O.J., Gray, A.I., 2008. Friedelanone and other triterpenoids from *Hymenocardia acida*. Int. J. Phys. Sci. 3, 156–158.

Iqbal, J., Kurose, Y., Canny, B., Clarke, I.J., 2006. Effects of central infusion of ghrelin on food intake and plasma levels of growth hormone, luteinizing hormone, prolactin, and cortisol secretion in sheep. Endocrinology 147, 510–519.

Iwasa, T., Matsuzaki, T., Murakami, M., Kinouchi, R., Gereltsetseg, G., Nakazawa, H., Yamamoto, S., Kuwahara, A., Yasui, T., Irahara, M., 2011. Changes in responsiveness of appetite, leptin and hypothalamic IL-1β and TNF-Zα to lipopolysaccharide in developing rats. J. Neuroimmunol. 236, 10–16.

Jean, A., Conductier, G., Manrique, C., Bouras, C., Berta, P., Hen, R., Charnay, Y., Bockaert, J., Compan, V., 2007. Anorexia induced by activation of serotonin 5-HT4 receptors is mediated by increases in CART in the nucleus accumbens. Proc. Natl. Acad. Sci. U. S. A. 104, 16335–40.

Jin, L., Zhang, S., Burguera, B.G., Couce, M.E., Osamura, R.Y., Kulig, E., Lloyd, R. V, 1999. Leptin and Leptin Receptor Expression in Rat and Mouse Pituitary Cells *. Endocrinology 141, 333–339.

Jolly, R.A., Goldstein, K.M., Wei, T., Gao, H., Chen, P., Huang, S., Colet, J.-M., Ryan, T.P., Thomas, C.E., Estrem, S.T., 2005. Pooling samples within microarray studies: a comparative analysis of rat liver transcription response to prototypical toxicants. Physiol. Genomics 22, 346–55.

Kao, T.-C., Wu, C.-H., Yen, G.-C., 2013. Bioactivity and Potential Health Benefits of Licorice. J. Agric. Food Chem. 524–553.

Kao, Y.H., Hiipakka, R.A., Liao, S., 2000. Modulation of Endocrine Systems and Food Intake by Green Tea Epigallocatechin Gallate. Endocr. Rev. 141, 980–987.

Karihaloo, J.L., 2015. DNA Fingerprinting Techniques for Plant Identification, in: Plant Biology and Biotechnology: Volume II: Plant Genomics and Biotechnology. pp. 205–221.

Kenicer, G.J., Kajita, T., Pennington, R.T., Murata, J., 2005. Systematics and biogeography of *Lathyrus* (Leguminosae) based on internal transcribed spacer and cpDNA sequence data. Am. J. Bot. 92, 1199–1209.

Kennedy, G.C., 1950. The hypothalamic control of food intake in rats. Proc. R. Soc. London. Ser. B, Biol. Sci. 137, 535–49.

Khandare, A.L., Ankulu, M., Aparna, N., 2013. Role of glutamate and nitric oxide in onset of motor neuron degeneration in neurolathyrism. Neurotoxicology 34, 269–274.

Kim, H., Jin, B., Oh, M., Shin, K., Choi, S., Kim, D., 2016. The effect of metformin on neuronal activity in the appetite-regulating brain regions of mice fed a high-fat diet during an anorectic period. Physiol. Behav. 184–190.

Kim, Y.J., Choi, M.S., Park, Y.B., Kim, S.R., Lee, M.K., Jung, U.J., 2013. *Garcinia cambogia* attenuates diet-induced adiposity but exacerbates hepatic collagen accumulation and inflammation. World J. Gastroenterol. 19, 4689–4701.

Kingston, D.G.I., 2011. Modern Natural Products Drug Discovery and its Relevance to Biodiversity Conservation. J. Nat. Prod. 74, 496–511.

Kirchgessner, T.G., Uysal, K.T., Wiesbrock, S.M., Marino, M.W., Hotamisligil, G.S., 1997. Tumor necrosis factor-α contributes to obesity-related hyperleptinemia by regulating leptin release from adipocytes. J. Clin. Invest. 100, 2777–2782.

Kitagawa, I., Zhou, J.L., Sakagami, M., Uchida, E., Yoshikawa, M., 1991. Licorice-saponins F3,G2,H2,J2,and K2,five new oleanene-triterpene oligoglycosides from the root of *Glycyrrhiza uralensis*. Chem. Pharm. Bull. (Tokyo). 39, 244–246.

Klok, M.D., Jakobsdottir, S., Drent, M.L., 2007. The role of leptin and ghrelin in the regulation of food intake and body weight in humans: A review. Obes. Rev. 8, 21–34.

Koehn, F.E., Carter, G.T., 2005. The evolving role of natural products in drug discovery. Nat. Rev. Drug Discov. 4, 206–220.

Kohyama, T., Hasumi, K., Murakawa, S., Endo, A., 1994. Inhibition of 15-lipoxygenase by Orobol. J. Antibiot. (Tokyo). 47, 1069–1071.

Kokot, F., Ficek, R., 1999. Effects of Neuropeptide Y on Appetite. Miner. Electrolyte Metab. 25, 303–5.

Kola, B., Hubina, E., Tucci, S. a., Kirkham, T.C., Garcia, E. a., Mitchell, S.E., Williams, L.M.,

Hawley, S. a., Hardie, D.G., Grossman, A.B., Korbonits, M., 2005. Cannabinoids and ghrelin have both central and peripheral metabolic and cardiac effects via AMP-activated protein kinase. J. Biol. Chem. 280, 25196–25201.

Koren, S., Fantus, I.G., 2007. Inhibition of the protein tyrosine phosphatase PTP1B: potential therapy for obesity, insulin resistance and type-2 diabetes mellitus. Best Pract. Res. Clin. Endocrinol. Metab. 21, 621–640.

Kostic, A.D., Howitt, M.R., Garrett, W.S., 2013. Exploring host – microbiota interactions in animal models and humans. Genes Dev. 27, 701–718.

Kotler, D.P., Tierney, a. R., Kral, J.G., Bjorntorp, P., 1984. Modification of weight gain by an α-glucosidase inhibitor during refeeding in rats. Am. J. Clin. Nutr. 40, 270–276.

Kristensen, P., Judge, M.E., Thim, L., Ribel, U., Christjansen, K.N., Wulff, B.S., Clausen, J.T., Jensen, P.B., Madsen, O.D., Vrang, N., Larsen, P.J., Hastrup, S., 1998. Hypothalamic CART is a new anorectic peptide regulated by leptin. Nature 393, 72–76.

Krude, H., Biebermann, H., Luck, W., Horn, R., Brabant, G., Grüters, a, 1998. Severe early-onset obesity, adrenal insufficiency and red hair pigmentation caused by POMC mutations in humans. Nat. Genet. 19, 155–157.

Kubota, N., Yano, W., Kubota, T., Yamauchi, T., Itoh, S., Kumagai, H., Kozono, H., Takamoto, I., Okamoto, S., Shiuchi, T., Suzuki, R., Satoh, H., Tsuchida, A., Moroi, M., Sugi, K., Noda, T., Ebinuma, H., Ueta, Y., Kondo, T., Araki, E., Ezaki, O., Nagai, R., Tobe, K., Terauchi, Y., Ueki, K., Minokoshi, Y., Kadowaki, T., 2007. Adiponectin Stimulates AMP-Activated Protein Kinase in the Hypothalamus and Increases Food Intake. Cell Metab. 6, 55–68.

Kumar, S., Kumar, V., Prakash, O., 2013. Enzymes inhibition and antidiabetic effect of isolated constituents from *Dillenia indica*. Biomed Res. Int. 2013.

Kwon, Y.I., Apostolidis, E., Shetty, K., 2008. *In vitro* studies of eggplant (*Solanum melongena*) phenolics as inhibitors of key enzymes relevant for type 2 diabetes and hypertension. Bioresour. Technol. 99, 2981–2988.

Langmead, B., Trapnell, C., Pop, M., Salzberg, S., 2009. Ultrafast and memory-efficient alignment of short DNA sequences to the human genome. Genome Biol. 10, R25.

Lantz, K. a, Hart, S.G.E., Planey, S.L., Roitman, M.F., Ruiz-White, I. a, Wolfe, H.R., McLane, M.P., 2010. Inhibition of PTP1B by trodusquemine (MSI-1436) causes fat-specific weight loss in diet-induced obese mice. Obesity (Silver Spring). 18, 1516–1523.

Lau, J., Herzog, H., 2014. CART in the regulation of appetite and energy homeostasis. Front. Neurosci. 8.

Lecomte, V., Kaakoush, N.O., Maloney, C.A., Raipuria, M., Huinao, K.D., Mitchell, H.M., Morris, M.J., 2015. Changes in gut microbiota in rats fed a high fat diet correlate with obesity-associated metabolic parameters. PLoS One 10.

Levitzki, A., Gazit, A., 1995. Tyrosine Kinase Inhibition : An Approach to Drug Development. Science (80-.). 267, 1782–1788.

Liu, P., Cheng, H., Roberts, T.M., Zhao, J.J., 2009. Targeting the phosphoinositide 3-kinase (PI3K)

pathway in cancer. Nat. Rev. Drug. Discov. 8, 627–644.

LOEB Classical Library, n.d. Epitome of Book LXXVII, A.D.208 [WWW Document]. Dio Cassius, Rom. Hist.

Lopaschuk, G.D., Ussher, J.R., Jaswal, J.S., 2010. Targeting intermediary metabolism in the hypothalamus as a mechanism to regulate appetite. Pharmacol. Rev. 62, 237–264.

Lotia, S., Montojo, J., Dong, Y., Bader, G.D., Pico, A.R., 2013. Cytoscape app store. Bioinformatics 29, 1350–1351.

Luque de Castro, M.D., Priego-Capote, F., 2010. Soxhlet extraction: Past and present panacea. J. Chromatogr. A 1217, 2383–9.

MacLean, D.B., Luo, L.G., 2004. Increased ATP content/production in the hypothalamus may be a signal for energy-sensing of satiety: Studies of the anorectic mechanism of a plant steroidal glycoside. Brain Res. 1020, 1–11.

Magni, P., Motta, M., Martinì, L., 2000. Leptin: a possible link between food intake, energy expenditure, and reproductive function. Regul. Pept. 92, 51–56.

Maljaars, P.W.J., Keszthelyi, D., Masclee, A.A.M., 2010. An ileal brake-through? Am. J. Clin. Nutr. 92, 467–468.

Malveira Cavalcanti, J., Henrique Leal-Cardoso, J., Leite Diniz, L.R., Gomes Portella, V., Oliveira Costa, C., Barreto Medeiros Linard, C.F., Alves, K., De Paula Rocha, M.V.A., Calado Lima, C., Marilande Cecatto, V., Coelho-De-Souza, A.N., 2012. The essential oil of *Croton zehntneri* and trans-anethole improves cutaneous wound healing. J. Ethnopharmacol. 144, 240–247.

Marles and Farnsworth, 1995 - antidiabetic plants and their active constituents, n.d.

Marrero-Faz, E., Harvey, A.L., 2015. Inhibitory effect of Persea americana Mill leaf aqueous extract and its fractions on PTP1B as therapeutic target for type 2 diabetes .

Martínez-Sotres, C., López-Albarrán, P., Cruz-de-León, J., García-Moreno, T., Rutiaga-Quiñones, J.G., Vázquez-Marrufo, G., Tamariz-Mascarúa, J., Herrera-Bucio, R., 2012. Medicarpin, an antifungal compound identified in hexane extract of *Dalbergia congestiflora* Pittier heartwood. Int. Biodeterior. Biodegrad. 69, 38–40.

McIntyre, L.M., Lopiano, K.K., Morse, A.M., Amin, V., Oberg, A.L., Young, L.J., Nuzhdin, S. V, 2011. RNA-seq: technical variability and sampling. BMC Genomics 12, 293.

Melorose, J., Perroy, R., Careas, S., 2015. World population prospects. United Nations 1, 587–92.

Meng, Y., Guan, Y., Zhang, W., Wu, Y., Jia, H., Zhang, Y., Zhang, X., Du, H., Wang, X., 2016. RNA-seq analysis of the hypothalamic transcriptome reveals the networks regulating physiopathological progress in the diabetic GK rat. Nat. Sci. Reports 6, 34138.

Mhalhal, T.R., Washington, M.C., Newman, K., Heath, J.C., Sayegh, A.I., 2016. Infusion of exogenous cholecystokinin-8, gastrin releasing peptide-29 and their combination reduce body weight in diet-induced obese male rats. Appetite 109, 172–181.

Minor, R.K., Chang, J.W., Cabo, R. De, 2009. Hungry for Life: How the arcuate nucleus and neuropeptide Y may play a critical role in mediating the benefits of calorie restriction. Mol. Cell 299, 79–88.

Mogale, M.A., Lebelo, S.L., Thovhogi, N., Freitas, A.N., Shai, L.J., 2011. α-Amylase and α-glucosidase inhibitory effects of *Sclerocarya birrea* [(A. Rich.) Hochst.] subspecies *caffra* (Sond) Kokwaro (Anacardiaceae) stem-bark extracts. African J. Biotechnol. 10, 15033–15039.

Moghaddam, M.G., Bin H. Ahmad, F., Samzadeh-Kermani, A., 2012. Biological Activity of Betulinic Acid: A Review. Pharmacol. Pharm. 3, 119–123.

Moran, O., Phillip, M., 2003. Leptin: obesity, diabetes and other peripheral effects - a review. Pediatr. Diabetes 4, 101–109.

Morrison, C.D., 2009. Leptin signaling in brain: A link between nutrition and cognition? Biochim. Biophys. Acta - Mol. Basis Dis. 1792, 401–408.

Mullan, B.P., Pluske, J.R., Trezona, M., Harris, D.J., Allen, J.G., Siddique, K.H.M., Hanbury, C.D., van Barneveld, R.J., Kim, J.C., 2009. Chemical composition and standardised ileal digestible amino acid contents of *Lathyrus (Lathyrus cicera)* as an ingredient in pig diets. Anim. Feed Sci. Technol. 150, 139–143.

Naef, L., Woodside, B., 2007. Prolactin/leptin interactions in the control of food intake in rats. Endocrinology 148, 5977–5983.

Nass, R.M., Gaylinn, B.D., Rogol, A.D., Thorner, M.O., 2010. Ghrelin and growth hormone: story in reverse. PNAS 107, 8501–8502.

National Biodiverstiy Network 2013b. *Lathyrus linifolius* (Reichard) Vassler [Bitter-vetch] [WWW Document], n.d. URL https://data.nbn.org.uk/Taxa/NHMSYS0000460181 (accessed 4.22.15).

NBN Gateway - Taxon - Lathyrus linifolius (Reichard) Bässler [Bitter-vetch] [WWW Document], n.d. URL https://data.nbn.org.uk/Taxa/NHMSYS0000460181 (accessed 4.22.15).

Neary, N.M., Goldstone, A.P., Bloom, S.R., 2004. Appetite regulation: From the gut to the hypothalamus. Clin. Endocrinol. (Oxf). 60, 153–160.

Newman, D.J., Cragg, G.M., 2016. Natural Products as Sources of New Drugs from 1981 to 2014. J. Nat. Prod. 79, 629–661.

Ng, W.L., Tan, S.G., 1994. Inter-Simple Sequence Repeat (ISSR) Markers: Are We Doing It Right ? ASM Sci. 9, 30–39.

Ohia, S.E., Opere, C. a., LeDay, A.M., Bagchi, M., Bagchi, D., Stohs, S.J., 2002. Safety and mechanism of appetite suppression by a novel hydroxycitric acid extract (HCA-SX). Mol. Cell. Biochem. 238, 89–103.

Omar, H.R., Komarova, I., El-Ghonemi, M., Fathy, A., Rashad, R., Abdelmalak, H.D., Yerramadha, M.R., Ali, Y., Helal, E., Camporesi, E.M., 2012. Licorice abuse: time to send a warning message. Ther. Adv. Endocrinol. Metab. 3, 125–38.

Ozek, C., Zimmer, D.J., De Jonghe, B.C., Kalb, R.G., Bence, K.K., 2015. Ablation of intact hypothalamic and/or hindbrain TrkB signaling leads to perturbations in energy balance. Mol. Metab. 4, 867–880.

Park, H.K., Ahima, R.S., 2014. Physiology of leptin: energy homeostasis, neuroendocrine function and metabolism. Metabolism. 64, 24–34.

Pastor-Cavada, E., Juan, R., Pastor, J.E., Alaiz, M., Vioque, J., 2010. Protein isolates from two

Mediterranean legumes: *Lathyrus clymenum* and *Lathyrus annuus*. Chemical composition, functional properties and protein characterisation. Food Chem. 122, 533–538.

Patwardhan, B., Mashelkar, R.A., 2009. Traditional medicine-inspired approaches to drug discovery: can Ayurveda show the way forward? Drug Discov. Today 14, 804–811.

Pavel, A.B., Vasile, C.I., 2012. PyElph - a software tool for gel images analysis and phylogenetics. BMC Bioinformatics 13, 9.

Pecket, R.C., 1959. The nature of the variation in flower colour in the genus *Lathyrus*. New Phytol. 59, 138–145.

Pelleymounter, M.A., Cullen, M.J., Baker, M.B., Hecht, R., Winters, D., Boone, T., Collins, F., 1995. Effects of the obese gene product on body weight regulation in ob/ob mice. Sci. Transl. Med. 269, 540–543.

Peng, X., Wood, C.L., Blalock, E.M., Chen, K.C., Landfield, P.W., Stromberg, A.J., 2003. Statistical implications of pooling RNA samples for microarray experiments. BMC Bioinformatics 4, 1–9.

Pérez, A.J., Kowalczyk, M., Simonet, A.M., Macías, F.A., Oleszek, W., Stochmal, A., 2013. Isolation and structural determination of triterpenoid glycosides from the aerial parts of alsike clover (*Trifolium hybridum* L.). J. Agric. Food Chem. 61, 2631–2637.

Perry, B., Wang, Y., 2012. Appetite regulation and weight control: the role of gut hormones. Nutr. Diabetes 2, e26.

Porter, A.E. a, Wynne Griffiths, D., Robertson, G.W., Sexton, R., 1999. Floral volatiles of the sweet pea *Lathyrus odoratus*. Phytochemistry 51, 211–214.

Poyraz, I., 2016. Comparison of ITS, RAPD and ISSR from DNA-based genetic diversity techniques. Comptes Rendus - Biol. 339, 171–178.

Queipo-Ortuño, M.I., Seoane, L.M., Murri, M., Pardo, M., Gomez-Zumaquero, J.M., Cardona, F., Casanueva, F., Tinahones, F.J., 2013. Gut Microbiota Composition in Male Rat Models under Different Nutritional Status and Physical Activity and Its Association with Serum Leptin and Ghrelin Levels. PLoS One 8.

Quennell, J.H., Howell, C.S., Roa, J., Augustine, R.A., Grattan, D.R., Anderson, G.M., 2011. Leptin deficiency and diet-induced obesity reduce hypothalamic kisspeptin expression in mice. Endocrinology 152, 1541–1550.

Ren, J., Zhang, Y., Jin, H., Yu, J., Zhou, Y., Wu, F., Zhang, W., 2014. Novel Inhibitors of Human DOPA Decarboxylase Extracted from *Euonymus glabra Rox*b.

Resnyk, C.W., Chen, C., Huang, H., Wu, C.H., Simon, J., Le Bihan-Duval, E., Duclos, M.J., Cogburn, L.A., 2015. RNA-seq analysis of abdominal fat in genetically fat and lean chickens highlights a divergence in expression of genes controlling adiposity, hemostasis, and lipid metabolism. PLoS One 10, 1–41.

Robeson, J., Harborne, J.B., 1980. A chemical dichotomy in phytoalexin induction within the tribe *Vicieae* of the Leguminosae. Phytochemistry 19, 2359–2365.

Rogge, G., Jones, D., Hubert, G.W., Lin, Y., Kuhar, M.J., 2008. CART peptides: regulators of body weight, reward and other functions. Nat. Rev. Neurosci. 9, 747–58.

Romanatto, T., Cesquini, M., Amaral, M.E., Roman, É. a., Moraes, J.C., Torsoni, M. a., Cruz-Neto, A.P., Velloso, L. a., 2007. TNF-α acts in the hypothalamus inhibiting food intake and increasing the respiratory quotient-Effects on leptin and insulin signaling pathways. Peptides 28, 1050–1058.

Rompelberg, C.J.M., Verhagen, H., van Bladeren, P.J., 1993. Effects of the naturally occurring alkenylbenzenes eugenol and trans-anethole on drug-metabolizing enzymes in the rat liver. Food Chem. Toxicol. 31, 637–645.

Sadot, E., 2014. Plant Comounds Acting on the Cytoskeleton. Appl. Plant Cell Biol., Plant Cell Monographs 22, 301–323.

Saito, M., Ueno, M., Ogino, S., Kubo, K., Nagata, J., Takeuchi, M., 2005. High dose of *Garcinia cambogi*a is effective in suppressing fat accumulation in developing male Zucker obese rats, but highly toxic to the testis. Food Chem. Toxicol. 43, 411–419.

Saleem, S., Jafri, L., Haq, I.U., Chang, L.C., Calderwood, D., Green, B.D., Mirza, B., 2014. Plants Fagonia cretica L. and Hedera nepalensis K. Koch contain natural compounds with potent dipeptidyl peptidase-4 (DPP-4) inhibitory activity. J. Ethnopharmacol. 156, 26–32.

Salinero, C., Feás, X., Mansilla, J.P., Seijas, J.A., Vázquez-Tato, M.P., Vela, P., Sainz, M.J., 2012. 1H-nuclear magnetic resonance analysis of the triacylglyceride composition of cold-pressed oil from *Camellia japonica*. Molecules 17, 6716–6727.

Sam Sik, K., Byung Tae, A., Ju Su, K., Bae, K., 1998. Lathyrus saponin, a new trisaccharide glycoside from *Lathyrus japonicu*s. J. Nat. Prod. 61, 299–300.

Sangster, S.A., Caldwell, J., Smith, R.L., Farmer, P.B., 1984. Metabolism of anethole. I. Pathways of metabolism in the rat and mouse. Food Chem. Toxicol. 22, 695–706.

Saravanan, G., Ponmurugan, P., Deepa, M.A., Senthilkumar, B., 2014. Anti-obesity action of gingerol: Effect on lipid profile, insulin, leptin, amylase and lipase in male obese rats induced by a high-fat diet. J. Sci. Food Agric. 94, 2972–2977.

Schaefer, H., Hechenleitner, P., Santos-Guerra, A., Menezes de Sequeira, M., Pennington, R.T., Kenicer, G., Carine, M. a, 2012. Systematics, biogeography, and character evolution of the legume tribe Fabeae with special focus on the middle-Atlantic island lineages. BMC Evol. Biol. 12, 250.

Scharp, S., Meester, I. De, Vanhoof, G., Hendriks, D., Sande, M. Van, Camp, K. Van, Yaron, A., 1988. Assay of Dipeptidyl Peptidase IV in Serum by Fluorometryof 4-Methoxy-2-naphthylamine. Clin. Chem. 34, 2299–2301.

Schwartz, M.W., Woods, S.C., Porte, D., Seeley, R.J., Baskin, D.G., 2000. Central nervous system control of food intake. Nature 404, 661–671.

Seminara, S.B., Messager, S., Chatzidaki, E.E., Thresher, R.R., Acierno Jr., J.S., Shagoury, J.K., Bo-Abbas, Y., Kuohung, W., Schwinof, K.M., Hendrick, A.G., Zahn, D., Dixon, J., Kaiser, U.B., Slaugenhaupt, S.A., Gusella, J.F., O'Rahilly, S., Carlton, M.B.L., Crowley Jr., W.F., Aparicio, S.A.J.R., Colledge, W.H., 2003. The GPR54Gene as a Regulator of Puberty. N. Engl. J. Med. 349, 1614–1627.

Senaris, R., Garcia-Caballero, T., Casabiell, X., Gallego, R., Castro, R., Considine, R. V, Dieguez, C., Casanueva, F.F., 1997. Synthesis Of Leptin In Human Placenta. Endocrinology 138, 5079–5082.

Senatore, F., Oliviero, F., Scandolera, E., Taglialatela-Scafati, O., Roscigno, G., Zaccardelli, M., De Falco, E., 2013. Chemical composition, antimicrobial and antioxidant activities of anethole-rich oil from leaves of selected varieties of fennel [*Foeniculum vulgare Mill. ssp. vulgare var. azoricum (Mill.) Thell*]. Fitoterapia 90, 214–219.

Sethi, J.K., Hotamisligil, G.S., 1999. The role of TNF alpha in adipocyte metabolism. Semin. Cell Dev. Biol. 10, 19–29.

Shahidi, F., Chavan, U.., Bal, a. ., McKenzie, D.., 1999. Chemical composition of beach pea (Lathyrus maritimus L.) plant parts. Food Chem. 64, 39–44.

Shahidi, F., Chavan, U.D., Naczk, M., Amarowicz, R., 2001. Nutrient distribution and phenolic antioxidants in air-classified fractions of beach pea (*Lathyrus maritimus* L.). J. Agric. Food Chem. 49, 926–933.

Shannon, P., Markiel, A., Ozier, O., Baliga, N.S., Wang, J.T., Ramage, D., Amin, N., Schwikowski, B., Ideker, T., 2005. Cytoscape: a software environment for integrated models of biomolecular interaction networks. Genome Res. 2498–2504.

Sheikh, B.A., Pari, L., Rathinam, A., Chandramohan, R., 2015. Trans-anethole, a terpenoid ameliorates hyperglycemia by regulating key enzymes of carbohydrate metabolism in streptozotocin induced diabetic rats. Biochimie 112, 57–65.

Shin, H.-S., Kindleysides, S., Yip, W., Budgett, S.C., Ingram, J.R., Poppitt, S.D., 2015. Postprandial effects of a polyphenolic grape extract (PGE) supplement on appetite and food intake: a randomised dose-comparison trial. Nutr. J. 14, 96.

Shin, H.S., Ingram, J.R., McGill, A.T., Poppitt, S.D., 2013. Lipids, CHOs, proteins: Can all macronutrients put a “brake” on eating? Physiol. Behav. 120, 114–123.

Siegrist-Kaiser, C. a, Pauli, V., Juge-Aubry, C.E., Boss, O., Pernin, a, Chin, W.W., Cusin, I., Rohner-Jeanrenaud, F., Burger, a G., Zapf, J., Meier, C. a, 1997. Direct effects of leptin on brown and white adipose tissue. J. Clin. Invest. 100, 2858–2864.

Singh, S., Rao, S., 2013. Lessons from neurolathyrism: A disease of the past & the future of *Lathyrus sativus (Khesari dal)*. Indian J. Med. Res. 138, 32–37.

Sneader, W., 2005. Drug Discovery: A History, John Wiley & Sons Ltd.

Sneddon, A. a, Tsofliou, F., Fyfe, C.L., Matheson, I., Jackson, D.M., Horgan, G., Winzell, M.S., Wahle, K.W.J., Ahren, B., Williams, L.M., 2008. Effect of a conjugated linoleic acid and omega-3 fatty acid mixture on body composition and adiponectin. Obesity (Silver Spring). 16, 1019–1024.

Sohn, J.W., 2015. Network of hypothalamic neurons that control appetite. BMB Rep. 48, 229–233.

Sominsky, L., Spencer, S.J., 2014. Eating behavior and stress: A pathway to obesity. Front. Psychol. 5, 1–8.

Sone, H., Kamiyama, S., Higuchi, M., Fujino, K., Kubo, S., Miyazawa, M., Shirato, S., Hiroi, Y.,

Shiozawa, K., 2016. Biotin augments acetyl CoA carboxylase 2 gene expression in the hypothalamus, leading to the suppression of food intake in mice. Biochem. Biophys. Res. Commun. 476, 134–139.

Sonita, B., Mooney, J., Gaudet, L., Touyz, R.M., 2008. Pseudohyperaldosteronism, Liquorice, and Hypertension. J. Clin. Hypertens. 10, 153–157.

Sousa-Cavada, B., Richardson, M., Yarwood, A., Pere, D., Rouge, P., 1986. The amino acid sequences of the alpha subunits of the lectins from *Lathyrus cicera, L. aphaca* and *L articulatus*. Phytochemistry 25, 115–118.

Southon, I.W., 1994. Phytochemical Dictionary of the Leguminosae.

Spiller, R.C., Trotman, I.F., Higgins, B.E., Ghatei, M. a, Grimble, G.K., Lee, Y.C., Bloom, S.R., Misiewicz, J.J., Silk, D.B., 1984. The ileal brake--inhibition of jejunal motility after ileal fat perfusion in man. Gut 25, 365–374.

Stanley, B.G., Leibowitz, S.F., 1984. Neuropeptide Y: Stimulation of feeding and drinking by injection into the paraventricular nucleus. Life Sci. 26, 2635–42.

Stark, R., Ashley, S.E., Andrews, Z.B., 2013. AMPK and the neuroendocrine regulation of appetite and energy expenditure. Mol. Cell. Endocrinol. 366, 215–223.

Stengel, A., Goebel-Stengel, M., Teuffel, P., Hofmann, T., Bußе, P., Kobelt, P., Rose, M., Klapp, B.F., 2014. Obese patients have higher circulating protein levels of dipeptidyl peptidase IV. Peptides 61, 75–82.

Tak, P.P., Firestein, G.S., Tak, P.P., Firestein, G.S., 2001. NF-kappaB: a key role in inflammatory diseases. J. Clin. Invest. 107, 7–11.

Tang-christensen, M., Jessop, D.S., Larsen, J., Jessop, S., 1996. Central administration food and water intake of GLP-1- (7-36) in rats amide inhibits. Am. J. Physiol. 271, R848–R856.

Tolson, K.P., Garcia, C., Yen, S., Simonds, S., Stefanidis, A., Lawrence, A., Smith, J.T., Kauffman, A.S., 2014. Impaired kisspeptin signaling decreases metabolism and promotes glucose intolerance and obesity. J. Clin. Invest. 124, 3075–3079.

Toriya, M., Maekawa, F., Maejima, Y., Onaka, T., Fujiwara, K., Nakagawa, T., Nakata, M., Yada, T., 2010. Long-term infusion of brain-derived neurotrophic factor reduces food intake and body weight via a corticotrophin-releasing hormone pathway in the paraventricular nucleus of the hypothalamus. J. Neuroendocrinol. 22, 987–995.

Tornatore, L., Thotakura, A.K., Bennett, J., Moretti, M., Franzoso, G., 2012. The nuclear factor kappa B signaling pathway: Integrating metabolism with inflammation. Trends Cell Biol. 22, 557–566.

Tropicos.org. Missouri Botanical Garden. [WWW Document], n.d. URL http://www.tropicos.org/Name/13044751 (accessed 4.22.15).

Truhaut, R., Le Bourhis, B., Attia, M., Glomot, R., Newman, J., Caldwell, J., 1989. Chronic toxicity/carcinogenicity study of trans-anethole in rats. Food Chem. Toxicol. 27, 11–20.

Tucci, S.A., 2010. Phytochemicals in the control of human appetite and body weight. Pharmaceuticals 3, 748–763.

Uddin, G., Waliullah, Siddiqui, B.S., Alam, M., Sadat, A., Ahmad, A., Uddin, A., 2011. Chemical

Constituents and Phytotoxicity of Solvent Extracted Fractions of Stem Bark of *Grewia optiva* Drummond ex Burret. Middle-East J. Sci. Res. 8, 85–91.

Urabe, H., Kojima, H., Chan, L., Terashima, T., Ogawa, N., Katagi, M., Fukino, K., Kumagai, A., Kawai, H., Asakawa, A., Inui, A., Yasuda, H., Eguchi, Y., Oka, K., Maegawa, H., Kashiwagi, A., Hiroshi, K., 2013. Haematopoietic cells produce BDNF and regulate appetite upon migration to the hypothalamus. Nat. Commun. 4.

Uribe, J.A.R., Perez, J.I.N., Kauil, H.C., Rubio, G.R., Alcocer, C.G., 2011. Extraction of oil from chia seeds with supercritical carbon dioxide. J. Supercrit. Fluids 56, 174–178.

Van Heerden, F., Vleggaar, R., Horak, R.M., Learmonth, R.A., Maharaj, V., Whittal, R.D., 2002. Pharmaceutical compositions having appetite suppressant activity.

van Heerden, F.R., Marthinus Horak, R., Maharaj, V.J., Vleggaar, R., Senabe, J. V., Gunning, P.J., 2007. An appetite suppressant from *Hoodia* species. Phytochemistry 68, 2545–2553.

Verhoeckx, K.C.M., Bijlsma, S., De Groene, E.M., Witkamp, R.F., Van Der Greef, J., Rodenburg, R.J.T., 2004. A combination of proteomics, principal component analysis and transcriptomics is a powerful tool for the identification of biomarkers for macrophage maturation in the U937 cell line. Proteomics 4, 1014–1028.

Vermaak, I., Viljoen, a. M., Chen, W., Hamman, J.H., 2011. In vitro transport of the steroidal glycoside P57 from Hoodia gordonii across excised porcine intestinal and buccal tissue. Phytomedicine 18, 783–787.

Vieira, M.N.N., Lyra e Silva, N.M., Ferreira, S.T., De Felice, F.G., 2017. Protein Tyrosine Phosphatase 1B (PTP1B): A Potential Target for Alzheimer's Therapy? Front. Aging Neurosci. 9, 1–9.

Vlahov, G., 1999. Application of NMR to the study of olive oils. Prog. Nucl. Magn. Reson. Spectrosc. 35, 341–357.

Wahle, K.W.J., Caruso, D., Ochoa, J.J., Quiles, J.L., 2004. Olive oil and modulation of cell signaling in disease prevention. Lipids 39, 1223–1231.

Wahle, K.W.J., Rotondo, D., Heys, S.D., 2003. Polyunsaturated fatty acids and gene expression in mammalian systems. Proc. Nutr. Soc. 349–360.

Walewski, J.L., Ge, F., Lobdell IV, H., Levin, N., Schwartz, G.J., Vasselli, J.R., Pomp, A., Dakin, G., Berk, P.D., 2014. Spexin is a novel human peptide that reduces adipocyte uptake of long chain fatty acids and causes weight loss in rodents with diet-induced obesity. Obesity 22, 1643–1652.

Wang, D., He, X., Zhao, Z., Feng, Q., Lin, R., Sun, Y., Ding, T., Xu, F., Luo, M., Zhan, C., 2015. Whole-brain mapping of the direct inputs and axonal projections of POMC and AgRP neurons. Front. Neuroanat. 9, 40.

Wang, L., Saint-Pierre, D.H., Tache, Y., 2002. Peripheral ghrelin selectively increases Fos expression in neuropeptide Y - synthesizing neurons in mouse hypothalamic arcuate nucleus. Neurosci. Lett. 325, 47–51.

Wiirzler, L.A.M., de Souza Silva-Comar, F.M., Silva-Filho, S.E., de Oliveira, M.J.A., Bersani-Amado, C.A., Cuman, R.K.N., 2015. Evaluation of immunomodulatory activity of transanethole

and estragole, and protective effect against cyclophosphamide-induced suppression of immunity in Swiss albino mice. Int. J. Appl. Res. Nat. Prod. 8, 26–33.

Williams, D., Fleming, I., 2007. Spectroscopic Methods in Organic Chemistry.

Withering, W., 1785. An account on the foxglove, and some of its medical uses with practical remark on dropsy and other diseases. G. G. J. J. Robinson, London.

Wold, B., Myers, R.M., 2007. Sequence census methods for functional genomics. Nat. Methods 5, 19–21.

Wolf, J.B.W., 2013. Principles of transcriptome analysis and gene expression quantification: An RNA-seq tutorial. Mol. Ecol. Resour. 13, 559–572.

Woods, S.C., D'Alessio, D. a, 2008. Central control of body weight and appetite. J. Clin. Endocrinol. Metab. 93, S37–S50.

Wortley, K.E., Anderson, K.D., Garcia, K., Murray, J.D., Malinova, L., Liu, R., Moncrieffe, M., Thabet, K., Cox, H.J., Yancopoulos, G.D., Wiegand, S.J., Sleeman, M.W., 2004. Genetic deletion of ghrelin does not decrease food intake but influences metabolic fuel preference. Proc. Natl. Acad. Sci. U. S. A. 101, 8227–32.

Wynne, K., Stanley, S., McGowan, B., Bloom, S.R., 2005. Appetite control. J. Endocrinol. 184, 291–318.

Xie, F., Xiao, P., Chen, D., Xu, L., Zhang, B., 2012. miRDeepFinder: A miRNA analysis tool for deep sequencing of plant small RNAs. Plant Mol. Biol. 80, 75–84.

Yamauchi, T., Kadowaki, T., 2008. Physiological and pathophysiological roles of adiponectin and adiponectin receptors in the integrated regulation of metabolic and cardiovascular diseases. Int. J. Obes. (Lond). 32 Suppl 7, S13–S18.

Yan, Z.Y., Spencer, P.S., Li, Z.X., Liang, Y.M., Wang, Y.F., Wang, C.Y., Li, F.M., 2006. *Lathyrus sativus* (grass pea) and its neurotoxin ODAP. Phytochemistry 67, 107–121.

Ye, J., Coulouris, G., Zaretskaya, I., Cutcutache, I., Rozen, S., Madden, T.L., 2012. Primer-BLAST: A tool to design target-specific primers for polymerase chain reaction. BMC Bioinformatics 13, 134.

Yeo, G.S.H., Heisler, L.K., 2012. Unraveling the brain regulation of appetite: lessons from genetics. Nat. Neurosci. 15, 1343–1349.

Yilmazer-Musa, M., Griffith, A.M., Michels, A.J., Schneider, E., Frei, B., 2012. Grape seed and tea extracts and catechin 3-gallates are potent inhibitors of α-amylase and α-glucosidase activity. J. Agric. Food Chem. 60, 8924–8929.

Yoshikawa, M., Morikawa, T., Nakano, K., Pongpiriyadacha, Y., Murakami, T., Matsuda, H., 2002. Characterization of new sweet triterpene saponins from *Albizia myriophylla. J*. Nat. Prod. 65, 1638–1642.

Yu, J.H., Kim, M.S., 2012. Molecular mechanisms of appetite regulation. Diabetes Metab. J. 36, 391–398.

Yuliana, N.D., Jahangir, M., Korthout, H., Choi, Y.H., Kim, H.K., Verpoorte, R., 2011. Comprehensive review on herbal medicine for energy intake suppression. Obes. Rev. 12, 499–

514.

Yulyaningsih, E., Zhang, L., Herzog, H., Sainsbury, A., 2011. NPY receptors as potential targets for anti-obesity drug development. Br. J. Pharmacol. 163, 1170–1202.

Zhang, B., Deng, Z., Ramdath, D.D., Tang, Y., Chen, P.X., Liu, R., Liu, Q., Tsao, R., 2015. Phenolic profiles of 20 Canadian lentil cultivars and their contribution to antioxidant activity and inhibitory effects on α-glucosidase and pancreatic lipase. Food Chem. 172, 862–872.

Zhang, W., Hong, D., Zhou, Y., Zhang, Y., Shen, Q., Li, J.-Y., Hu, L.-H., Li, J., 2006. Ursolic acid and its derivative inhibit protein tyrosine phosphatase 1B, enhancing insulin receptor phosphorylation and stimulating glucose uptake. Biochim. Biophys. Acta 1760, 1505–1512.

Zhang, X., Zhao, Y., Xu, J., Xue, Z., Zhang, M., Pang, X., Zhang, X., Zhao, L., 2015. Modulation of gut microbiota by berberine and metformin during the treatment of high-fat diet-induced obesity in rats. Sci. Rep. 5, 14405.

Zhang, Y., Proenca, R., Maffei, M., Barone, M., Leopold, L., Friedman M., J., 1994. Positional cloning of the mouse obese gene and its human homologue. Nature 372, 425–432.

Zhao, T., Liang, G., Lin, R., Xie, X., Sleeman, M.W., Murphy, A.J., Valenzuela, D.M., Yancopoulos, G.D., Goldstein, J.L., Brown, M.S., 2010. Ghrelin O-acyltransferase (GOAT) is essential for growth hormone-mediated survival of calorie- restricted mice. PNAS 107, 7467–7472.

Zhong, L., Furne, J.K., Levitt, M.D., 2006. An extract of black, green, and mulberry teas causes malabsorption of carbohydrate but not of triacylglycerol in healthy volunteers. Am. J. Clin. Nutr. 84, 551–555.

Zhou, J., Xie, G., Yan, X., 2011. Encyclopedia of Traditional Chinese Medicines: Molecular Structures, Pharamcological Activities, Natural Sources and Applications, Volume 4.

Zietkiewicz, E., Rafalski, A., Labuda, D., 1994. Genome fingerprinting by simple sequence repeat (SSR)-anchored polymerase chain reaction amplification. Genomics 20, 176–183.

Zigman, J.M., Bouret, S.G., Andrews, Z.B., 2016. Obesity Impairs the Action of the Neuroendocrine Ghrelin System. Trends Endocrinol. Metab. 27, 54–63.

APPENDIX 1, Interview with Dr Brian Moffat regarding *Lathyrus Linifolius* tubers

Date of Interview:	07 March 2016
Present:	Nicola Woods (N), Ann Mitchell (A), Brian Moffat (B)
Location:	Edinburgh Central Library

Quotations from interview transcript published with permission from Dr. Brian Moffat.

- [Preparation of LL tuber]

"…it is only processed through drying, and this is what you have to call air drying. More or less the root mass is slung over rafters inside peasant's hobbles and left until it is needed. No period is recommended, I assume no period is required, just come and use it as you need it. The second thing is, it tends to be dug up when it is needed, in season – in other words in winter time, which obliges a very strange way of doing it nowadays as that's the last time you dig up tiny little roots under ice and snow. But it appears to be required. The third thing is dosage – there is no measure of the size or weight of the roots offered at all, but what crops up persistently in probably a dozen of these informants is the tubers are of a similar mass to a hazelnut and that is what is taken. There is no mention of multiples of hazelnuts, a number of them and there is no mention of fractions of hazelnuts. So they are more or less taking what nature provides – a hazelnut sized tuber. Now that must mean the dosage is very variable."

- [History of LL tuber]

"…no one has ever identified this plant at an archaeological site apart from, only one exception, Stonehenge. Which is quite an exception. There is a subdivision Stonehenge – Robin Hoods Ball – now I don't know what that means but the tubers have been identified there, whole. Now I am sure you will appreciate the Stonehenge is traditionally associated with seasonal banqueting - that doesn't fit – you don't have this thing at a banquet. That's the only record of the tubers and you'll appreciate if you

encounter something tiny like that you are not going to build up a sense of its importance in the economy/ecology provision of the plant to the society."

"That's the overview of the largest root mass we have encountered and got out. The calculations sas to how long that would allow 100 people to survive is months – now that is quite an interesting calculation – based entirely on Sibbald. Now he might be right or he might be wrong. It's my viewing Sibbald and both he and I have a rather optimistic outlook of the properties of this plant."

"Now I should mention Sibbald – you have seen that publication haven't you – [To a Marvellous Plant article written by Brian]. You will appreciate there is a letter incorporated in that dated 1685 – now, intriguingly it's with the collection of Sibbalds letters in the National Library. There aren't any publications centred on him - perhaps due to Sibbald writing in 6 different languages."

"So the encyclopaedia, Scotia Illustrata, 1684 has 7 distinct references allocated to the plant… essentially he is saying it is the food of the ancient Britain's upon the arrival of the romans – and it allows them to do extra ordinary things. Now the really weird thing about this is that this is being picked and incorporated in the carton books – Asterix Gaul. He is a superhero in the face of the roman invasion of Gaul who has a large colleague – it has been made into a feature film – with Gerard Edpatuer as his psychic Obulus who is a large bulky man. They have a medicine man in the village Gaul called Getafix. He issues a potion which bestows superhuman powers – the point is in the contemporary histories of the roman invasion of Britain and account which says that there is a plant, of which they use a small nut sized volume."

"Well, there is a contemporary account of the invasion of Britain by a Roman Historian called Deo cassius and he maintains that the people of Britain have been able to resist the invasion of the roman army by eating nut sized roots and this allows them to be extraordinarily strong, to live without food and drink – the only drawback to this is Deo cassius doesn't name the plant – so it's been overlooked. Sibbald says this is the plant that Deo Cassiss meant."

"This is one of the latest sources – Colin MacDonald – who passed away quite recently – this is a book that nobody would look at for purposes of a traditional plant and the science in it but this man is extremely competent observer who wrote a memoir of his childhood – now these can be good, or they can be bad, they can be detailed or not, but there is the account. I checked with his daughter who lived in his old house. [Section from Colin MacDonald book] *"I wonder if the boys at my old school … know what carochans are – they are little lumps or nodules that grow on the roots of certain purple flowered vetch, when we came on a bed of them we carefully pulled away the grass then with our knives, dig down into the earth until we got the much prized carochan – it's believed to have the special virtue imparting strength and what boy does now want to be strong."* The interesting thing is caroachns have a Gaelic equivalent – cracchan – now it's impossible for me to be confused by that – it's just local variant. Nobody looks at memoirs of childhood growing up in a certain remote place – his daughter tells me which crossroads he went through his way to school – the plant is still there."

"…the other key one we follow is Special Operations Executive. It's the organisation which coordinate commandos – and commando training, in Scotland, centred on three castles in the far North West. And they were given courses on living off the land – they were told about Heath Pea. It's in the course records. The main historian of the Special Operation commandos in general, is a curator at Edinburgh castle and in a book of his – called the Last Commandos – actually reviewed that they went on a course to Achnacarry which I have visited – which is absolutely surrounded by heath pea. They were quite simply told to dig in fox holes, make holes for themselves and live off what they could make and they weren't allowed to light fires. And not surprisingly when the special op executives, particularly the officers, die, you get a review of what they did in their lives and almost certainly a memoir so we are using obituaries as a way in to who might give an account of the use of the plant. There all taught in the vicinity of Achnacarry Castle and all they can be shown is what grows around the castle so no matter where they parachute in they will be looking for the plant which they know about and which is found useful – and those tubers are on the record."

"It took me a long time to identify the tubers from scratch – there are no botanists who take an interest in tiny tubers. The list of useful plants from the past is usually considered in modern terms, the range of cereals, the range of pulses, but none of those are part of the growing plant. It took us 25 years to get our tubers identified. Because no one, the experts, more or less said they have no interest to us, there is no evidence they have ever been used – now if they said that to me now I would whip out that as being evidence (large file of documents on LL)."

"Sibbald calls this plant 'Herba Scotia Miraculosa' in his letters"

- [Possible active compounds]

"As far as I know, [one of the active components is] *trans*-anethole – one of our large files centred on a comprehensive review of the Journal of Phytochemistry, it was the only journal then, and we got in touch in the team who seem to be central in research into this plant and related plants – Prof. Jeffery Barry Harbourne, University of Reading."

"…his research interests were iso-flavonoids. I discussed a bit with him about what was distinctive about the chemical profile of this plant – and you will appreciate there is not much work being done on it, and a string of rather anonymous, nondescript chemicals have surfaced particularly from the flowers. Orobol is the distinctive chemical which lead me to prick up my interest. And you will appreciate Orobus is the traditional name in the scientific way – so turning on its head it's the chemical first identified in our plant."

- [Identifying the tubers]

"The key thing for me is no tendrils, but with tubers – there are perhaps 30 native or introduced vetches in British Isles, only 3 or 4 have tubers. Absence of tendrils is the pointer. The key one to me is a rarity – not in this part of Scotland – its botanical name is *Vicia Orobus* – that is a thumping great clue, and it does look superficially similar but the flower colours is quite different and it bears tubers – but you might have a

problem gathering it, wherever it grows where I have encountered it, it's an endangered species."

- [Eating the tubers and dosage]

"I'd eat one tuber. You do tend to be chewing for quite a while, now I don't know if that is stage release. It doesn't go away - it's not like... the only think I can compare it with, and it's a related plant, its liquorice root – your left with the root even after hours of chewing."

"About 1h to 1.5h after eating it, I g*et al*most a sort of quivery elation – 2 or 3 other people have said something along those lines. It's quite a pleasant feeling. I think we all have agreed that appetite just disappears, it's not even a consideration.

"It is said that you would not eat, not want to eat and not miss eating for weeks and even into months"

"I don't feel hungry and regardless I don't go by the clock in the sense that a lot of people do –all I can say is we just get on in the absence of wanting to eat or drink. Anything that tastes of liquorice coats the mouth and you want to rinse the mouth but I don't think that's having to drink.

"I'd have to say that the first time I took it the effects were more striking than subsequent times but it's not tailing off – you get to a norm."

"It would work out 1 every 3 or 4 days"

APPENDIX 2, EMAIL CORRECPONDANCE: MR MARK GOFF

Email sent: 04 Nov 2016

Val hi!

I have no pride in authorship and you are free to edit,distribute as you see fit or return for a rewrite! It's all a bit longwinded but I wanted to put in the preamble before the final paragraph to demonstrate that I didn't fall into this by luck – I believe it was Mark Twain who said "Luck is when preparation and opportunity meet". I also have another unattributed quote which looking back is equally apt - "It is because opportunities come dressed in overalls and look like hard work that so many people fail to act upon them". Everything from helping my grandfather culture and incubate his orchids through to the countless books I've read and people I've met have brought me to where I am today and I salute and thank them all.

Plants have always been present in my life. As a small boy I spent a great deal of time with my Grandfather, an amateur orchid grower, who had his Oncidium hybrid "Ann Dore" recognised by the RHS on 1st Jan 1962. My father was a farmer (I spent six years farming as a young man) and our next door neighbour, the botanist Laura Ponsonby, was a great source of inspiration, as was Arthur Jewell, the curator of the Haslemere Education Museum (David Bellamy began his career under Arthur's tutelage). I still relish the many happy hours I spent in Arthur's company absorbing his encyclopaedic knowledge of how different cultures around the world use plants and fungi (often deemed poisonous) for medical, cultural and recreational use.

I have always been fascinated how different cultures (mis) appropriate aspects of other cultures to camouflage their intentions or to win over their target audience - the early church's adoption of the pagan Green Man being one of my favourite examples. Somewhere in this I was aware that the early English church followed the Ordination of the Signatures – if the plant looks like a bladder then God has put it in this world to treat bladder problems; if the patient doesn't improve then it is God's will (a classic lose:lose). By comparison, I was aware that whilst England was mired in superstitious bunk, Scotland went down the Arabic route of evidence based medicinal treatment.

In 2008 I read a newspaper article in which Dr Brian Moffatt extolle the appetite suppressing properties of Bitter Vetch and this, reinforced by the Scottish/medical link, caught my attention. I was also particularly tickled by the delicious irony that a plant once used in times of famine might have a future in times of plenty. I began researching the plant and greater

credence came when I read that in the Nordic countries the plant's presence is often an indication of the site of a settlement by early man – our ancestors didn't have the luxury of following too many blind alleys! It took me a couple of intensive weeks to find a source of the seeds. Their scarcity spurred me on and I determined to make the cultivation of Bitter Vetch my particular niche of expertise. I was confident that if the plant truly possessed appetite suppressing qualities then, at some stage, possibly with a little help from me, the spotlight would fall upon it and I would be in a prime position to supply the tubers. I imagined that interest might come from a commercial entity but was overjoyed when Strathclyde University contacted me. Supporting this project is a source of great pride.

Regards

Mark

APPENDIX 3, SUMMARY OF HISTORICAL REFERENCES TO LL

Table A3-1: Summary of literature from Flora Celtica mentioning LL

Quote	Year
"*[Bitter vetch (Lathyrus linifolius)] when infused in whisky was said to be an "agreeable beverage and, like the Nepenthe of the Greeks, exhilarates the mind." Nepenthe roughly means 'banisher of grief', so the combination must have been potent indeed*!" – Pennant	1774
"*In the Highlands of Scotland, where the Bitter-Vetch abounds, they are collected by the people, dried and used for chewing, like the betel-nut in India, or the coca in Peru and are said to increase the strength and improve the lungs of those addicted to the habit. They are likewise considered to give a relish to the whisky so largely consumed in those mountain districts. . . . . The tubers are considered in the Highlands to promote expectoration when chewed, and thus to be serviceable in lung disorders, but have probably no medical action beyond what is due to their liquorice-like sweetness*."	1777
[Called Orobus tuberosus, by Lightfoot]. "*The Highlanders have great esteem for the tubercles of the roots of this plant; they dry and chew them in general to give better relish to their liquor; they also affirm them to be good against most disorders of disorders of the thorax, and that by the use of them they are able to repel hunger and thirst for a long time. In Breadalbane and Rosshire they sometimes bruise and steep them in water and make an agreeable fermented liquor with them. They have a sweet taste, something like the root of liquorice, and when boiled, we are told, are well flavoured and nutrative, and in times of scarcity have served as a substitute for bread*." – Lightfoot	1777
"*The tuberous roots of this plant constitute the Cormeille of the Highlanders, and are very highly esteemed by them. They are dried in the sun, and afterwards chewed in order to add a relish to their whiskey; and according to the Highlanders, they have the power of allaying both hunger and thirst*." – Pratt	1899

Quote	Year
"…the tuberous roots [of bitter vetch] were dug up and eaten raw, or tied in bundles and hung up to the kitchen roof to dry, and afterwards roasted. Used for flavouring whisky." – McNeil	1910
"*The tubers of bitter-vetch were formerly dried and used to ward off hunger, being both acid and sweet. It also was used as a food flavouring and in brewing. Although there is no current use, it could have potential for use as a flavouring in soft drinks, ice cream and other dairy products*." – Highlands and Islands Enterprise	1995
"*A plant which seems likely to be the ubiquitous bitter, or tuberous vetch (Lathyrus linifolius) is mentioned in classical sources (including Julius Caesar) as having been added to beer for use in brewing by the native Britons. Up until the 1950s, this practice is thought to have continued, it having been included in a home-brewed heather ale by older Highland folk. It is likely that the addition of L. linifolius, with its stimulant properties, may have complemented the intoxicating effects of the beer and potentially enhanced its ritual significance to the various Celtic tribal groupings who used it.*" – Beith	1995

APPENDIX 4, ISSR PCR Primer Optimisation

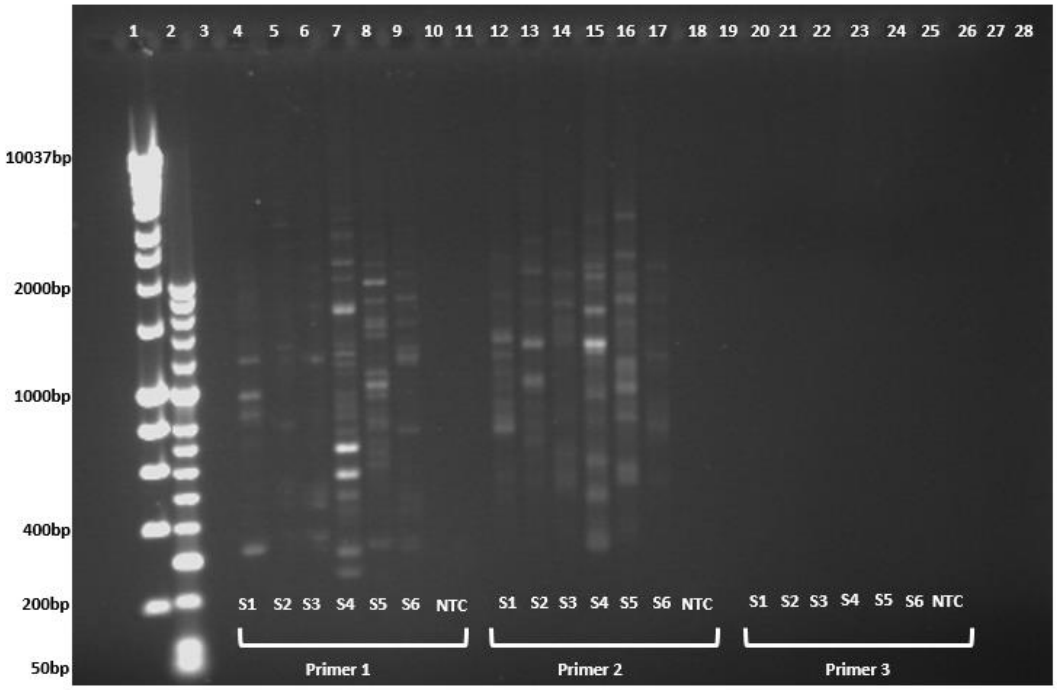

Figure A4-1: ISSR PCR of *Lathyrus* DNA Samples with ISSR Primers 1-3

Aliquots of ISSR PCR products following amplification of *Lathyrus* DNA samples, S1-6 (as detailed in Table 2.5) with ISSR Primers 1-3 (as detailed in Table 2.7) were resolved on a 2% agarose gel and visualised by ethidium bromide staining. NTC lanes contain aliquots of the reactions from the no template control reactions for each ISSR PCR assay. The size markers (measured in basepairs) were Hyperladder 1kb (lane 1) and 50bp (lane 2). Unique banding patterns for each sample are evident with primer 1 and primer 2. No banding patterns can be seen with Primer 3.

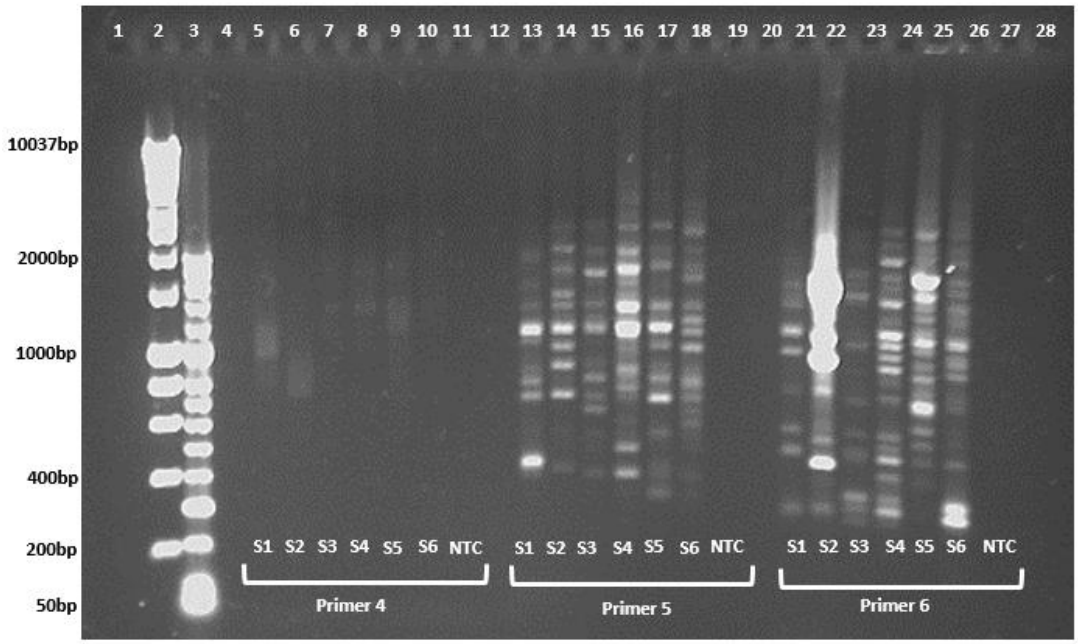

Figure A4-2: ISSR PCR of *Lathyrus* DNA Samples with ISSR Primers 4-6

Aliquots of ISSR PCR products following amplification of *Lathyrus* DNA samples, S1-6 (as detailed in Table 2.5) with ISSR Primers 4-6 (as detailed in Table 2.7) were resolved on a 2% agarose gel and visualised by ethidium bromide staining. NTC lanes contain aliquots of the reactions from the no template control reactions for each ISSR PCR assay. The size markers (measured in basepairs) were Hyperladder 1kb (lane 2) and 50bp (lane 3). Unique banding patterns are evident with Primer 5 and Primer 6, but not Primer 4.

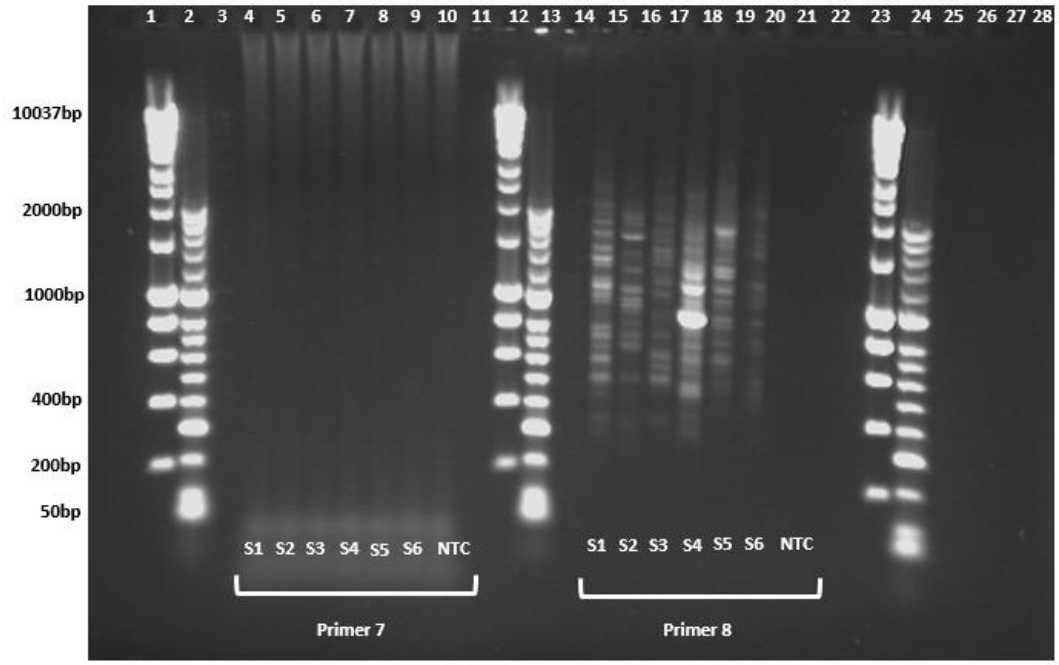

Figure A4-3: ISSR PCR of *Lathyrus* DNA Samples with ISSR Primers 7 and 8

Aliquots of ISSR PCR products following amplification of *Lathyrus* DNA samples, S1-6 (as detailed in Table 2.5) with ISSR Primers 7 and 8 (as detailed in Table 2.7) were resolved on a 2% agarose gel and visualised by ethidium bromide staining. NTC lanes contain aliquots of the reactions from the no template control reactions for each ISSR PCR assay. The size markers (measured in basepairs) were Hyperladder 1kb (lanes 1, 12 and 23) and 50bp (lanes 2, 13 and 24). A unique banding pattern for each sample is evident with Primer 8 but not Primer 7.

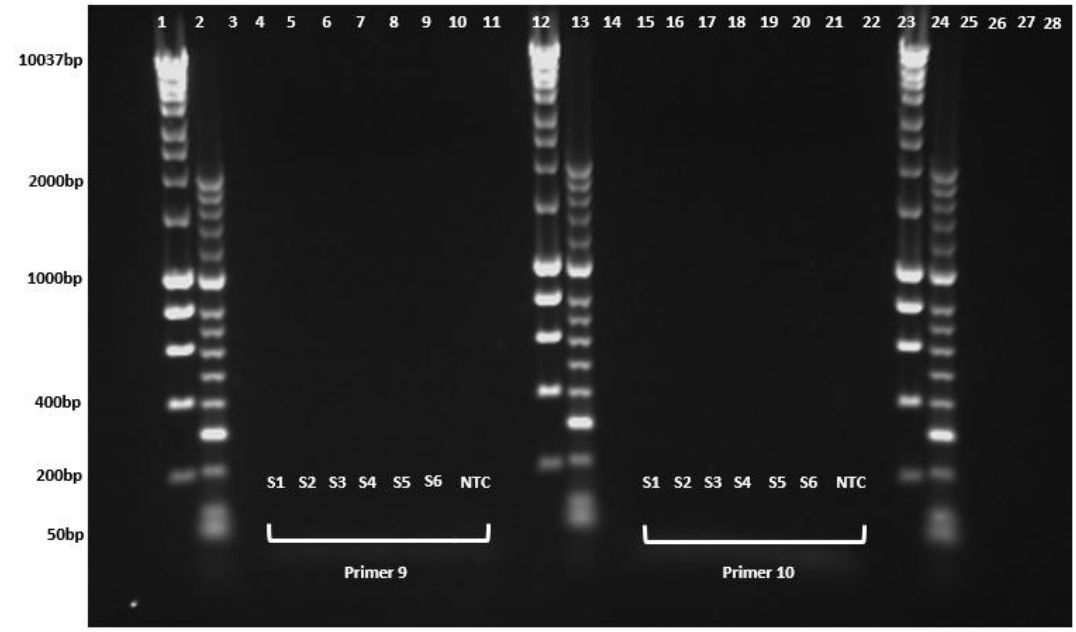

Figure A4-4: ISSR PCR of *Lathyrus* DNA Samples with ISSR Primers 9 and 10

Aliquots of ISSR PCR products following amplification of *Lathyrus* DNA samples, S1-6 (as detailed in Table 2.5) with ISSR Primers 9 and 10 (as detailed in Table 2.7) were resolved on a 2% agarose gel and visualised by ethidium bromide staining. NTC lanes contain aliquots of the reactions from the no template control reactions for each ISSR PCR assay. The size markers (measured in basepairs) were Hyperladder 1kb (lanes 1, 12 and 23) and 50bp (lanes 2, 13 and 24). Neither primer resulted in unique banding patterns for the samples tested.

APPENDIX 5, NMR Spectra for LL-EthA-2 Extract

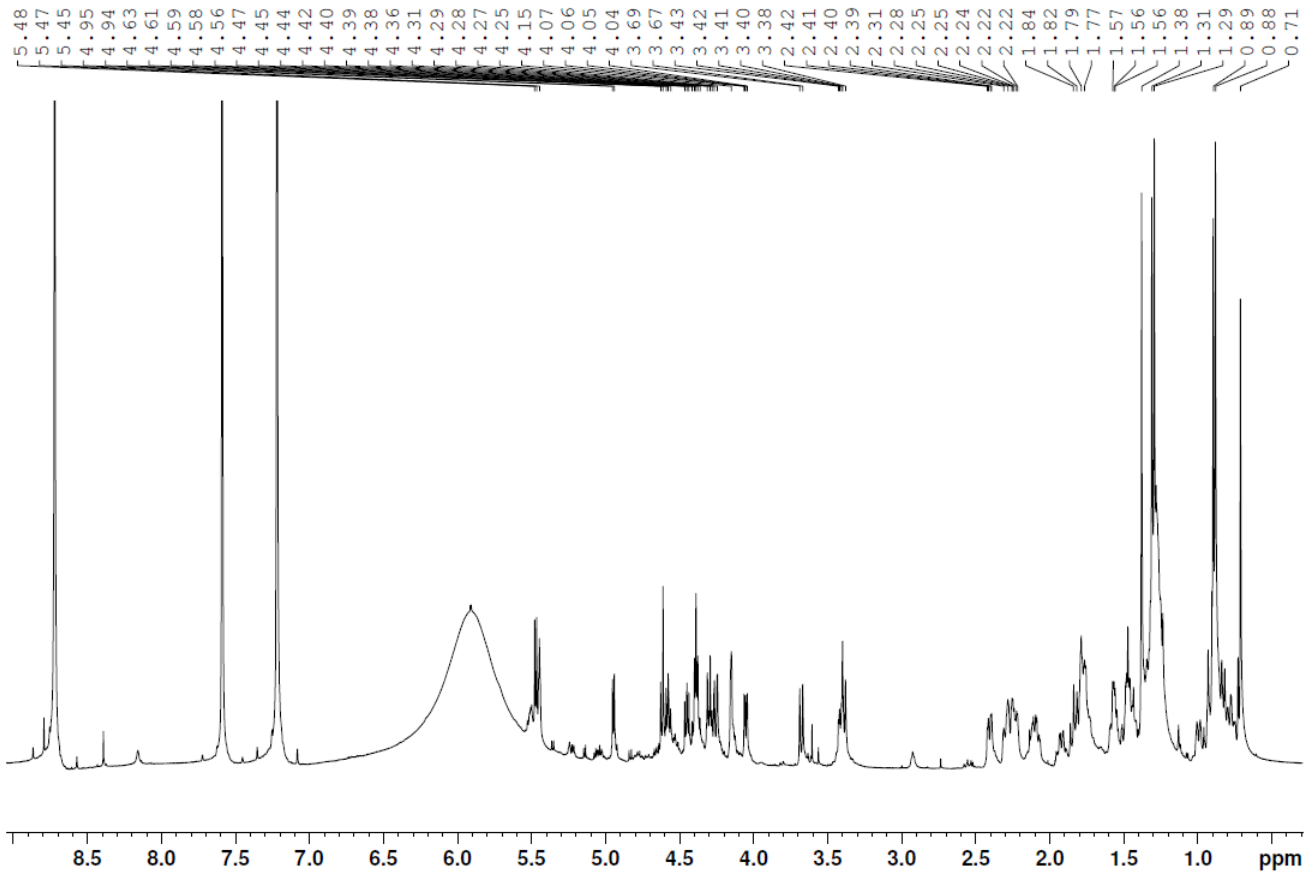

Figure A5-1: 1H NMR (Full Spectra) of LL-EthA-2 (Pyridine-D_5, 600MHz). Numbering along the top of the figure represents the peaks (ppm) mentioned in Section 2.4.3.2.1. Pyridine peaks shown at δ 7.22, 7.58 and 8.74. Broad peak at around δ 5.60-6.50 indicates the presence of water in the sample.

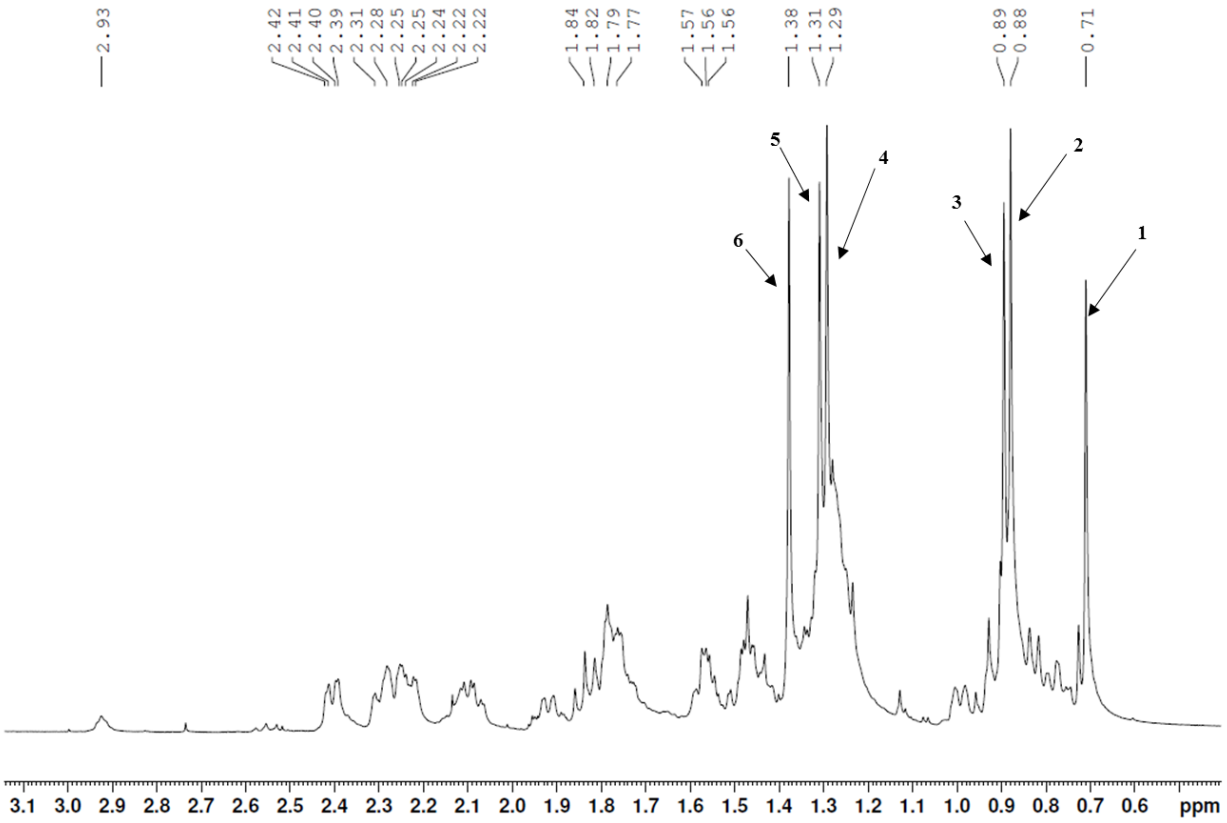

Figure A5-2: 1H NMR (Expanded region, 0 ppm to 3.1 ppm) of LL-EthA-2 (Pyridine-D_5, 600MHz). Numbering along the top of the figure represents the peaks (ppm). Numbering alongside the peaks within the spectra represent the 6 methyl groups mentioned in section 2.4.3.2.1 which form part of the aglycone structure of LL-EthA-2 [Number 1 to 6 represent peaks δ 0.71, 0.88, 0.89, 1.29, 1.31 and 1.38, respectively].

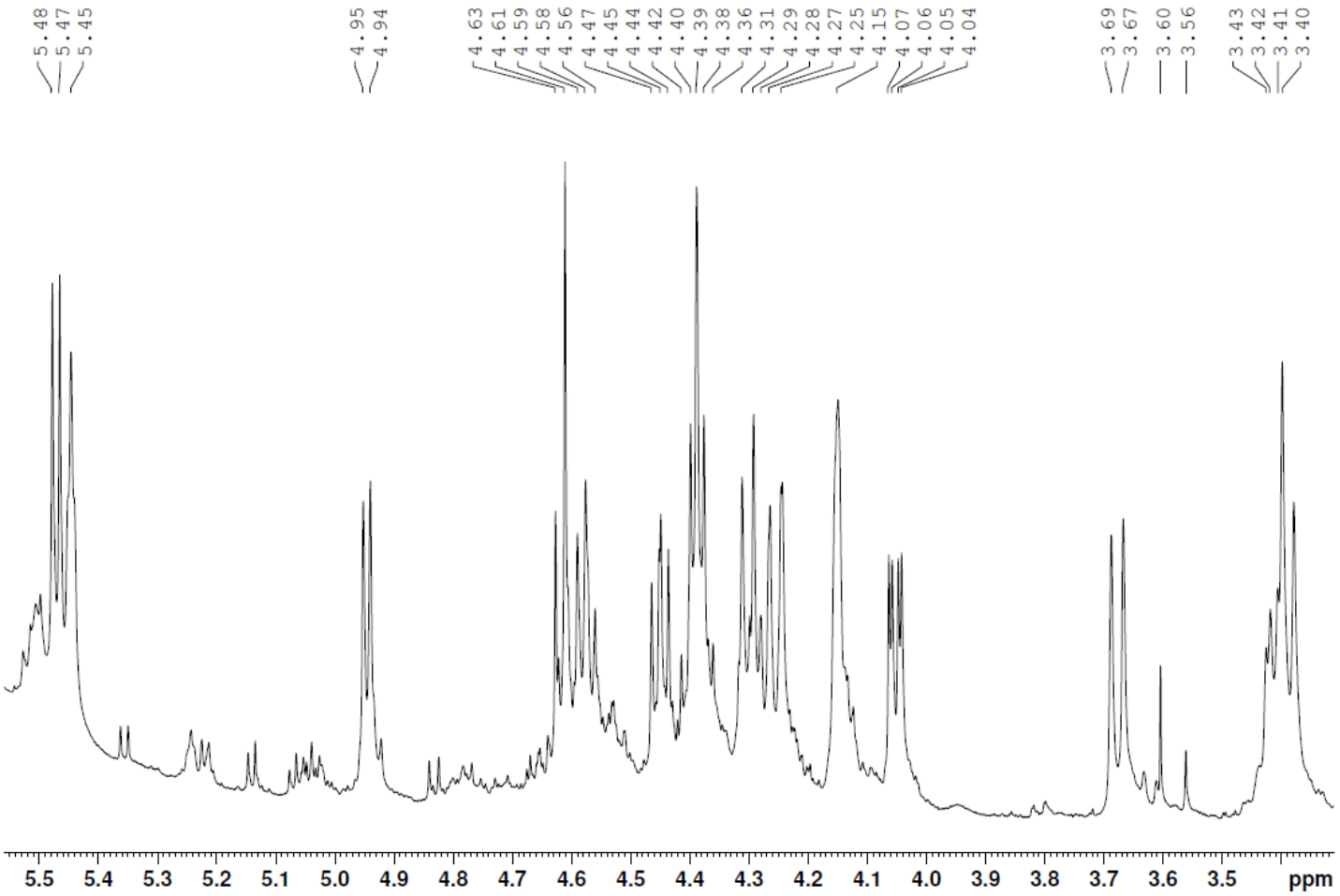

Figure A5-3: ^{1}H NMR (Expanded region, 3.5 ppm to 6.0 ppm) of LL-EthA-2 (Pyridine-d_5,, 600MHz).

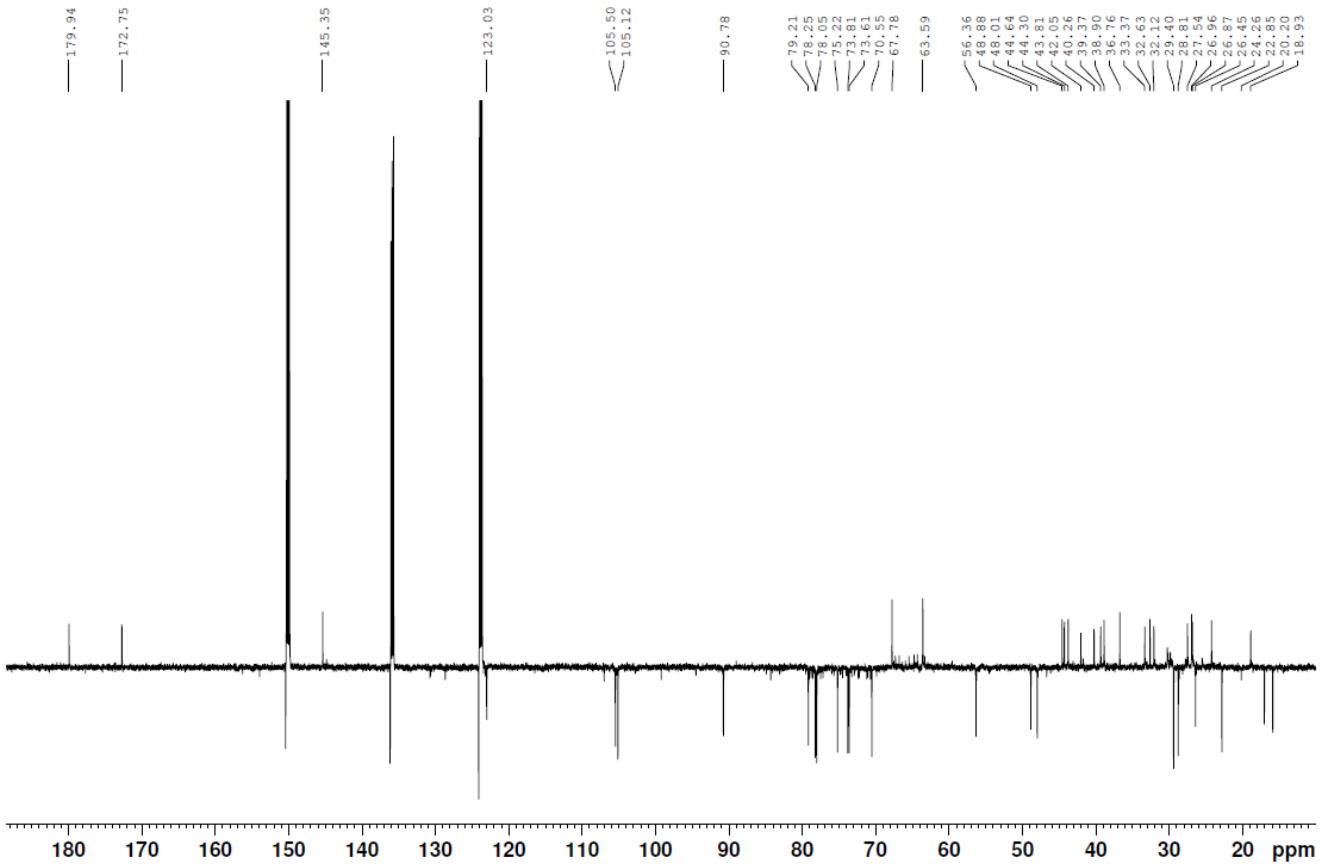

Figure A5-4: 13C NMR (Full spectra) of LL-EthA-2 (Pyridine-d_5, 600MHz). Proton and carbon assignments shown in Chapter 2, Table 2.14.

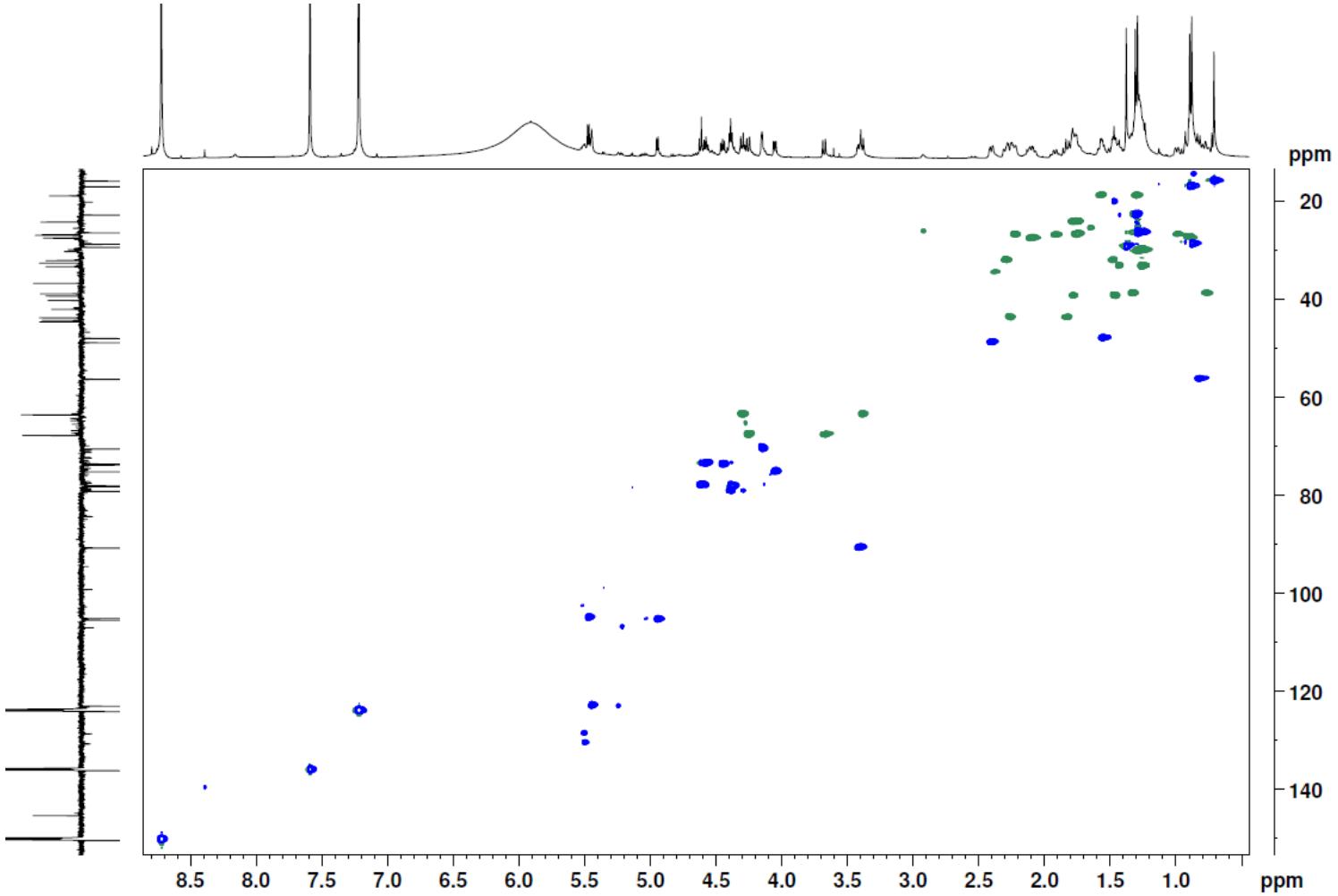

Figure A5-5: HSQC NMR (Full spectra) of LL-EthA-2 (Pyridine-D$_5$, 600MHz). Blue represents correlations between ^{1}H and C or CH_3. Green represents correlations between ^{1}H and CH_2.

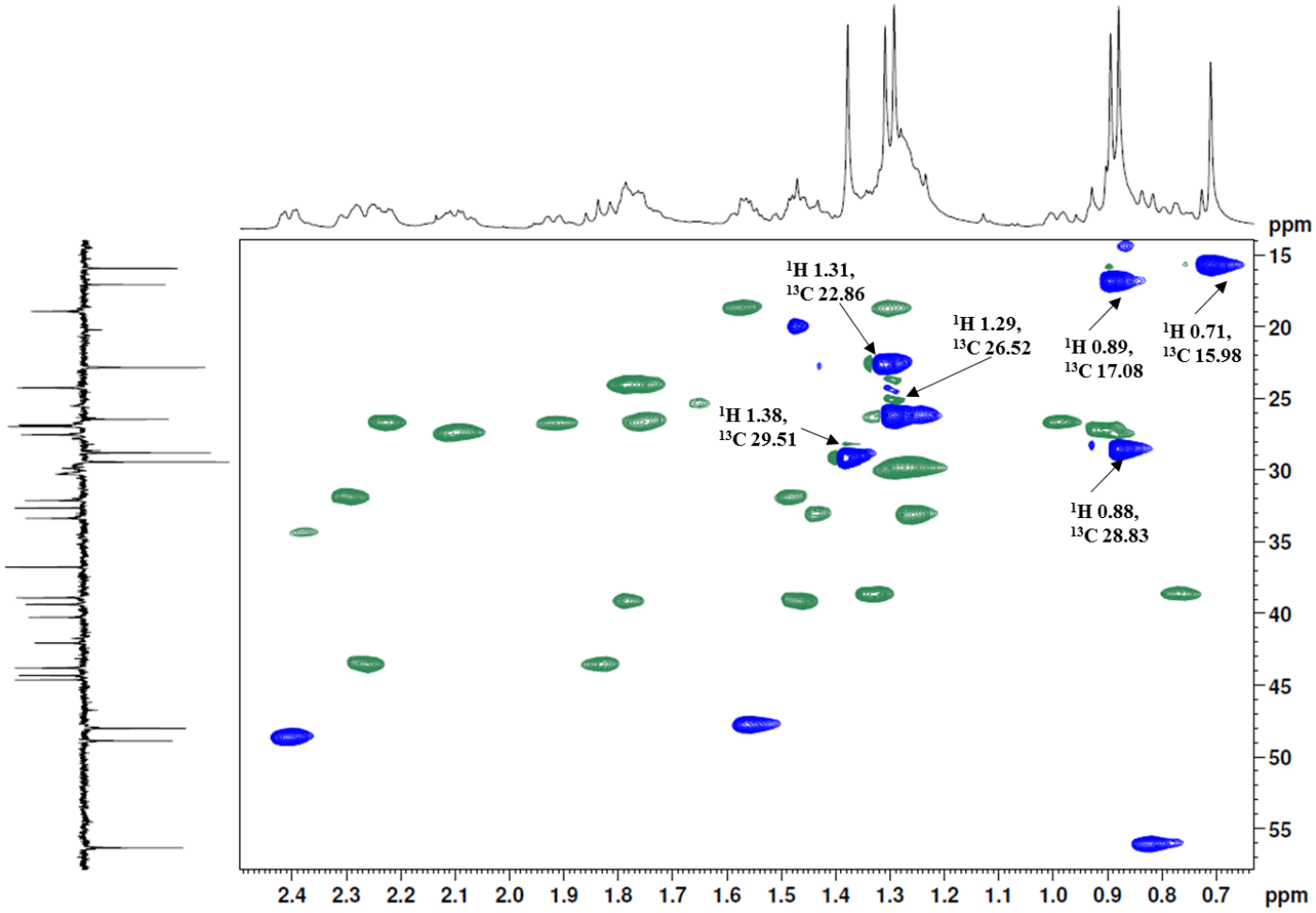

Figure A5-6: HSQC NMR (Expanded region) of LL-EthA-2 (Pyridine-D_5, 600MHz). Green represents correlations between ^1H and C or CH_3. Blue represents correlations between ^1H and CH_2. Arrows highlight the six methyl groups mentioned in section 2.4.3.2.1. Signals are shown for both proton and carbon atoms (ppm).

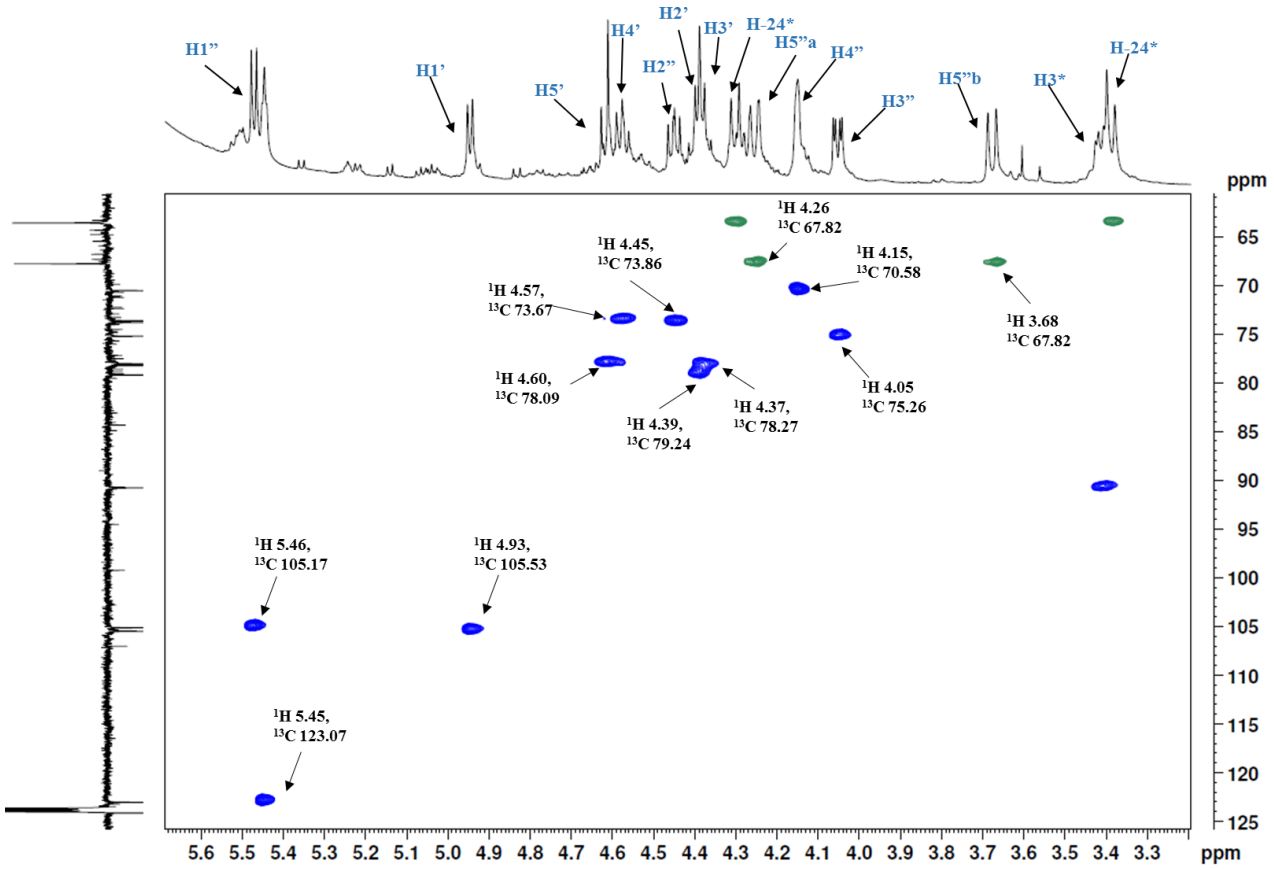

Figure A5-7: HSQC NMR (Expanded sugar region) of LL-EthA-2 (Pyridine-D_5, 600MHz). Blue represents correlations between ^{1}H and C or CH_3. Green represents correlations between ^{1}H and CH_2. Blue labelling along the top of the spectra represents the assignments for both the glucuronic acid and arabinose molecules identified in LL-EthA-2, shown in Chapter 2, Table 2.15. H#’ indicates a hydrogen atom which is part of glucuronic acid. H#” indicates a hydrogen atom which is part of the arabinose molecule. H#* indicates a hydrogen atom which is part of the aglycone structure.

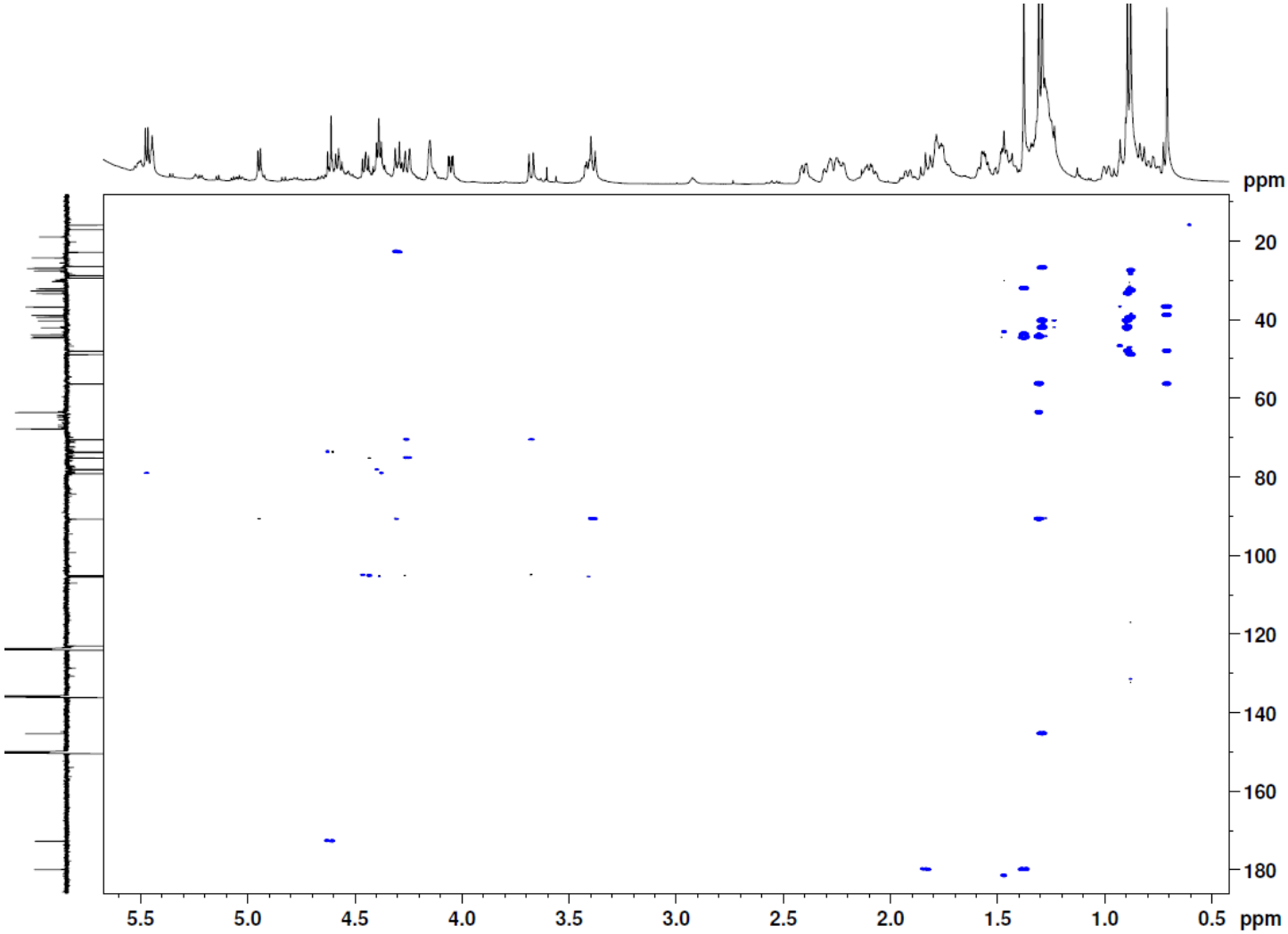

Figure A5-8: HMBC NMR (Full spectra) of LL-EthA-2 (Pyridine-D_5, 600MHz).

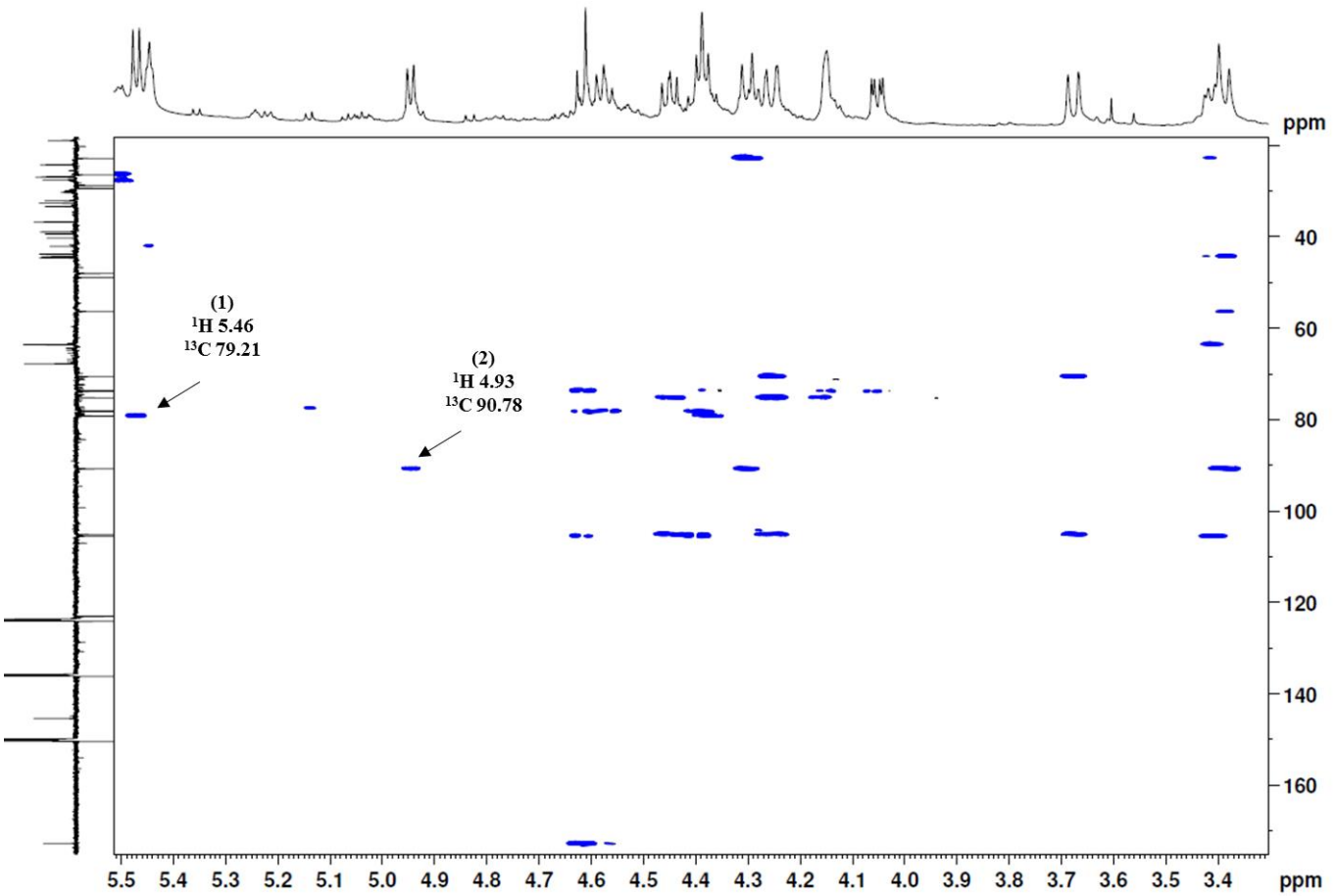

Figure A5-9: HMBC NMR (Sugar region) of LL-EthA-2 (Pyridine-D_5, 600MHz). HMBC detects long range heteronuclear correlations (^{1}H to ^{13}C), typically over 2-4 bonds. (1) highlights the correlation between H1" on arabinose to C2' on glucuronic acid, where both sugars are connected. (2) highlights the correlation between H1' on glucuronic acid with C3 on the aglycone structure, indicating this is where they are joined.

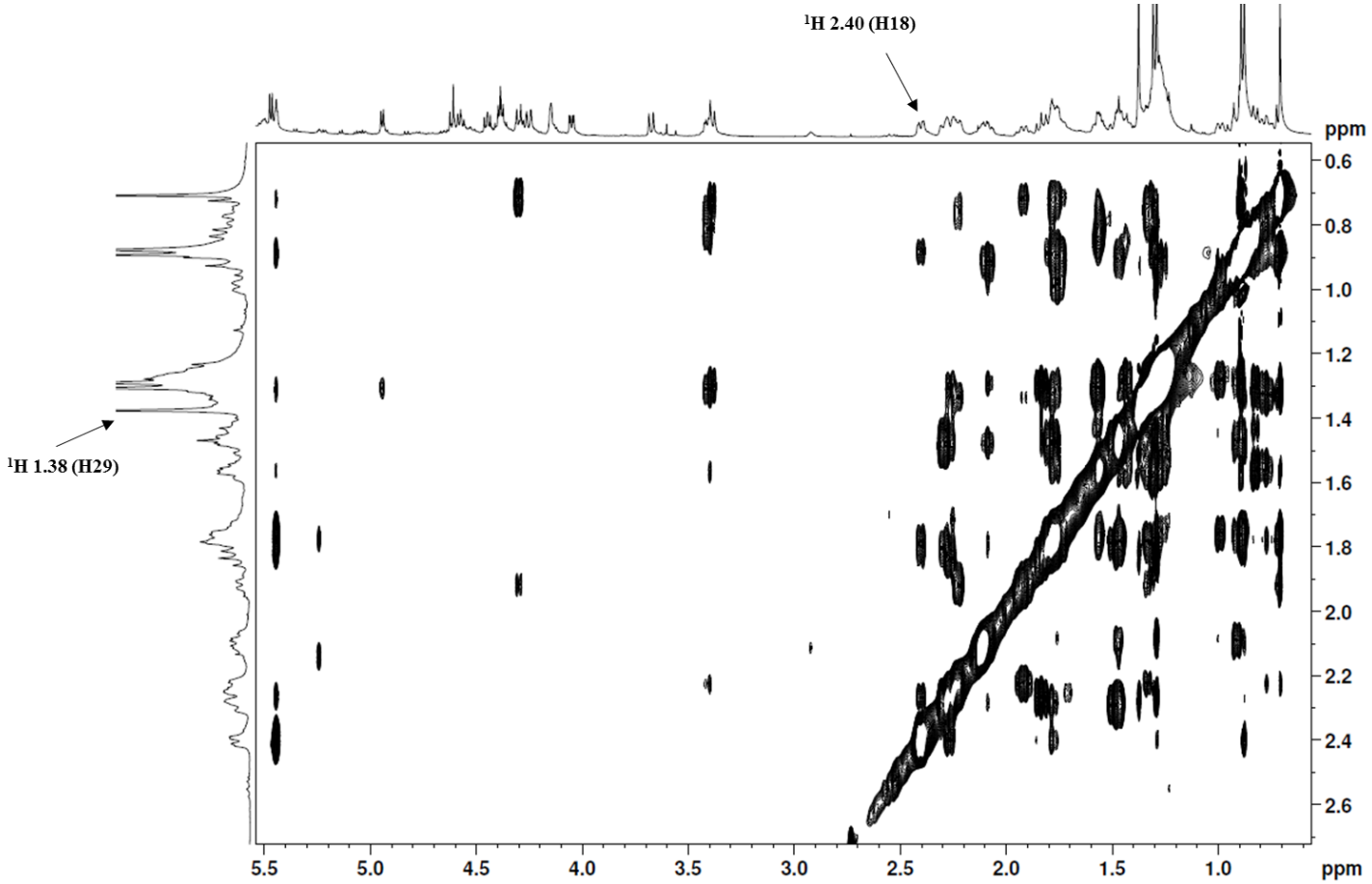

Figure A5-10: NOESY NMR of LL-EthA-2 taken in Pyridine-D_5 at 600MHz. Arrows highlight peaks for H18 and H29 which are part of the aglycone structure of LL-EthA-2. This spectra shows no correlation between both of these hydrogen atoms, thus confirming the structure has a different stereochemistry in comparison to the compound identified by Perez *et al.* (2013) who identified a correlation using ROESY NMR between H18 and H30. This hydrogen has been assigned H29 due to the difference in position.

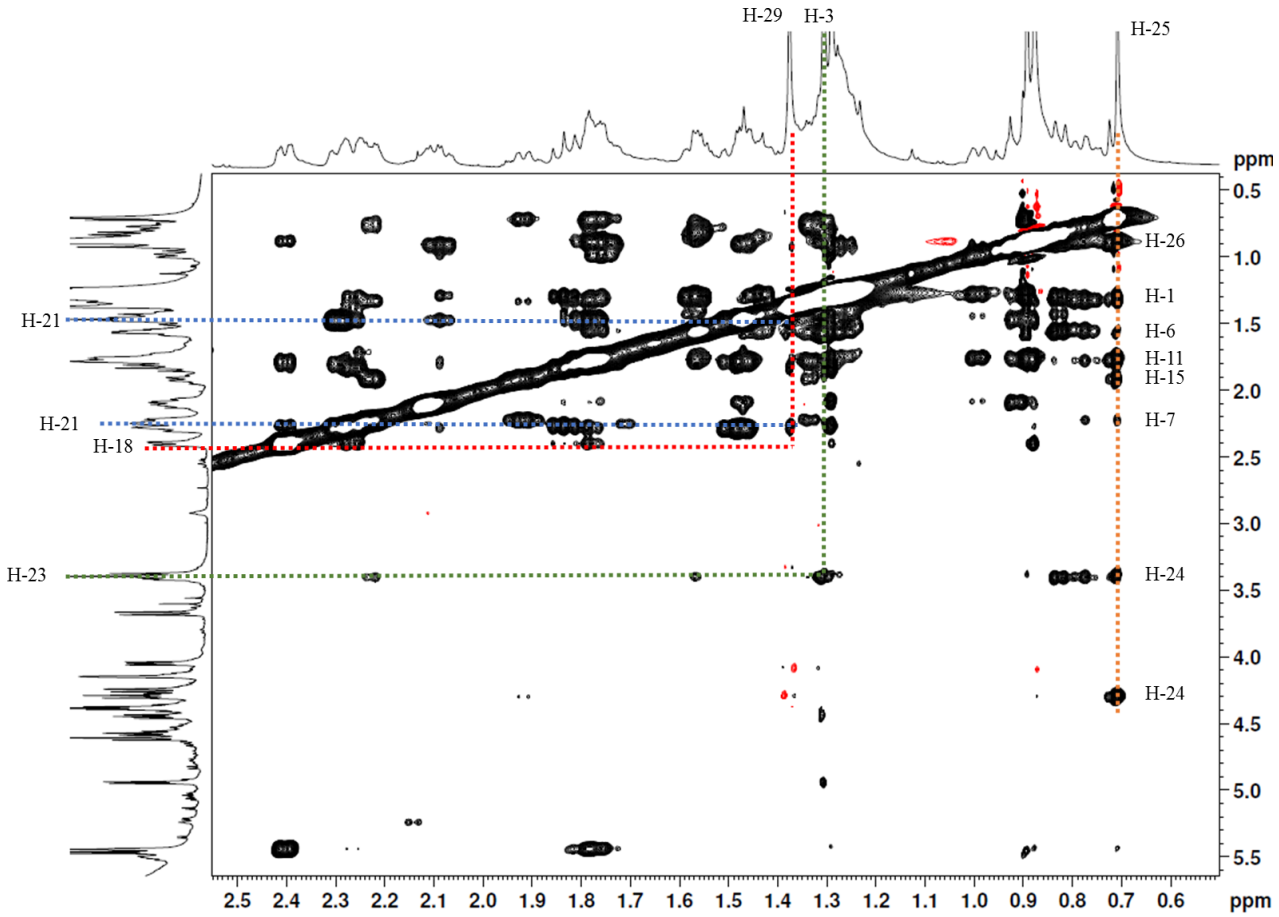

Figure A5-11: NOESY NMR of LL-EthA-2 taken in Pyridine-D_5 at 600MHz. The red lines highlight no correlation between H18 and H29, confirming stereochemistry of H29 and H30. Blue lines which are horizontal to the red line show which hydrogen atoms are visible to H29 – the two protons highlighted are both from C21 (thus labelled H21). The green line show correlations between H3 and H23, which are close to the two sugar moieties. The orange vertical line highlights the protons visible to H25.

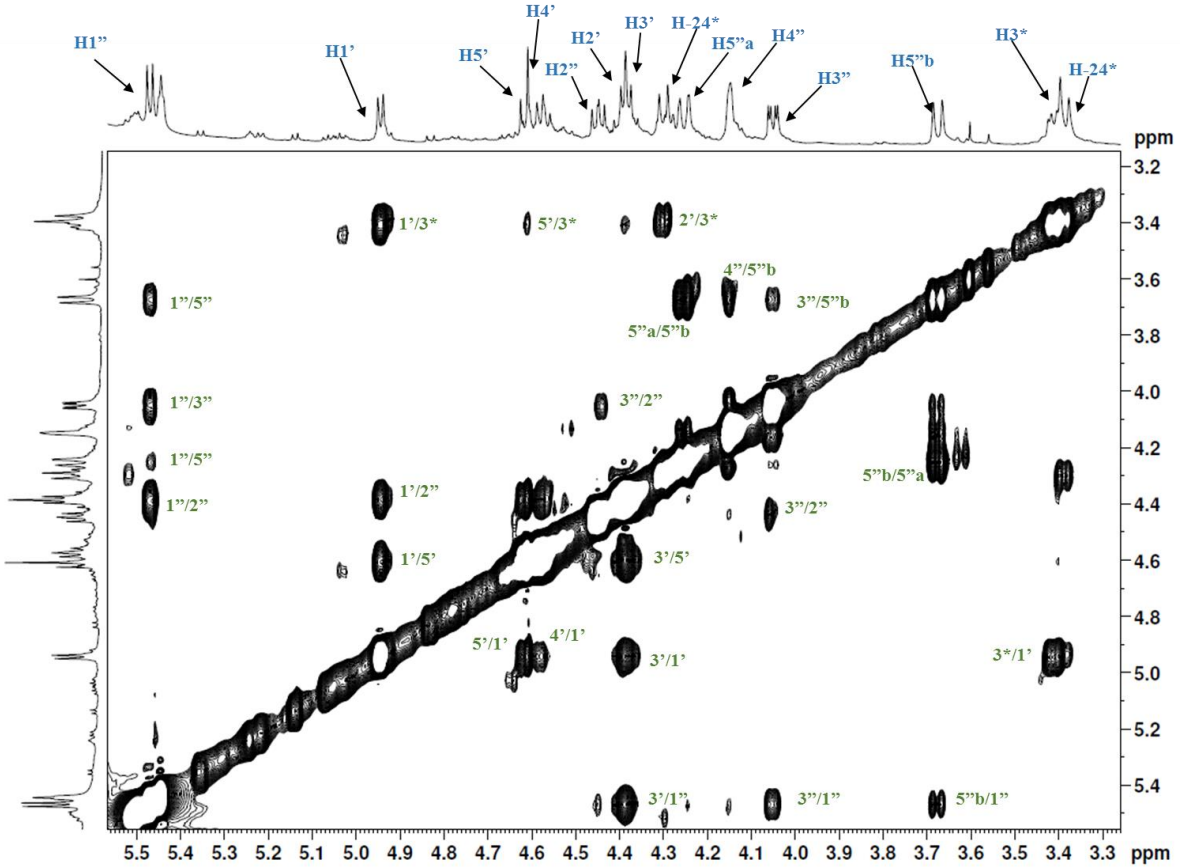

Figure A5-12: NOESY NMR of LL-EthA-2 sugar region taken in Pyridine-D_5 at 600MHz. Blue numbering on the top spectrum indicates protons of both sugar molecules as well as protons on the aglycone structure which correlate to the sugars. H#’ indicates a hydrogen atom which is part of glucuronic acid. H#” indicates a hydrogen atom which is part of the arabinose molecule. H#* indicates a hydrogen atom which is part of the aglycone structure. Blue numbering within the spectra highlights which hydrogens are able to ‘see’ each other through space rather than as a direct bond.